

‘Role of  
Class II Phosphoinositide 3-Kinase  
PI3K-C2 $\alpha$   
in pancreatic  $\beta$  cell function’

Simona Mazza

Supervisor: Dr. Tania Maffucci

Co-supervisor: Prof. Marco Falasca

Thesis submitted for the degree of Doctor of Philosophy

Inositide Signalling Group, Centre for Diabetes, Blizard Institute,

Barts and the London School of Medicine and Dentistry,

Queen Mary University of London

May 2014

I, Simona Mazza, confirm that the research included within this thesis is my own work or that where it has been carried out in collaboration with, or supported by others, that this is duly acknowledged below and my contribution indicated. Previously published material is also acknowledged below.

I attest that I have exercised reasonable care to ensure that the work is original, and does not to the best of my knowledge break any UK law, infringe any third party's copyright or other Intellectual Property Right, or contain any confidential material.

I accept that the College has the right to use plagiarism detection software to check the electronic version of the thesis.

I confirm that this thesis has not been previously submitted for the award of a degree by this or any other university.

The copyright of this thesis rests with the author and no quotation from it or information derived from it may be published without the prior written consent of the author.

Signature:

Date:

## Abstract

Phosphoinositide 3-kinases (PI3Ks) are a family of enzymes that catalyse the synthesis of different lipid second messengers, regulating a plethora of intracellular functions. Deregulation of their signalling pathway has different functional consequences, and it has been associated with a variety of human diseases. The existence of eight distinct isoforms, divided into three classes, has raised in the past many questions on whether and to which extent their role was redundant or overlapping. The study of their intracellular signalling pathways and cellular functions is crucial, because some of these isoforms have been identified as important therapeutic targets.

The most investigated PI3Ks belong to the class I subfamily, and they have a well established role in the regulation of cell growth, survival and proliferation. In the past years, attention and research efforts focussed on class I isoforms and alteration of their signalling pathways, one of the most common causes of cancer. More recently, evidence indicated that the least investigated class II PI3Ks have different intracellular roles.

This work focussed on the class II isoform PI3K-C2 $\alpha$ , the study of its intracellular function(s) in pancreatic  $\beta$  cells and the implications of its inhibition through downregulation in pancreatic  $\beta$  cells homeostasis. It was reported that PI3K-C2 $\alpha$  has a crucial role insulin granules exocytosis. This study has demonstrated that this enzyme synthesises the lipid product PtdIns3P specifically at the plasma membrane of pancreatic  $\beta$  cells upon depolarisation of the plasma membrane and stimulation of insulin secretion. Moreover, the data herein presented indicated for the first time that glucose-induced activation of PI3K-C2 $\alpha$  is able to protect  $\beta$  cells from cell death induced by nutrients deprivation. Analysis of the intracellular pathways stimulated by glucose indicated that PI3K-C2 $\alpha$  is able to modulate the activity of mTOR and its downstream effectors, key regulators of cell proliferation and growth. Importantly, the activation of mTOR pathway upon glucose does not seem to involve the activation of the upstream regulator Akt or class I PI3K, suggesting a novel intracellular pathway stimulated by glucose.

# Table of contents

Abstract .....	3
Table of contents .....	4
List of Tables.....	10
List of Figures .....	11
List of Abbreviations .....	18
Publications.....	23
Acknowledgements.....	23
Chapter 1.....	24
Introduction .....	24
1.1 Phosphoinositide 3-kinases.....	24
1.1.1 PI3Ks products: 3-phosphorylated phosphoinositides.....	25
1.1.2 Classification of PI3Ks .....	28
1.1.3 Physiological roles of PI3K in insulin target cells .....	35
1.1.4 Physiological roles of PI3K in insulin producing cells.....	41
1.1.5 Dysregulation of PI3K signalling pathway and type 2 diabetes.....	53
1.2 PI3K-C2 $\alpha$ .....	60
1.2.1 Activation of PI3K-C2 $\alpha$ .....	60
1.2.2 Lipid product of PI3K-C2 $\alpha$ .....	63
1.2.3 Functions of PI3K-C2 $\alpha$ .....	66
1.2.4 Mouse models .....	70
1.2.5 PI3K-C2 $\alpha$ and diabetes.....	72
1.3 Aims of the project .....	75

Chapter 2.....	76
Materials and Methods.....	76
2.1 Cell culture.....	76
2.1.1 Cell culture and propagation .....	76
2.1.2 Cell amplification and passage .....	77
2.1.3 Cryo-preservation and recovery of cell lines .....	77
2.2 Biochemistry.....	78
2.2.1 Protein sample preparation from cell lysates .....	78
2.2.2 Measurement of Protein Concentration using Bradford protein assay .....	79
2.2.3 SDS-PAGE and Western blot.....	81
2.2.4 Immunoblotting and analysis .....	84
2.2.5 Co-Immunoprecipitation .....	87
2.3 Cell Biology .....	88
2.3.1 Cell counting .....	88
2.3.2 MTT assay .....	89
2.3.3 Sodium Palmitate treatment .....	90
2.3.4 GFP-2XFYVE <sup>Hrs</sup> transfection .....	91
2.4 Molecular Biology.....	92
2.4.1 RNA extraction .....	92
2.4.2 RNA Reverse transcription.....	92
2.4.3 Real Time quantitative Polymerase Chain Reaction (RT-qPCR).....	94
2.5 Imaging methods.....	95

2.5.1 Confocal Microscopy Analysis .....	95
2.6 Lipid analysis.....	96
2.6.1 HPLC analysis of intracellular phosphoinositides .....	96
2.7 Statistical Analysis .....	97
Chapter 3.....	98
Mechanisms of PI3K-C2 $\alpha$ downregulation.....	98
3.1 Introduction.....	98
3.2 Results .....	101
3.2.1 Optimisation .....	101
3.2.2 Lipotoxic growth conditions reduce the protein expression levels of PI3K-C2 $\alpha$ .....	106
3.2.3 Lipotoxic growth conditions do not affect mRNA levels of PI3K-C2 $\alpha$ .....	107
3.2.4 Protein levels of other members of the PI3K family upon lipotoxic growth conditions .....	109
3.3 Discussion .....	114
Chapter 4.....	118
Intracellular functions regulated by PI3K-C2 $\alpha$ .....	118
Cell viability .....	118
4.1 Introduction.....	118
4.2 Results .....	121
4.2.1 Downregulation of PI3K-C2 $\alpha$ does not sensitise INS1 cells towards death in lipotoxic conditions.....	121

4.2.2 Glucose alone is able to sustain survival of INS1 cells upon nutrients deprivation.....	124
4.2.3 Glucose rescue upon nutrient deprivation is not inhibited by classical PI3Ks inhibitors.....	126
4.2.4 Glucose-induced survival upon nutrient deprivation requires the activation of PI3K-C2 $\alpha$ .....	129
4.2.5 Nutrients deprivation and apoptosis.....	135
4.2.6 Nutrients deprivation and autophagy .....	139
4.3 Discussion .....	142
Chapter 5.....	148
Intracellular functions regulated by PI3K-C2 $\alpha$ .....	148
Signalling pathways.....	148
5.1 Introduction.....	148
5.2 Results .....	154
5.2.1 Effects of stimulatory glucose concentrations on the activation of mTOR and its direct downstream effectors in INS1 cells.....	154
5.2.2 Glucose-induced stimulation of mTOR is affected by rapamycin .....	158
5.2.3 Effects of rapamycin treatment on glucose-induced cell survival .....	161
5.2.4 Role of PI3K-C2 $\alpha$ in the activation of mTOR pathway induced by stimulatory concentrations of glucose .....	165
5.2.5 Effects of stimulatory glucose concentrations on the activation of other components of mTOR pathway .....	171
5.2.6 Akt activation upon nutrients starvation and glucose stimulation .....	174
5.2.7 PI3K-C2 $\alpha$ has a role in AMPK signalling .....	176

5.2.8 Short term signalling following 24 hours of nutrients deprivation. ....	179
5.3 Discussion .....	189
Chapter 6.....	194
Mechanisms of PI3K-C2 $\alpha$ activation .....	194
6.1 Introduction.....	194
6.2 Results .....	201
6.2.1 Optimisation – Labelling and starvation.....	201
6.2.2 Optimisation – HPLC analysis.....	203
6.2.3 Stimulation of INS1 cells with KCl induces PtdIns3P <i>de novo</i> synthesis.....	207
6.2.4 Stimulation of INS1 sh-scrambled and sh-PI3K-C2 $\alpha$ cells with KCl induces <i>de novo</i> synthesis of PtdIns3P .....	211
6.2.5 Glucose induces the synthesis of the lipid product PtdIns3P.....	213
6.3 Discussion .....	218
Chapter 7.....	223
Mechanisms of PI3K-C2 $\alpha$ action .....	223
7.1 Introduction.....	223
7.2 Results .....	227
7.2.1 Analysis of calpain family members protein expression .....	227
7.2.2 Investigation of potential effects of PI3K-C2 $\alpha$ downregulation on SNAREs interaction.....	228
7.2.3 Optimisation of GFP-2XFYVE <sup>Hrs</sup> plasmid transfection.....	232
7.2.4 GFP-2XFYVE <sup>Hrs</sup> translocates to the plasma membrane upon KCl treatment	234



7.3 Discussion .....	243
Chapter 8.....	247
Final conclusions and future work .....	247
8.1 Conclusions.....	247
8.2 Future work .....	251
Function of PI3K-C2 $\alpha$ .....	251
Lipid product of PI3K-C2 $\alpha$ in pancreatic $\beta$ cells .....	252
mTORC1 activation .....	252
Bibliography .....	253
Copyright permission .....	273

## List of Tables

Table 1.1: PI3Ks lipid products and interaction with protein domains .....	27
Table 2.1: BSA Standard curve protein concentration .....	79
Table 2.2: 5X Denaturing Sample Buffer .....	81
Table 2.3: 10% separating gel solution .....	82
Table 2.4: 5% stacking gel solution. ....	82
Table 2.5: Running Buffer.....	83
Table 2.6: Transfer buffer .....	83
Table 2.7: List of primary antibodies used .....	86
Table 2.8: Reagents used for cDNA synthesis. ....	93
Table 2.9: Program used for PCR thermal cyclers. ....	93
Table 2.10: Primers used for the amplification of Rat PI3K-C2 $\alpha$ and 18S ribosomal subunit .....	94

## List of Figures

Figure 1.1: Structure of PI3Ks lipid products .....	26
Figure 1.2: Schematic structure of class I PI3Ks.....	29
Figure 1.3: PI-dependent activation of a target protein .....	31
Figure 1.4: Schematic structure of class II PI3Ks.....	34
Figure 1.5: Schematic structure of class III PI3Ks.....	35
Figure 1.6: Activation of class I PI3Ks signalling pathway upon insulin stimulation..	37
Figure 1.7: Glucose uptake via insulin-stimulated GLUT4 translocation and fusion in muscle and adipose tissues.....	38
Figure 1.8: Schematic representation of the intracellular pathways triggered in insulin target cells .....	40
Figure 1.9: Mechanism of insulin granules exocytosis upon glucose stimulation in pancreatic $\beta$ cells.....	42
Figure 1.10: Schematic representation of Akt signalling downstream of class I PI3K in pancreatic $\beta$ cells.....	46
Figure 1.11: Schematic representation of PI3K/Akt/mTORC1 signalling pathway..	48
Figure 2.11: Program used for RT-qPCR reaction using the ABI 7500 Real-Time PCR system software.....	94
Figure 3.1: Expression of PI3K-C2 $\alpha$ in the presence or absence of BSA and sodium palmitate .....	102

Figure 3.2: Expression of PI3K-C2 $\alpha$ upon 24 and 48 hours treatment with sodium palmitate dissolved in methanol.....	103
Figure 3.3: Expression of PI3K-C2 $\alpha$ upon 24 and 48 hours treatment with medium containing sodium palmitate or ethanol .....	104
Figure 3.4: Cell viability in lipotoxic conditions.....	105
Figure 3.5: Expression of PI3K-C2 $\alpha$ upon treatment with increasing concentrations of sodium palmitate .....	107
Figure 3.6: Levels of PI3K-C2 $\alpha$ mRNA determined by qPCR .....	108
Figure 3.7: Expression of p110 $\alpha$ upon 24 and 48 hours treatment with sodium palmitate.....	110
Figure 3.8: Expression of p110 $\beta$ upon 24 and 48 hours treatment with sodium palmitate.....	111
Figure 3.9: Expression of p110 $\gamma$ upon 24 and 48 hours treatment with sodium palmitate.....	112
Figure 3.10: Expression of hVps34 upon 24 and 48 hours treatment with sodium palmitate.....	113
Figure 4.1: Expression levels of PI3K-C2 $\alpha$ were analysed by Western blot analysis in stable INS1 sh scrambled and INS1 sh PI3K-C2 $\alpha$ cells .....	121
Figure 4.2: Cell viability of INS1 sh scrambled and sh PI3K-C2 $\alpha$ in the presence of palmitate.....	122
Figure 4.3: Cell viability of INS1 sh scrambled and sh PI3K-C2 $\alpha$ in the presence of palmitate.....	124

Figure 4.4: Cell viability upon nutrients deprivation and glucose reintroduction...	125
Figure 4.5: Cell viability upon nutrients deprivation and glucose reintroduction, in the presence or absence of wortmannin.....	127
Figure 4.6: Cell viability upon nutrients deprivation and glucose reintroduction, in the presence or absence of LY294002 .....	128
Figure 4.7: Cell viability assessed by manual cell counting - Effect of downregulation of PI3K-C2 $\alpha$ on cell viability upon nutrients deprivation and glucose reintroduction....	130
Figure 4.8: Cell viability assessed by MTT assay - Effect of downregulation of PI3K-C2 $\alpha$ on cell viability upon nutrients deprivation and glucose reintroduction .....	131
Figure 4.9: Cell viability assessed by manual cell counting - Effect of downregulation of PI3K-C2 $\alpha$ on cell viability upon nutrients deprivation and reintroduction of stimulatory or substimulatory glucose concentrations .....	133
Figure 4.10: Cell viability was assessed by MTT assay - Effect of downregulation of PI3K-C2 $\alpha$ on cell viability upon nutrients deprivation and reintroduction of stimulatory or substimulatory glucose concentrations .....	134
Figure 4.11: Activation of caspase 3 upon nutrients deprivation and glucose reintroduction .....	137
Figure 4.12: Activation of autophagy upon nutrients deprivation and glucose reintroduction .....	140
Figure 5.1: Diagram of mTORC1 and mTORC2 components and intracellular functions .....	150

Figure 5.2: Schematic diagram of mTORC1 signalling pathway. ....	152
Figure 5.3: Activation of mTOR upon nutrients deprivation and glucose reintroduction in INS1 parental cells .....	155
Figure 5.4: Phosphorylation of 4EBP1 upon nutrients deprivation and glucose reintroduction .....	156
Figure 5.5: Activation of S6K upon nutrients deprivation and glucose reintroduction.. .....	157
Figure 5.6: Activation of mTOR upon nutrients deprivation and glucose reintroduction in the presence of rapamycin .....	158
Figure 5.7: Activation of S6 upon nutrients deprivation and glucose reintroduction.....	160
Figure 5.8: Cell viability upon nutrients deprivation and glucose reintroduction, in the presence or absence of rapamycin.....	162
Figure 5.9: Cell viability upon nutrients deprivation and glucose reintroduction, in the presence or absence of rapamycin.....	164
Figure 5.10: Activation of mTOR upon nutrients deprivation and glucose reintroduction .....	165
Figure 5.11: Activation of 4EBP1 upon nutrients deprivation and glucose reintroduction .....	166
Figure 5.12: Densitometric analysis of Western Blots for p4EBP1 (Thr 37/46).....	167
Figure 5.13: Activation of S6K upon prolonged nutrients deprivation and 24 hours glucose reintroduction .....	168

Figure 5.14: Activation of S6K upon nutrients deprivation and 24 or 48 hours of glucose reintroduction .....	169
Figure 5.15: Densitometric analysis of Western Blots for pS6K (Thr 389).....	170
Figure 5.16: Representative blot (A) and densitometric analysis (B) of Western Blots for pS6 (Ser 235/236) .....	172
Figure 5.17: Representative blot (A) and densitometric analysis (B) of Western Blots for pS6 (Ser 240/244) .....	173
Figure 5.18: Activation of Akt upon nutrients deprivation and glucose reintroduction. ....	175
Figure 5.19: Activation of AMPK upon nutrients deprivation and glucose reintroduction .....	177
Figure 5.20: Densitometric analysis of Western Blots for pAMPK .....	178
Figure 5.21: Activation of Akt and S6 upon nutrients deprivation and short time points of glucose stimulation .....	180
Figure 5.22: Activation of Akt and S6 upon nutrients deprivation and short time points of glucose stimulation (II).....	182
Figure 5.23: Activation of Akt upon nutrients deprivation and glucose reintroduction. ....	183
Figure 5.24: Activation of S6K upon nutrients deprivation and glucose reintroduction .....	184
Figure 5.25: Activation of S6 upon nutrients deprivation and short time points of glucose stimulation .....	186

Figure 5.26: Activation of 4EBP1 upon nutrients deprivation and short time points of glucose stimulation .....	187
Figure 6.1: Chemical structure of phosphatidylinositol (PtdIns), the building block of all PIs. ....	196
Figure 6.2: Schematic diagram of PtdIns(3,4,5)P <sub>3</sub> . ....	197
Figure 6.3: Schematic diagram of the non linear HPLC gradient .....	199
Figure 6.4: Representative blot of the indicated INS1 cell lines untreated or stimulated with 100 nM insulin for 30 min.....	202
Figure 6.5: Representative chromatogram of glycerophosphoinositides extracted from INS1 cells and analysed by HPLC. ....	204
Figure 6.6: Representative chromatogram of glycerophosphoinositides extracted from INS1 cells and analysed by HPLC. ....	205
Figure 6.7: Representative chromatogram of glycerophosphoinositides extracted from INS1 cells and analysed by HPLC. ....	206
Figure 6.8: Analysis of the levels of PtdIns3P in INS1 cells upon stimulation with KCl... ..	208
Figure 6.9: Analysis of the levels of PtdIns3P in INS1 cells upon stimulation with KCl... ..	209
Figure 6.10: Analysis of the levels of PIs in INS1 cells upon stimulation with KCl ...	210
Figure 6.11: Analysis of the levels of PtdIns3P in INS1 sh-scrambled and sh-PI3K-C2α cells upon stimulation with KCl.....	211



Figure 6.12: Analysis of the levels of PIs in INS1 sh-scrambled and sh-PI3K-C2 $\alpha$ cells upon stimulation with KCl.....	212
Figure 6.13: Analysis of the levels of PtdIns3P in INS1 cells upon stimulation with 15mM glucose.....	214
Figure 6.14: Analysis of the levels of PtdIns3P in INS1 cells upon stimulation with 15mM glucose.....	216
Figure 7.1: SNAREs core complex. Interactions between VAMP2, SNAP 23/25 and syntaxin are shown. ....	224
Figure 7.2: Analysis of calpain family members protein expression. ....	228
Figure 7.3: Association between syntaxin 1 and VAMP 2 in the presence or absence of KCl.. ....	230
Figure 7.4: Association between syntaxin 1 and VAMP 2 in the presence or absence of KCl. ....	231
Figure 7.5: Analysis of intracellular localisation of PtdIns3P – 30 mins KCl.....	235
Figure 7.6: Analysis of intracellular localisation of PtdIns3P – 2.5 and 5 mins KCl..	237
Figure 7.7: Analysis of intracellular localisation of PtdIns3P – syntaxin 1 staining..	239
Figure 7.8: Quantitative analysis of GFP-2XFYVE <sup>Hrs</sup> translocation.....	241

## List of Abbreviations

4EBP1	Eukaryotic translation initiation factor 4E-binding protein 1
AMP	Adenosine Monophosphate
AMPK	AMP-activated protein kinase
AS160	Akt substrate of 160 kDa
ATP	Adenosine triphosphate
BSA	Bovine Serum Albumin
cDNA	Complementary DNA
CHO-IR	Chinese Hamster Ovary cells expressing IR
ddH <sub>2</sub> O	Double-distilled water
DMEM	Dulbecco's modified Eagle's medium
DMSO	Dimethyl sulfoxide
DNA	Deoxyribonucleic Acid
dNTP	Deoxynucleotide triphosphate
EDTA	Ethylenediaminetetraacetic acid
eEF2	eukaryotic Elongation Factor 2
eIF4B	eukaryotic Initiation Factor 4B
ERK	Extracellular-signal-related-kinase
FBS	Foetal Bovine Serum
FFA	Free Fatty Acid
FFA-free BSA	Free Fatty Acid-free BSA
FYVE	Fab1p, YOTB, Vac1, EEA1
GAPDH	Glyceraldehyde-3-phosphates dehydrogenase

GFP	Green fluorescent protein
GH	Growth Hormone
GK	Glucokinase
GLUT	Glucose transporter
GPCR	G-protein-coupled-receptor
GSK3	Glycogen synthase kinase 3
GTP	Guanosine-5'-triphosphate
HBSS	Hank's Balanced Salt Solution
HPLC	High Pressure Liquid Chromatography
HUVEC	Humbilical Vein Endothelial Cells
IGF	Insulin-like growth factor 1
IgG	Immunoglobulin G
IR	Insulin receptor
IRS	Insulin Receptor Substrate
LC3	Microtubule-associated protein 1A/1B-light chain 3
MEF	Mouse embryonic fibroblasts
mRNA	Messenger RNA
MTM	Myotubularin
mTOR	Mechanistic Target of Rapamycin
mTORC1/2	Mechanistic Target of Rapamycin complex 1/2
MTT	[3-(4,5-Dimethylthiazol-2-yl)-2,5-Diphenyltetrazolium Bromide]
N	Number of experiments
PAGE	Polyacrylamide gel electrophoresis
PBS	Phosphate buffer saline

PCR	Polymerase chain reaction
PDCD4	Programmed Cell Death Protein 4
PDK1	3-Phosphoinositide-Dependent-Protein-Kinase-1
PFA	Paraformaldehyde
PH	Pleckstrin homology
PI	Phosphoinositide
PI3K	Phosphoinositide 3-kinase
PIP3	Phosphatidylinositol-3,4,5-trisphosphate
PtdIns	Phosphatidylinositol
PtdIns(3,4) $P_2$	Phosphatidylinositol-3,4-bisphosphate
PtdIns(3,4,5) $P_3$	Phosphatidylinositol-3,4,5-trisphosphate
PtdIns(3,5) $P_2$	Phosphatidylinositol-3,5-bisphosphate
PtdIns(4,5) $P_2$	Phosphatidylinositol-4,5-bisphosphate
PtdIns3P	Phosphatidylinositol-3-phosphate
PTEN	Phosphatase and tensin homolog
PX	Phox
Rheb	Ras homolog enriched in brain
RNA	Ribonucleic acid
RPM	Revolutions per minute
RT	Room temperature
RT-qPCR	Reverse transcription quantitative polymerase chain reaction
S6 /rpS6	Ribosomal protein S6
S6K	p70 ribosomal protein S6 Kinase
SDS	Sodium-dodecyl-sulphate

SEM	Standard error of the mean
SH	Src homology domain
shRNA	Short hairpin RNA
siRNA	Small interfering RNA
SNAP 23/25	Synaptosomal-Associated Protein of 23/25 kDa
SNARE	Soluble N-ethylmaleimide-sensitive factor attachment protein receptor
T2D	Type 2 Diabetes
TFIIIC	Transcription Factor 3C
TIRF	Total Internal Reflection Fluorescence microscope
RTK	Receptor Tyrosine Kinase
TSC1/2	Tuberous sclerosis protein 1/2
ULK1	Unc-51-like kinase 1
Vps-34	Vacuolar sorting protein 34
WB	Western blot

## Publications

**Mazza, S.** and T. Maffucci (2011). "Class II phosphoinositide 3-kinase C2alpha: what we learned so far." *Int J Biochem Mol Biol* 2(2): 168-182.

**Mazza, S.** and T. Maffucci (2014). "Autophagy and pancreatic beta-cells." *Vitam Horm* 95: 145-164.

## Acknowledgements

It would not have been possible to write this doctoral thesis without the guidance of my supervisors, Dr Tania Maffucci and Prof Marco Falasca. Their knowledge and scientific passion inspired me throughout my project and their constant support encouraged my research for the past three years.

I would also like to thank the members of my group, for the priceless technical and moral support. I am glad I had the chance to work with each one of them, and for all the different things I had the opportunity to learn. I am thankful for the friendship and the cheerful moments I shared with my colleagues in and out of the lab, it would not have been the same without them.

A special thanks goes to the people from my 'adoptive' lab and my friends, who supported me during my writing.

Last, I am deeply grateful to my family for always being there for me. From close, far or very far their unconditional love is always with me and it strengthens me every day.

# Chapter 1

## Introduction

### 1.1 Phosphoinositide 3-kinases

Phosphoinositide 3-kinases (PI3Ks) are enzymes that regulate several biological functions, including cell growth, differentiation, survival, proliferation, migration, intracellular vesicular transport and metabolism (Vanhaesebroeck et al. 2010). PI3Ks were first discovered in 1984 and subsequently found in all eukaryotic cell types examined (Foster et al. 2003). It has subsequently emerged that PI3Ks are a family of structurally related enzymes, that can use different lipid substrates and can be differently regulated, which explains the plethora of biological functions that the enzymes control (Foster et al. 2003). Because of their multiple intracellular functions, dysregulation of their signalling pathway is associated to the onset and/or progression of several human diseases. For instance, impaired signalling downstream of PI3Ks is one of the major contributors towards the progression of Type 2 diabetes (T2D), while hyperactivation of PI3K-dependent signalling has been reported in human cancers (Engelman et al. 2006). PI3Ks share high sequence homology within their kinase domain and they have been divided into three main classes, based on their substrate specificity and structure (Vanhaesebroeck et al. 2010). All PI3K isoforms catalyse the phosphorylation of the 3-OH position within



the inositol head groups of their lipid substrates phosphoinositides (PIs), generating 3-phosphorylated lipids (Vanhaesebroeck et al. 2001).

### **1.1.1 PI3Ks products: 3-phosphorylated phosphoinositides**

PIs consist of a glycerol backbone attached to two fatty acids and an inositol 1-phosphate group. The unphosphorylated form of phosphoinositide is phosphatidylinositol (PtdIns). The hydroxyl groups of the inositol ring can be phosphorylated in position 3, 4, and 5 in different combinations, generating seven distinct PIs, all naturally occurring in cell membranes of higher eukaryotes (Maffucci 2012). PIs have several intracellular functions, from being part of the cellular membranes to acting as intracellular second messengers. Because of their lipid tail, they bind intracellular membranes and therefore mark cellular compartments. As amphipathic molecules, they also possess a polar inositol head, which can interact with cytosolic proteins and regulate the activation of signalling molecules both temporally and spatially (Maffucci 2012).

As mentioned before, PI3Ks are able to catalyse the phosphorylation of the position 3 of the inositol ring of PtdIns, phosphatidylinositol 4-phosphate (PtdIns4P) and phosphatidylinositol 4,5-bisphosphate [PtdIns(4,5)P<sub>2</sub>], generating phosphatidylinositol 3-phosphate (PtdIns3P), phosphatidylinositol 3,4-bisphosphate [PtdIns(3,4)P<sub>2</sub>] and phosphatidylinositol 3,4,5-trisphosphate [PtdIns(3,4,5)P<sub>3</sub>] respectively (Fig 1.1). The 3-phosphorylated PI phosphatidylinositol 3,5-

bisphosphate [PtdIns(3,5)P<sub>2</sub>] is not a direct enzymatic product of PI3Ks and it is generated by further phosphorylation of PtdIns3P in position 5 (Maffucci 2012).

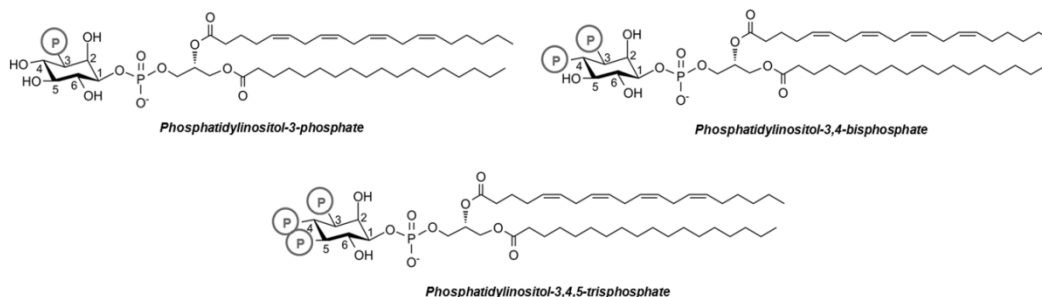


**Figure 1.1: Structure of PI3Ks lipid products. Phosphorylation sites on hydroxyl groups of the inositol head of the molecules are indicated. Adapted from Maffucci 2012**

Another characteristic of some phosphorylated PIs, crucial for their role as second messengers, is their rapid rate of synthesis and turnover, which allows the activation of intracellular signalling pathways only when they are needed. Also, PIs are associated to cellular membranes, and this limits their intracellular localisation. At the same time, the fact that they are compartmentalised, and that they are able to recruit different proteins in distinct subcellular compartments is a clear indication of the specificity of their action (Vanhaesebroeck et al. 2001).

The number and the position of the phosphate groups on the inositol head of PIs define the type of protein(s) that can interact and be activated by them. Therefore, distinct intracellular pathways can be regulated by PI3Ks, depending on their lipid product. Intracellular levels of PtdIns(3,4)P<sub>2</sub> and PtdIns(3,4,5)P<sub>3</sub> are undetectable in

normal resting cells, but they rapidly increase upon cellular stimulation, consistent with their well established role as second messengers (Sotsios and Ward 2000, Hinchliffe 2001, Falasca and Maffucci 2009). PtdIns(3,4) $P_2$  and PtdIns(3,4,5) $P_3$  can bind the pleckstrin homology (PH) domain of several proteins, including protein kinase B/Akt. Binding of PtdIns(3,4) $P_2$  and PtdIns(3,4,5) $P_3$  to Akt PH domain allows translocation of the enzyme to the plasma membrane and subsequent activation (Maffucci 2012). Another well characterised protein domain that is able to bind 3-phosphorylated PIs is the phox homology (PX) domain, which can interact with PtdIns(3,4) $P_2$  but preferentially binds the monophosphorylated lipid PtdIns3 $P$  (Table 1.1).

Phosphoinositide	Binding domain
PtdIns3 $P$	FYVE, PX, PH
PtdIns(3,4) $P_2$	PX, PH
PtdIns(3,4,5) $P_3$	PH

**Table 1.1: PI3Ks lipid products and interaction with protein domains**

The fact that different types of phosphorylated PIs are able to interact with different protein domains, therefore binding distinct proteins, suggests that they have specific intracellular roles.

The lipid PtdIns3 $P$  is constitutively present in eukaryotic cells and it is the most abundant 3-phosphorylated PI in resting conditions, representing 0.1-0.5% of all PIs

(Falasca and Maffucci 2006). Several lines of evidence indicated that at least two distinct pools of PtdIns3P are present within the cells: a constitutive pool, which regulates endosomal trafficking and membrane dynamics and is detectable in unstimulated cells, and a regulated pool, synthesised upon cellular stimulation (Falasca and Maffucci 2009, Maffucci 2012). PtdIns3P can selectively bind the zinc finger domain conserved in F<sub>ab</sub>1p-YOPB-Vac1-EEA1 (FYVE).

Another key regulator of PtdIns3P homeostasis is the family of phosphatases myotubularins (MTMs). They catalyse the dephosphorylation of the position 3 of the inositol ring of PtdIns3P and PtdIns(3,5)P<sub>2</sub>. In humans, this family comprises 14 members, 6 of which are mutated in their catalytic domain, and are predicted to be inactive (Falasca and Maffucci 2009, Maffucci 2012). Interestingly, it appears that the inactive MTMs have a regulatory role on the active isoforms, although the precise mechanisms of MTMs activation are not completely understood. Also, an isoform-specific intracellular localisation of some MTMs has been reported, which may represent a mechanism of regulation of their activity (Maffucci 2012).

### **1.1.2 Classification of PI3Ks**

#### Class I

Class I PI3Ks are the best characterised and they are further divided into class IA and IB. Class IA PI3Ks consist of a catalytic subunit of 110 kDa which interacts with a

regulatory subunit through a specific binding domain (p85 binding domain, Fig 1.2). The regulatory subunit is able to bind phosphotyrosine residues of other proteins through its Src Homology (SH2) domain and it can be of 85 or 55 kDa (Sotsios and Ward 2000, Engelman et al. 2006). Class IA catalytic subunits are p110 $\alpha$ , p110 $\beta$  and p110 $\delta$ , which are encoded by separate genes. p110 $\alpha$  and p110 $\beta$  isoforms are ubiquitous, while p110 $\delta$  is primarily expressed in thymus, lung, spleen and cells of the haematopoietic lineage, such as B and T cells (Domin and Waterfield 1997, Vanhaesebroeck et al. 2001, Herman and Johnson 2012). They have multiple intracellular roles, including regulation of cell size, motility, metabolism, survival and proliferation (Foster et al. 2003). The catalytic subunits of class I PI3Ks comprise the PI3K core shared by all PI3K isoforms, which includes the catalytic domain, a p85 domain that ensures the interaction with the regulatory subunit, and a Ras binding domain which enables activation via Ras signalling.

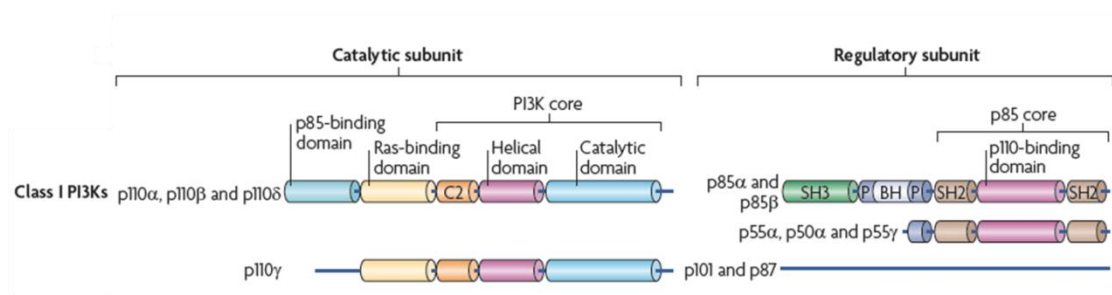


**Figure 1.2: Schematic structure of class I PI3Ks. Catalytic and regulatory subunits are shown, and the domains comprised in class I PI3Ks are indicated (Vanhaesebroeck et al. 2010).**

Class IB catalytic subunit p110 $\gamma$  can bind the regulatory subunits p87 or p101. Tissue distribution for p110 $\gamma$  indicated that this isoform is mainly found in leukocytes and its function is to modulate inflammation and allergy (Foster et al. 2003).

Originally, class IA PI3Ks were thought to be specifically activated upon stimulation of receptor tyrosine kinases (RTKs) by several growth factors and hormones such as insulin (Vanhaesebroeck et al. 2001), while class IB was believed to be solely activated upon stimulation of G-protein coupled receptors (GPCRs) (Sotsios and Ward 2000, Vanhaesebroeck et al. 2001). More recently it has been shown that p110 $\beta$  can also be activated downstream of GPCRs, and p110 $\gamma$  can be activated downstream of RTKs (Vanhaesebroeck et al. 2010). Also, Ras can be activated downstream of both RTKs and GPCRs, and it can in turn activate class I PI3K signalling by direct interaction and regardless of the type of receptor activated (Vanhaesebroeck et al. 2010).

*In vitro*, class I PI3Ks are able to phosphorylate the substrates PtdIns, PtdIns4P and PtdIns(4,5)P<sub>2</sub>. However, *in vivo*, the preferred substrate is PtdIns(4,5)P<sub>2</sub> and therefore the main lipid product is the trisphosphate PtdIns(3,4,5)P<sub>3</sub> (Vanhaesebroeck et al. 2001). The action of class I PI3Ks can be counteracted by intracellular phosphatases, which are able to remove specific phosphate groups from the inositol head of PIs. These enzymes act in direct antagonism to PI3Ks, degrading their lipid products. For example, PtdIns(3,4,5)P<sub>3</sub> can be converted into PtdIns(4,5)P<sub>2</sub> by the phosphatase and tensin homolog (PTEN) which removes the

phosphate group in position 3, or into  $\text{PtdIns}(3,4)P_2$  by 5-phosphatases (such as SHIP2, SKIP, INPP5E) which remove the phosphate group in position 5 (Maffucci 2012).

$\text{PtdIns}(3,4,5)P_3$  can activate several downstream targets and therefore it is responsible for regulation of many intracellular functions (Hinchliffe 2001, Maffucci 2012). The most studied downstream effector of class I PI3Ks is the Ser/Thr kinase Akt, which exists in three isoforms: Akt1/PKB $\alpha$ , Akt2/PKB $\beta$  and Akt3/PKB $\gamma$  (Schultze et al. 2011). The PH domain of Akt can directly bind  $\text{PtdIns}(3,4,5)P_3$  and  $\text{PtdIns}(3,4)P_2$ . This leads to Akt translocation to the plasma membrane, where it can be phosphorylated at two key regulatory residues, Thr 308 and Ser 473 (Alessi et al. 1996).

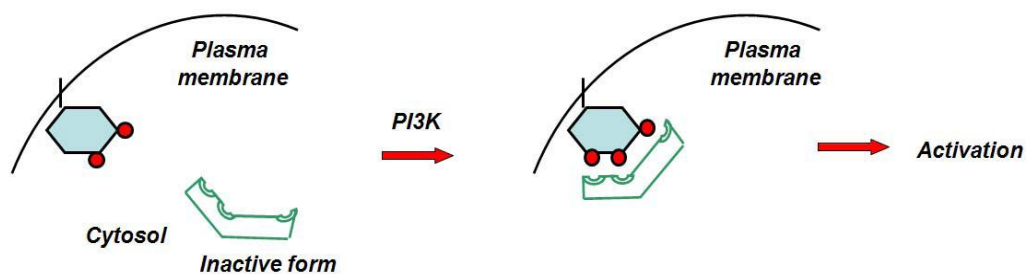


**Figure 1.3: PI-dependent activation of a target protein. PH domain of Akt can bind  $\text{PtdIns}(3,4,5)P_3$  synthesised by class I PI3Ks, leading to its translocation to the plasma membrane and activation (Maffucci 2012).**

The residue Thr 308 is phosphorylated by the enzyme 3'phosphoinositide dependent protein kinase 1 (PDK1), which can also be activated by  $\text{PtdIns}(3,4,5)P_3$ . The residue

Ser 473 of Akt can be phosphorylated by the mechanistic target of rapamycin (mTOR) complex 2, mTORC2 (Sarbasov et al. 2006). The concomitant phosphorylation of these two amino acid residues allows full activation of Akt, which in turn activates intracellular signalling pathways that regulate multiple cellular functions, such as cell metabolism, growth, survival, motility, proliferation and protein synthesis (Manning and Cantley 2007). Deregulation of this signalling pathway is associated with metabolic conditions such as diabetes (discussed later in this chapter) and also with the onset and the progression of cancer. Indeed, deregulation of PI3K signalling has been detected in many types of human cancers (Engelman et al. 2006). For instance, several mutations of the gene encoding for p110 $\alpha$  have been found in tumours, suggesting that mutant p110 $\alpha$  could function as an oncogene (Samuels et al. 2004). More recently, it has been suggested that amplification of other class I PI3K isoforms can also be associated with cancer. For example, immunohistochemical screening and Western blot analysis revealed that the isoform p110 $\gamma$  was overexpressed in human pancreatic cancer tissues and in several cancer cell lines (Edling et al. 2010). Similarly, it has been reported that p110 $\delta$  was expressed at high level in leukemic blasts from patients with acute myeloid leukemia (Sujobert et al. 2005). Furthermore, PTEN is a well established tumour suppressor and its inhibition, either through mutations or epigenetic modifications, is associated with hyperactivation of PI3K signalling pathway and it is detected in many cancer types (Leslie and Downes 2002). Consistent with this, it was reported that heterozygous inactivation of PTEN in mice models was sufficient to



increase the incidence of tumours (Suzuki et al. 1998). Other lines of evidence also indicate that alteration of the signalling pathway downstream of class I PI3Ks is relevant in cancer. For instance, amplification of Akt has also been found in many human cancers (Cheng et al. 1996, Fresno Vara et al. 2004).

## Class II

Class II PI3Ks are high molecular weight monomers, that lack the regulatory subunit present in class I isoforms (Fig 1.4). They were discovered on the basis of their sequence homology with the members of other classes and their physiological roles are still poorly understood (Vanhaesebroeck et al. 2010, Falasca and Maffucci 2012). In humans, three class II isoforms were discovered: PI3K-C2 $\alpha$  and PI3K-C2 $\beta$ , which have a broad tissue distribution and PI3K-C2 $\gamma$ , whose expression is limited to liver, prostate and testis (Kok et al. 2009). The three isoforms PI3K-C2 $\alpha$ , PI3K-C2 $\beta$  and PI3K-C2 $\gamma$  are encoded by three separate genes and differ from each other at their N-terminus region (Vanhaesebroeck and Waterfield 1999).

*In vitro*, class II PI3Ks are able to phosphorylate the substrates PtdIns and PtdIns4P, with a stronger preference for PtdIns over the other PIs (Maffucci 2012). As for their *in vivo* product, contrasting results were originally reported, but strong evidence now suggest that the lipid product of class II PI3Ks is the monophosphorylated PtdIns3P (Falasca et al. 2007, Falasca and Maffucci 2009, Mazza and Maffucci 2011, Yoshioka et al. 2012). Class II PI3Ks differ from other isoforms for their large N-

terminal region and their C-terminus region, which contains a C2 domain that binds phospholipids *in vitro* in a  $\text{Ca}^{2+}$ -independent manner. Also, it has been also observed that *in vitro* PI3K-C2 $\alpha$  and PI3K-C2 $\beta$  can use  $\text{Ca}^{2+}$ /ATP for their kinase activity (Vanhaesebroeck and Waterfield 1999). PI3K-C2 $\alpha$  will be discussed more extensively later in this chapter. In terms of cellular functions, it was reported that PI3K-C2 $\beta$  is involved mainly in the regulation of cell migration (Domin et al. 2005, Maffucci et al. 2005, Tibolla et al. 2013), cell cycle (Visnjic et al. 2003) and activation of  $\text{Ca}^{2+}$  activated  $\text{K}^+$  channel (Srivastava et al. 2009), through the synthesis of  $\text{PtdIns}3\text{P}$ . Less information are available on the functional role of PI3K-C2 $\gamma$ . It has been reported that has a role in liver regeneration (Ono et al. 1998).

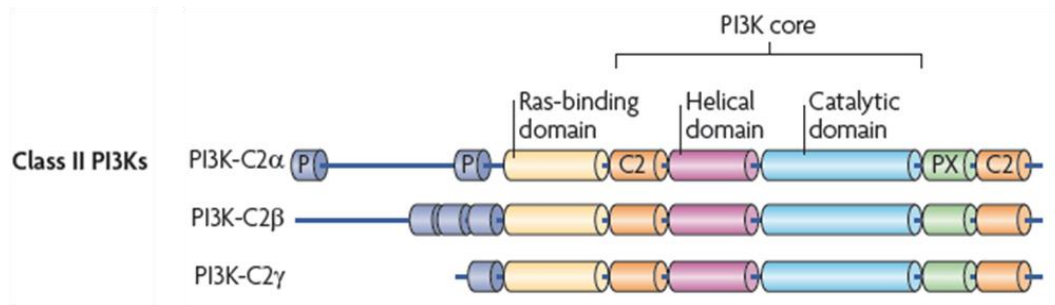


**Figure 1.4: Schematic structure of class II PI3Ks (Vanhaesebroeck et al. 2010)**

### Class III

Vacuolar protein sorting 34 (Vps34) was first discovered in yeast. It is the only member of class III PI3K and its sequence is conserved from unicellular organisms to plants and vertebrates (Backer 2008). Mammals ubiquitously express its homologue,

the protein hVps34. The enzyme associates with a subunit of 150 kDa (in yeast Vps15, in humans hVps15, Figure 1.5) that possesses kinase activity required for Vps34 function (Foster et al. 2003), although its precise role is not fully understood (Backer 2008). Class III PI3K hVps34 is implicated in endosomal trafficking, phagocytosis and autophagy (Vanhaesebroeck et al. 2010). It can only phosphorylate PtdIns both *in vitro* and *in vivo*, and it is generally accepted that this isoform is responsible for the majority of the intracellular pool of PtdIns3P (Vanhaesebroeck and Waterfield 1999, Falasca and Maffucci 2007).

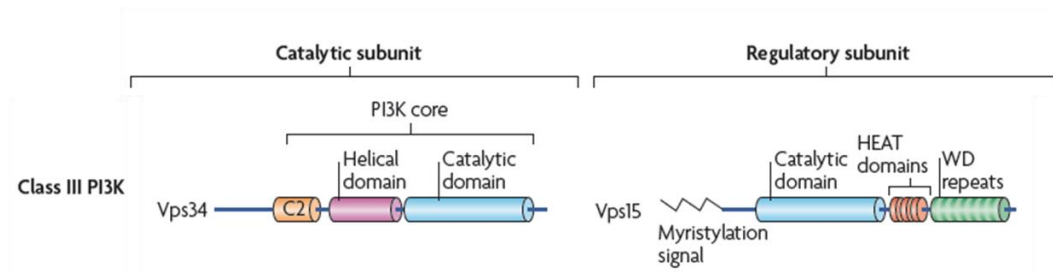


**Figure 1.5: Schematic structure of class III PI3Ks (Vanhaesebroeck et al. 2010)**

### 1.1.3 Physiological roles of PI3K in insulin target cells

Following food consumption, glucose blood concentration rises, and this stimulates the secretion of insulin by pancreatic  $\beta$  cells. Insulin in turn stimulates glucose uptake in insulin target tissues, mainly skeletal muscle and adipocytes, and reduces hepatic gluconeogenesis (Muioio and Newgard 2008, Foukas and Withers 2010). The binding of insulin to its membrane receptor activates intracellular signalling

pathways that are regulated, among others, by PI3Ks, mainly by class I PI3Ks. The binding of insulin to insulin receptor (IR) results in receptor activation through autophosphorylation on tyrosine residues on its cytosolic domain. This allows recruitment and binding to the receptor of insulin receptor substrate (IRS) proteins (Figure 1.6), mainly insulin receptor substrate 1 (IRS 1) in skeletal muscle and adipocytes, and insulin receptor substrate 2 (IRS 2) in liver (Taniguchi et al. 2006). Upon tyrosine phosphorylation by the activated IR, IRS can bind SH2 domain-containing proteins, including the regulatory subunits of class IA PI3K. Recruitment of the regulatory subunit leads to the activation of PI3K and synthesis of the lipid second messenger  $\text{PtdIns}(3,4,5)\text{P}_3$ . Enzymes like Akt and PDK1, which possess a PH domain, are then able to bind  $\text{PtdIns}(3,4,5)\text{P}_3$  and become activated (Saltiel and Kahn 2001).

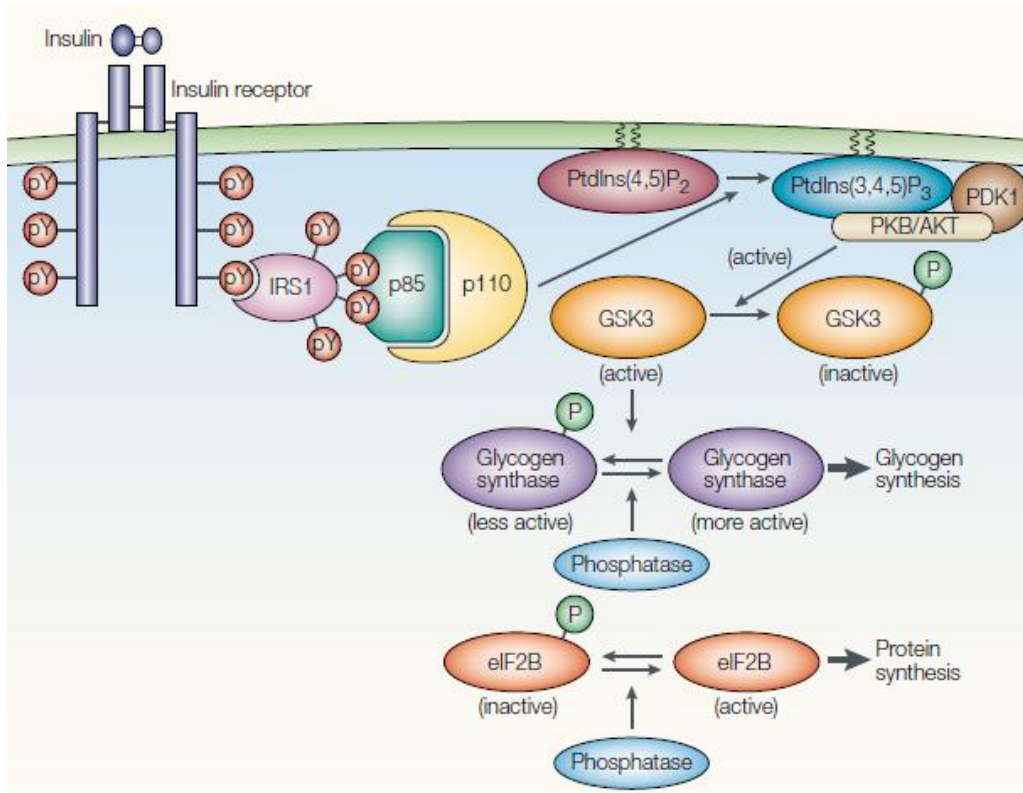


**Figure 1.6: Activation of class I PI3Ks signalling pathway upon insulin stimulation. Main molecules involved in the intracellular signalling of insulin (Cohen and Frame, 2001).**

Activated Akt is able to modulate several processes through its many downstream targets. For instance, Akt can regulate glucose uptake and storage in insulin sensitive tissues by increasing the number of glucose transporters (GLUT) at the plasma membrane. GLUT family comprises 14 proteins, which are involved in the transport of glucose against its concentration gradient. They are membrane-associated proteins, which possess 12 transmembrane domains. GLUT isoforms differ between them for their affinity to glucose and their tissue distribution (Bogan 2012). The isoform GLUT4 has a very high affinity for glucose and it is the predominant isoform in adipose and muscle tissues. It is stored on the membrane of intracellular vesicles

in unstimulated conditions. Insulin stimulates the translocation and fusion to the plasma membrane of GLUT4-containing vesicles, allowing the internalisation of glucose and its removal from the bloodstream.

In the final steps of GLUT4 translocation, fusion of GLUT4-containing vesicles to the plasma membrane occurs. This process involves soluble N-ethylmaleimide-sensitive factor attachment protein receptor (SNARE) proteins, which facilitate GLUT4 integration into the plasma membrane. Specifically, the vesicle-associated SNARE vesicle-associated membrane protein 2 (VAMP2) and the membrane-associated SNAREs syntaxin 4 and synaptosomal-associated protein of 23 kDa (SNAP23) are required for GLUT4 fusion to the plasma membrane, which leads to glucose internalisation in skeletal muscle cells (Jewell et al. 2011). The steps of the complex process of GLUT4 translocation are schematically represented in Figure 1.7.

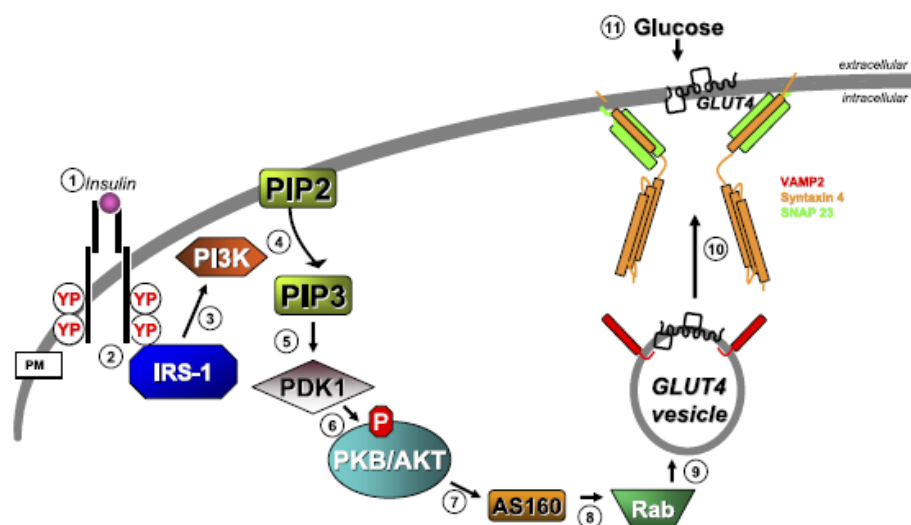


**Figure 1.7: Glucose uptake via insulin-stimulated GLUT4 translocation and fusion in muscle and adipose tissues. Numbers indicate sequential steps of the process (Jewell et al. 2010).**

GLUT4 translocation is a very complex process that requires several proteins. Among these, the PI3K/Akt pathway plays a central role. Specifically, Akt phosphorylates and activates Akt substrate of 160 kDa (AS160), and it was shown that insulin-induced phosphorylation of AS160 was associated with GLUT4 translocation in 3T3-L1 adipocytes (Sano et al. 2003). AS160 can indeed regulate the activation of Rab proteins, which facilitate intracellular trafficking of GLUT4 vesicles and their docking to the plasma membrane (Jewell et al. 2011). However, it is worth mentioning that while activation of class I PI3K/Akt signalling is necessary for GLUT4 translocation, it is not sufficient and evidence suggested that other signalling pathways are also required for glucose uptake (Czech and Corvera 1999). For instance, it has been demonstrated that GLUT4 translocation also requires the activation of the small GTP-binding protein TC10 (Chiang et al. 2001) and the synthesis of the lipid second messenger PtdIns3P (Maffucci et al. 2003). Specifically, a key role for class II PI3K-C2 $\alpha$  has been demonstrated and this will be discussed later in this chapter.

Once glucose is internalised by the cells, it is converted into glycogen, ensuring long-term storage of energy supplies within the cells. This process requires the phosphorylation of glycogen synthase kinase 3 (GSK3), the first physiological substrate identified for Akt (Figure 1.6). Phosphorylation of GSK3 by Akt has an inhibitory effect, preventing GSK-mediated phosphorylation of its substrate glycogen synthase, a crucial process for the conversion of glucose into glycogen in muscle cells and liver (Cross et al. 1995).

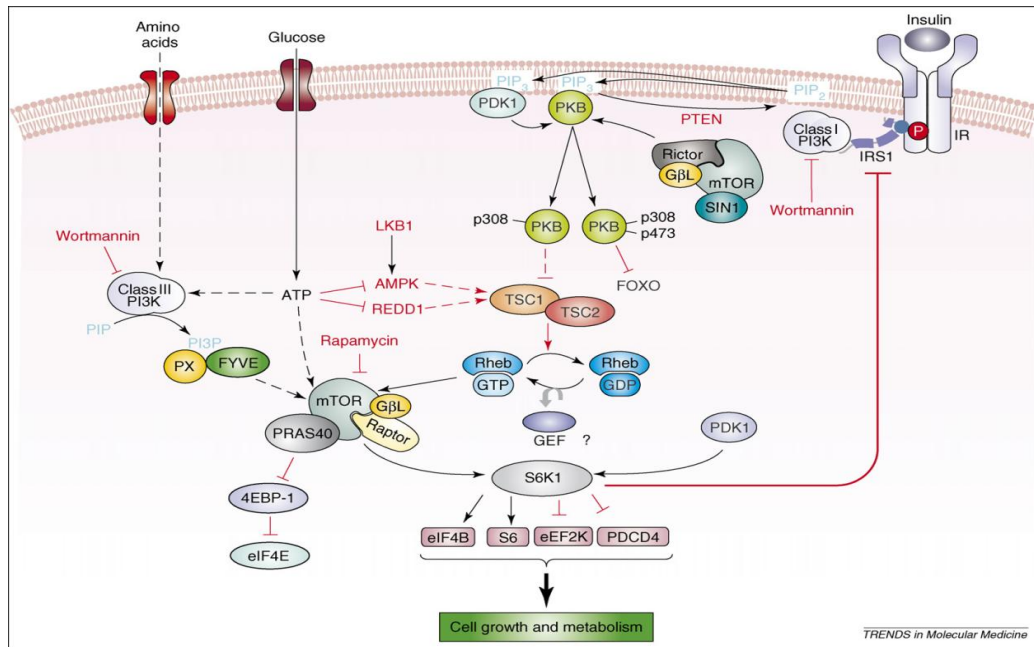


**Figure 1.8: Schematic representation of the intracellular pathways triggered in insulin target cells. Arrows indicate activation, whereas blunt-end lines indicate inhibition. The resulting positive or negative regulation is indicated by black and red colours, respectively (Dann et al. 2007).**

In addition, PI3K/Akt signalling modulates lipogenic and adipogenic processes, and the release of leptin in adipocytes in response to insulin stimulation (Mannaa et al. 2013). Specifically, it was reported that pharmacological inhibition of PI3K-dependent pathway inhibited adipocytes differentiation (Tomiyama et al. 1995, Cho et al. 2004) and prevented the accumulation of lipid droplets in 3T3-L1 adipocytes (Cho et al. 2004).

Akt can further control cell metabolism by regulating the winged helix or forkhead (FOXO) class of transcription factors (Figure 1.8), some of which have a role in insulin signalling. For instance, activation of PI3K/Akt signalling in liver cells can inhibit the



transcription of gluconeogenic enzymes, such as phosphoenolpyruvate carboxykinase and glucose-6-phosphatase, which results in the inhibition of hepatic glucose production (Engelman et al. 2006).

#### **1.1.4 Physiological roles of PI3K in insulin producing cells**

The endocrine region of pancreas is organised in clusters of cells called islets of Langerhans, named after the German pathologist who discovered them around 150 years ago. There are ~1 million pancreatic islets in a human pancreas, representing 1-2% of its total mass, and they comprise different types of cells. The most important pancreatic endocrine cells are the glucagon-releasing pancreatic  $\alpha$  cells (35–40% of pancreatic human islets), the insulin-secreting pancreatic  $\beta$  cells (50%) and the somatostatin-releasing  $\delta$  cells (10–15%) (Rorsman and Braun 2013). The function of endocrine pancreas is essential for glucose metabolism and regulation of glycaemia. In physiologic conditions, pancreatic  $\beta$  cells respond to increased glucose levels in the bloodstream by releasing insulin. Specifically, glucose enters pancreatic  $\beta$  cells via the specific transporters of the GLUT family constitutively present on the plasma membrane. In particular, the subtype GLUT2 allows glucose uptake in rodent pancreatic  $\beta$  cells, while GLUT1 and GLUT3 have this function in humans (McCulloch et al. 2011, Rorsman and Braun 2013, Bernal-Mizrachi et al. 2014). This process is schematically represented in Figure 1.9 (step 1). Glucose is then metabolised, through glycolysis and Krebs cycle, resulting in

adenosine triphosphate (ATP) production (Figure 1.9, step 2). The first step of this process is the phosphorylation of glucose to glucose-6-phosphate catalysed by the enzyme glucokinase (GK), and this conversion is the rate limiting step of the biochemical reaction. The subsequent increase of ATP/ADP ratio closes the ATP-sensitive  $K^+$  channels, causing the depolarisation of the plasma membrane and opening of the voltage-gated  $Ca^{2+}$  channel (Figure 1.9, steps 3, 4, 5). Intracellular concentration of  $Ca^{2+}$  subsequently increases and this event triggers the exocytosis of insulin granules, in a mechanism still not fully understood (Figure 1.9, steps 6, 7) (Jewell et al. 2011). The proteins involved in insulin granules exocytosis belong to the SNARE family, and specifically the isoforms syntaxin 1 and synaptosomal-associated protein of 25 kDa (SNAP25) on the plasma membrane and VAMP2 on the insulin granule form a complex that allows insulin exocytosis (Rorsman and Braun 2013).

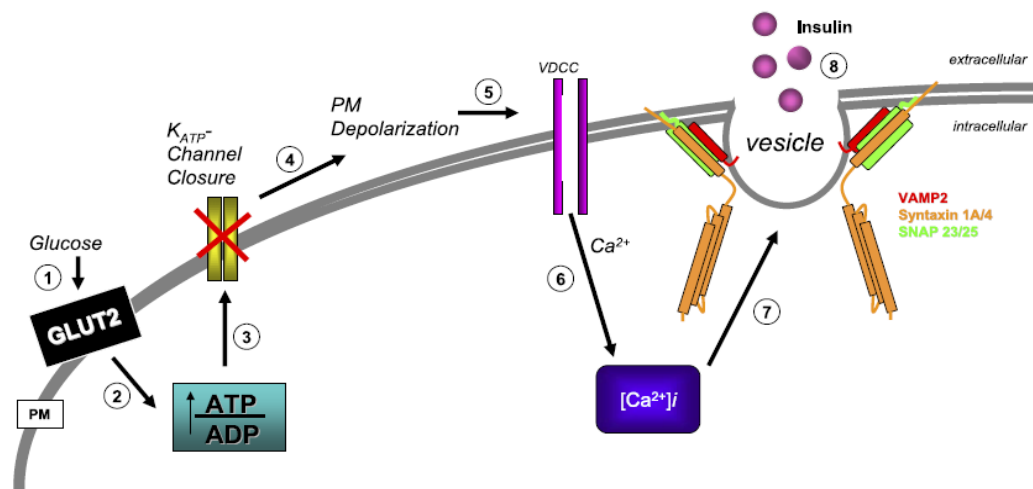


**Figure 1.9: Mechanism of insulin granules exocytosis upon glucose stimulation in pancreatic  $\beta$  cells. Numbers indicate sequential steps of the process (Jewell et al. 2010).**

Insulin exocytosis follows a biphasic time course, comprising a rapid first-phase secretion (15 insulin granules secreted/min in humans) which is induced ~5 min after glucose increase in the bloodstream, followed by a slower second-phase secretion (5 granules/min) (Rorsman and Braun 2013). Insulin granules in pancreatic  $\beta$  cells form distinct functional pools, based on their competence and their proximity to the plasma membrane. It was thought that insulin granules in close proximity to the plasma membrane formed a 'ready releasable pool' that was involved in the first phase of insulin secretion. According to this model, when this pool was depleted new granules were recruited and docked to the plasma membrane, accounting for the slower second phase of insulin release (Rorsman and Braun 2013). More recently, this model has been challenged by evidence suggesting that both first and second phase of insulin release rely on the recruitment, docking and immediate fusion of granules to the plasma membrane. This hypothesis is based on data obtained with total internal reflection fluorescence (TIRF) microscopy, that allows observation of events within the first 100–200 nm to the plasma membrane, and on intracellular signalling similarities between first and second phase of insulin release, which suggested that the late phase is probably a reiteration of the first. However, more studies are required to fully elucidate these mechanisms (Prentki et al. 2013, Rorsman and Braun 2013).

PI3Ks have a well established role in pancreatic  $\beta$  cells, as they are involved in the regulation of both pancreatic  $\beta$  cell mass and function. It was shown that mRNA of all members of class I and II PI3Ks was expressed in human islets of Langerhans,

along with members of class I PI3K signalling cascade, such as IR-A, IR-B, IRS1, IRS2, PDK1 and Akt. Even more important is the finding that the mRNA coding for the aforementioned proteins was expressed specifically in human pancreatic  $\beta$  cells (Muller et al. 2006), which suggests a relevant role of PI3K-dependent signalling in this specific cell type.

#### *Pancreatic $\beta$ cell mass*

The class I PI3K/Akt pathway has a crucial role in cell proliferation (increase in cell number), cell survival (protection from death) and cell growth (increase in cell size). For instance, Akt is able to control cell proliferation by modulating cell cycle progression. Specifically, Akt is able to stabilise the proteins c-Myc and cyclin D1 through inhibition of GSK3, and to promote the transition from G1 to S phase, by blocking the transcription of cell cycle inhibitors regulated by FOXO (Engelman et al. 2006, Marchetti et al. 2008).

In addition, Akt can regulate cell survival through inhibition of apoptotic processes. Apoptosis is a type of programmed cell death, used by multicellular organisms to eliminate unwanted or damaged cells in a diversity of settings. During apoptosis, cells are dismantled in a controlled way, minimising the damage to the neighbouring cells (Taylor et al. 2008). This cellular process is finely regulated by a number of antiapoptotic (BCL2, BCL-XL) and proapoptotic (BAD, BAK, PUMA) proteins. Activated Akt can inactivate the proapoptotic protein BAD by direct

phosphorylation, and therefore inhibiting the initiation of apoptotic processes (Figure 1.10).

Furthermore, apoptosis involves activation of the caspase family of proteases, which normally exist as inactive precursor enzymes (zymogens) in healthy cells. Once they are activated, they can initiate the apoptotic process (isoforms 8 and 9) and modulate the proteasome proteolysis once the apoptotic process is triggered (Taylor et al. 2008). In addition, it was reported that Akt can directly phosphorylate and inhibit caspase 9, therefore preventing apoptosis (Figure 1.10).

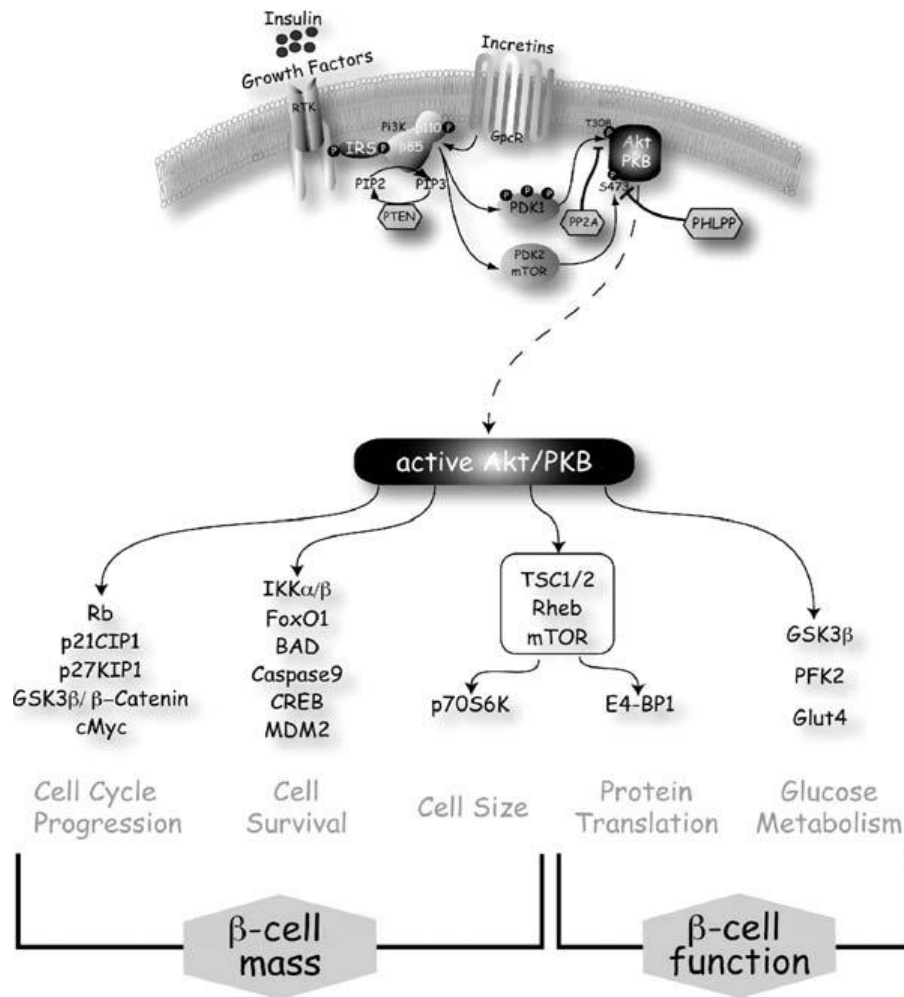


**Figure 1.10: Schematic representation of Akt signalling downstream of class I PI3K in pancreatic β cells. Akt is a signalling hub, able to regulate both pancreatic β cell mass and function (Elghazi 2007).**

Furthermore, Akt regulates the activation of mTOR, a key enzyme that is conserved through evolution and has a critical role in cell growth and proliferation (Huang and Manning 2008, Blandino-Rosano et al. 2012). The kinase core of mTOR can associate with several other proteins, forming two large complexes (1 MDa) named mTORC1 and mTORC2. Both mTOR complexes comprise mammalian lethal with Sec13 protein 8 (mLST8) and DEP domain-containing mTOR-interacting protein (DEPTOR). The

presence of other adaptor proteins distinguishes the two mTOR complexes: mTORC1 associates with the regulatory-associated protein of mTOR (raptor) and proline-rich Akt substrate of 40 kDa (PRAS40), while rapamycin insensitive companion of mTOR (rictor), mammalian stress-activated map kinase-interacting protein1 (mSin1) and protein observed with rictor (protor)1/protor2 are found in mTORC2 (Mavrommati and Maffucci 2011, Lamming and Sabatini 2013).

A very simplified representation of PI3K/Akt/mTOR signalling pathway is presented in Figure 1.11. Activated Akt can inhibit the tuberous sclerosis complex (TSC1/TSC2). The function of TSC1 is to stabilise the other subunit TSC2, preventing its degradation. Direct phosphorylation of TSC2 by different proteins results in enhanced or reduced activity of the TSC1/TSC2 complex, depending on the specific site of phosphorylation. For instance, Akt phosphorylates TSC2 on multiple residues, and studies using phosphorylation-site mutants of TSC indicated that Akt activity results in inhibition of the TSC1/TSC2 complex (Huang and Manning 2008). Specifically, Akt-dependent phosphorylation of TSC2 prevents the GTPase activity of the complex towards the protein Ras homolog enriched in brain (Rheb), allowing the accumulation of GTP-bound Rheb which in turn activates mTORC1 (Engelman et al. 2006). On the other hand, activated AMP-Activated Protein Kinase (AMPK) can directly phosphorylate TSC2 on Ser1345 and Thr1227, resulting in the activation of TSC2 and inhibition of mTORC1 (Inoki et al. 2003, Huang and Manning 2008).

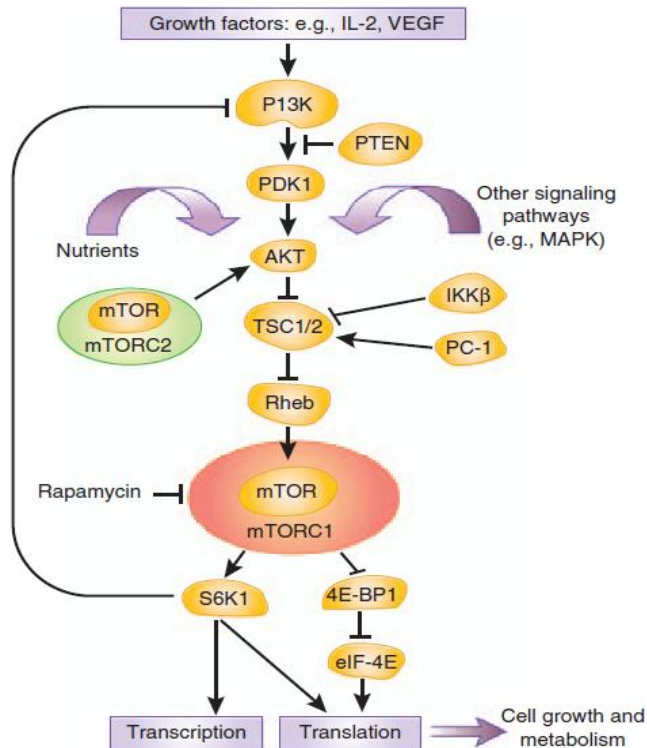


**Figure 1.11:** Schematic representation of PI3K/Akt/mTORC1 signalling pathway. PI3K-dependent stimulation of mTOR contributes to the regulation of cell growth and metabolism (Geissler and Schlitt 2010).

Once activated, mTOR can regulate several cellular functions that are crucial for pancreatic  $\beta$  cells. For instance, mTORC1 can induce phosphorylation of eIF4E binding proteins (4EBPs), releasing the eukaryotic translation initiation factor 4E which can then associate to the multisubunit complex that recruits 40S ribosomal subunits to the 5' end of mRNAs. This allows protein translation initiation, the rate limiting step process of protein synthesis (Figure 1.11), which is under strict control in eukaryotic cells (Modrak-Wojcik et al. 2013). The mTOR-dependent activation of protein translation results in the expression, among others, of proteins promoting cell cycle progression (Xie and Herbert 2012). Another downstream target of



mTORC1 is the protein S6K, which in turn phosphorylates several substrates. The most studied is ribosomal protein S6 (S6), which positively regulates  $\beta$  cell growth. However, it cannot be excluded that S6K-dependent functions in  $\beta$  cells are mediated by other targets of S6K, such as the eukaryotic elongation factor 2 (eEF2), eukaryotic initiation factor 4B (eIF4B) and programmed cell death protein 4 (PDCD4). Other mTORC1 targets include transcription factor 3C (TFIIIC), which regulates ribosome and tRNA biogenesis (Xie and Herbert 2012).

In addition, mTORC1 can negatively regulate autophagy, by modulating the initial steps of this intracellular process. Autophagy is a cellular process through which the recycling of cellular proteins and organelles is ensured, allowing *de novo* protein synthesis (Mazza and Maffucci 2014). Basal autophagy (often referred to as 'constitutive' autophagy) occurs in many cell types and it is crucial to maintain cellular homeostasis, ensuring the removal of protein aggregates, ubiquitinated proteins, damaged organelles (i.e. mitochondria and ribosomes) (Fujitani et al. 2010, Mazza and Maffucci 2014). Also, autophagy is important during starvation, allowing the cells to recycle existing macromolecules to sustain energy requirements and to maintain neosynthesis of essential proteins and glucose. This process is often termed as 'adaptive' or 'protective' autophagy (Mazza and Maffucci 2014). Autophagy is emerging as a key process in maintaining pancreatic  $\beta$  cell homeostasis. Impairment of autophagy in pancreatic  $\beta$  cells resulted in mitochondrial dysfunction, oxidative stress (Wu et al. 2009), degeneration of

pancreatic islets (Ebato et al. 2008) and decreased  $\beta$  cell mass, due to both reduced proliferation and increased apoptosis (Jung et al. 2008) in mice models.

The complex formed by Unc-51-like kinase 1 (ULK1), autophagy-related gene 13 (ATG13) and focal adhesion kinase family-interacting protein of 200 kDa (FIP200) is essential in the initial stages of autophagy and it is regulated by mTOR. Evidence indicate that overexpression of an inactive form of mTOR, rapamycin treatment or nutrient starvation inhibited phosphorylation of ULK1 and ATG13, activating ULK1-ATG13-FIP200 complex and promoting autophagy (Ganley et al. 2009, Hosokawa et al. 2009). Specifically, mTORC1 was associated with the complex ULK1-ATG13-FIP200 when HEK cells were cultured in complete medium, and mTORC1 component Raptor directly interacted with ULK1. Nutrient starvation caused the dissociation of the two complexes, inhibited ULK1 and ATG13 phosphorylation and promoted autophagy (Hosokawa et al. 2009).

Class I PI3K/Akt/mTORC1 axis integrates signals from nutrients and growth factors and is one of the most important intracellular signalling pathways in the regulation of  $\beta$  cell proliferation/survival, because of its crucial effect on pancreatic  $\beta$  cell mass and protein translation. Its key role in pancreatic  $\beta$  cell homeostasis has been confirmed by mouse models. For instance, knockout mice model for S6K isoforms have indicated its crucial role in the regulation of pancreatic  $\beta$  cell mass. Deletion of both S6K 1 and S6K 2 caused perinatal lethality in mice, while the knockout of S6K 1 alone produced a more severe phenotype compared to the knockout of S6K 2.

Specifically, S6K 1 deficient mice were smaller at birth compared to both S6K 2 deficient mice and wild type controls, and had reduced levels of circulating insulin. The observation of their phenotype suggested a preponderant role for S6K 1 over S6K 2 in the regulation of pancreatic  $\beta$  cell mass and function, as it appeared that S6K 1 is able to compensate for the lack of S6K 2 isoform but not vice versa (Pende et al. 2004). Interestingly, mice deficient for S6K 1 showed a selective decrease in pancreatic  $\beta$  cell mass and an impaired glucose-induced insulin secretion. This was not caused by defects in glucose sensing or insulin production, and it was due to a reduction in pancreatic endocrine mass, and specifically due to a selective decrease in  $\beta$  cell size (Pende et al. 2000). These observations supported the conclusion that mTOR has a key role in regulation of pancreatic  $\beta$  cell mass. Whether class I PI3Ks are the only PI3K isoforms able to activate mTOR remains to be established.

In this respect, a role for class III PI3K in regulating mTORC1 has been reported. Indeed, overexpression of hVps34 or the presence of inhibitory anti-hVps34 antibodies were able to positively or negatively regulate S6K activation, respectively. In the same study, the authors proposed that amino acid or glucose starvation and activation of AMPK were able to regulate mTORC1 activation through class III PI3K, while the involvement of hVps34 in insulin stimulated pathway was ruled out (Byfield et al. 2005). Interestingly, the presence of a FYVE domain sequestering PtdIns3P inhibited insulin-stimulated activation of S6K (Byfield et al. 2005), clearly suggesting the involvement of a PtdIns3P-producing enzyme upstream of mTORC1/S6K. More recently, it was suggested that class II PI3K-C2 $\alpha$  had a role in

mTORC1 and S6K activation, by producing PtdIns3P upon stimulation with insulin. Interestingly, evidence indicated that Akt pathway upstream of mTOR was not involved (Bridges et al. 2012).

### *Pancreatic $\beta$ cell function*

More recent lines of evidence suggest that, besides its key role in the regulation of pancreatic  $\beta$  cell mass, class I PI3Ks can also be directly involved in control of pancreatic  $\beta$  cell function. For instance, it was shown that knockdown of Akt target AS160 in both MIN6 cells and primary mouse  $\beta$  cells increased insulin secretion in unstimulated conditions, while glucose-induced insulin release was abolished (Bouzakri et al. 2008). Also, using specific knockout mice models lacking the regulatory subunits of class I PI3Ks in  $\beta$  cells ( $\beta$ DKO mice), it has been shown that PI3K signalling is crucial for maintaining  $\beta$  cell function (Kaneko et al. 2010). The authors reported that inhibition of class I PI3K signalling pathway resulted in an impaired glucose-induced insulin secretion in this mice model. Consistent with this, isolated islets from either  $\beta$ DKO mice or mice lacking the regulatory subunit p85 $\alpha$  alone, displayed impaired KCl-induced insulin secretion. In addition, the authors reported decreased protein expression of SNAREs involved in insulin secretion, which might account, at least in part, for the impaired exocytosis (Kaneko et al. 2010).

Similarly, homozygous knockout for p110 $\gamma$  showed impaired glucose-induced insulin secretion both *in vivo* and in *ex vivo* perfused pancreas (MacDonald et al. 2004). In this study, insulin exocytosis was impaired, despite greater pancreatic insulin content and compensatory hypertrophy of pancreatic  $\beta$  cells. This indicated that the isoform p110 $\gamma$  has a role specifically in insulin secretion while it does not regulate pancreatic  $\beta$  cell mass. This suggest that the role and the intracellular signalling activated by p110 $\gamma$  is different from other class I PI3K isoforms. Subsequently, the role of p110 $\gamma$  in pancreatic  $\beta$  cells was investigated using specific inhibitors and downregulation of p110 $\gamma$  with siRNA in INS1 cells (Pigeau et al. 2009). Results indicated that insulin secretion induced by depolarisation was modulated by p110 $\gamma$ , as this enzyme regulates the recruitment of the insulin granules pool associated to the plasma membrane in both INS1 cell lines and human pancreatic islets (Pigeau et al. 2009).

### **1.1.5 Dysregulation of PI3K signalling pathway and type 2 diabetes**

As discussed so far PI3Ks, mainly class I isoforms, have a central role in regulation of insulin action and production. Several lines of evidence indicate that deregulation of PI3K pathway is associated with the onset and progression of metabolic diseases such as T2D.

### *Type 2 diabetes*

Diabetes is the most common metabolic disease, with 382 million people affected worldwide in the year 2013 and the prediction that the number of affected people will rise to 592 million by 2035 (Guariguata et al. 2014). It is characterised by impaired glucose handling in response to a physiological stimulus to produce insulin. The molecular mechanisms involved in T2D development and progression are at the level of both insulin target tissues and insulin producing tissues. Individuals affected by T2D show impaired insulin signalling in insulin target tissues (i.e. muscle cells, adipose tissue, liver), with a defective response in terms of blood glucose uptake and storage. In physiological conditions, insulin is produced by pancreatic  $\beta$  cells in response to a rise in blood glucose levels. When insulin signalling is impaired in target tissues, glucose is not adequately removed from the bloodstream and internalised in muscle and fat cells. This stage is termed 'insulin resistance' and it is temporarily compensated through increased insulin secretion, either by increased pancreatic  $\beta$  cell mass or increased  $\beta$  cell efficiency (Bonner-Weir 2000). It was originally thought that insulin resistance always preceded pancreatic  $\beta$  cell dysfunction and full blown diabetes, but more recent studies have shown that this paradigm is not always true (Bartolome and Guillen 2014). Indeed, in the UK Prospective Diabetes Study it was observed that pancreatic  $\beta$  cell function was already reduced by 50% in patients at the time of diagnosis and it progressively declined regardless of the therapy used (U.K. prospective diabetes study 16, 1995). Nevertheless, the state of insulin resistance often accompanies the diabetic

condition and it is considered a major risk factor for T2D (Taylor 2012). It is now generally accepted that T2D appears when pancreatic  $\beta$  cells are no longer able to compensate, either because insulin resistance exceeds insulin production capacity, or because of a decline in their function ( $\beta$  cell failure) (Bartolome and Guillen 2014). This causes the progression to overt diabetes, which is characterised by reduced pancreatic  $\beta$  cell function, and reduced pancreatic  $\beta$  cell mass and viability (Butler et al. 2003, Muoio and Newgard 2008).

The loss of pancreatic  $\beta$  cell mass and viability can be ascribed, at least in part, to the elevated circulating levels of glucose and free fatty acids (FFA), typical of the diabetic condition (Barlow and Affourtit 2013). Indeed, the metabolic deregulation caused by T2D leads to impaired handling of glucose and fatty acids, which subsequently circulate at higher levels in the bloodstream. Several lines of evidence suggested that increased glucose and FFA levels are toxic and induce apoptosis, and they are one of the main factors contributing to the decrease of  $\beta$  cell mass (Lee et al. 1994, McGarry 2002, El-Assaad et al. 2003). These toxic effects on cell viability are defined as glucotoxicity, lipotoxicity and glucolipotoxicity. It was observed that pancreatic  $\beta$  cell mass mainly decreases because of increased apoptosis in diabetic subjects (Butler et al. 2003). Interestingly, recent lines of evidence indicated a crucial role for autophagy in the regulation of  $\beta$  cell mass and function. For instance, using mice models, it has been shown that genetic impairment of autophagic processes in pancreatic  $\beta$  cells results in glucose intolerance (Ebato et al. 2008, Jung et al. 2008). Also, these mice showed decreased  $\beta$  cell mass and pancreatic insulin content and

lower fasting serum insulin concentration, which suggested a crucial role for autophagy in pancreatic function (Jung et al. 2008). In addition, analysis of human islets of diabetic patients indicated that 50% of  $\beta$  cells showed signs of autophagy-associated cell death (Masini et al. 2009). Due to the key role of PI3K in regulation of pancreatic  $\beta$  cell mass, survival and autophagy, it is not surprising that alterations of PI3K pathway have been detected in diabetes.

#### *Role of PI3K-dependent pathway in diabetes*

Analysis of mice models demonstrated that genetic manipulation of PI3K pathway could cause alteration of insulin signalling and induce T2D. It was reported that the lack of IRS1 in knockout mice retards growth and causes mild insulin resistance but overt diabetes does not develop. Specifically, IRS1 knockout mice were able to compensate the impaired insulin signalling by increasing pancreatic  $\beta$  cell mass and increasing the secretion of insulin. This indicated that other IRS isoforms are able to compensate in insulin signalling for IRS1 absence. On the other hand, the lack of IRS2 causes overt diabetes in knockout mice, because of their selective decrease in  $\beta$  cell mass (Withers et al. 1998). Importantly, this was already observed in newborn mice and therefore it was not the consequence of a metabolic phenotype (Withers et al. 1998).

Homozygous knockout of p110 $\alpha$  or p110 $\beta$  are lethal in embryo (Bi et al. 1999, Bi et al. 2002). Mice with heterozygous loss of p110 $\alpha$  or p110 $\beta$  showed no impairment in



insulin signalling, while the double heterozygous  $p110\alpha^{+/-} p110\beta^{+/-}$  had a mild defect in insulin response, namely a slight glucose intolerance and hyperinsulinemia in fasting state (Brachmann et al. 2005), suggesting a complementary role of the two isoforms. Nevertheless, several studies supported the conclusion of a predominant role for p110 $\alpha$  in insulin response: chemical inhibitors of p110 $\alpha$  (but not of p110 $\beta$  or p110 $\delta$ ) have been shown to prevent insulin-induced phosphorylation of Akt in 3T3 adipocytes and L6 myotubes, and to decrease insulin sensitivity and glucose transport in mice (Knight et al. 2006). Mice with homozygous mutation inactivating p110 $\alpha$  kinase activity died in embryo (E10-11), while heterozygous mice carrying this mutation were viable and showed impaired insulin signalling, with insulin resistance and glucose intolerance (Foukas et al. 2006). On the other hand, homozygous inactivation of p110 $\beta$  kinase activity in mice did not always result in embryonic lethality. Specifically, homozygosity for a catalytically inactive form of p110 $\beta$  caused embryonic lethality with incomplete penetrance, as the number of viable mice was lower than expected. In addition, heterozygous mice displayed only mild increase in blood glucose (Ciraolo et al. 2008).

Selective knockout models for Akt isoforms have also been developed. Global knockout of Akt2 in mice models caused metabolic effects such as hyperglycemia and compensatory hyperinsulinemia, and impaired repression of gluconeogenesis in the liver (Cho et al. 2001).

Taken together, data from mice models indicated that deregulation of PI3K pathway can impair insulin signalling and pancreatic  $\beta$  cell function and lead to T2D. Deletion of mTORC1 downstream effector 4EBP1 increased ER-stress-induced susceptibility to apoptosis in MIN6 cells and decreased insulin secretion and pancreatic insulin content in mice models fed a high fat diet. In the same study, the authors reported that deletion of 4EBP1 in diabetic mice models accelerated  $\beta$  cell loss and decreased protein synthesis, suggesting a deregulated translational control under ER stress conditions (Yamaguchi et al. 2008).

Importantly, evidence of deregulation of PI3K pathway in T2D has also been reported. For instance, human islets carrying the Arg972 polymorphism of IRS1, which has been associated with T2D, showed reduced insulin secretion, reduced number of insulin granules and increased apoptosis following serum deprivation (Marchetti et al. 2002, Marchetti et al. 2008). Moreover, studies on the db/db mouse model (a well established mouse model of obesity-induced diabetes) showed that insulin secretion is impaired, probably through downregulation of class I PI3K/Akt pathway (Kaneko et al. 2010). Specifically, the authors showed that plasma insulin levels are transiently increased in this diabetic mice model, along with the expression of regulatory subunits of class I PI3K, p110 $\alpha$ , insulin receptor and IRS2, only to subsequently decline in a later stage marked by insulin deficiency. In addition, it was demonstrated that the downstream effector of Akt AS160, is expressed in human islets, and it is phosphorylated in human islets and primary mouse  $\beta$  cells following glucose stimulation and activation of Akt (Bouzakri et al.

2008). Importantly, AS160 expression was decreased in type 2 diabetic subjects and this can be associated with reduced  $\beta$  cell function, since knockdown of AS160 impairs glucose-induced insulin secretion, increases apoptosis and decreases proliferation in both MIN6 cells and primary mouse  $\beta$  cells (Bouzakri et al. 2008).

## 1.2 PI3K-C2 $\alpha$

Human PI3K-C2 $\alpha$  was first cloned from the cell line U937. Studies showed a wide tissue distribution of the mRNA encoding for PI3K-C2 $\alpha$ , with the highest levels of expression found in the heart, placenta and ovary (Domin et al. 1997). As the other class II PI3K isoforms, PI3K-C2 $\alpha$  lacks the regulatory subunit binding domain. Class II PI3Ks differ between them for the N-terminus extension; specifically, PI3K-C2 $\alpha$  possesses a clathrin-binding region in its N terminus domain (Mazza and Maffucci 2011). One of the specific features of PI3K-C2 $\alpha$  is its low sensitivity to classical PI3K inhibitors wortmannin and LY294002 (Domin et al. 1997), which has been used as a tool to identify the involvement of this specific isoform in biological processes.

### 1.2.1 Activation of PI3K-C2 $\alpha$

One of the first studies on PI3K-C2 $\alpha$  *in vivo* activation reported that the enzyme was activated by insulin in the insulin-responsive cell lines Chinese hamster ovary cells expressing insulin receptor (CHO-IR), L5L6 myotubes, and 3T3-L1 adipocytes but not in 3T3-L1 preadipocytes, undifferentiated L5L6 myoblasts, or HEK 293 cells (Brown et al. 1999). Consistent with this, insulin-induced activation of PI3K-C2 $\alpha$  was also reported in intact rat skeletal muscle, suggesting the involvement of PI3K-C2 $\alpha$  in insulin signalling in a central insulin-responsive tissue (Soos et al. 2001). Subsequently, work from our laboratory showed that insulin stimulation of L6 muscle cells was able to activate PI3K-C2 $\alpha$  through TC10 (Maffucci et al. 2003), a

small GTPase which has been implicated in insulin-dependent GLUT4 translocation to the plasma membrane (Chiang et al. 2001). Further investigation revealed that PI3K-C2 $\alpha$  translocated to the plasma membrane of L6 cells upon insulin stimulation, promoting the synthesis of the lipid product PtdIns3P (Falasca et al. 2007). Consistent with this, PI3K-C2 $\alpha$ -like activity was observed in immunocomplexes of IR-B but not IR-A in insulin stimulated HIT-T15  $\beta$  cells. This suggested that insulin activates PI3K-C2 $\alpha$  through its association to IR-B at the plasma membrane, in a distinct mechanism compared to class I PI3Ks, which associate to IR-A (Leibiger et al. 2001). The authors further reported a codistribution of PI3K-C2 $\alpha$  and IR-B at the plasma membrane in MIN6 cells upon either insulin or glucose stimulation (Leibiger et al. 2010). In contrast with this, Brown and colleagues reported that PI3K-C2 $\alpha$  did not form a complex with the insulin receptor, since PI3K-C2 $\alpha$  and insulin receptor did not coimmunoprecipitate in insulin-stimulated CHO-IR cells (Brown et al. 1999). In this study, the authors suggested that PI3K-C2 $\alpha$  associated with two tyrosine phosphorylated proteins, one of 207 kDa and the other of 160 kDa but their identity remains unknown (Brown et al. 1999). More recently, and in a different cellular and functional context, relocalisation of PI3K-C2 $\alpha$  was also described. Specifically, it was observed that PI3K-C2 $\alpha$  translocated from the cytoplasm to plasma membrane and vesicular compartments at the periphery of the cells in HeLa cells following dynamin-independent endocytotic processes (Krag et al. 2010). Taken together, these data suggest that one of the mechanisms of PI3K-C2 $\alpha$  activation may involve its translocation to the plasma membrane, at least in certain conditions.

Since PI3K-C2 $\alpha$  lacks a regulatory subunit, different mechanisms of activation for PI3K-C2 $\alpha$  were proposed. In the original report showing an insulin-dependent activation of PI3K-C2 $\alpha$ , it was proposed that the enzyme may undergo phosphorylation, but this hypothesis was not further investigated. Specifically, Western Blot analysis showed that the enzyme PI3K-C2 $\alpha$  was detected as a single band in unstimulated cells, and as a doublet upon insulin stimulation, suggesting a post-translational modification dependent on insulin treatment (Brown et al. 1999). The fact that PI3K-C2 $\alpha$  possesses several binding domains led to the hypothesis that they could be involved in its activation. It was reported that PI3K-C2 $\alpha$  could directly bind clathrin through its N-terminal domain, and that its activity was enhanced *in vitro* in the presence of clathrin (Gaidarov et al. 2001). Also, PI3K-C2 $\alpha$  has been shown to be enriched on clathrin-coated vesicles in fibroblasts (Domin et al. 2000), whereas no detectable PI3K-C2 $\alpha$  association with clathrin-coated vesicles was found in chromaffin cells (Meunier et al. 2005). More recently, it was reported that PI3K-C2 $\alpha$  regulates clathrin-mediated endocytosis in the COS7 fibroblast-like cell line, by regulating the maturation of clathrin coated vesicles (Posor et al. 2013).

In addition, several lines of evidence reported that PI3K-C2 $\alpha$  activity was regulated by Ca<sup>2+</sup>. Specifically, kinase assay was performed on recombinant PI3K-C2 $\alpha$  immunoprecipitated from HEK cells and results showed that Ca<sup>2+</sup> was able to directly activate PI3K-C2 $\alpha$  (Wen et al. 2008). Consistent with this, the activity of PI3K-C2 $\alpha$  immunoprecipitated from de-endothelialised rabbit aortic vascular smooth muscle increased upon stimulation with KCl, noradrenaline or ionomycin, and extracellular

$\text{Ca}^{2+}$  depletion prevented the noradrenaline-induced activation of PI3K-C2 $\alpha$ . This indicated that PI3K-C2 $\alpha$  stimulation was  $\text{Ca}^{2+}$ -dependent (Wang et al. 2006). Interestingly, it was recently shown that PI3K-C2 $\alpha$  is implicated in KCl-induced insulin secretion in INS1 cells, a process dependent on intracellular  $\text{Ca}^{2+}$  increase (Dominguez et al. 2011). However, further studies are needed to determine whether  $\text{Ca}^{2+}$  alone is sufficient to induce the activation of PI3K-C2 $\alpha$  *in vivo*.

### **1.2.2 Lipid product of PI3K-C2 $\alpha$**

As reported for the other members of class II PI3K, PI3K-C2 $\alpha$  is able to phosphorylate the substrates PtdIns and PtdIns4P *in vitro*, with a strong substrate preference for PtdIns (Mazza and Maffucci 2011, Falasca and Maffucci 2012). Evidence from *in vivo* studies indicated that cells have different pools of PtdIns3P: a constitutive pool, regulated by class III PI3K and associated with intracellular endosomes, and an inducible pool which is emerging as the product of class II PI3Ks, generated at the plasma membrane (Falasca and Maffucci 2009).

Indeed, studies on L6 muscle cells and 3T3-L1 adipocytes indicated for the first time that an insulin dependent pool of PtdIns3P was synthesised at the plasma membrane of the cells, and that its synthesis was resistant to classical PI3Ks inhibitors (Maffucci et al. 2003, Falasca et al. 2007). The fact that class II PI3K-C2 $\alpha$  is the most resistant isoform among PI3Ks to treatment with classical inhibitors wortmannin and LY294002 suggested its involvement in the insulin-induced

neosynthesis of PtdIns3P (Maffucci et al. 2003). Subsequent studies showed that PtdIns3P was the sole product of PI3K-C2 $\alpha$ , through specific downregulation of PI3K-C2 $\alpha$  expression in L6 cells and analysing the levels of intracellular PIs, and the intracellular localisation of PtdIns3P (Falasca et al. 2007). Specifically, HPLC analysis showed that insulin stimulation induced synthesis of PtdIns3P, which was significantly reduced upon downregulation of PI3K-C2 $\alpha$ . No changes were detected in the insulin-stimulated levels of PtdIns(3,4)P<sub>2</sub> and PtdIns(3,4,5)P<sub>3</sub> in PI3K-C2 $\alpha$  knock down cells. Consistent with these data, it was reported that the steady-state levels of PtdIns3P were reduced in pheochromocytoma (PC12) cells expressing a catalytically inactive mutant of PI3K-C2 $\alpha$  (Meunier et al. 2005). In addition, these authors also showed that the synthesis of a pool of PtdIns3P on neurosecretory vesicles is dependent on PI3K-C2 $\alpha$  activation (Wen et al. 2008). Specifically, in this study they demonstrated that PI3K-C2 $\alpha$  knockdown or expression of a catalytically inactive mutant of PI3K-C2 $\alpha$  in PC12 cells inhibited the nicotine-induced, Ca<sup>2+</sup>-dependent production of PtdIns3P on neurosecretory vesicles, and that knockdown of PI3K-C2 $\alpha$  abolished the wortmannin-insensitive pool of PtdIns3P in PC12 cells (Wen et al. 2008). Consistent with these data, it was recently shown that simultaneous knockdown of class II PI3K-C2 $\alpha$  and PI3K-C2 $\beta$  reduced the levels of PtdIns3P, with no effect on PtdIns4P or PtdIns(4,5)P<sub>2</sub> in mouse embryonic fibroblasts (MEF) cultured in complete medium (Devereaux et al. 2013). Importantly, it has been recently observed that the total cellular content of PtdIns3P, but not of PtdIns(3,4)P<sub>2</sub>, PtdIns(3,5)P<sub>2</sub> or PtdIns(3,4,5)P<sub>3</sub>, was reduced in PI3K-C2 $\alpha$ <sup>-/-</sup> MEFs, and



that the endosomal localisation of a fluorescent PtdIns3P probe was decreased in umbilical vein endothelial cells (HUVEC) upon downregulation of PI3K-C2 $\alpha$ , but not p110 $\alpha$  or Vps34 (Yoshioka et al. 2012). Consistent with this, a very recent study using MEF with homozygous deletion for PI3K-C2 $\alpha$  confirmed the conclusion that PtdIns3P is the lipid product of this enzyme (Franco et al. 2014). Specifically, the authors reported that staining wild type MEF with a PtdIns3P-selective GFP-2XFYVE fluorescent probe or with anti-PtdIns3P antibodies revealed an intracellular pool of PtdIns3P localised at the base of the cilium, an organelle that has crucial roles in vertebrate development, regulating cell proliferation, polarity, differentiation and tissue organization. The levels of PtdIns3P at the base of the cilium was significantly reduced in PI3K-C2 $\alpha$  knockout MEF. Interestingly, the localisation of PtdIns3P detected in the rest of the cell did not show significant changes. This indicates that PI3K-C2 $\alpha$  is able to regulate a specific intracellular pool of PtdIns3P. These data were confirmed by HPLC analysis of intracellular PIs, and specifically the authors reported a significant reduction in PtdIns3P levels upon metabolic labelling of serum-starved PI3K-C2 $\alpha$ <sup>-/-</sup> MEFs, confirming the conclusion that PI3K-C2 $\alpha$  modulates the levels of a specific pool of PtdIns3P.

In contrast with these data, HPLC analysis of intracellular PIs showed that PI3K-C2 $\alpha$  specifically generated PtdIns(3,4)P<sub>2</sub> in MIN6 cells upon insulin stimulation, while no changes in the levels of PtdIns3P and PtdIns(3,4,5)P<sub>3</sub> were observed (Leibiger et al. 2010). Recently, using specific PI-binding domain based sensors and an anti-

PtdIns(3,4) $P_2$  antibody, it was reported that PtdIns(3,4) $P_2$  is synthesised by PI3K-C2 $\alpha$  in COS7 cells (Posor et al. 2013).

### **1.2.3 Functions of PI3K-C2 $\alpha$**

Studies on the intracellular functions regulated by PI3K-C2 $\alpha$  revealed that this enzyme is involved in many intracellular processes. In the past few years, it has been reported that PI3K-C2 $\alpha$  has a role in exocytotic and endocytotic processes, glucose transport and insulin secretion. Although these processes seem distinct, they share some similarities that might suggest a common mechanism of action for PI3K-C2 $\alpha$ . In addition, it was shown that PI3K-C2 $\alpha$  is able to regulate cell survival and apoptotic processes.

#### *Exocytosis/endocytosis*

Several lines of evidence indicate that PI3K-C2 $\alpha$  is involved in exocytotic processes. PI3K-C2 $\alpha$  is required for the ATP-dependent priming phase of neurosecretory granules exocytosis in chromaffin cells, in a process that requires synthesis of PtdIns3P (Meunier et al. 2005). In particular, the authors showed that neurosecretion in PC12 cells was increased by overexpression of PI3K-C2 $\alpha$ , while its catalytically-inactive mutant or expression of a probe sequestering PtdIns3P had an inhibitory effect. In a subsequent study, the authors demonstrated that knockdown of PI3K-C2 $\alpha$  inhibited the Ca<sup>2+</sup>-dependent synthesis of PtdIns3P on neurosecretory

vesicles of PC12 cells (Wen et al. 2008), confirming the role of PI3K-C2 $\alpha$  in this context.

More recent studies have also shown that PI3K-C2 $\alpha$  is required for exocytotic processes in different cellular contexts. For example, it was reported that PI3K-C2 $\alpha$  is involved in glucose-induced insulin secretion in MIN6 cells (Leibiger et al. 2010). In addition, previous work indicated that KCl-induced insulin granules exocytosis is impaired by downregulation of PI3K-C2 $\alpha$  (Dominguez et al. 2011). Specifically, it was reported that stable knockdown of PI3K-C2 $\alpha$  in the insulin secreting cell line INS1 strongly reduced KCl-induced fusion of insulin granules to the plasma membrane, without affecting the total insulin content of the cells. Moreover, downregulation of PI3K-C2 $\alpha$  also impaired proteolysis of the protein SNAP 25, an event associated with insulin secretion. As KCl stimulation specifically induces the fusion of insulin granules to the plasma membrane, these data suggested that PI3K-C2 $\alpha$  was specifically involved in the late steps of insulin exocytosis, namely the fusion of insulin containing granules to the cellular plasma membrane.

Consistent with this observation, several lines of evidence reported a role for PI3K-C2 $\alpha$  in exocytotic-like processes in different cellular contexts, supporting the hypothesis that PI3K-C2 $\alpha$  is critical for fusion events in distinct cellular contexts. In particular, in the context of insulin signalling, it was shown that downregulation of PI3K-C2 $\alpha$  in L6 muscle cells impaired GLUT4 translocation to the plasma membrane in response to insulin stimulation (Falasca et al. 2007). Also, it was shown that a

maximal GLUT4 translocation requires the synthesis of PtdIns3P at the plasma membrane.

The fusion of GLUT4 vesicles to the plasma membrane required the same family of accessory proteins involved in insulin granules fusion, and that the SNAREs machinery required in both GLUT4 translocation and insulin secretion is also similar to that implicated in neurosecretion (Jewell et al. 2010). In addition, it has recently been reported that depletion of PI3K-C2 $\alpha$  in MEF caused impaired activation of Rab11, a small GTPase member of the Rab family, which modulate delivery and docking of secretory vesicles at the base of the cilium in MEF (Franco et al. 2014). Also, results from this study showed that GFP-tagged PI3K-C2 $\alpha$  in wild type MEF was localised in vesicular structures surrounding the ciliary basal body, which is involved in primary cilium biogenesis. These results were confirmed by analysing the intracellular localisation of endogenous PI3K-C2 $\alpha$  in inner medullary collecting duct 3 (IMCD3) cells, a cell line widely used in cilium studies. The authors proposed that the loss of PI3K-C2 $\alpha$  in MEF caused Rab11 delocalisation/deactivation, which in turn impaired cilia formation, likely as a consequence of defective trafficking of ciliary components.

A role for PI3K-C2 $\alpha$  has also been reported in the context of endocytosis. Specifically, it was shown that silencing of PI3K-C2 $\alpha$  in HeLa cells reduced fluid-phase endocytosis and internalisation of diphtheria toxin, in a dynamin-independent process that did not require other PI3K isoforms (Krag et al. 2010). Similarly, it was

reported that PI3K-C2 $\alpha$  was able to modulate clathrin-mediated endocytosis. Specifically, overexpression of PI3K-C2 $\alpha$  impaired endocytosis of transferrin and clathrin-mediated membrane trafficking to plasma membrane and trans-Golgi network, without affecting the overall Golgi structure (Gaidarov et al. 2001).

### *Cell viability*

It was reported that downregulation of PI3K-C2 $\alpha$  caused decreased proliferation and increased apoptosis in HeLa cells, without affecting class I PI3K/Akt survival pathway (Elis et al. 2008). The same study analysed the viability of several normal and cancer cell lines upon downregulation of PI3K-C2 $\alpha$  and in normal growth conditions. Results indicated that the majority of the cell lines tested (21 of 23) showed decreased viability upon downregulation of PI3K-C2 $\alpha$ , and in more than a half of them (13 of 23) viability was decreased by more than 50% (Elis et al. 2008). Consistent with this, it has been recently shown that downregulation of PI3K-C2 $\alpha$  specifically induced apoptosis in HUVEC cells (Yoshioka et al. 2012, Tibolla et al. 2013). Also, downregulation of PI3K-C2 $\alpha$  mRNA in DLD1 cells caused dosage-dependent inhibition of cell growth (Schepeler et al. 2012). In contrast with these results, downregulation of PI3K-C2 $\alpha$  cells had no effect on cell proliferation in the muscle cell line L6 (Falasca et al. 2007), while only a slight increase of the percentage of cells in the sub-G1 phase of the cell cycle was observed in INS1 cells (Dominguez et al.

2011). In addition, other findings suggested that PI3K-C2 $\alpha$  has a role as survival factor. For instance, downregulation of PI3K-C2 $\alpha$  induced apoptosis in CHO-IR cell lines cultured in normal growth medium (Kang et al. 2005). Similarly, it was observed that downregulation of PI3K-C2 $\alpha$  decreased proliferation and the ability to form colonies in 3D soft agar assays and increased apoptosis of hepatocarcinoma cell line Mahlavu (Ng et al. 2009).

#### **1.2.4 Mouse models**

The first PI3K-C2 $\alpha$  null mouse model was reported in 2011 by Harris and colleagues (Harris et al. 2011). First, they generated heterozygous PI3K-C2 $\alpha$ <sup>+/-</sup> mice, which had normal size, were fertile and were intercrossed to obtain progeny carrying homozygous deletion for PI3K-C2 $\alpha$ . PI3K-C2 $\alpha$ <sup>-/-</sup> mice were viable but smaller in size compared to control mice. At 4 to 6 weeks of age, PI3K-C2 $\alpha$ <sup>-/-</sup> mice showed lower body weight and both lean and fat mass were reduced compared to control littermates. PI3K-C2 $\alpha$ <sup>-/-</sup> mice became progressively sick as they aged, and 30% of them died within 6 months of age, compared to 5% of control animals. This indicated that PI3K-C2 $\alpha$  was important for post-natal development of the animals. Analysis of blood and urine samples from animals at 6 weeks of age indicated kidney failure in PI3K-C2 $\alpha$ <sup>-/-</sup> mice. Subsequent analysis revealed that kidney damage became apparent in mice of 4 weeks of age, with glomerular leakage, proteinuria

and severe lesions to podocytes, critical components of the glomerular filtration barrier.

A second knockout model has been generated in 2012 (Yoshioka et al. 2012). The authors reported that PI3K-C2 $\alpha$ <sup>-/-</sup> genotype was lethal, as mice embryos showed retarded growth at day E8.5, and they died at day E10.5-11.5. This indicated a crucial and specific role for PI3K-C2 $\alpha$  in embryonic development. In particular, data showed that lack of PI3K-C2 $\alpha$  affected vascular development, as the major blood vessels were disorganised or absent in PI3K-C2 $\alpha$ <sup>-/-</sup> embryos. In order to further study the function of PI3K-C2 $\alpha$ , tissue specific and inducible knockout models were created. Results showed that endothelial-cell-specific PI3K-C2 $\alpha$ <sup>-/-</sup> also presented embryonic lethal phenotype, with impairment of vessels formation and development. The generation of a tamoxifen-inducible and endothelial-cell-specific PI3K-C2 $\alpha$  knockout mice allowed studying postnatal physiological angiogenesis. Evidence indicated increased apoptosis in retinas upon PI3K-C2 $\alpha$  depletion and an impairment in retinal angiogenesis, suggesting a crucial role for PI3K-C2 $\alpha$  in vascular formation. These data are consistent with the observation that downregulation of PI3K-C2 $\alpha$  impaired morphogenesis, inhibited cell survival and increased apoptosis in human endothelial cells (Tibolla et al. 2013).

More recently, global knockout for PI3K-C2 $\alpha$  was performed and the phenotype of MEF was analysed. In contrast with the mice model previously reported by Harris and colleagues, where a truncated form of PI3K-C2 $\alpha$  was still detected, in this case

the authors reported a complete ablation of PI3K-C2 $\alpha$  (Franco et al. 2014). Similarly to what observed by Yoshioka and colleagues, these authors reported that homozygous deletion of PI3K-C2 $\alpha$  caused growth defects at embryonic day 8.5 and lethality between E10.5 and E11.5. However, while Yoshioka and colleagues indicated that loss of PI3K-C2 $\alpha$  was lethal during vasculogenesis due to endothelial abnormalities, this study indicated that lethality in PI3K-C2 $\alpha$ <sup>-/-</sup> embryos was caused by defective trafficking of ciliary components, in a developmental stage preceding vasculogenesis (Franco et al. 2014).

### **1.2.5 PI3K-C2 $\alpha$ and diabetes**

The link between class I PI3Ks and human diseases such as diabetes and cancer is well established. On the other hand, much less is known about class II PI3Ks and their physiologic and pathophysiologic roles. The precise role of class II PI3K-C2 $\alpha$  remains to be understood. However, evidence suggest a potential link between PI3K-C2 $\alpha$  and T2D. Indeed, it was shown that the mRNA encoding for class II enzymes PI3K-C2 $\alpha$  and PI3K-C2 $\gamma$  was expressed in the majority of human islets of Langerhans (more than 75%), with frequency even higher than class I PI3Ks (Muller et al. 2006). Also, human islets from T2D individuals showed reduced mRNA levels of PI3K-C2 $\alpha$ , compared to islets from non diabetic subjects. No difference in the levels of the mRNA encoding PI3K-C2 $\beta$  or PI3K-C2 $\gamma$  was reported (Dominguez et al. 2011).



Whether or not PI3K-C2 $\alpha$  downregulation is linked to type 2 diabetes, or whether it could be a cause or an effect of the diabetic condition remains to be understood.

As briefly mentioned before, a crucial role for PI3K-C2 $\alpha$  in pancreatic  $\beta$  cell function has also recently emerged. For instance, it was shown that insulin-induced expression of  $\beta$ -glucokinase mRNA did not involve the activation of class I PI3Ks and was not impaired by the use of classical PI3K inhibitors wortmannin and LY294002, which suggested the involvement of PI3K-C2 $\alpha$  (Leibiger et al. 2001). Indeed, it was later demonstrated by the same group that this process specifically involved the action of PI3K-C2 $\alpha$  in MIN6 cells (Leibiger et al. 2010). In this study, the authors also showed that downregulation of PI3K-C2 $\alpha$  impaired glucose-induced insulin secretion in MIN6 cells (Leibiger et al. 2010). Consistent with this, it was also shown that downregulation of PI3K-C2 $\alpha$  in INS1 cells decreased KCl-induced insulin secretion (Dominguez et al. 2011). Taken together, these data indicate that PI3K-C2 $\alpha$  has a crucial role in regulation of pancreatic  $\beta$  cell function.

Interestingly, it has been recently suggested that PI3K-C2 $\alpha$  might be involved in the activation of mTOR. Indeed, it was reported that PI3K-C2 $\alpha$  was required for mTORC1 activation and its translocation to the plasma membrane in 3T3-L1 adipocytes (Bridges et al. 2012). Specifically, the authors reported that downregulation of PI3K-C2 $\alpha$  impaired mTORC1 activity, as assessed by phosphorylation of its downstream effector S6K upon serum starvation and stimulation with insulin. Importantly, no effect on the phosphorylation of Akt was observed, indicating that PI3K-C2 $\alpha$  is not

involved in the 'classical' Akt/mTOR axis. Furthermore, it was shown that downregulation of PI3K-C2 $\alpha$  impaired endogenous mTORC1 translocation to the plasma membrane in response to insulin and amino acids stimulation in the same cell line (Bridges et al. 2012).

### 1.3 Aims of the project

Evidence discussed in this chapter indicated that PI3Ks have a central role in both insulin producing and insulin target cells. Most of our knowledge comes from the study on class I PI3Ks but more recently it became evident that PI3K-C2 $\alpha$  also has an important role in insulin producing and insulin target cells. However, many questions on the functional role of PI3K-C2 $\alpha$  and its mechanisms of action and activation are still unanswered.

The rationale of the present study was mainly based on the findings published by my research group (Dominguez et al. 2011). In this study, it was shown that downregulation of PI3K-C2 $\alpha$  impaired insulin granule exocytosis in the rat insulinoma cell line INS1. Interestingly, it was also shown that the mRNA encoding for PI3K-C2 $\alpha$  was significantly lower in pancreatic islets from T2D patients compared to non diabetic individuals. This suggested a crucial involvement of PI3K-C2 $\alpha$  in the regulation of pancreatic  $\beta$  cell function.

Therefore, the aims of this project were:

- Investigation of the mechanisms of downregulation of PI3K-C2 $\alpha$
- Investigation of the functions and the signalling pathways regulated by PI3K-C2 $\alpha$  in pancreatic  $\beta$  cells
- Investigation of the mechanisms of activation of PI3K-C2 $\alpha$  in pancreatic  $\beta$  cells

## Chapter 2

### Materials and Methods

#### 2.1 Cell culture

##### 2.1.1 Cell culture and propagation

Rat insulinoma cells INS1 were cultured in RPMI (powder medium, Sigma-Aldrich, UK), supplemented with 11mM D-glucose (Sigma-Aldrich, UK), 26 mM sodium bicarbonate (Sigma-Aldrich, UK), 10 mM HEPES (Sigma-Aldrich, UK), 50  $\mu$ M  $\beta$ -mercaptoethanol (Sigma-Aldrich, UK), pH 7.4. Dissolved medium was filtered using sterile bottles with a 0.22 $\mu$ m top bottle filter (Merck Millipore, UK) and it was supplemented with 10% v/v Foetal Bovine Serum (FBS) (Life Technologies), 1X L-Glutamine/Penicillin/Streptomycin (PAA), 1% v/v Sodium Pyruvate (Life Technologies).

Cells were seeded in T75 vented flasks, with gas-permeable caps, tissue culture treated or multi-well dishes (BD, UK) and grown in humidified incubator at 37°C in a 5% CO<sub>2</sub> atmosphere.

Stable cell lines lacking the enzyme PI3K-C2 $\alpha$  were previously generated in Dr. Maffucci's laboratory by retroviral infection of a pSuper vector containing a specific short hairpin RNA sequence (sh RNA). Stable control cells were generated at the same time using a non-targeting, 'scrambled' shRNA (Dominguez et al., 2011).

### **2.1.2 Cell amplification and passage**

INS1 were passaged every 2 days, when 80% confluent. Medium was removed and cells were washed with sterile, pre-warmed, calcium free phosphate buffered saline solution 1X (PBS) (PAA, Austria). Then, 4ml of trypsin-EDTA (PAA, Austria) were added, in order to detach the cells, and flasks were put back in the incubator for 2-3 minutes. Trypsin was inactivated with 8ml of pre-warmed complete growth medium and cells were gently harvested, pipetting up and down to disperse the medium on the flask surface. Cells were collected in 15ml or 50ml centrifuge tubes (Falcon-BD, UK) and centrifuged at 250g for 5 minutes at room temperature. Medium was gently aspirated, cells were resuspended in complete growth medium and seeded as required in new T75 tissue culture flasks or multiwell plates.

### **2.1.3 Cryo-preservation and recovery of cell lines**

Cells in a T75 tissue culture flask were detached when 80% confluent. Cells were washed, detached, harvested and pelleted as previously described 2.1.2. Cell pellets were resuspended in 1ml of 90% FBS:10% DMSO (Sigma Aldrich, UK) freezing solution and the total volume of 1 ml was transferred in cryovials (VWR). Cells were stored at -80°C in a polystyrene box for a maximum of 10 days. For long term storage, cells were placed in dry ice and transferred into liquid nitrogen.

## 2.2 Biochemistry

### 2.2.1 Protein sample preparation from cell lysates

Cells were detached from T75 flasks when 80% confluent as previously described for cell passage. The pellet was resuspended in 10 ml of growth medium and an aliquot was transferred into a Bürker chamber for manual counting. Cells were then seeded at the desired confluence in 6 or 12 wells plates. When required, the following day after being plated cells were washed using sterile PBS and cultured in serum free medium for further 24 hours before stimulation. Alternatively, cells were starved in Krebs-Ringer buffer (0.1% w/v BSA, 125mM NaCl, 25mM Hepes, 5mM KCl, 2mM MgSO<sub>4</sub>, 1.67mM D-glucose, 1.2mM KH<sub>2</sub>PO<sub>4</sub>) and stimulated as required.

Cells were then washed twice in ice-cold, non sterile PBS and lysed in 200µl of cold Triton X-100 lysis buffer (50mM Tris-pH 8.0, 150mM NaCl and 1% v/v Triton-X100) containing 1X protease inhibitor cocktail (Sigma-Aldrich, UK) and 1X phosphatase inhibitor cocktail II (Sigma-Aldrich, UK). In order to detach the cells, disposable cell scrapers were used. Lysates were then transferred in 1.5 ml tubes (VWR, UK) and centrifuged at 10,000g for 3 minutes at 4°C to remove debris and cellular membranes. The supernatants were collected and transferred into new 1.5 ml tubes and kept on ice until protein quantification. Lysates were stored at -20°C or -80°C for long conservation.

### 2.2.2 Measurement of Protein Concentration using Bradford protein assay

Protein concentration was determined using the Bio-Rad Protein Assay, based on the method of Bradford. This was necessary to ensure equal loading of lysates during Western Blot experiments. Bradford solution (Bio-Rad, UK) was diluted to 1X with ddH<sub>2</sub>O and Bovine Serum Albumin (BSA, Sigma-Aldrich, UK) was used to generate a calibration curve for protein quantification. In a 96 wells plate, six dilutions of BSA/Bradford solution were prepared in duplicates, with concentrations range from 0 to 2 µg/µl (Table 2.1).

Biorad protein assay	1X Bradford reagent (µl)	BSA 200 µg/ml (µl)	BSA (µg)
Standard Curve	200	0	0 µg
	198	2	0.4 µg
	196	4	0.8 µg
	196	6	1.2 µg
	192	8	1.6 µg
	190	10	2 µg

**Table 2.1: BSA Standard curve protein concentration**

Aliquots of cellular lysates were diluted 1:200, using the same Bradford solution. Duplicates were prepared for each sample and the absorbance at 595 nm was

measured using a microplate reader. A linear calibration curve was set, using Microsoft Excel® and plotting BSA concentration (X axis) and absorbance value (Y axis). The unknown protein concentration of the samples was calculated using the following formula:

$$\text{Abs} = mx+b$$

Abs=Absorbance; m=slope of the line; x=protein concentration; b=Y intercept

Protein samples were then diluted in 5X denaturing sample buffer (Table 2.2) and heated at 95°C for 5 minutes to allow denaturation. Samples were analysed by SDS-Polyacrylamide Gel Electrophoresis (SDS-PAGE) and Western blot. Denatured samples were stored at +4°C for short period or at -20°C for long-term storage.



5X denaturing sample buffer (per 16 ml)	
ddH <sub>2</sub> O	6.8 ml
0.5M Tris-HCl pH 6.8	2 ml
Glycerol 87%	4 ml
SDS 20%	1.6 ml
Bromophenol Blue solution (6mg/ml)	1.6 ml

**Table 2.2: 5X Denaturing Sample Buffer**

### **2.2.3 SDS-PAGE and Western blot**

A resolving polyacrilamide gel solution was prepared using Tris-HCl pH 8.8, H<sub>2</sub>O, Acrylamide, 10% APS and Temed (Table 2.3). The volume of Tris-HCl, Acrylamide and H<sub>2</sub>O was adjusted according to the desired final concentration of Acrylamide, in order to obtain a 7%, 10% or 15% resolving gel solution. The solution was poured into an assembled electrophoresis apparatus (Bio-Rad Laboratories, UK), overlaid with 1ml of ddH<sub>2</sub>O and left at room temperature (RT) until polymerised.

10% separating gel solution (per 5 ml)5X	
ddH <sub>2</sub> O	1.9 ml
1.5M Tris, pH 8.8	1.3 ml
Acrylamide mix ProtoGel (30% (w/v) acrylamide, 0.8% (w/v) bisacrylamide stock solution (37.5:1)	1.7 ml
SDS 20%	0.05 ml
10% APS	0.05 ml
TEMED	0.02 ml

**Table 2.3: 10% separating gel solution. The volume of Tris-HCl, Acrylamide and H<sub>2</sub>O was adjusted according to the desired final concentration of acrylamide for 7% and 15% separating gel solutions**

Then, H<sub>2</sub>O was removed and a 5% stacking gel solution (Table 2.4) was prepared and poured on top of the prepared gel. A 10 or 15 sample comb was used and polymerisation was allowed at RT.

5% stacking gel solution (per 1 ml)	
ddH <sub>2</sub> O	0.67 ml
1M Tris, pH 6.8	0.13 ml
Acrylamide mix ProtoGel (30% (w/v) acrylamide, 0.8% (w/v) bisacrylamide stock solution (37.5:1)	0.17 ml
SDS 20%	0.01 ml
10% APS	0.01 ml
TEMED	0.01 ml

**Table 2.4: 5% stacking gel solution.**

After removing the comb, gel wells were washed with ddH<sub>2</sub>O to remove residues and the gels were mounted in a tank with 1X Running Buffer (Table 2.5). Gel electrophoresis was performed applying a constant voltage of 110V, allowing the separation of proteins according to their molecular weight.

1X Running Buffer
25 mM tris, pH 8.3
192 mM Glycine
0.2% SDS

**Table 2.5: Running Buffer**

Proteins were then transferred from the gel onto a Protran<sup>®</sup> nitrocellulose membrane filter (Whatman, UK) by electroblotting in a dedicated tank (Bio-Rad Laboratories), using ice cold 1X Blotting Buffer (Table 2.6) supplied with 20% v/v methanol.

1X Transfer Buffer
25 mM tris, pH 8.3
192 mM Glycine
20% v/v Methanol

**Table 2.6: Transfer buffer**

Transfer was allowed for 90 minutes at a constant current of 400mA at RT. Overheating was prevented by the presence of an icepack in the tank.

Then, the nitrocellulose membrane was incubated with Ponceau-S solution (Applichem GmbH, UK) for 1-2 minutes at room temperature to assess correct protein transfer. Excess of Ponceau-S solution was removed by rinsing the membrane with ddH<sub>2</sub>O.

#### **2.2.4 Immunoblotting and analysis**

Nitrocellulose membrane was incubated for 30 minutes with PBS-0.05%Tween-20 (v/v), supplemented with 5% milk (w/v) (Invitrogen), in order to achieve blocking of non-specific binding. Then, the membrane was incubated overnight at 4°C under agitation with a solution of PBS-0.05%Tween-20 (v/v) containing the primary antibody (Table 2.7). The solution was removed the following day and the membrane was washed in PBS-0.05%Tween-20 (v/v) 3X for 7-8 minutes.

Primary Antibody	Company	Cat. No	Secondary Antibody	Dilution
PI3K-C2 $\alpha$	BD Transduction Laboratories	611046	Anti-Mouse IgG	1:500
PI3K-C2 $\beta$	BD Transduction Laboratories	611343	Anti-Mouse IgG	1:500
p110 $\alpha$	Cell Signalling Technology	4249	Anti-Rabbit IgG	1:1000
p110 $\beta$	Cell Signalling Technology	3011	Anti-Rabbit IgG	1:1000
p110 $\gamma$	Santa Cruz Biotechnology	sc-7177	Anti-Rabbit IgG	1:1000
hVps34	Zymed Laboratories	38-2100	Anti-Rabbit IgG	1:1000
pmTOR (Ser 2448)	Cell Signalling Technology	5536	Anti-Rabbit IgG	1:1000
P4EBP1 (Ser37/46)	Cell Signalling Technology	2855	Anti-Rabbit IgG	1:1000
pAkt (Ser473)	Cell Signalling Technology	4060	Anti-Rabbit IgG	1:1000
pAkt (Thr308)	Cell Signalling Technology	2965	Anti-Rabbit IgG	1:1000
pS6K (Thr389)	Cell Signalling Technology	9234	Anti-Rabbit IgG	1:1000
pS6 (Ser235/236)	Cell Signalling Technology	4858	Anti-Rabbit IgG	1:1000
pS6 (Ser240/244)	Cell Signalling Technology	5364	Anti-Rabbit IgG	1:1000
pAMPK $\alpha$ (Thr 172)	Cell Signalling Technology	2531	Anti-Rabbit IgG	1:1000
Akt 1/2/3	Santa Cruz Biotechnology	Sc-8312	Anti-Rabbit IgG	1:1000

S6K	Cell Signalling Technology	9202	Anti-Rabbit IgG	1:1000
S6	Cell Signalling Technology	2317	Anti-Mouse IgG	1:1000
AMPK	Cell Signalling Technology	2603	Anti-Rabbit IgG	1:1000
Caspase 3	Cell Signalling Technology	9665	Anti-Rabbit IgG	1:1000
LC-3	Cell Signalling Technology	2775	Anti-Rabbit IgG	1:1000
ERK1/2	Santa Cruz Biotechnology	sc-135900	Anti-Rabbit IgG	1:1000
Tubulin	Sigma-Aldrich	T9026	Anti-Mouse IgG	1:10000
Calpain 1	Cell Signalling Technology	2556	Anti-Rabbit IgG	1:1000
Calpain 2	Cell Signalling Technology	2539	Anti-Rabbit IgG	1:1000
Calpain 10	Kindly provided by Dr. M. Turner	N/A	Anti-Mouse IgG	1:1000
Syntaxin 1	Santa Cruz Biotechnology	sc-12736	Anti-Mouse IgG	1:1000
Vamp 2	Kindly provided by Dr. G. Schiavo	N/A	Anti-Mouse IgG	1:1000

**Table 2.7: List of primary antibodies used**

Membrane was then incubated with a solution of PBS-0.05%Tween-20 (v/v) containing a dilution 1:15000 of the appropriate peroxidase-conjugated secondary antibodies anti-rabbit IgG (Sigma Aldrich, UK) or anti-mouse IgG (GE Healthcare, UK)

for 1 hour at RT. In order to remove the excess of secondary antibody, the membrane was washed 3X in PBS-0.05%Tween-20 (v/v) for 7-8 minutes and dried with chromatography paper (Whatman). Then, the membrane was incubated for 5 minutes with ECL Prime solution (Amersham Bioscience, UK), dried, sealed in a plastic sheet, placed in a dedicated autoradiography cassette and exposed to an X-ray film (Kodak) in a dark room. Exposure time varied depending on the amount of protein and antibody potency and was usually between 15 second and 10 minutes.

### **2.2.5 Co-Immunoprecipitation**

INS1 cells were cultured in 100mm tissue culture treated Petri dishes (BD, UK). When cells reached ~70% confluence, they were starved with Krebs-ringer buffer for 30 minutes and stimulated with Krebs-ringer buffer supplemented with 60mM KCl + 1mM Ca<sup>2+</sup> for the indicated time. Then, cells were washed 3x with ice cold PBS, lysed on ice using lysis buffer containing 50mM Tris-pH 8.0, 150mM NaCl and 1% Triton-X100 as previously described for preparation of cell lysates. Protein concentration was measured using the Bradford method and an aliquot of cell lysate was kept and processed as described for Western blot sample preparation. Then, 1 mg of cellular lysate for each sample was transferred in 1.5 ml eppendorf tubes and incubated overnight with 4 µg of anti VAMP2 antibody at +4°C in agitation. The following day, samples were incubated for 1 hour with 30 µl of Protein G Sepharose Fast Flow beads (GE Healthcare) to pull down the complex antibody/protein of interest.

Samples were centrifuged at 3,000 g for 5 minutes and supernatant was carefully removed. An aliquot of supernatant was kept and processed for Western Blot analysis to assess the efficiency of immunoprecipitation, and it was indicated as 'unbound'. Pellets were then washed 3X with PBS and samples were processed for Western Blot analysis, by adding 2X denaturing sample buffer and by heating at 95°C for 5 minutes to allow denaturation of the proteins and dissociation from the beads. Samples were then loaded on a 15% gel for SDS-PAGE.

## **2.3 Cell Biology**

### **2.3.1 Cell counting**

INS1 cells were seeded in 12 well plates ( $15 \times 10^5$  cells/plate) in complete growth medium. They were left in the incubator for at least 12 hours, in order to let them attach to the plate, before being washed 1X with sterile PBS and incubated with serum-free medium. Culture medium was changed every 24 hours with fresh medium supplemented with the amount of glucose indicated in each experiment. Where indicated, medium also contained inhibitors. Cells were then detached using trypsin solution, harvested using complete growth medium and centrifuged at 2,000 rpm for 5 minutes. The supernatant was carefully removed, the pellet was resuspended in complete growth medium (400 to 800  $\mu$ l, depending on the experiments) and 10  $\mu$ l of cell resuspension were placed in a Bürker chamber.



Usually, 4 or 5 fields were counted and the number of cells/ml was calculated with the formula:

$$\text{average number of cells/field} * 10,000 = \text{number of cells/ml}$$

All the measurements were performed in duplicate.

### **2.3.2 MTT assay**

INS1 cells were seeded and treated as previously described for the cell counting. MTT 10X stock solution was prepared dissolving Thiazolyl Blue Tetrazolium Bromide (#M2128, Sigma-Aldrich, UK) 5mg/ml in serum free RPMI, filtered with a 0.22 µm syringe filter (Merck Millipore, UK) and kept at 4°C for a maximum of 5 days for further use. 100 µl of MTT 10X stock were added to 900 µl of serum free medium in a 12 well plate. Cells were placed in humidified incubator at 37°C in a 5% CO<sub>2</sub> atmosphere for 2 hours and 30 minutes. Then, medium was carefully removed from the plate with a vacuum aspirator and adherent cells were lysed in 600 µl of DMSO. The plate was placed on a shaker for 2 minutes in order to dissolve the formazan crystals completely and 100 µl of the solution were transferred to a 96 well plate. Triplicates of each sample and triplicates of a dilution 1:2 of each sample were analysed, measuring the absorbance at 570nm using a microplate reader, subtracting a background absorbance at 650nm.

### **2.3.3 Sodium Palmitate treatment**

INS1 cells were detached from T75 flasks when 80% confluent as previously described for cell passage. The pellet was resuspended in growth medium and manually counted into a Bürker chamber. Then,  $12 \times 10^5$  cells were seeded in complete growth medium in 6 wells plates for lysates or 12 wells plates for cell counting and MTT assays. Cells were then left to attach to the plate for a minimum of 12 hours, in humidified incubator at 37°C in a 5% CO<sub>2</sub> atmosphere.

Fresh aliquots of sodium palmitate (#P9767, Sigma-Aldrich, UK) 100mM were prepared for every experiment. Palmitate was administered to cells after conjugation with free fatty acid-free bovine serum albumin (FFA-free BSA, Sigma). Sodium palmitate was dissolved in 100% Ethanol or Methanol (Sigma-Aldrich, UK) by vigorous vortexing followed by sonication, until it appeared as a milky solution. Complete growth medium was supplemented with 1% w/v BSA (Sigma-Aldrich, UK-Aldrich, UK), filter sterilised and warmed up to 55°C. Then, medium was supplemented with the required amount of palmitate solution, cooled down to room temperature and administrated to INS1 cells for 24 or 48 hours.

#### **2.3.4 GFP-2XFYVE<sup>Hrs</sup> transfection**

Round coverlips of 60mm diameter were kept in ethanol. Then, coverslips were transferred to 12-well plates and ethanol was allowed to evaporate in a sterile environment. Cells were seeded (100000 cells/coverslip) in 12-well plates and incubated at 37°C and 5% CO<sub>2</sub> atmosphere for 24 hours. Transfection of GFP-2XFYVE<sup>Hrs</sup> contained in pEGFP-C2 plasmid was optimised using 0.5µg of plasmid DNA and 2µl Lipofectamine<sup>®</sup> reagent according to the manufacturer's instructions in serum free OPTIMEM medium. Two separate mixes were prepared, a 'mix A' containing 2µl Lipofectamine<sup>®</sup> (LifeTechnologies) in 50µl OPTIMEM and 'mix B' containing 0.5µg GFP-2XFYVE<sup>Hrs</sup> plasmid in 50µl OPTIMEM (LifeTechnologies). The two solutions were incubated for 10 minutes at room temperature before being gently mixed and left to incubate for further 20 minutes at room temperature. Cells were washed with 1X PBS and 400µl serum free OPTIMEM were added to each well. Then, 100µl of transfection mix was added and cells were incubated for 4 hours at 37°C and 5% CO<sub>2</sub> atmosphere in a humidified incubator. Medium was then carefully removed and replaced with pre-warmed complete growth medium.

## **2.4 Molecular Biology**

### **2.4.1 RNA extraction**

Total RNA was extracted from INS1 cells treated with sodium palmitate for 24 or 48 hours. Attached cells were trypsinised, collected and pelleted by centrifugation. RNA was immediately extracted using RNeasy kit (Qiagen, UK) following the manufacturer's instructions. Total RNA was then quantified using Nanodrop and used for cDNA synthesis or stored at -80°C for subsequent use.

### **2.4.2 RNA Reverse transcription**

cDNA was synthesised following the manufacturer's instructions (Cat.No. EP0742, Thermo Scientific) using total RNA extracted from INS1 cells. Preparation for the reverse transcription reaction was performed on ice. Total RNA was diluted to a final concentration of 1µg/µl using RNase-free water. Then, 1µg of template RNA was used for retrotranscription reaction, adding random primers, dNTPs, RT buffer, Ribolock RNase Inhibitor and Maxima Reverse Transcriptase as indicated in Table 2.8.

Component	Amount
Template RNA	1µg
Random Primers (#S0131)	1µl
dNTP Mix, 10mM (#R0191)	1µl
Nuclease free H <sub>2</sub> O	To 12.5µl
5X RT Buffer	4µl
Ribolock RNase Inhibitor (#E00381)	0.5µl
Maxima Reserve Transcriptase	1µl
Total Volume	20µl

**Table 2.8: Reagents used for cDNA synthesis.**

The PCR thermal-cycler was programmed as indicated in Table 2.9.

Time (min)	Temperature (°C)
10	25
30	50
5	85
∞ (until collection)	4

**Table 2.9: Program used for PCR thermal cycler.**

### 2.4.3 Real Time quantitative Polymerase Chain Reaction (RT-qPCR)

Mix for RT-qPCR was prepared using 12.5 µl of 2X Maxima® SYBR green qPCR master mix (Fermentas), a final concentration of 0.25µM of forward and reverse primers and nuclease free H<sub>2</sub>O to a final volume of 25 µl. Then, 200ng of cDNA was added. For each qPCR reaction a 18S ribosomal subunit cDNA was amplified as internal control. ABI 7500 Real-Time PCR system was programmed as indicated in Figure 2.11.

Primer	Sequence
PI3K-C2α Fw	5' TGTGGACCTCTGCTGTCAAG 3'
PI3K-C2α Rv	5' AACTTTGTGGCAATGCTTCC 3'
18S Fw	5' TCTTCCACAGGAGGCCTACACG 3'
18S Rv	5' GCCCCACACCCTTAATGGCAGT 3'

Table 2.10: Primers used for the amplification of Rat PI3K-C2α and 18S ribosomal subunit

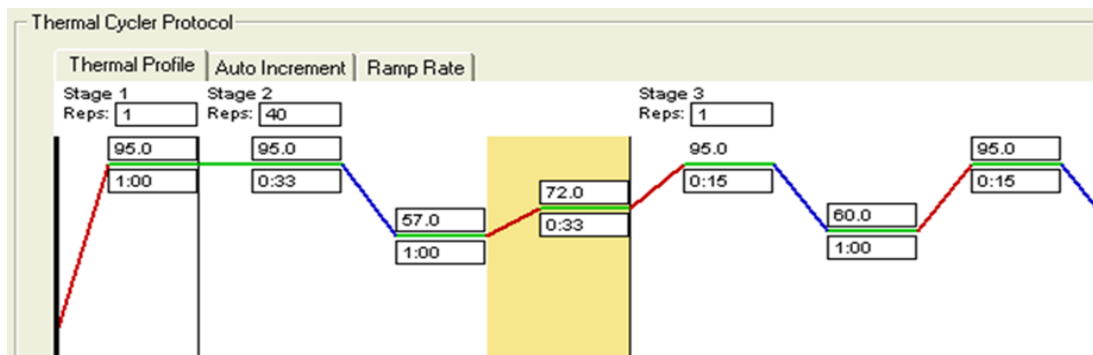


Figure 2.11: Program used for RT-qPCR reaction using the ABI 7500 Real-Time PCR system software.

Relative quantification of gene was calculated using the relative ddCT method and the ABI 7500 Real-Time PCR system software.

## **2.5 Imaging methods**

### **2.5.1 Confocal Microscopy Analysis**

INS1 cells were seeded on coverslips and transfected with GFP-2XFYVE<sup>Hrs</sup> as previously described. 48 hours post transfection, cells were starved for 30 minutes in Krebs-Ringer buffer and then stimulated with Krebs-Ringer Buffer + 60mM KCl and 1mM Ca<sup>2+</sup>. After stimulation, cells were washed 3x in PBS and fixed in 4% paraformaldehyde for 30 minutes. Cells were then permeabilised with PBS-0.25% Triton-X-100 for 2.5 minutes, washed 3x in PBS and incubated with PBS/0.1% BSA, 0.3M glycine for 30 minutes to increase antibody specificity and reduce autofluorescence. Syntaxin 1 antibody (Santa Cruz Biotechnology) was diluted 1:50 in PBS/0.1% BSA, and incubated for 2 hours at room temperature in a humidified chamber, 50µl/coverslip. Coverslips were washed 3x in PBS and incubated with Alexa Fluor 555 Goat Anti-Mouse IgG (1:500) in PBS 0.1% BSA for 1h at room temperature. Coverslips were then washed 3x in PBS, 1x in dH<sub>2</sub>O, mounted with Vectashield mounting media and analysed with a Zeiss Confocal Microscope 710. 63x objective was used to observe cells and take pictures. Alternatively, coverslips

were analysed with a Leica DM5000 automated epifluorescence microscope, using 63x objective to observe cells.

## **2.6 Lipid analysis**

### **2.6.1 HPLC analysis of intracellular phosphoinositides**

INS1 cells were plated in 6 wells plates ( $18 \times 10^5$  cells/well) and left for 24 hours. Then, cells were incubated for 24 hours in M199 media (inositol-free media) supplemented with 1% v/v penicillin/streptomycin/glutamine and  $5 \mu\text{Ci/well}$  myo-[ $^3\text{H}$ ]inositol. Cells were then starved in Krebs-Ringer buffer for 30 minutes and stimulated with Krebs-Ringer buffer containing 60mM KCl and 1mM  $\text{Ca}^{2+}$  for the indicated time points. Where necessary, cells were appropriately starved and stimulated as indicated in the text. Cells were lysed in HCl 1M/1mM EDTA and scraped from the well surface. Lysates were collected in glass chromacol vials and phospholipids were extracted by phase separation using 500  $\mu\text{l}$  1M hydrochloric acid, 670  $\mu\text{l}$  methanol and 1.3 ml chloroform. Samples were vigorously vortexed and subsequently centrifuged until the aqueous and the organic phase appeared completely separated. The organic phase containing PIs was manually retrieved and solvents were removed using a rotary evaporator. Then, PIs were deacylated by resuspending the pellet in a mix of monomethylamine, water, butanol and methanol (5:4:3:1) and by incubating for 30-45 minutes at  $53^\circ\text{C}$  in a waterbath. Samples were



allowed to cool down and a second phase separation was performed. Aqueous phase containing glycerophosphoinositides was separated by the organic phase containing acyl chains using a mix of butanol, petroleum ether and ethyl acetate (20:4:1). Evaporation of the solvents was allowed in a rotary evaporator before samples were resuspended in 600  $\mu$ l of ddH<sub>2</sub>O or stored at -20°C for subsequent use. HPLC separation of the samples was performed using a PartiSphere 5- $\mu$ m strong anion exchange column (Whatman) and a non-linear gradient of 1mM EDTA (buffer A) and 1.3M (NH<sub>4</sub>)<sub>2</sub>HPO<sub>4</sub> + 1mM EDTA (buffer B) as described in Figure 6.3. Eluted samples were collected in fractions of 1ml/min and the radioactivity was evaluated with a beta counter, using a scintillation liquid specific for samples with high levels of phosphate salt (#6013599 Ultima Flo-AP, Perkin Elmer).

## **2.7 Statistical Analysis**

Statistical analysis was carried out performing one-tailed paired t-test by Microsoft Excel software. Error bars in graphs indicate the standard error of the mean (S.E.M.).

## Chapter 3

### Mechanisms of PI3K-C2 $\alpha$ downregulation

#### 3.1 Introduction

A condition of insulin resistance, where insulin signalling is impaired in target tissues, generally precedes overt T2D. Obese individuals present an increased risk to develop T2D, which is the result of both genetic and environmental factors (Prentki and Nolan 2006). Healthy  $\beta$  pancreatic cells respond to chronic nutrients overload with a compensatory increase in insulin production in order to restore normoglycaemia. T2D develops only when  $\beta$  cell compensatory response fails (Prentki and Nolan 2006, Muoio and Newgard 2008), resulting ultimately in a defective insulin secretion. Impaired insulin secretion and insulin signalling cause metabolic defects, and the increase of glucose and fatty acids levels in the bloodstream. In particular, high levels of fatty acids can further aggravate the failure of pancreatic  $\beta$  cells.

In particular, high circulating free fatty acid levels are generally associated with cell death and secretory defects of pancreatic  $\beta$  cells. This pathological link is often called ' $\beta$  cell lipotoxicity', although to date, the molecular mechanisms underlying this process have not been fully understood (Barlow and Affourtit 2013). Studies on lipotoxicity have indicated that different types of fatty acids do not exert the same toxic effects; toxicity on  $\beta$  cells is greater when long chain (C16 or greater), saturated

fatty acids are involved (Morgan and Dhayal 2010). Palmitic acid is a 16-carbon saturated molecule commonly used in lipotoxicity studies, as it normally circulates at the highest concentration in the bloodstream in humans (Morgan and Dhayal 2010). Also, *in vitro* studies using palmitate indicated that it is responsible for cytotoxic effects on pancreatic  $\beta$  cell lines (Koshkin et al. 2008).

Failure of pancreatic  $\beta$  cells in T2D is caused by a decrease in both  $\beta$  cell mass and  $\beta$  pancreatic function (Butler et al. 2003). Several lines of evidence in literature indicated a role of PI3K-dependent signalling pathways in the regulation of pancreatic  $\beta$  cell mass and survival (Franke et al. 1997, Ueki et al. 2002, Kulkarni 2005) and, more recently, evidence also suggested their involvement in the regulation of insulin secretion (Pigeau et al. 2009, Kaneko et al. 2010).

To date, class II PI3Ks remains the least investigated. Interestingly, it has been shown that the mRNA encoding for class II enzymes PI3K-C2 $\alpha$  and PI3K-C2 $\gamma$  is expressed in more than 75% of human islets of Langerhans, and its frequency is higher than other class I PI3K isoforms (Muller et al. 2006). Recently, it has also been reported that PI3K-C2 $\alpha$  has a role in glucose-induced insulin secretion (Leibiger et al. 2010). Previous work in my laboratory further demonstrated that the mRNA encoding for PI3K-C2 $\alpha$  was expressed at lower levels in human islets from T2D individuals compared to islets from non diabetic subjects and that downregulation of this enzyme impaired insulin secretion in rat insulinoma cells (Dominguez et al. 2011). These lines of evidence clearly indicated a specific role for PI3K-C2 $\alpha$  in insulin

granules exocytosis in pancreatic  $\beta$  cells. Therefore, I investigated whether the downregulation of PI3K-C2 $\alpha$  might play a role in the functional failure of pancreatic  $\beta$  cells, contributing to the progression of diabetes. Also, I focussed on whether metabolic dysregulation, typical of T2D and mimicked *in vitro* by using lipotoxic concentrations of sodium palmitate, could be responsible for the downregulation of PI3K-C2 $\alpha$ , both at a protein and mRNA level. Protein levels of other members of the PI3Ks family were also assessed.

## 3.2 Results

### 3.2.1 Optimisation

In order to incubate INS1 cells in lipotoxic growth conditions, sodium palmitate was used. The manufacturer's data sheet recommends to dissolve this product in methanol or ethanol, at a maximum concentration of 50 mg/ml. I chose to prepare a stock concentration of 100mM, corresponding to 27.8 mg/ml. At first, sodium palmitate powder was insoluble at this concentration, in either methanol or ethanol, at room temperature and after vigorous vortexing. Therefore, I tried different protocols: incubation in a waterbath, at temperatures from 37 to 50°C for up to 2 hours, or overnight incubation on a rotating wheel at room temperature. However, these procedures did not improve palmitate solubility. Finally, I obtained a milky solution of 100mM sodium palmitate in either methanol or ethanol by sonicating repeatedly the solution for 10-sec bursts at 200 W on ice (Peng et al. 2011).

Then, I tested the effect of 0.5 mM sodium palmitate on INS1 cells. INS1 were plated in a 6 well plate and treated the following day as described below. An aliquot of INS1 complete medium (containing 10% FBS as described in Materials and Methods) was supplemented with 1% FFA-free BSA and sterile filtered. FFA-free BSA works as a carrier, ensuring the shuttling of fatty acids inside cells (Zhao and Wang 2012). Medium with or without FFA-free BSA was then warmed up to 60°C and the required amount of sodium palmitate solution was added (Peng et al. 2011). Medium was allowed to cool down slowly by incubation in a waterbath at 37°C for

at least 2 hours before being used, to ensure the binding of sodium palmitate to the BSA. An equivalent amount (v/v) of methanol or ethanol was added to complete medium, with or without FFA-free BSA, to evaluate the effect of the vehicle alone.

Growth medium was removed carefully from the plate and replaced with fresh complete medium, with or without FFA-free BSA and sodium palmitate or methanol alone. After 24 hours incubation, medium was removed, cells were lysed and samples were prepared for Western Blot analysis as described in the Materials and Methods section.

Then, protein levels of PI3K-C2 $\alpha$  were analysed, and the result of this experiment is shown in Figure 3.1.

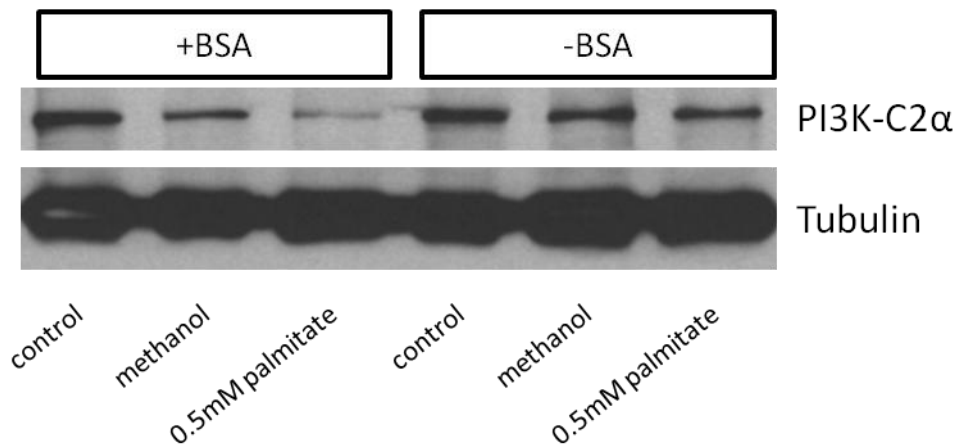


**Figure 3.1:** Expression of PI3K-C2 $\alpha$  in the presence or absence of BSA and sodium palmitate. INS1 cells were left untreated (“control”) or treated for 24 hours with medium containing 0.5mM sodium palmitate or methanol, with or without 1% w/v FFA-free BSA. PI3K-C2 $\alpha$  expression was determined by Western Blot. Tubulin was used as control of equal loading.

Results showed that sodium palmitate treatment had no effect on the protein level of PI3K-C2 $\alpha$  in absence of FFA-free BSA. This confirms that sodium palmitate is unable to pass through the cellular membrane without forming a complex with an appropriate carrier. Also, this suggests that the BSA already contained in the complete growth medium has no effect as a carrier, in these experimental conditions. On the other hand, 24 hours treatment with 0.5 mM sodium palmitate, in the presence of FFA-free BSA, reduced the protein level of PI3K-C2 $\alpha$ .

Pancreatic islets of diabetic patients are chronically exposed to lipotoxic conditions. In order to study the time-dependence of the effects of palmitate on INS1 cells, I extended the treatment of INS1 cells with FFA-free BSA conjugated sodium palmitate for further 24 hours.

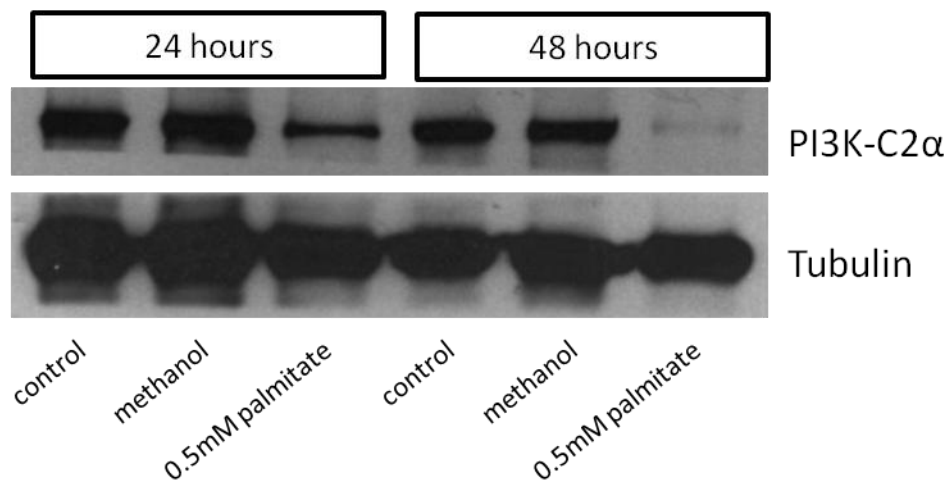


**Figure 3.2:** Expression of PI3K-C2 $\alpha$  upon 24 and 48 hours treatment with sodium palmitate dissolved in methanol. INS1 cells were left untreated (“control”) or treated for 24 or 48 hours with medium containing 0.5mM sodium palmitate or methanol and conjugated with FFA-free BSA. PI3K-C2 $\alpha$  expression was determined by Western Blot. Tubulin was used as control of equal loading.

The result of this experiment showed that 0.5 mM sodium palmitate was able to significantly reduce the level of PI3K-C2 $\alpha$  after 24 hours of treatment. A further decrease was visible after 48 hours of treatment.

In parallel experiments, cells were incubated with sodium palmitate dissolved in ethanol, following the same procedure previously described for methanol. Then, the expression levels of PI3K-C2 $\alpha$  were analysed by Western Blot.

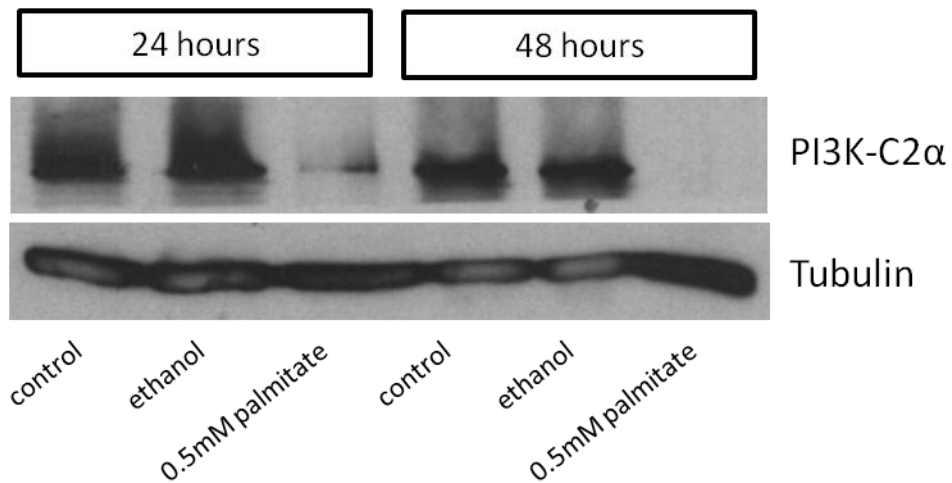


**Figure 3.3: Expression of PI3K-C2 $\alpha$  upon 24 and 48 hours treatment with medium containing sodium palmitate or ethanol. INS1 cells were treated for 24 or 48 hours with medium containing 0.5mM sodium palmitate or ethanol and conjugated with FFA-free BSA. Protein levels were determined by Western Blot analysis. Representative blot of 3 independent experiments is shown.**

Consistent with the results shown in Figures 3.1 and 3.2, incubation of INS1 cells with 0.5 mM palmitate decreased the protein levels of PI3K-C2 $\alpha$  after 24 hours treatment, with a further decrease after 48 hours.



It is well established that treatment of pancreatic  $\beta$  cells with increasing concentrations of sodium palmitate reduces cell viability (Morgan and Dhayal 2010). Consistent with these data, microscope observation of INS1 cells treated with 0.5 mM palmitate suggested a decrease in cell viability. Therefore, cell counting analysis was performed in order to estimate the toxic effects of sodium palmitate.

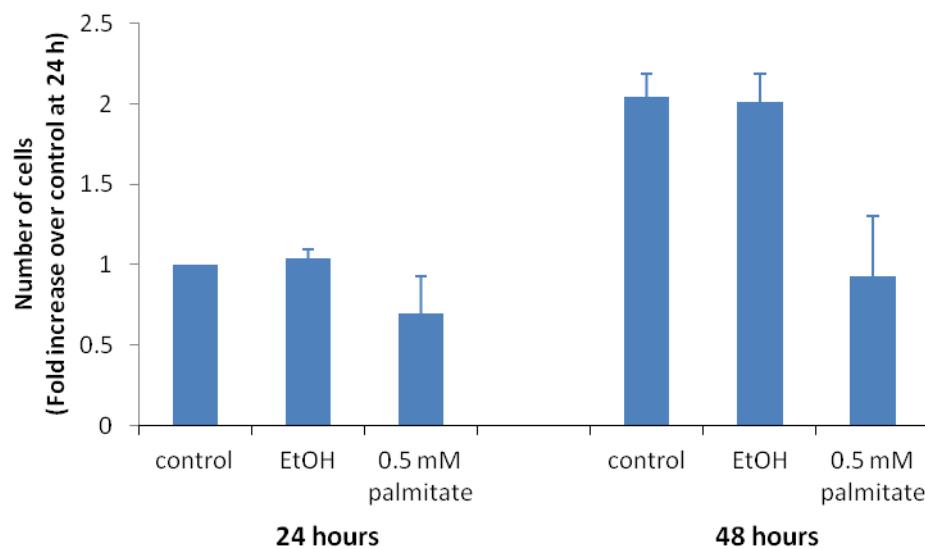


**Figure 3.4: Cell viability in lipotoxic conditions. INS1 cells were left untreated (“control”) or treated with 0.5 mM sodium palmitate dissolved in ethanol and conjugated with FFA-free BSA (or ethanol alone in complete medium supplemented with FFA-free BSA). Number of cells was determined after 24h or 48h by manual counting. Data are expressed as fold increase of the number of untreated cells (“control”) at 24 hours and are means  $\pm$  s.e.m. from 3 independent experiments.**

Results shown in Figure 3.4 indicate the viability of INS1 cells treated with vehicle alone (0.5% ethanol in complete medium) or 0.5 mM sodium palmitate for 24 and 48 hours. Ethanol alone did not affect cell viability compared to control, untreated

cells. On the other hand, viability of INS1 was decreased by ~30% after 24 hours and ~50% after 48 hours treatment with sodium palmitate.

These explorative data were necessary to set the experimental conditions for my subsequent analysis of the effect of lipotoxic conditions on PI3Ks levels. Taken together, these data indicate that preparation of sodium palmitate as described in the Materials and Methods section was able to affect INS1 cells viability and also reduce the protein levels of PI3K-C2 $\alpha$ . Ethanol alone had no effect on the viability of INS1 cells, compared to complete growth medium and therefore it was chosen as vehicle to dissolve sodium palmitate.

### **3.2.2 Lipotoxic growth conditions reduce the protein expression levels of PI3K-C2 $\alpha$**

In order to investigate the effects of lipotoxic growth conditions on the levels of PI3K-C2 $\alpha$ , I tested different concentrations of sodium palmitate.

Following the protocol optimised in my preliminary experiments, INS1 cells were incubated for 24 and 48 hours in medium containing FFA-free BSA-conjugated sodium palmitate, at concentrations ranging from 0.05 mM to 0.5 mM. Western Blot experiments were performed to assess the expression levels of PI3K-C2 $\alpha$ .

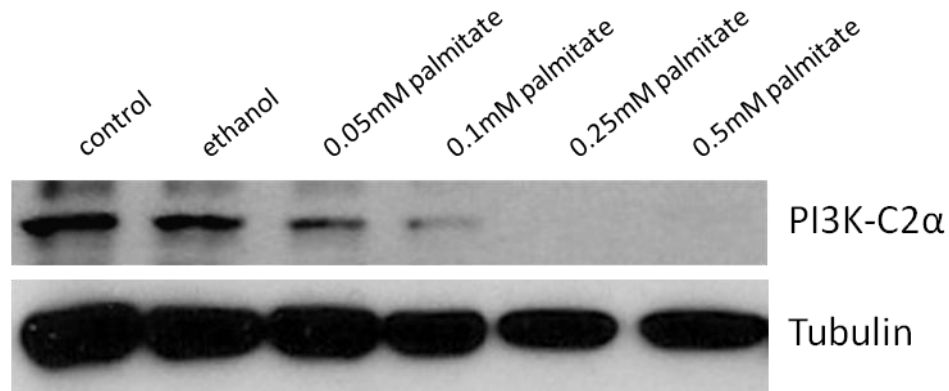


**Figure 3.5: Expression of PI3K-C2 $\alpha$  upon treatment with increasing concentrations of sodium palmitate.** INS1 cells in complete growth medium were left untreated (“control”) or treated for 48 hours with increasing concentrations of sodium palmitate dissolved in ethanol and conjugated with FFA-free BSA. Control with ethanol had the equivalent (v/v) as the maximum concentration of sodium palmitate used. PI3K-C2 $\alpha$  expression was determined by Western Blot analysis and tubulin was used as loading control. Blot is representative of 3 independent experiments.

Results showed that treatment with sodium palmitate downregulated PI3K-C2 $\alpha$  levels in a dose-dependent manner. The decrease in protein level of PI3K-C2 $\alpha$  was maximal when a concentration of 0.25 mM palmitate was used, with comparable results at 0.5 mM.

These data indicated that lipotoxic conditions are able to reduce the protein expression of class II PI3K-C2 $\alpha$  in INS1 cells.

### **3.2.3 Lipotoxic growth conditions do not affect mRNA levels of PI3K-C2 $\alpha$**

To further investigate the mechanisms of PI3K-C2 $\alpha$  downregulation, I performed quantitative analysis of the mRNA encoding for PI3K-C2 $\alpha$ . INS1 cells were incubated

for 48 hours with a range of concentrations of FFA-free BSA-conjugated sodium palmitate, from 0.05 mM to 0.5 mM, as previously described. Then, cells were trypsinised, collected and pellet was stored at -80°C for subsequent RNA extraction.

Specific primers for rat PI3K-C2 $\alpha$  were designed (Table 2.10), total RNA was extracted from samples and retrotranscribed to cDNA. Then, qPCR was performed, using primers targeting rat PI3K-C2 $\alpha$  and 18S ribosomal subunit as housekeeping control gene.

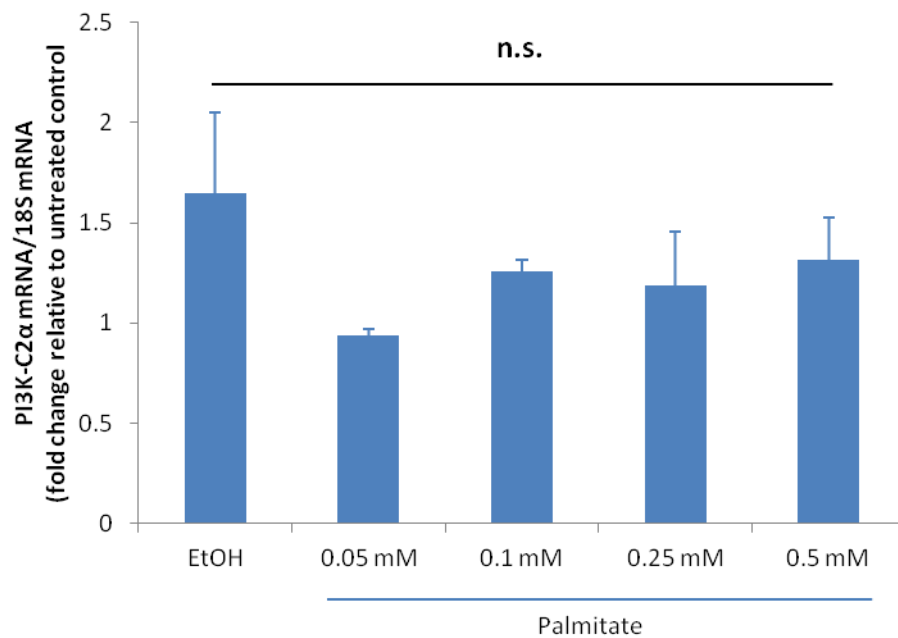


**Figure 3.6:** Levels of PI3K-C2 $\alpha$  mRNA were determined by qPCR, after 48 h incubation in the indicated experimental conditions. Data are expressed as fold change relative to untreated control and are means  $\pm$  s.e.m. from 3 independent experiments.

Results from qPCR experiments are shown in Figure 3.6: mRNA levels of PI3K-C2 $\alpha$  were not significantly modified by lipotoxic growth conditions after 48 hours treatment. This indicates that the decreased protein levels of PI3K-C2 $\alpha$  observed after 48 hours treatment with sodium palmitate are likely due to a defective translation or to an increased degradation of the protein, rather than a reduced protein transcription.

#### **3.2.4 Protein levels of other members of the PI3K family upon lipotoxic growth conditions**

To determine whether treatment with sodium palmitate specifically affects PI3K-C2 $\alpha$  protein expression, I then analysed the effect on the protein levels of other members of the PI3K family. Since treatment with sodium palmitate decreased the protein levels of PI3K-C2 $\alpha$  irrespective of the solvent used (Figures 3.2 and 3.3), I performed the following experiments using either ethanol or methanol. First, I analysed the expression levels of class I PI3K p110 $\alpha$  by Western Blot, upon treatment with sodium palmitate for 24 and 48 hours.

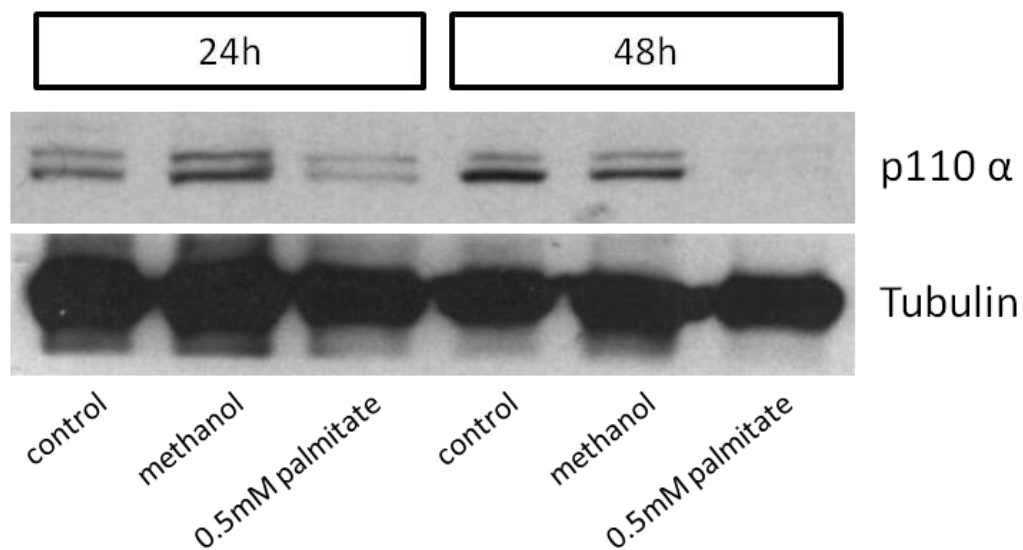


**Figure 3.7: Expression of p110 $\alpha$  upon 24 and 48 hours treatment with sodium palmitate. INS1 cells in complete medium were left untreated or treated for 24 and 48 hours with vehicle alone or 0.5mM sodium palmitate conjugated with FFA-free BSA. Protein levels of p110 $\alpha$  were determined by Western Blot and tubulin was used as loading control. Representative blot of 3 independent experiments is shown.**

Results showed that incubation of INS1 cells with sodium palmitate for 24 hours decreased the protein levels of p110 $\alpha$ , which were further reduced after 48 hours treatment (Figure 3.7).

In contrast, treatment with sodium palmitate did not affect the protein levels of class I p110 $\beta$ , upon either 24 or 48 hours incubation (Fig 3.8).

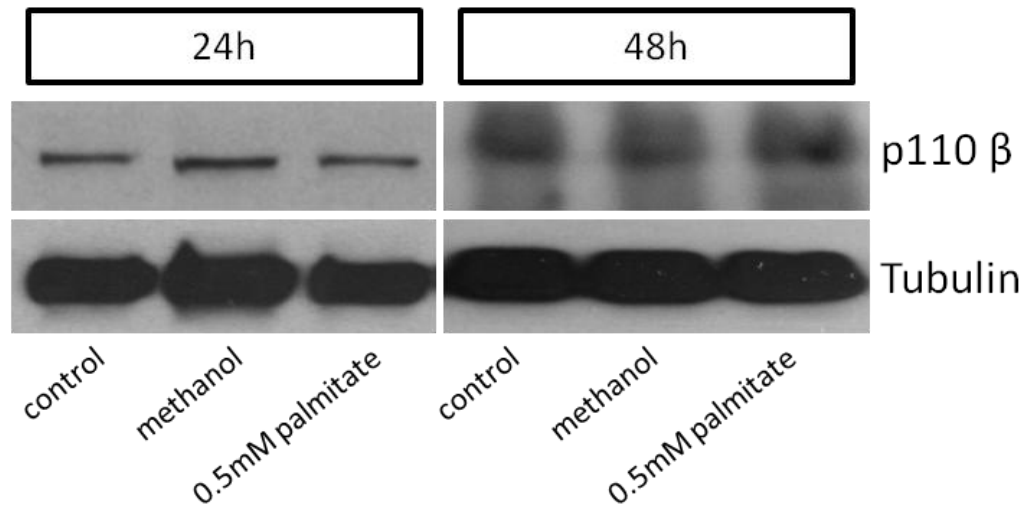


**Figure 3.8: Expression of p110 $\beta$  upon 24 and 48 hours treatment with sodium palmitate.** INS1 cells in complete medium were left untreated or treated for 24 and 48 hours with vehicle alone or 0.5mM sodium palmitate conjugated with FFA-free BSA. Protein levels of p110 $\beta$  were determined by Western Blot and tubulin was used as loading control. Representative blot of 3 independent experiments is shown.

Evidence in literature suggests that class I PI3K p110 $\gamma$  has a crucial role in pancreatic  $\beta$  cells. Indeed, it has been shown that p110 $\gamma$  has an important role in insulin secretion in insulinoma cell lines and human  $\beta$  cells (Pigeau et al. 2009). Therefore, I assessed the effect of palmitate on p110 $\gamma$  levels.

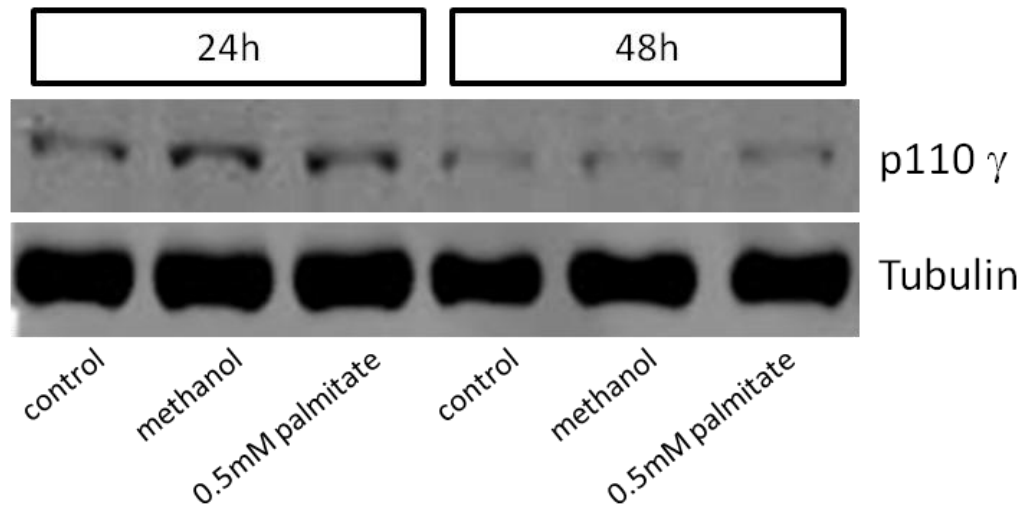


**Figure 3.9: Expression of p110 $\gamma$  upon 24 and 48 hours treatment with sodium palmitate. INS1 cells in complete medium were left untreated (“control”) or treated for 24 and 48 hours with vehicle alone or 0.5mM sodium palmitate conjugated with FFA-free BSA. Protein levels of p110 $\gamma$  were determined by Western Blot and tubulin was used as loading control. Representative blot of 2 independent experiments is shown.**

Figure 3.9 shows a representative blot of the protein levels of p110 $\gamma$  upon treatment with palmitate for 24 and 48 hours. Lipotoxic conditions did not affect p110 $\gamma$  protein levels in these experimental conditions.

In addition, I analysed protein levels of class III PI3K hVps34 upon treatment with sodium palmitate.



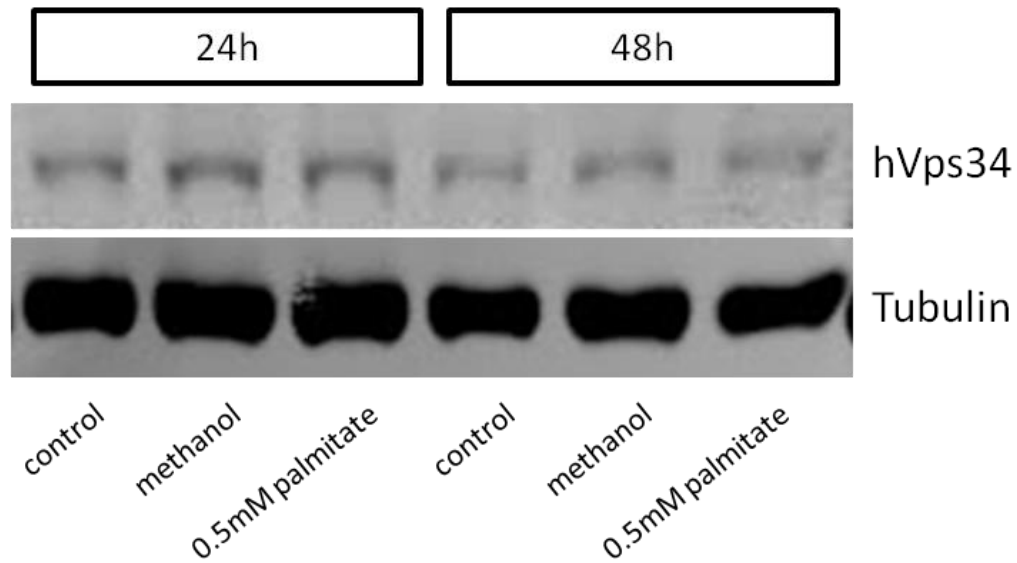


**Figure 3.10: Expression of hVps34 upon 24 and 48 hours treatment with sodium palmitate.** INS1 cells in complete medium were left untreated (“control”) or treated for 24 and 48 hours with vehicle alone or 0.5mM sodium palmitate conjugated with FFA-free BSA. Protein levels of hVps34 were determined by Western Blot and tubulin was used as loading control. Representative blot of 2 independent experiments is shown.

Results showed that incubations of INS1 cells with palmitate for 24 or 48 hours did not affect protein levels of hVps34 in these experimental conditions.

Taken together, these data indicate that treatment with sodium palmitate specifically decreased the protein levels of PI3K-C2 $\alpha$  and p110 $\alpha$ , with no effect on the protein levels of the other PI3Ks examined.

### 3.3 Discussion

In this chapter, I analysed the effects of lipotoxic growth conditions on the expression levels of PI3K-C2 $\alpha$  and other members of the PI3K family in INS1 cells. The mRNA coding for PI3K-C2 $\alpha$  is expressed in the majority of human pancreatic  $\beta$  cells isolated from non diabetic donors, with a higher frequency compared to class I catalytic subunits (Muller et al., 2006), which suggests a role for the enzyme specifically in  $\beta$  cells. Interestingly, PI3K-C2 $\alpha$  mRNA levels are downregulated in islets from diabetic patients (Dominguez et al. 2011), and this observation suggests a link between diabetes and PI3K-C2 $\alpha$  function. These findings, together with the fact that diabetic patients have elevated levels of fatty acids circulating in the bloodstream, led us to hypothesise that lipotoxicity might be one of the causes of PI3K-C2 $\alpha$  mRNA downregulation, leading to a reduced amount of enzyme. Furthermore, since we (Dominguez et al. 2011) and others (Leibiger et al. 2010) observed that PI3K-C2 $\alpha$  has a role in insulin secretion, this could be associated with an impairment of pancreatic  $\beta$  cell function. Because of the large amount of sample required for protein studies and the scarcity of human pancreatic islets available for medical research, it was necessary to use an *in vitro* model of pancreatic  $\beta$  cells. Cell lines are a very useful tool to study physiological and pathophysiological conditions and INS1 cells are a well established model of pancreatic  $\beta$  cells. However, limitations of their use must always be considered. *In vitro* studies have to take into account the disadvantages of working with artificial cell lines, which might

encounter changes in cell characteristics due to the continuous growth and to genetic manipulation. More importantly, *in vitro* models cannot accurately reproduce the complexity of interactions of an intact organ in the context of a whole organism, due to the disruption of cell-cell interactions (Skelin et al. 2010). Also, pancreatic islets constitute a unique micro environment, where islets hormones finely modulate the activity of different cell types through autocrine and paracrine mechanisms (Barker et al. 2013).

To the best of my knowledge, modification of the protein levels of PI3K family in  $\beta$  cells subjected to lipotoxic conditions has not been investigated before. Western Blot analysis of the levels of different PI3Ks revealed that PI3K-C2 $\alpha$  and p110 $\alpha$  are specifically decreased upon treatment with sodium palmitate for 24 hours, with a further decrease observed after 48 hours treatment (Figures 3.3 and 3.7). No difference in the levels of other PI3Ks was detected. Quantitative analysis of PI3K-C2 $\alpha$  mRNA was performed and results indicated that the levels of PI3K-C2 $\alpha$  mRNA do not undergo significant modifications upon treatment with palmitate for 48 hours. This result appears to be in contrast with the observation that PI3K-C2 $\alpha$  mRNA is downregulated in human pancreatic islets from diabetic patients (Dominguez et al. 2011). This discrepancy might be explained by the difference between human pancreatic islets and the cellular system used, and by the limited time of treatment with sodium palmitate in this study, which is not comparable to the chronic lipotoxic conditions that islets of diabetic patients are exposed to. The correct functioning of PI3K pathway is particularly important in pancreatic  $\beta$  cells.

Insights from studies on mice models revealed that the disruption of the pathway involving IR/IRS2/PI3K/Akt axis leads to defects in  $\beta$  cell development and function. For instance, IRS2 knockout mice models develop diabetes, show  $\beta$  cell deficiency at birth and lack  $\beta$  cell compensation in the stages preceding overt diabetes (Withers et al. 1998, Kubota et al. 2000). Also, mice models deficient for S6K1, a class I PI3K downstream effector, show a reduction in pancreatic mass and a selective decrease in  $\beta$  cell size, as a result of the disruption of PI3K signalling pathway (Pende et al. 2000). More recently, a specific role for PI3K isoforms in insulin secretion has also been reported, irrespective of their role in regulating  $\beta$  cell mass. For instance, it has been found that insulin secretion is impaired in db/db mice probably through a downregulation of class I PI3K/Akt pathway (Kaneko et al. 2010). Using  $\beta$ DKO mice models, which, as mentioned before lack the regulatory subunits of class I PI3Ks specifically in  $\beta$  cells, it has been shown that PI3K signalling is crucial for maintaining  $\beta$  cell function (Kaneko et al. 2010). Indeed, the activity of class I PI3K is blunted in these mice models, and this impairs insulin secretion. More recently, a role for class II PI3K and specifically for PI3K-C2 $\alpha$  has also been reported, as this PI3K isoform is involved in glucose-induced insulin release in MIN6 cells (Leibiger et al. 2010). Also, in the pancreatic  $\beta$  cell line INS1 the downregulation of PI3K-C2 $\alpha$  has been found to cause a decreased insulin secretion (Dominguez et al. 2011).

My data suggest that an excess of free fatty acids is able to downregulate the protein levels of two PI3K isoforms (class I p110 $\alpha$  and class II PI3K-C2 $\alpha$ ) in the pancreatic  $\beta$  cell line INS1. Since it was previously reported that downregulation of

PI3K-C2 $\alpha$  impairs insulin secretion (Dominguez et al. 2011), this data suggests that an excess of free fatty acids might be accountable for the malfunctioning of the aforementioned signalling pathways, contributing to the reduced pancreatic  $\beta$  cell function.

In addition, results show that lipotoxic conditions do not affect the levels of class I p110 $\beta$ , p110 $\gamma$  and class III hVps34 (Figures 3.8, 3.9 and 3.10, respectively). This suggests that the observed decrease in the protein levels of PI3K-C2 $\alpha$  and p110 $\alpha$  is a specific effect of the lipotoxic growth conditions and it is not due to a general cytotoxic action of free fatty acids supplemented in the growth medium.

Taken together, these findings underline how PI3K activity is essential to maintain both  $\beta$  cells mass and secretory ability. The fact that lipotoxic conditions are able to affect the protein levels of two PI3K isoforms might shed new light into the mechanisms of lipotoxicity and diabetes progression.

## Chapter 4

### Intracellular functions regulated by PI3K-C2 $\alpha$

#### Cell viability

##### 4.1 Introduction

As mentioned in the previous chapter, the transition to overt diabetes is characterised by a failure of pancreatic  $\beta$  cells, in terms of insulin secreting function, pancreatic  $\beta$  cell mass and viability (Muio and Newgard 2008). Increased  $\beta$  cell mass and function resulting from the correct balance between pancreatic  $\beta$  cell neogenesis, proliferation and cell size allows the organism to respond to defects in insulin signalling (insulin resistance). The failure of  $\beta$  cell to compensate is responsible for the progression of diabetes (Bonner-Weir 2000).

Class I PI3Ks have a well established role in regulating cell mass, as they are activated upon serum and growth factors stimulation and they induce activation of several downstream effectors, including Akt (Franke et al. 1997). This leads to stimulation of cell proliferation, survival, growth and inhibition of apoptotic mechanisms in multiple organs (Elghazi et al. 2007).

Interestingly, studies on class II PI3Ks also outlined a role for the enzyme PI3K-C2 $\alpha$  in regulation of cell survival. Specifically, downregulation of PI3K-C2 $\alpha$  is associated with increased apoptosis in cancer and endothelial cell lines (Elis et al. 2008, Yoshioka et al. 2012, Tibolla et al. 2013). In contrast with these data, downregulation of PI3K-C2 $\alpha$  in L6 cells did not affect cell proliferation (Falasca et al. 2007), and only slightly increased the percentage of INS1 cells in the sub-G1 phase of the cell cycle, at least in normal growing conditions (Dominguez et al. 2011). However, the effect of PI3K-C2 $\alpha$  downregulation on cell survival in lipotoxic growth conditions, mimicking the metabolic alterations typical of diabetic patients, was not assessed in the previous study. Therefore, the possibility that the lipotoxicity-induced downregulation of PI3K-C2 $\alpha$  underlies the reduced cell proliferation/survival in INS1 cells was examined.

Moreover, it has been reported that glucose deprivation can contribute to  $\beta$  cell death through induction of apoptotic process (Guillen et al. 2008). The correct functioning of pancreatic  $\beta$  cells ensures the essential function of glucose homeostasis. In most cell types, glucose metabolism depends on ATP and metabolic requirements, while in pancreatic  $\beta$  cells it is modulated by glucose catabolism and glycaemia. Glucose sensing and metabolism are critical for pancreatic  $\beta$  cell function, in order to ensure an appropriate insulin secretion rate.

The central role of glucose in pancreatic  $\beta$  cells is also underlined by other findings: glucose alone can induce cell proliferation in INS1 cells, upon 24 hours of nutrients

deprivation (Hugl et al. 1998). Indeed, it was shown that glucose deprivation (0 - 0.5 mM) inhibited proliferation in INS1 cells, inducing a quiescent state. Substimulatory concentrations of glucose alone (1 - 3 mM) induced a modest increase in INS1 proliferation, up to 1.4 fold compared to glucose deprived cells, while stimulatory concentrations (6 - 18 mM) were able to increase proliferation of INS1 cells up to 20 fold (Hugl et al. 1998). In addition, it was reported that glucose can potentiate the mitogenic signals induced by IGF1 and growth hormone (GH) (Hugl et al. 1998, Cousin et al. 1999), stimulate the activity of PI3Ks (Cousin et al. 2001) and that PI3Ks have a role in glucose-dependent mitogenesis (Hugl et al. 1998, Cousin et al. 1999). Interestingly, further studies on glucose and IGF1-dependent  $\beta$  cell proliferation demonstrated that a constitutive activation of class I PI3Ks (which on its own did not affect  $\beta$  cell proliferation) was able to enhance IGF1-dependent mitogenesis, with no further increase when the cells were stimulated with 15 mM glucose alone (Dickson et al. 2001). This result suggests that the proliferation signalling triggered by glucose is mediated by another enzyme/class of enzymes than class I PI3K.

Therefore, the potential contribution of PI3K-C2 $\alpha$  to the glucose-induced proliferation/survival was investigated.



## 4.2 Results

### 4.2.1 Downregulation of PI3K-C2 $\alpha$ does not sensitise INS1 cells towards death in lipotoxic conditions

In order to determine the potential role of PI3K-C2 $\alpha$  in regulation of cell survival, I used stable cell lines previously generated in my laboratory. INS1 'sh PI3K-C2 $\alpha$ ' and 'sh scrambled' were obtained by retroviral infection of rat insulinoma cells INS1. The constructs used contained shRNA oligomers designed based on the sequence of rat PI3K-C2 $\alpha$  and a scrambled control (Dominguez et al. 2011). The shRNA construct targeting PI3K-C2 $\alpha$ , once introduced in INS1 cells, is able to downregulate both PI3K-C2 $\alpha$  mRNA and protein expression levels, without affecting the expression of other PI3Ks (Dominguez et al. 2011).

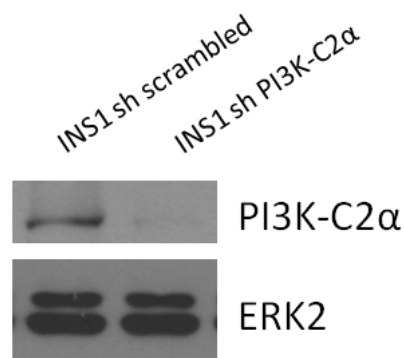


**Figure 4.1:** Expression levels of PI3K-C2 $\alpha$  were analysed by Western blot analysis in stable INS1 sh scrambled and INS1 sh PI3K-C2 $\alpha$  cells. A representative blot is shown.

Western blot analysis confirmed downregulation of PI3K-C2 $\alpha$  in the corresponding stable cell line, compared to the control scrambled cells (Figure 4.1), as previously described (Dominguez et al. 2011). Importantly, it was reported that INS1 sh PI3K-C2 $\alpha$  cells do not present any defect in terms of proliferation, compared to the scrambled control (Dominguez et al. 2011).

First, I investigated the effects of PI3K-C2 $\alpha$  downregulation on cell viability in lipotoxic conditions. INS1 sh scrambled and INS1 sh PI3K-C2 $\alpha$  cells were plated in 6-wells plates and incubated in normal growth medium, supplemented with 1% FFA-BSA and increasing concentrations of sodium palmitate, for 24 or 48 hours. Then, they were trypsinised, collected and manually counted in a Bürker chamber.

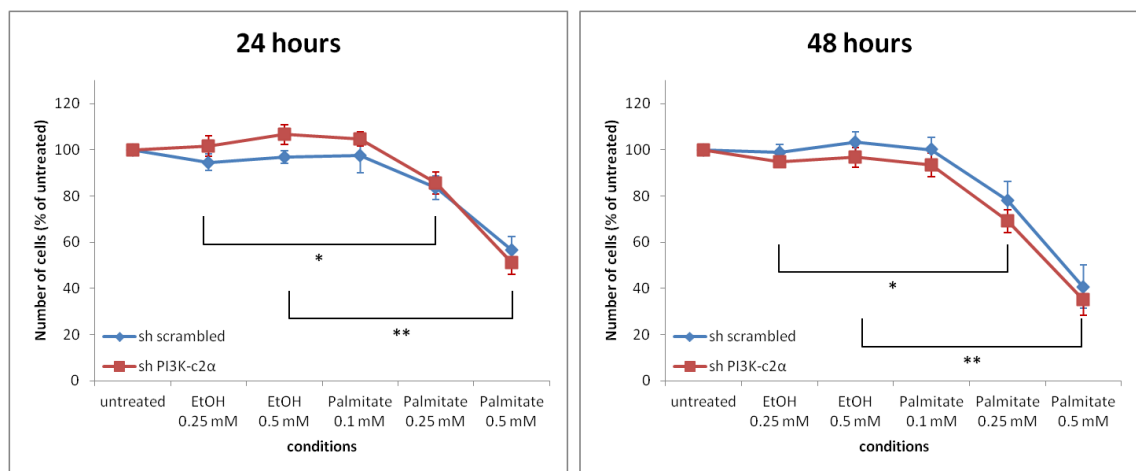


**Figure 4.2: Cell viability of INS1 sh scrambled and sh PI3K-C2 $\alpha$  in the presence of palmitate. Stable INS1 cell lines expressing a shRNA specifically targeting PI3K-C2 $\alpha$  or a scrambled shRNA were treated with the indicated concentrations of palmitate or vehicle alone. Number of cells was determined after 24h or 48h by manual counting. Data are expressed as percentage of untreated cells and are means  $\pm$  s.e.m. from 4 independent experiments performed in duplicate. \* $p$ <0.05; \*\* $p$ <0.01 vs corresponding control treated with ethanol.**

As shown in Figure 4.2, a significant reduction in the number of cells was detected upon 24 and 48 hours treatment with sodium palmitate. Consistent with data in literature, these results indicated that lipotoxic conditions reduce cell viability of INS1. No difference was observed between INS1 sh scrambled and sh PI3K-C2 $\alpha$  cells, suggesting that downregulation of PI3K-C2 $\alpha$  does not enhance cell death in lipotoxic growth conditions.

To further validate these results, MTT assay was performed to assess cell viability. The MTT assay is based on the cleavage of the yellow MTT [3-(4,5-Dimethylthiazol-2-yl)-2,5-diphenyltetrazolium bromide] to a purple formazan by mitochondrial succinate dehydrogenase of living cells (Loveland et al. 1992). The amount of formazan is proportional to the number of living cells present during the incubation with MTT. Cells were treated as described before and incubated with MTT solution during the final 3 hours of treatment. Then, cells were lysed in DMSO and absorbance was read with a spectrophotometer (using a wavelength of 570nm and subtracting a background measurement at 650nm).

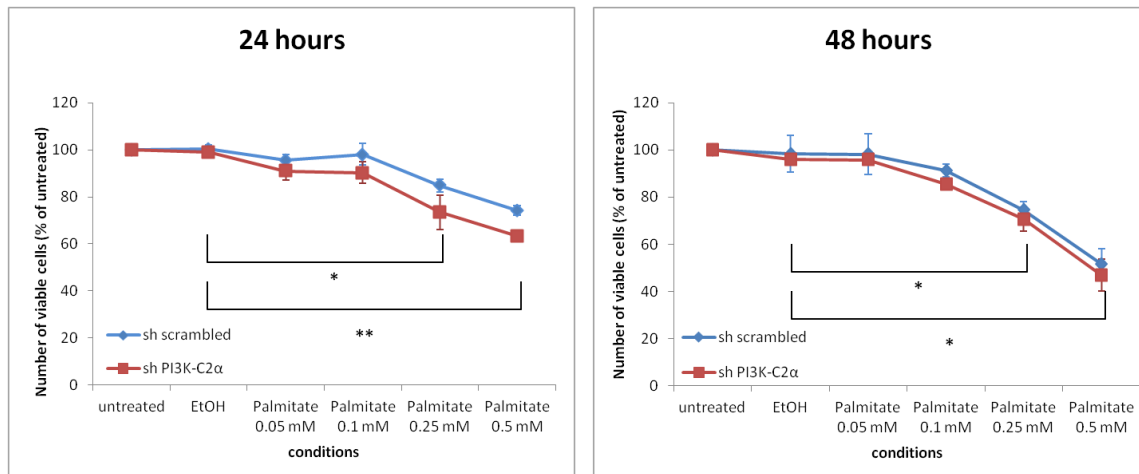


**Figure 4.3: Cell viability of INS1 sh scrambled and sh PI3K-C2α in the presence of palmitate. Stable INS1 cell lines expressing a shRNA specifically targeting PI3K-C2α or a scrambled shRNA were treated with the indicated concentrations of palmitate or vehicle alone. Cell viability was determined after 24h or 48h by MTT assay. Data are expressed as percentage of untreated cells and are means  $\pm$  s.e.m. from 3 independent experiments performed in duplicates. \* $p < 0.05$ ; \*\* $p < 0.01$  vs corresponding control treated with ethanol.**

Consistent with results from cell counting, MTT assay showed a decrease in cell viability in response to increasing concentrations of sodium palmitate. Furthermore, downregulation of PI3K-C2α did not alter the effect of palmitate on cell viability.

Taken together, these data indicate that downregulation of PI3K-C2α does not sensitise pancreatic  $\beta$  cells towards death when cultured in lipotoxic growth conditions.

#### **4.2.2 Glucose alone is able to sustain survival of INS1 cells upon nutrients deprivation**

One of the mechanisms that allows the progression of diabetes is a decrease in  $\beta$  cell mass, as a result of reduced proliferation and increased cell death. Several lines of

evidence highlight the role of glucose as a key regulator of proliferation in pancreatic  $\beta$  cells (Bonner-Weir et al. 1989). It was previously reported that glucose-dependent proliferation in  $\beta$  cells requires activation of mTOR, a key regulator of cell proliferation, and its downstream effector S6K, independently of Akt activation (Dickson et al. 2001).

In order to determine whether glucose can also stimulate cell survival, INS1 cells were incubated with serum free RPMI, supplemented with 0.5 mM glucose and 1% fresh glutamine (hereinafter referred to as 'nutrients deprivation') for 24 hours. Then, stimulatory concentrations of glucose (15 mM) were re-introduced in the serum-free medium for further 24 or 48 hours. Control cells were left in the absence of serum and reduced glucose levels.

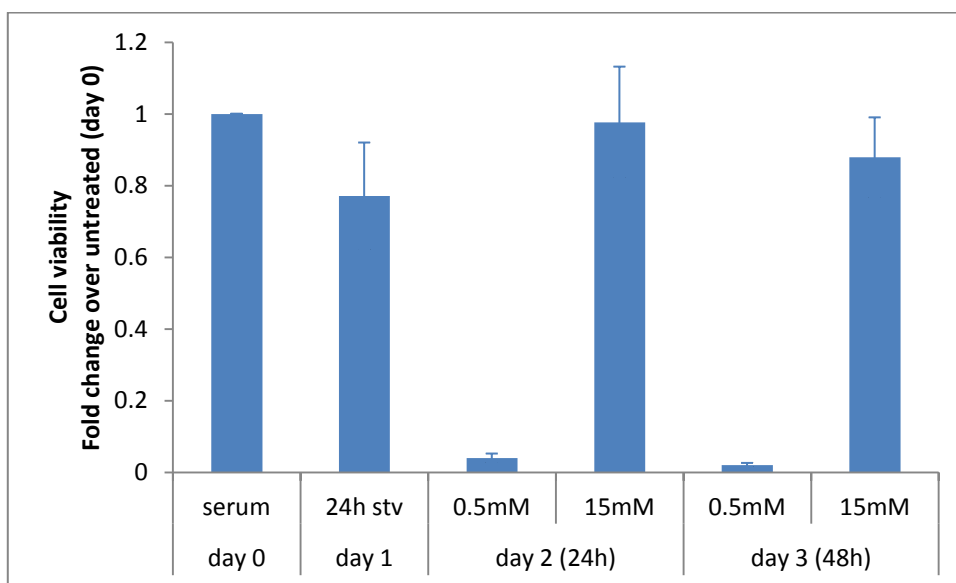


**Figure 4.4: Cell viability upon nutrients deprivation and glucose reintroduction.** INS1 cells were deprived of nutrients for 24 hours and then incubated with the indicated concentrations of glucose. Cell viability was assessed by MTT assay. Data are expressed as fold increase relative to day 0 and are means  $\pm$  s.e.m. from 3 independent experiments performed in duplicate.

Results from these experiments are presented in Figure 4.4. The viability of INS1 cells dramatically decreased when cells were cultured for more than 24 hours in serum and glucose starvation. Interestingly, after 24 hours of nutrients deprivation, re-introduction of 15 mM glucose alone was able to induce survival in INS1 cells, protecting them from death for further 48 hours.

### **4.2.3 Glucose rescue upon nutrient deprivation is not inhibited by classical PI3Ks inhibitors**

PI3Ks are activated following several extracellular stimuli and their action triggers a plethora of intracellular responses. Previous studies have shown that PI3Ks activity is important for glucose-dependent  $\beta$ -cell mitogenesis and that glucose is able to activate PI3Ks (Cousin et al. 2001).

Therefore, in order to test whether glucose-induced survival signal is transmitted intracellularly through PI3K family, I tested the effect of classical PI3Ks inhibitors wortmannin and LY294002.

As described in the previous experiment, INS1 cells were deprived from serum and glucose for 24 hours and then they were incubated in serum free RPMI supplemented with 15mM glucose for further 24 or 48 hours, in the presence or absence of 100nM wortmannin. At this concentration, wortmannin is able to irreversibly inhibit all the PI3K isoforms except PI3K-C2 $\alpha$ , by binding covalently to

the enzymes. Control cells were left in nutrients deprivation, with or without wortmannin.

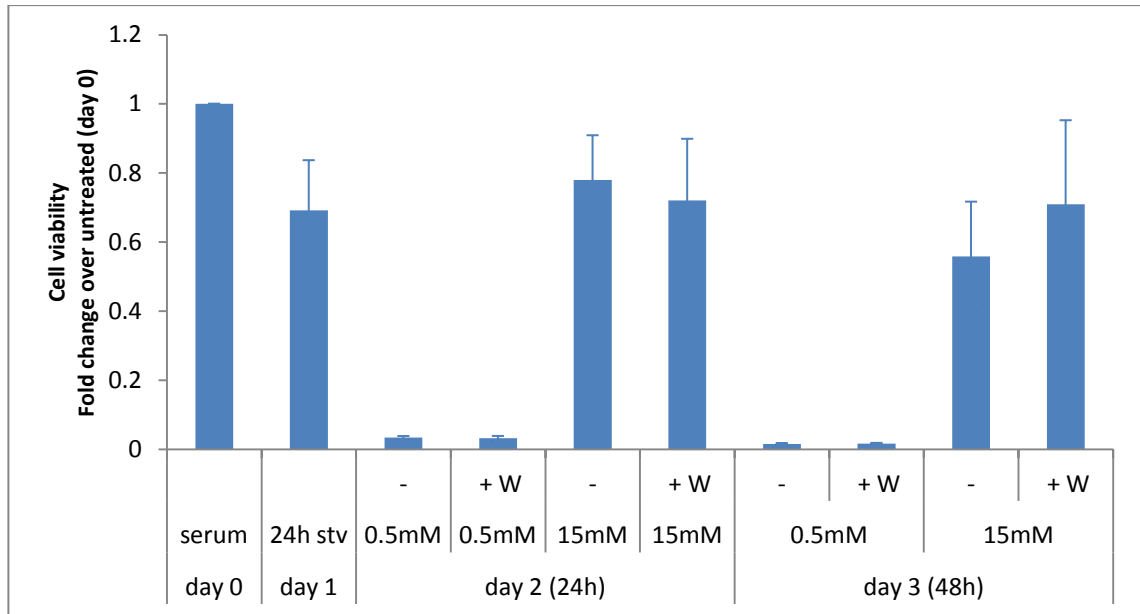


**Figure 4.5: Cell viability upon nutrients deprivation and glucose reintroduction, in the presence or absence of wortmannin.** INS1 cells were deprived of nutrients for 24 hours and then incubated with the indicated concentrations of glucose. Classical PI3Ks inhibitor wortmannin (W) was used at a concentration (100nM) that is effective on all PI3Ks isoforms except PI3K-C2 $\alpha$ . Cell viability was assessed by MTT assay. Data are expressed as fold increase relative to day 0 and are means  $\pm$  s.e.m. from 3 independent experiments performed in duplicate.

Results from these experiments are shown in Figure 4.5: as previously shown, re-introduction of glucose alone was able to induce cell survival for further 48 hours. Also, in these experimental conditions, treatment with wortmannin did not affect glucose-induced cell survival. Similar results were obtained by cell counting (experiments performed by Dr. Maffucci).

I then tested the effect of another classical PI3Ks inhibitor, LY294002, which is an ATP-competitive inhibitor able to bind PI3Ks in a reversible manner and is structurally unrelated to wortmannin (Blommaert et al. 1997).

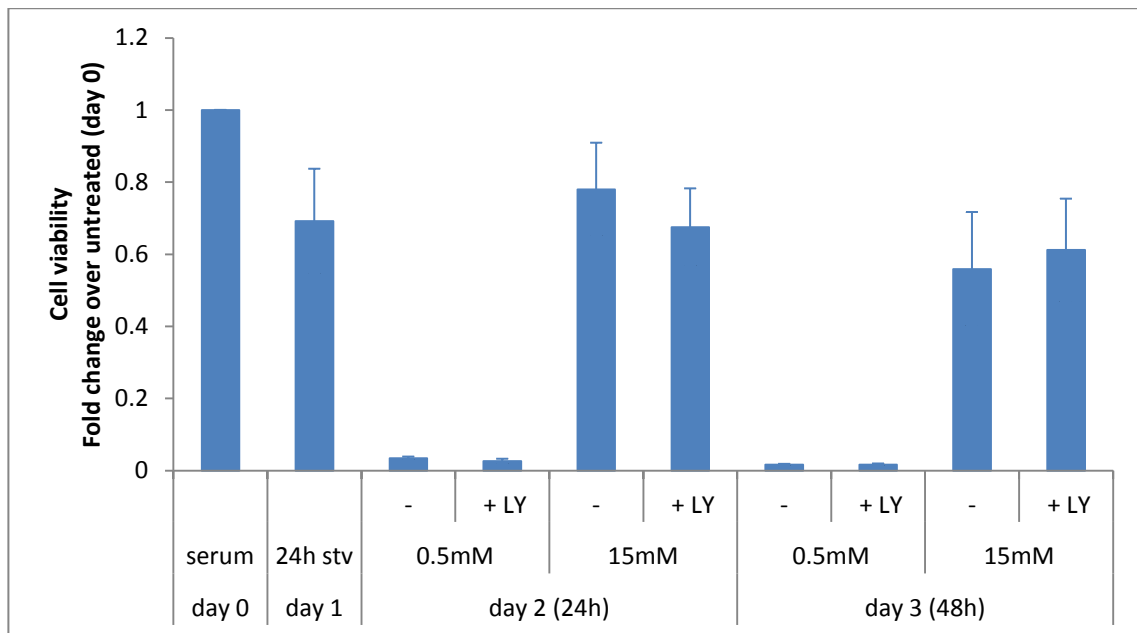


**Figure 4.6: Cell viability upon nutrients deprivation and glucose reintroduction, in the presence or absence of LY294002. INS1 cells were deprived of nutrients for 24 hours and then incubated with the indicated concentrations of glucose. Classical PI3Ks inhibitor LY294002 (LY) was used at a concentration (10 $\mu$ M) that is effective on all PI3Ks isoforms except PI3K-C2 $\alpha$  and, to a lesser extent, PI3K-C2 $\beta$ . Cell viability was assessed by MTT assay. Data are expressed as fold increase relative to day 0 and are means  $\pm$  s.e.m. from 3 independent experiments performed in duplicate.**

Consistent with data obtained with wortmannin, glucose alone was able to protect INS1 cells from death induced by nutrients deprivation. Data showed that LY294002 did not affect the protective effect of glucose in INS1 cells after 24 or 48 hours of treatment. Similar results were obtained by cell counting (experiments performed by Dr. Maffucci).



These data indicate that glucose-induced cell survival is not inhibited by classical PI3K inhibitors. This suggests that the intracellular signalling activated by glucose in this context is either mediated by another enzyme/class of enzymes or it involves the activation of PI3K-C2 $\alpha$ , which is insensitive to the concentration of inhibitors used in these experiments.

#### **4.2.4 Glucose-induced survival upon nutrient deprivation requires the activation of PI3K-C2 $\alpha$**

In order to determine whether PI3K-C2 $\alpha$  is required for glucose-induced cell survival, INS1 sh scrambled and sh PI3K-C2 $\alpha$  cells were used.

Following the same protocol used for the previous experiments, both INS1 sh scrambled and sh PI3K-C2 $\alpha$  cell lines were seeded in 6 wells plates and starved for 24 hours from serum and glucose. Then, they were incubated with serum free RPMI medium supplemented with 15mM glucose.

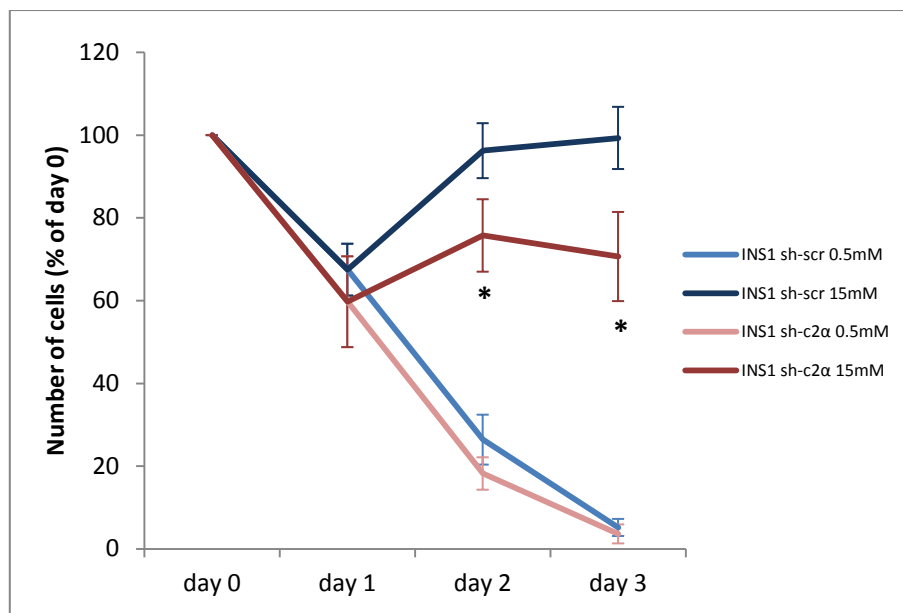


**Figure 4.7: Cell viability assessed by manual cell counting - Effect of downregulation of PI3K-C2α on cell viability upon nutrients deprivation and glucose reintroduction. Stable INS1 cell lines were deprived of nutrients for 24 hours and then incubated with 15 mM glucose or left in nutrients deprivation. Data are expressed as percentage relative to day 0 and are means ± s.e.m. from 5 independent experiments performed in duplicates. \*p<0.01 vs corresponding value in sh scrambled cells.**

Consistent with the data previously shown, cell viability was significantly ameliorated by reintroduction of stimulatory glucose concentration after 24 hours of nutrients deprivation in both cell lines (Figure 4.7). Glucose reintroduction was able to induce survival in INS1 sh scrambled and sh PI3K-C2α cells for further 48 hours, compared to cells left in nutrients deprivation.

Interestingly, INS1 sh PI3K-C2α cells showed a decreased viability compared to the scrambled control upon glucose reintroduction, at both 24 and 48 hours post treatment. These data indicate that downregulation of PI3K-C2α in INS1 cells impairs the protective effect of glucose reintroduction and, as a consequence, the viability of sh PI3K-C2α cells is significantly reduced compared to control cells.

In order to confirm these data, similar experiments were performed using MTT assay. Cells were plated in 12 wells plates and duplicates were analysed for each condition.

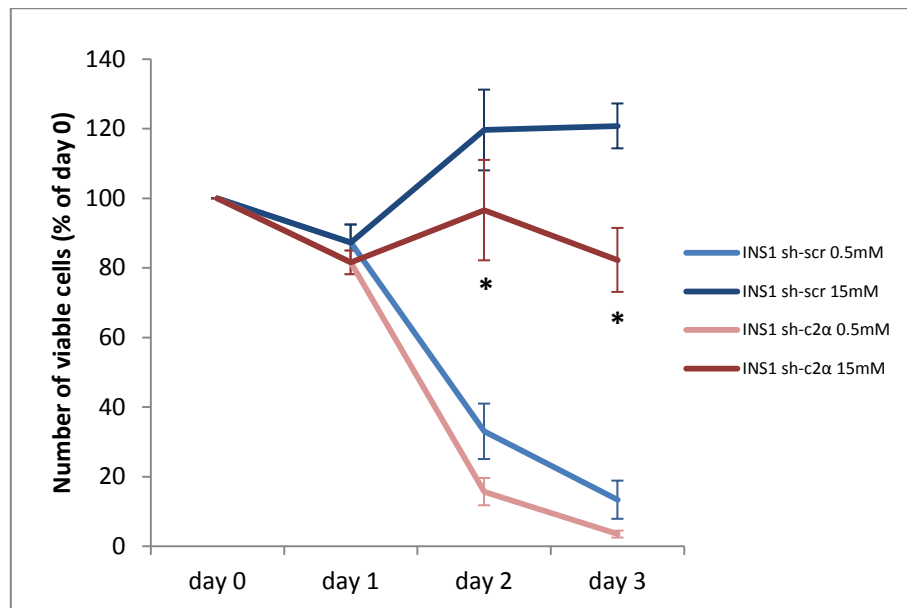


**Figure 4.8: Cell viability assessed by MTT assay - Effect of downregulation of PI3K-C2 $\alpha$  on cell viability upon nutrients deprivation and glucose reintroduction. Stable INS1 cell lines were deprived of nutrients for 24 hours and then incubated with 15 mM glucose or left in nutrients deprivation. Data are expressed as percentage relative to day 0 and are means  $\pm$  s.e.m. from 4 independent experiments performed in duplicates. \* $p < 0.01$  vs corresponding value in sh scrambled cells.**

Consistent with results from cell counting experiments, INS1 sh PI3K-C2 $\alpha$  cells showed a significantly decreased viability, compared to the scrambled control upon nutrients deprivation and glucose reintroduction (Figure 4.8).

Taken together, these data indicate that PI3K-C2 $\alpha$  is involved in glucose-induced survival of INS1 cells following nutrients deprivation. These data, together with data

obtained with classical inhibitors previously performed in my laboratory, indicate that reintroduction of stimulatory concentrations of glucose is able to protect INS1 from cell death induced by nutrients and glucose deprivation, through a mechanism that specifically involves the action of PI3K-C2 $\alpha$  and not other PI3Ks.

In order to further investigate the mechanisms of glucose-induced survival in INS1 cells, I assessed the effect of substimulatory glucose concentrations in these experimental conditions (Briaud et al. 2003).

To this end, INS1 sh scrambled and sh PI3K-C2 $\alpha$  cell lines were starved for 24 hours from serum and glucose. Then, they were incubated with serum free RPMI supplemented with 3 mM glucose (substimulatory concentrations) or left in starvation medium as a control.

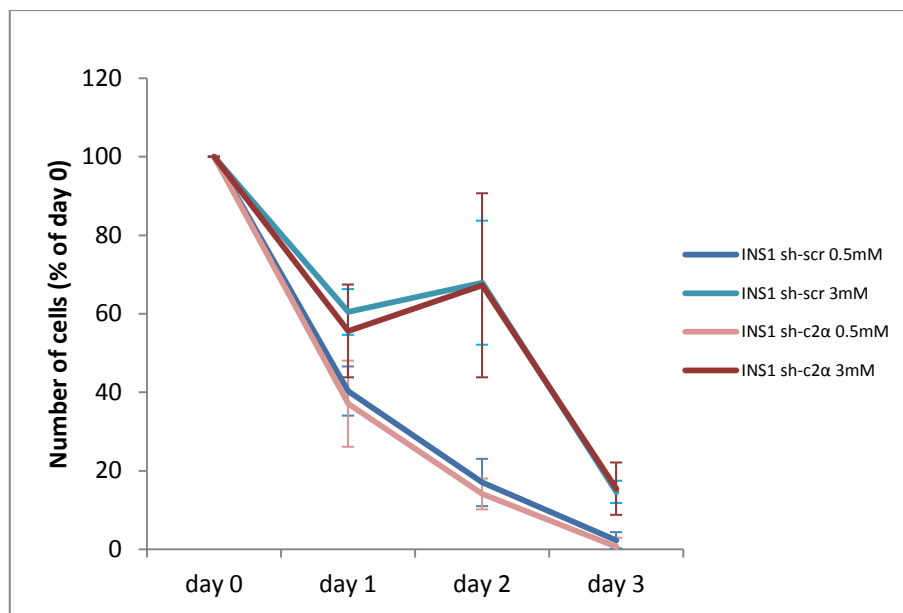


**Figure 4.9: Cell viability assessed by manual cell counting - Effect of downregulation of PI3K-C2α on cell viability upon nutrients deprivation and reintroduction of stimulatory or substimulatory glucose concentrations. Stable INS1 cell lines were deprived of nutrients for 24 hours and then incubated with 3 mM glucose or left in nutrients deprivation. Data are expressed as percentage relative to day 0 and are means  $\pm$  s.e.m. from 2 independent experiments performed in duplicates.**

Data show that after 24 hours in starvation medium the proliferation of both cell lines arrested and cell viability was slightly decreased (Figure 4.9). When cells were left in starving conditions for further 24 or 48 hours, cell viability dramatically and rapidly reduced, with no difference between the two cell lines. Reintroduction of a substimulatory concentration of glucose was able to protect INS1 from cell death for further 24 hours, but cell viability then decreased. The survival curves observed in these experimental conditions were comparable between INS1 sh scrambled and sh PI3K-C2α cells. This indicates that PI3K-C2α is not required for cell survival induced by reintroduction of substimulatory glucose concentrations.

In order to confirm the data obtained with cell counting, similar experiments were performed using MTT assay. Cells were plated in 12 wells plates, using duplicates for each condition.

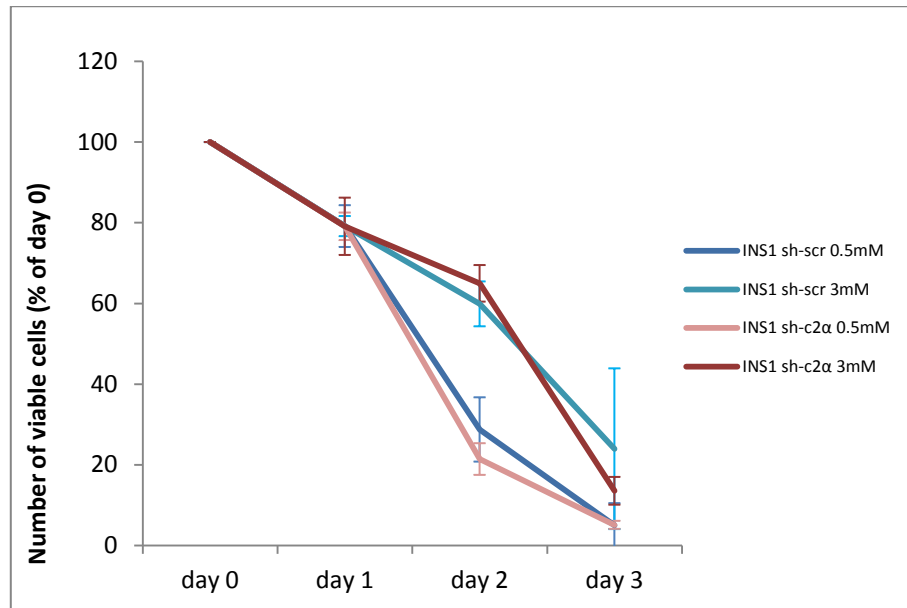


**Figure 4.10:** Cell viability was assessed by MTT assay - Effect of downregulation of PI3K-C2 $\alpha$  on cell viability upon nutrients deprivation and reintroduction of stimulatory or substimulatory glucose concentrations. Stable INS1 cell lines were deprived of nutrients for 24 hours and then incubated with 3 mM glucose or left in nutrients deprivation. Data are expressed as percentage relative to day 0 and are means  $\pm$  s.e.m. from 2 independent experiments performed in duplicates.

As observed in cell counting experiments, cells growing in serum and glucose deprivation for more than 24 hours showed a rapid decrease in cell viability. Introduction of a substimulatory concentration of glucose induced cell survival for further 24 hours before significantly decreasing cell viability. As observed before,

downregulation of PI3K-C2 $\alpha$  did not affect cell viability compared to control cells in these experimental conditions (Figure 4.10).

These data indicate that substimulatory concentration (3 mM) of glucose is less effective in preventing cell death compared to reintroduction of stimulatory concentration (15 mM) glucose, upon 24 hours of nutrients deprivation. Interestingly, using substimulatory glucose concentrations, the survival of control cells was comparable to that observed in PI3K-C2 $\alpha$  knock down cells, while a significant difference between the two cell lines was observed upon reintroduction of glucose at stimulatory concentrations. This suggests that PI3K-C2 $\alpha$  is involved in cell survival triggered by stimulatory but not by substimulatory concentrations of glucose. Furthermore, after 24 hours of glucose reintroduction, the number of surviving cells is higher upon reintroduction of 15 mM glucose compared to 3 mM glucose. Based on this observation, it is possible to conclude that reintroduction of 15 mM glucose induces both cell survival and proliferation.

#### **4.2.5 Nutrients deprivation and apoptosis**

MTT and cell counting assays can quantitatively evaluate the viability of cellular populations, with no indication on the ongoing cellular death processes. My data indicated that 24 hours of nutrients deprivation caused a slight decrease in INS1 cells viability and that downregulation of PI3K-C2 $\alpha$  was responsible for a reduced cellular response to stimulatory concentrations of glucose. Therefore, I decided to

investigate whether the observed decrease in cell viability was caused by increased apoptosis. Also, in order to analyse the specific role for PI3K-C2 $\alpha$  in this context and in the aforementioned experimental conditions, I sought to assess whether the improvement in cell viability upon reintroduction of stimulatory concentration of glucose occurred through inhibition of apoptosis.

The protein caspase 3 is a critical executioner of apoptosis and it is activated by cleavage of its aspartic acid residue (Asp 175). This converts the inactive zymogen into activated fragments of 17 and 12 kDa, which are detectable by Western Blot analysis and their formation is used to assess an ongoing apoptotic process.

Therefore, I performed a Western Blot analysis on INS1 sh scrambled and INS1 sh PI3K-C2 $\alpha$  cells upon nutrients deprivation and reintroduction of stimulatory concentrations of glucose, as previously described, using specific antibodies recognising the uncleaved form and the cleaved fragments of caspase 3.



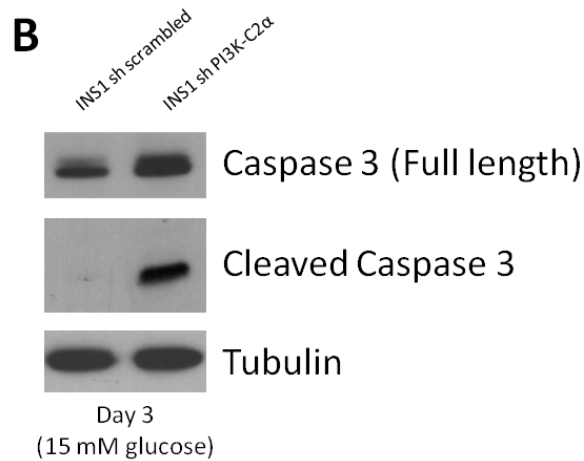
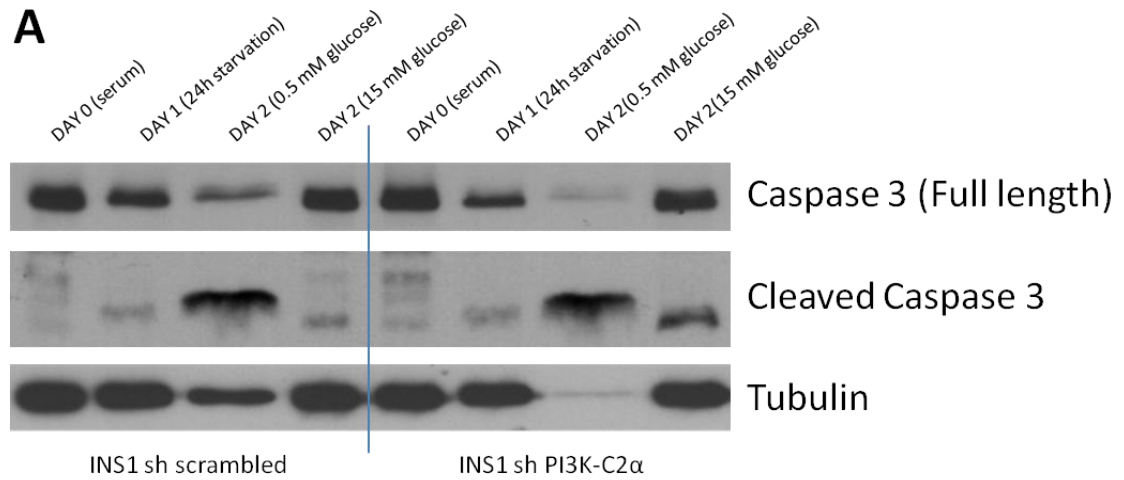


**Figure 4.11: Activation of caspase 3 upon nutrients deprivation and glucose reintroduction. Stable INS1 cell lines were deprived of nutrients for 24 hours and then incubated with the indicated concentrations of glucose. Lysates were analysed by Western Blot analysis and incubated with an antibody anti caspase 3, detecting both the full length protein and the cleaved fragments. Representative blot of 3 independent experiments is shown.**

Results showed that nutrients deprivation induced the accumulation of the cleaved fragment of caspase 3, indicating that apoptosis was activated in both INS1 sh scrambled and sh PI3K-C2α cell lines, following 24 hours of starvation (Day 1, Figure 4.11). After further 24 hours of nutrients deprivation, the fragment corresponding to cleaved caspase 3 had an increased intensity (Day 2, 0.5mM glucose), indicating that

apoptosis was fully ongoing in these experimental conditions. Interestingly, reintroduction of stimulatory glucose concentrations in sh scrambled cells decreased the amount of cleaved caspase 3 (Day 2, sh scrambled 15mM glucose), compared to samples kept in starvation medium. This data indicates that stimulatory glucose concentrations are able to inhibit the apoptotic process, protecting cells from death. The protective effect of stimulatory concentrations of glucose was even more evident when analysing samples from sh scrambled cells upon 48 hours of glucose reintroduction (Day 3, sh scrambled 15mM glucose), where caspase 3 fragment is no longer detectable. This further suggests an effective inhibition of the apoptotic process in these experimental conditions. These data are consistent with the increase in cell viability observed in INS1 sh scrambled cells upon reintroduction of stimulatory glucose concentrations described in Chapter 4.2.4.

Interestingly, a clear band corresponding to cleaved caspase 3 fragment was still detectable in INS1 sh PI3K-C2 $\alpha$  cells upon glucose reintroduction (Day 2, sh PI3K-C2 $\alpha$  15mM glucose). This indicates that INS1 sh PI3K-C2 $\alpha$  cells have a reduced ability to stop the apoptotic process, compared to the scrambled control, and therefore are more prone to cell death in these experimental conditions. This observation is even clearer upon 48 hours treatment with stimulatory glucose concentrations in PI3K-C2 $\alpha$  knock down cells (Day 3, sh PI3K-C2 $\alpha$  15mM glucose), since cleaved caspase 3 fragment is still intense and clearly detectable by Western blot analysis. This further suggests that reintroduction of glucose is not able to inhibit apoptosis in PI3K-C2 $\alpha$

knock down cells in these experimental conditions, and is consistent with the data on cell viability showed in Figures 4.7 and 4.8.

#### **4.2.6 Nutrients deprivation and autophagy**

Autophagy is a critical process for cellular homeostasis. It ensures the recycling of damaged cellular components and misfolded proteins, which are enclosed in intracellular vacuoles (autophagosomes), then fused to lysosomes and degraded to simpler molecules (mostly amino acids). This, at the same time, supplies the cells with amino acids, which can be used for the synthesis of new proteins, especially during periods of starvation. It is a finely regulated process, essential for survival in a low energy state, but it can lead to cell death when it is deregulated, or during prolonged starvation. Recent data in literature demonstrate that basal autophagy is particularly important for the homeostasis of pancreatic  $\beta$  cells, contributing to their survival (Ebato et al. 2008, Jung et al. 2008)

Data in section 4.2.2 showed that nutrient deprivation induces apoptosis in INS1 cells. I then decided to investigate whether autophagy is also involved in these experimental conditions. Therefore, INS1 cells were deprived from nutrients for 24h and then incubated with serum free medium containing 15mM glucose, as previously described. Cellular lysates were then analysed by Western Blot using antibodies anti Light chain 3 (LC3), which is a commonly used autophagy marker. LC3 is detected as two bands, LC3-I (16-18 kDa) and LC3-II (14-16). LC3-I is the cytosolic

form of the protein, which is post transcriptionally modified with a phosphatidylethanolamine (PE) tag (and converted to LC3-II) when it is bound to the autophagosome membrane during autophagy. Although LC3-II molecular weight is increased by the PE tag, due to its hydrophobicity it migrates faster than LC3-I in a Western blot gel and it appears as a band of lower molecular weight. The ratio between LC3-I and LC3-II provides an indicator of autophagic activity.

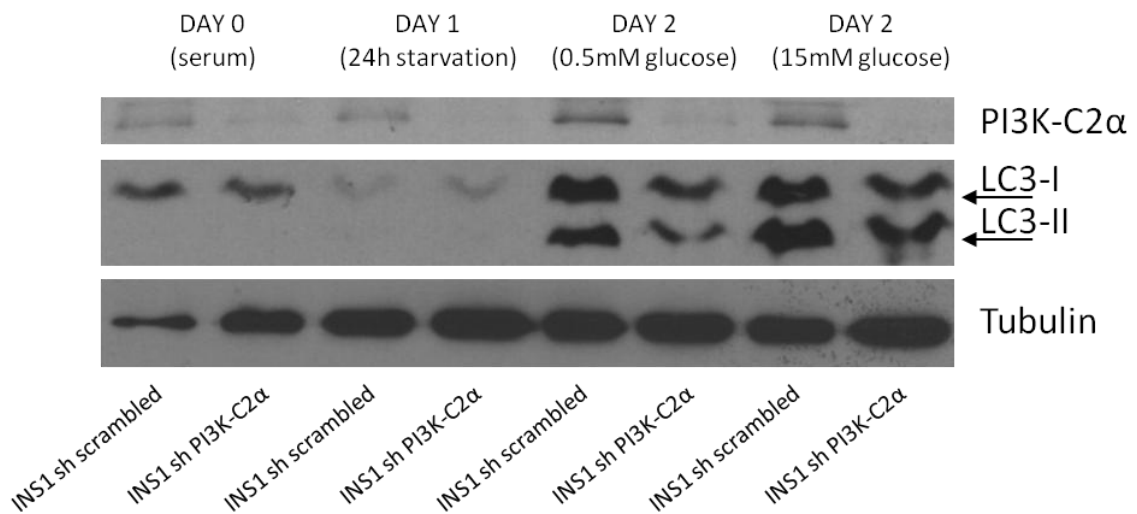


**Figure 4.12: Activation of autophagy upon nutrients deprivation and glucose reintroduction. Stable INS1 cell lines were deprived of nutrients for 24 hours and then incubated with the indicated concentrations of glucose. Lysates were analysed by Western Blot analysis and incubated with an antibody anti LC3. Tubulin was used as equal loading control. Representative blot of 3 independent experiments is shown.**

Results showed that, in these experimental conditions, nutrients deprivation induced an increase in the Western Blot band corresponding to LC3-II, suggesting an increase in autophagosomes formation (Figure 4.12). This suggests that an autophagic process is activated in these experimental conditions. Reintroduction of

stimulatory concentrations of glucose did not significantly modify the intensity of LC3-I and LC3-II bands compared to the control left in nutrients deprivation. Also, no difference was observed between scrambled and PI3K-C2 $\alpha$  knock down cells, indicating that reintroduction of glucose alone does not seem to inhibit autophagosome formation. Moreover, downregulation of PI3K-C2 $\alpha$  does not seem to affect the autophagic process.

### 4.3 Discussion

PI3Ks activity controls many intracellular functions, including cell proliferation, survival and growth. The fact that multiple isoforms of PI3Ks exist, and the unanswered questions on whether their roles are overlapping or redundant complicate the investigation of this class of enzymes. Recently, several lines of evidence suggest a role for the class II isoform PI3K-C2 $\alpha$  as a cellular survival factor. Specifically, downregulation of PI3K-C2 $\alpha$  in HUVEC cells increased apoptosis (Yoshioka et al. 2012, Tibolla et al. 2013) and decreased proliferation upon stimulation with serum (Yoshioka et al. 2012). Furthermore, knockdown of PI3K-C2 $\alpha$  also decreased proliferation and increased apoptosis in HeLa cells, without affecting class I PI3K/Akt survival pathway (Elis et al. 2008). Also, the viability of several cancer cell lines is affected upon downregulation of PI3K-C2 $\alpha$  and in normal growth conditions (Elis et al. 2008), although, in the pancreatic  $\beta$  cell line INS1, no significant modification of cell viability was observed upon downregulation of PI3K-C2 $\alpha$  (Dominguez et al. 2011).

The effect of PI3K-C2 $\alpha$  downregulation in pancreatic  $\beta$  cells upon stressful growth conditions was not investigated before. Therefore, I sought to investigate whether under adverse growth conditions PI3K-C2 $\alpha$  downregulation might sensitise INS1 cells towards death. First, I focused on lipotoxicity, since one of the common metabolic alterations caused by diabetes is an increased free fatty acids concentration in the bloodstream, which can negatively affect pancreatic  $\beta$  cell viability. Using INS1 sh

scrambled and sh PI3K-C2 $\alpha$  cell lines, I measured cell viability by both cell counting and MTT assay upon treatment for 24 and 48 hours with sodium palmitate. As expected, lipotoxic growth conditions caused a decrease in cell viability. Also, my results indicated that PI3K-C2 $\alpha$  downregulation did not render INS1 cells more prone to cell death, in these experimental conditions (Figures 4.2 and 4.3). Considering that treatment with sodium palmitate caused a significant decrease in the protein levels of PI3K-C2 $\alpha$  (Figure 3.5), the comparable decrease in viability upon palmitate treatment in the two cell lines can be due to a reduction of PI3K-C2 $\alpha$  levels in control cells. Sodium palmitate concentrations of 0.25 and 0.5 mM, which caused a decrease in cell viability (Figures 4.2 and 4.3), were also able to affect PI3K-C2 $\alpha$  protein levels in control cells (Figure 3.5), rendering them phenotypically similar to INS1 sh PI3K-C2 $\alpha$  cells. However, the fact that cell viability is only slightly affected by concentrations of palmitate (0.25 mM upon 24h treatment, Figures 4.2 and 4.3) that strongly affect the protein levels of PI3K-C2 $\alpha$  (Figure 3.5), suggests that PI3K-C2 $\alpha$  might not be involved in the regulation of cell viability, in these experimental conditions.

Then, I investigated the effects of other stressful growth conditions, such as nutrients deprivation, upon downregulation of PI3K-C2 $\alpha$ . Data in literature suggest the central role of glucose on  $\beta$  cell proliferation (Hugl et al. 1998, Cousin et al. 1999, Dickson et al. 2001, Briaud et al. 2003), although the molecular mechanisms underlying this intracellular signalling are not fully understood.

It was reported that stimulatory concentrations of glucose can induce cell proliferation, with a maximal effect observed using 15 mM glucose upon 24 hours of serum and glucose deprivation in INS1 cells (Hugl et al. 1998). The stimulatory effect of glucose is potentiated by treatment with IGF-1, while no significant proliferation effect is observed using glucose concentrations up to 3 mM, with or without IGF-1 (Hugl et al. 1998). Similar results were then obtained by the same group, using GH to potentiate glucose proliferation signal (Cousin et al. 1999). Interestingly, class I PI3Ks seem not to be involved in the intracellular signalling upon glucose stimulation. Indeed, constitutive activation of class I PI3K resulted in an enhanced IGF-1-induced proliferation, with no effect on glucose-induced signalling (Dickson et al. 2001).

This suggests that the intracellular signalling triggered by stimulatory glucose concentrations involves other enzymes rather than class I PI3Ks and therefore I decided to investigate the potential role of class II PI3K-C2 $\alpha$  in this context. To this end, INS1 sh scrambled and sh PI3K-C2 $\alpha$  cells were deprived from serum and nutrients for 24 hours and then incubated with serum free medium supplemented with 15 mM glucose. Consistent with data in literature, my data show that, upon 24 hours nutrient deprivation, glucose alone is able to protect INS1 cells from death, ameliorating cell viability upon treatment with a concentration of 3 mM glucose and with a further improvement on cell viability using 15 mM glucose.

My data show for the first time that the enzyme PI3K-C2 $\alpha$  is involved in the intracellular signalling of stimulatory concentrations of glucose, as INS1 cells



downregulating PI3K-C2 $\alpha$  show a decreased viability upon nutrients deprivation and glucose reintroduction, compared to the control (Figures 4.7 and 4.8). After the 24 hours starvation period and treatment of INS1 cells with serum free medium supplemented with substimulatory concentrations of glucose, no difference in cell viability was observed between sh scrambled and sh PI3K-C2 $\alpha$  cells. This suggests that the intracellular mechanisms activated by 3 or 15 mM glucose are distinct, and only 15 mM glucose stimulation is able to activate PI3K-C2 $\alpha$ . Furthermore, the extent of glucose-induced increase in cell viability depends on glucose concentration, being more pronounced with high glucose than with lower concentrations. This is in line with previous reports suggesting that both survival and proliferation mechanisms are activated upon high glucose stimulation (Hugl et al. 1998, Cousin et al. 1999, Dickson et al. 2001). Further studies are needed to investigate whether these intracellular mechanisms are activated upon these experimental conditions.

In addition, my data show that glucose-induced cell survival is not inhibited by classical PI3Ks inhibitors wortmannin and LY294002. This observation is consistent with data in literature showing that class I PI3Ks are not necessary for glucose-induced cell proliferation (Dickson et al. 2001) and further support the hypothesis that the intracellular signalling upon glucose stimulation is mediated by PI3K-C2 $\alpha$ , which is the only PI3K isoform resistant to both inhibitors (Domin et al. 1997).

An appropriate pancreatic  $\beta$  cell mass is the result of a balance between cell signals protecting from death (i.e. cell survival, proliferation, growth) and promoting death (i.e. apoptosis, necrosis). In order to study which cellular processes were responsible for the increase in cell viability upon treatment with stimulatory concentrations of glucose, I examined the activation of apoptosis and autophagy by Western Blot using the markers Caspase 3 and LC3, respectively. Results showed that nutrients deprivation in INS1 cells triggers both autophagy and apoptosis (Figures 4.11 and 4.12). Interestingly, autophagy was not reverted by the reintroduction of stimulatory concentrations of glucose (Figure 4.12) in the time frame examined. On the other hand, treatment with stimulatory glucose concentrations was able to gradually stop the apoptotic process (Figure 4.11), which is consistent with the observed increase in cell viability.

Furthermore, no difference was observed in terms of conversion from LC3-I to LC3-II upon downregulation of PI3K-C2 $\alpha$ , suggesting that PI3K-C2 $\alpha$  does not regulate autophagy in these experimental conditions. This is in contrast with the findings recently reported by Devereaux and colleagues, who showed that simultaneous downregulation of PI3K-C2 $\alpha$  and PI3K-C2 $\beta$  was able to affect autophagy (Devereaux et al. 2013). This discrepancy could be explained by the different cellular system and experimental conditions used, or with the potential compensatory role of PI3K-C2 $\beta$  in our experiments.

Interestingly, my data showed that downregulation of PI3K-C2 $\alpha$  has a role in overturning the apoptotic process upon reintroduction of stimulatory glucose concentrations. In fact, while treatment with glucose cause the progressive decrease of the fragment corresponding to cleaved caspase 3 in INS1 sh scrambled cells, the intensity of the band corresponding to the fragment does not decrease in PI3K-C2 $\alpha$  knock down cells, indicating the inability of this cell line to inhibit the apoptotic process upon treatment with stimulatory concentrations of glucose. This suggests that PI3K-C2 $\alpha$  is involved in the anti-apoptotic role of stimulatory glucose concentrations.

## Chapter 5

### Intracellular functions regulated by PI3K-C2 $\alpha$

#### Signalling pathways

##### 5.1 Introduction

In the previous chapter I described how class II PI3K-C2 $\alpha$  regulates a signalling pathway which is able to prevent death of pancreatic  $\beta$  cells upon nutrients deprivation and reintroduction of stimulatory concentrations of glucose.

In order to further investigate the intracellular mechanisms triggered by stimulatory concentrations of glucose, the activation of the mTOR pathway was examined. mTOR is a serine/threonine kinase which can interact with several other proteins, forming two different complexes named mTORC1 and mTORC2. The understanding of mTORC signalling is complex and, more than 20 years after mTOR discovery, is still evolving (Laplante and Sabatini 2012).

Both mTOR complexes are large (1 MDa). They share the catalytic core mTOR, mammalian lethal with Sec13 protein 8 (mLST8) and DEP domain-containing mTOR-interacting protein (DEPTOR). The other components of the complex are specific,

with mTORC1 being associated with the regulatory-associated protein of mTOR (raptor) and proline-rich Akt substrate of 40 kDa (PRAS40) while rapamycin insensitive companion of mTOR (rictor), mammalian stress-activated map kinase-interacting protein1 (mSin1) and protein observed with rictor (protor)1/protor2 interact with mTORC2 (Figure 5.1) (Mavrommati and Maffucci 2011).

The name mTOR was originally chosen as acronym of 'mammalian Target Of Rapamycin', (or, more recently, 'mechanistic TOR') because of the discovery that mTOR was the target of rapamycin, an antibiotic, immunosuppressive and anticancer drug discovered in 1975. Rapamycin forms a gain-of-function complex binding the regulatory protein FK506-binding protein (FKBP12), which can directly interact and inhibit mTOR when it is part of mTORC1 but not mTORC2 (Laplante and Sabatini 2012). As a result, the complex mTORC1 is rapidly and acutely inhibited by rapamycin, while mTORC2 is resistant to acute treatment and can be inhibited only by prolonged rapamycin treatment. The long-term inhibition of mTORC2 induced by rapamycin is probably due to the lack of free mTOR, as the complex cannot be incorporated into newly synthesised mTORC2 (Sarbasov et al. 2006, Xie and Herbert 2012).

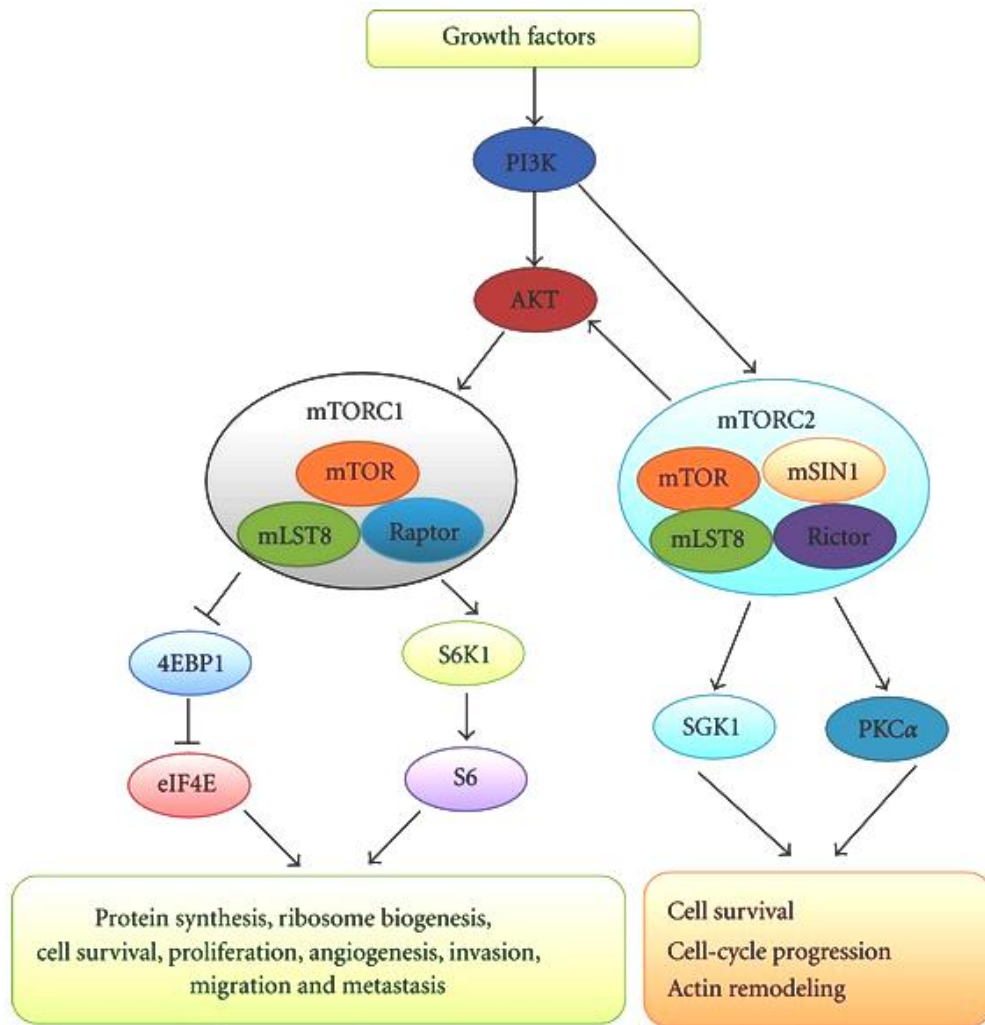


**Figure 5.1: Diagram of mTORC1 and mTORC2 components and intracellular functions. The two mTOR complexes have different downstream effectors (Gao et al. 2012).**

mTOR is an intracellular signalling hub which can integrate different cellular stimuli, such as nutrients availability, cellular stress, and growth factors stimulation, controlling anabolic or catabolic pathways based on the energy requirements. Its role is particularly important in pancreatic  $\beta$  cells, as it regulates  $\beta$  cell mass,

viability, function and metabolism, playing a crucial role especially during conditions of insulin resistance and  $\beta$  cell compensation (Xie and Herbert 2012).

Of the two mTOR complexes, mTORC1 is the best characterised (Laplante and Sabatini 2012). Its function is mediated mainly by its direct downstream target effectors 4EBPs and S6K (Figure 5.2), which are recruited through the specific mTORC1 component Raptor and phosphorylated by mTOR (Xie and Herbert 2012). Importantly, lack of S6K can cause a reduction in pancreatic endocrine mass and specifically it decreased pancreatic  $\beta$  cell size in knockout mice models (Pende et al. 2000). 4EBPs promote protein synthesis and cell cycle progression when hyperphosphorylated. Indeed, phosphorylation of 4EBPs leads to the release of eukaryotic translation initiation factor 4E and the expression, among others, of proteins promoting cell cycle progression (Wang and Proud 2009, Xie and Herbert 2012). Also, it has been reported that 4EBPs mediate mTORC1 proliferative signal and regulate cell proliferation in low serum conditions in MEFs (Dowling et al. 2010). Both mTORC1 and mTORC2 can be activated by growth factors and hormones. However, nutrients such as amino acids and glucose can only activate mTORC1 (Dann et al. 2007). Hormones and growth factors are able to activate mTORC1 through the canonical class I PI3K/Akt pathway (Dann et al. 2007, Vanhaesebroeck et al. 2010). It has also been reported that class III Vps34 is involved in mTORC1-dependent activation of S6K (Byfield et al. 2005).

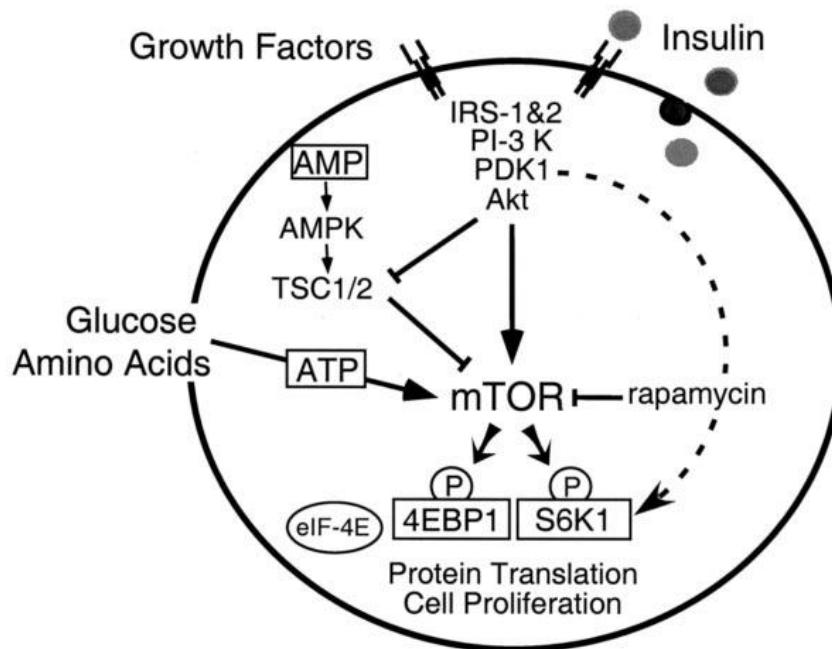


**Figure 5.2: Schematic diagram of mTORC1 signalling pathway. mTOR can be activated by a variety of stimuli, leading to protein translation and cell proliferation through its downstream effectors 4EBP1 and S6K (Kwon et al. 2004).**

In addition, it has been reported that glucose can indirectly activate mTORC1 signalling through the serine/threonine kinase AMPK. Specifically, AMPK acts as a cellular energy sensor, since it is allosterically activated by adenosine monophosphate (AMP) when the cell is in a low energy status (Hardie et al. 1999). Activation of AMPK causes its phosphorylation and subsequent inhibition of mTORC1, preventing the activation of intracellular anabolic pathways.

The fact that mTOR, and particularly mTORC1 can be activated by glucose, and can regulate both cell proliferation and cell size underlines its role in the context of T2D progression. Indeed, failure of pancreatic  $\beta$  cells observed in diabetic patients is due



to decrease in both  $\beta$  cell mass and size. As mentioned before, these processes are regulated, among others, by mTORC1 downstream effectors, S6K and 4EBP1.

Therefore, in this chapter I analysed the effects of glucose stimulation on the intracellular signalling involving mTOR pathway and the potential role of PI3K-C2 $\alpha$ .

## 5.2 Results

### 5.2.1 Effects of stimulatory glucose concentrations on the activation of mTOR and its direct downstream effectors in INS1 cells

Data presented in the previous chapter demonstrate that stimulatory concentrations of glucose can protect INS1 cells from death induced by nutrients deprivation, through an intracellular mechanism involving the enzyme PI3K-C2 $\alpha$ .

Since mTOR is one of the key regulators of cell proliferation, I decided to investigate whether stimulatory glucose concentrations were able to induce the activation of mTOR pathway by Western blot.

Previous studies have shown that phosphorylation of the residue Ser 2448 of mTOR depends on mTOR kinase activity and that this residue is not an autophosphorylation site (Sekulic et al. 2000). Subsequently it was reported that mTOR Ser 2448 phosphorylation is mediated by S6K (Chiang and Abraham 2005). These lines of evidence indicate that mTOR phosphorylation at its residue Ser 2448 occurs upon mTOR activation. Therefore, this specific post translational modification of mTOR can be used to monitor mTOR activity (Chiang and Abraham 2005, Subbiah et al. 2013).

INS1 cells were deprived from nutrients as previously described, and then left in nutrients deprivation or treated with stimulatory concentrations of glucose for further 24 hours.

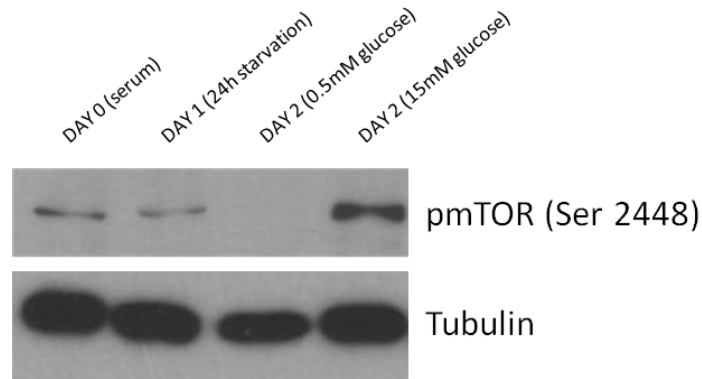


**Figure 5.3: Activation of mTOR upon nutrients deprivation and glucose reintroduction in INS1 parental cells.** INS1 cells were deprived from nutrients for 24 hours and then incubated in serum free medium supplemented with 15 mM glucose or left in nutrients deprivation. Lysates were analysed by Western Blot and incubated with a specific antibody recognising phosphorylated Ser 2448 of mTOR. Tubulin was used as loading control.

As shown in Figure 5.3, Ser 2448 of mTOR was phosphorylated in INS1 cells grown in complete medium. This indicated that mTOR was activated, contributing to the normal cell proliferation. Upon nutrients deprivation, phosphorylation of Ser 2448 of mTOR was progressively reduced. Reintroduction of stimulatory concentrations of glucose in the culture medium triggered the phosphorylation of this amino acid residue, indicating mTOR activation in these conditions.

In order to further investigate mTOR signalling cascade, phosphorylation of 4EBP1 was also examined. INS1 cells were deprived from nutrients for 24 hours as previously described, and then treated for further 24 hours with stimulatory concentrations of glucose or left in nutrients deprivation as a control.

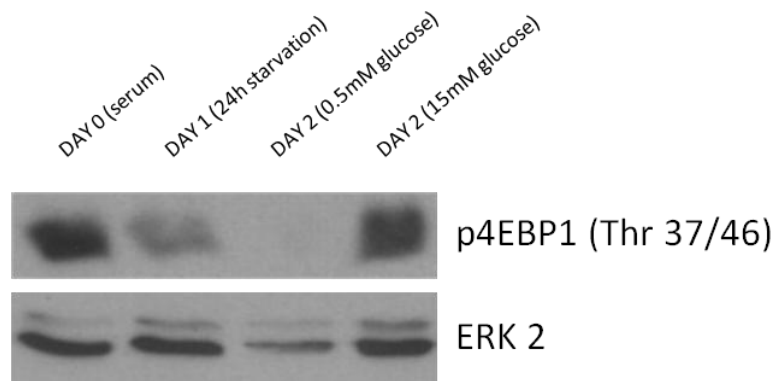


**Figure 5.4: Phosphorylation of 4EBP1 upon nutrients deprivation and glucose reintroduction.** INS1 cells were deprived from nutrients for 24 hours and then incubated in serum free medium supplemented with 15 mM glucose or left in nutrients deprivation. Lysates were analysed by Western Blot and incubated with a specific antibody recognising phosphorylated Thr 37/46 of 4EBP1. ERK2 was used as loading control.

Results showed that residues Thr 37/46 of 4EBP1 were phosphorylated in cells grown in complete medium. Upon nutrients deprivation, phosphorylation of 4EBP1 was gradually decreased, until it was undetectable upon 48 hours of nutrients deprivation. Reintroduction of stimulatory concentrations of glucose induced a strong phosphorylation of the residues Thr 37/46 of 4EBP1, indicating that glucose is able to induce activation of mTOR-dependent signals.

I then analysed the phosphorylation and activation of the protein S6K at its residue Thr 389, which is directly phosphorylated by mTOR.

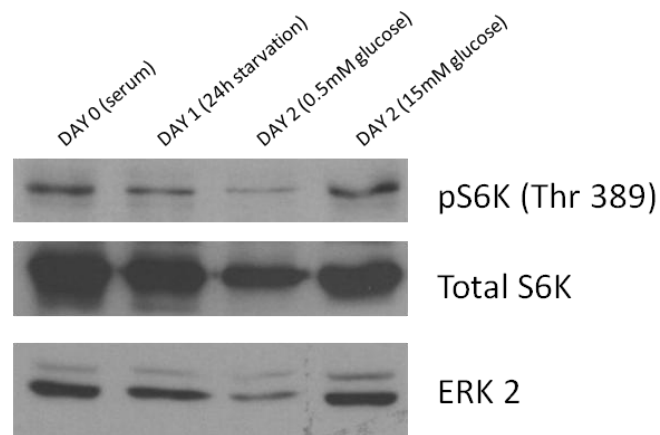


**Figure 5.5: Activation of S6K upon nutrients deprivation and glucose reintroduction. INS1 cells were deprived from nutrients for 24 hours and then incubated in serum free medium supplemented with 15 mM glucose or left in nutrients deprivation. Lysates were analysed by Western Blot and incubated with a specific antibody recognising S6K when phosphorylated at Thr 389, then stripped and incubated with an antibody recognising total S6K. ERK2 was also used as loading control. Representative blot of 3 independent experiments is shown.**

S6K was phosphorylated when INS1 cells were cultured in serum, consistent with the activation of mTOR and 4EBP1 in these experimental conditions shown in Figures 5.3 and 5.4.

S6K phosphorylation at its residue Thr 389 was slightly decreased upon 24 hours of nutrients deprivation and further reduced after additional 24 hours. Reintroduction of stimulatory concentrations of glucose increased the phosphorylation of residue Thr 389.

These data indicate that reintroduction of stimulatory concentrations of glucose in INS1 cells deprived from nutrients for 24 hours is able to induce the phosphorylation and activation of mTOR and its direct downstream effectors 4EBP1 and S6K.

### 5.2.2 Glucose-induced stimulation of mTOR is affected by rapamycin

Once assessed that glucose is able to activate mTOR pathway, I decided to determine the role of glucose-induced mTOR activation. To this end, I first tested the effect of mTOR inhibition on glucose-induced cell survival. Therefore, I determined which concentrations of rapamycin would inhibit glucose-induced mTOR activation. First, I analysed mTOR phosphorylation at Ser 2448. INS1 cells were deprived from growth factors and glucose for 24 hours. Then, cells were treated for 24 hours with stimulatory glucose concentrations in the absence of growth factors, following the same experimental conditions described in Chapter 4. Different rapamycin concentrations were used, ranging from 20 nM to 1  $\mu$ M.

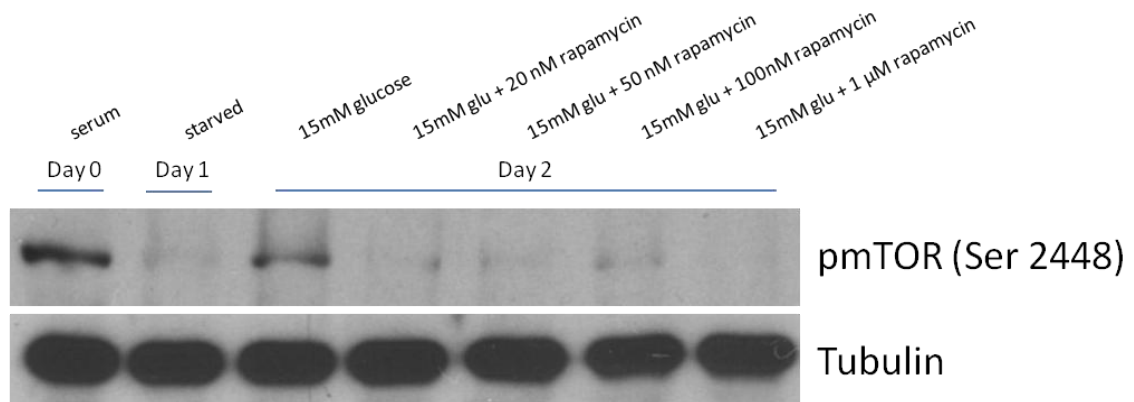


**Figure 5.6: Activation of mTOR upon nutrients deprivation and glucose reintroduction is inhibited by rapamycin.** INS1 cells were deprived of nutrients for 24 hours and then incubated with 15 mM glucose, with or without the indicated concentrations of rapamycin. Lysates were analysed by Western Blot and incubated with antibodies recognising phosphorylated Ser 2448 of mTOR. Tubulin was used as control of equal loading.

As described before, in normal growth conditions, Ser 2448 of mTOR was phosphorylated and after 24 hours of nutrients deprivation the phosphorylation of mTOR was decreased, indicating that mTOR was inhibited (Figure 5.6). Reintroduction of stimulatory glucose concentrations was able to induce the phosphorylation of Ser 2448. Treatment with rapamycin prevented the phosphorylation of Ser 2448, confirming the role of mTOR in this activation.

In the same experimental conditions, the phosphorylation of ribosomal protein S6, an indirect downstream effector of mTOR, was also analysed. S6 is phosphorylated by the protein S6K upon growth factors and mitogens stimulation (Dufner and Thomas 1999). The activation of S6 is often used as readout for mTOR activation and it is assessed by analysing the phosphorylation of the residues Ser 235/6 and Ser 240/4.

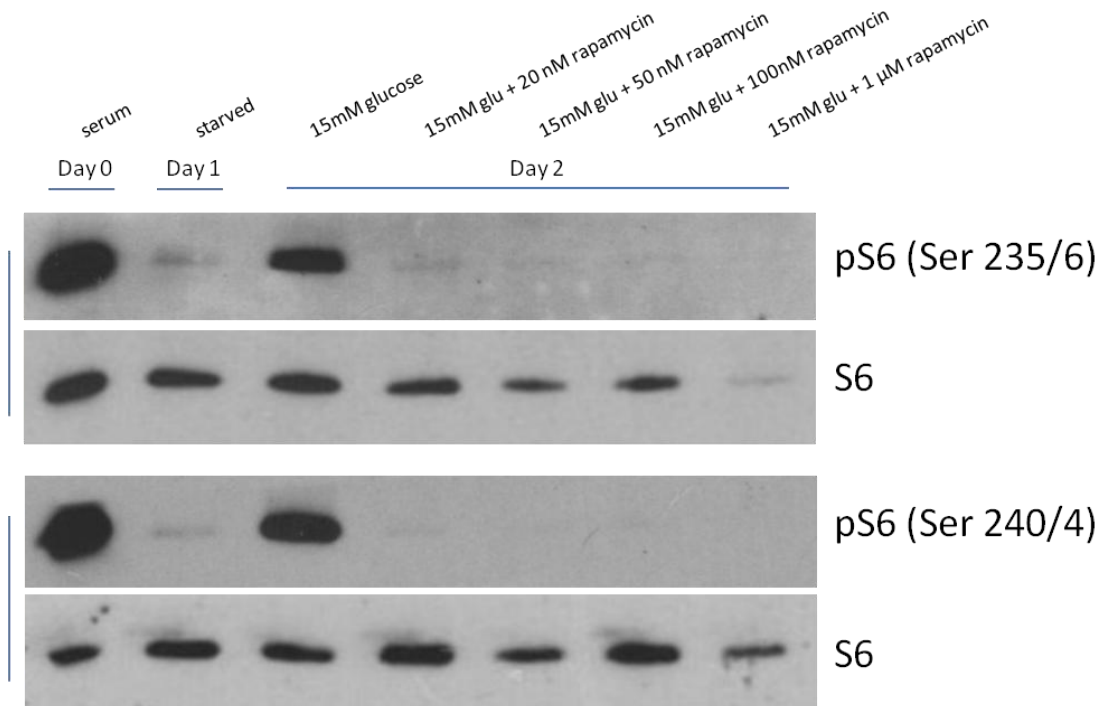


**Figure 5.7: Activation of S6 upon nutrients deprivation and glucose reintroduction.** INS1 cells were deprived of nutrients for 24 hours and then incubated with 15 mM glucose, with or without the indicated concentrations of rapamycin. Lysates were analysed by Western Blot and incubated with antibodies recognising phosphorylated S6, then stripped and incubated with a specific antibody for total S6.

Results from this experiment showed that S6 was phosphorylated at both residues Ser 235/236 and 240/244 in normal growth conditions. The phosphorylation of these residues was decreased upon 24 hours of nutrients deprivation. Reintroduction of stimulatory concentrations of glucose was able to induce the phosphorylation S6 at both residues examined, and this process was inhibited by treatment with rapamycin. These data are consistent with the data shown in Chapter 5.2.1, and confirm that stimulatory concentrations of glucose are able to activate mTORC1 in INS1 cells. Furthermore, these data confirmed that



concentrations of rapamycin as low as 20 nM were sufficient to inhibit mTOR and S6 phosphorylation.

### **5.2.3 Effects of rapamycin treatment on glucose-induced cell survival**

Once assessed that glucose was able to activate mTORC1 in INS1 cells, and set the concentrations of rapamycin necessary to inhibit its activation, I then decided to determine whether mTORC1 had a role in the glucose-induced survival/proliferation effect observed in INS1 cells (Chapter 4). To this end, I assessed the effect of rapamycin on cell viability. INS1 control cells were deprived from nutrients and then stimulated with 15 mM glucose, in the presence or absence of 20 and 50 nM rapamycin or left in nutrients deprivation as previously described. Cell viability was assessed by MTT assay.

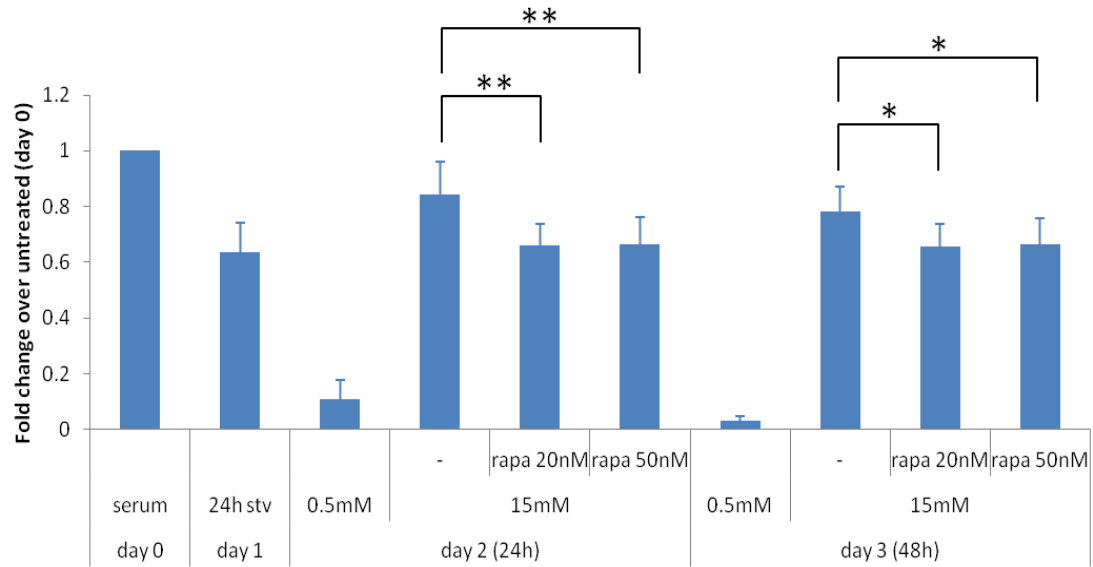


**Figure 5.8: Cell viability upon nutrients deprivation and glucose reintroduction, in the presence or absence of rapamycin.** INS1 sh scrambled cells were deprived from nutrients for 24 hours and then incubated in serum free medium supplemented with 15 mM glucose, with or without the indicated concentrations of rapamycin, or left in nutrients deprivation. Cell viability was assessed by MTT assay. Data are expressed as fold increase relative to day 0 and are means  $\pm$  s.e.m. from 6 independent experiments. \* p value < 0.05; \*\* p value < 0.01 vs corresponding untreated control.

Consistent with data presented in Chapter 4, results in Figure 5.8 showed that stimulatory concentrations of glucose were able to protect INS1 sh scrambled cells from death, upon 24 and 48 hours treatment. Also, the presence of rapamycin significantly reduced glucose-induced survival, at both 24 and 48 hours post-treatment. The effect of 20 nM rapamycin was not further enhanced by higher concentration of the drug, suggesting that a concentration of 20 nM already maximally inhibited the effect of glucose on cell viability.

Taken together, these data indicate that the intracellular signalling triggered by reintroduction of stimulatory concentrations of glucose activates mTORC1, which in turn is involved in glucose-induced cell survival.

My results showed that both rapamycin and downregulation of PI3K-C2 $\alpha$  affected glucose-induced cell proliferation (Figures 5.8 and 4.7, respectively), and that glucose was also able to activate mTOR pathway. Therefore, in order to assess the potential contribution of PI3K-C2 $\alpha$  in glucose-induced activation of mTOR pathway, in parallel with experiments presented in Figure 5.8, I also assessed the effect of rapamycin in sh PI3K-C2 $\alpha$  cells. The viability of sh PI3K-C2 $\alpha$  cells upon nutrients deprivation and glucose reintroduction and in the presence or absence of rapamycin was compared to that observed in sh scrambled cells (Fig 5.8) and is shown in Figure 5.9.

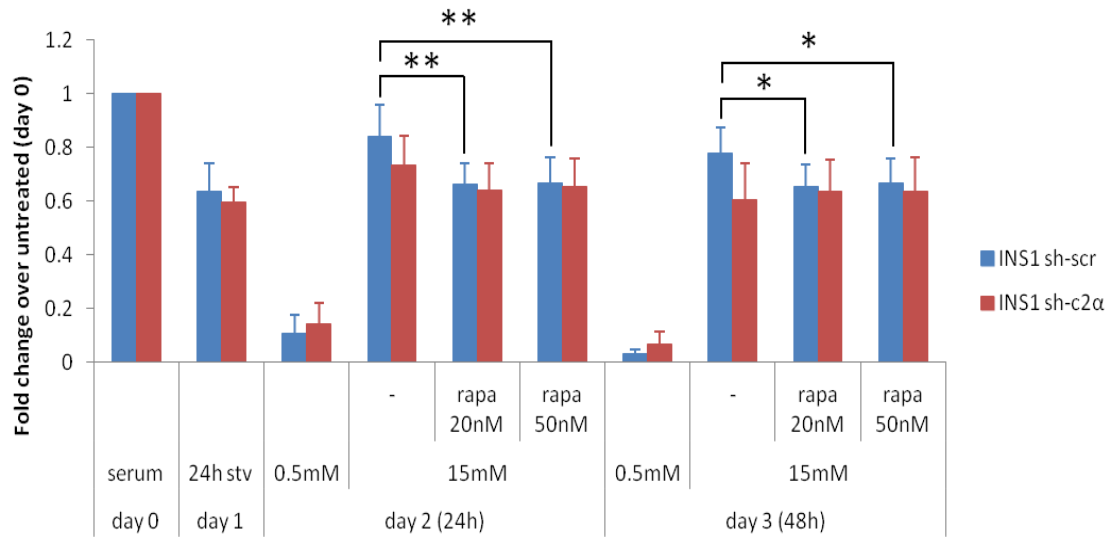


**Figure 5.9: Cell viability upon nutrients deprivation and glucose reintroduction, in the presence or absence of rapamycin. Stable INS1 cell lines were deprived of nutrients for 24 hours and then incubated in serum free medium supplemented with 15 mM glucose, with or without the indicated concentrations of rapamycin, or left in nutrients deprivation. Cell viability was assessed by MTT assay. Data are expressed as fold increase relative to day 0 and are means  $\pm$  s.e.m. from 6 independent experiments. \* p value < 0.05; \*\* p value < 0.01.**

Reintroduction of glucose alone was able to improve cell viability in both cell lines. Consistent with data described in Chapter 4.2.4, cell viability was reduced in INS1 sh PI3K-C2α cells compared to the scrambled control.

Notably, the viability of scrambled control cells treated with glucose and rapamycin was comparable to that observed in INS1 sh PI3K-C2α cells treated with glucose only. More importantly, rapamycin treatment did not affect the viability of PI3K-C2α knock down cells. These data indicate that rapamycin treatment has no further effect in PI3K-C2α knock down cells in terms of viability. This suggests that mTOR and PI3K-C2α might be part of the same signalling cascade activated by stimulatory concentrations of glucose upon nutrients deprivation.

## 5.2.4 Role of PI3K-C2 $\alpha$ in the activation of mTOR pathway induced by stimulatory concentrations of glucose

To directly investigate whether PI3K-C2 $\alpha$  is involved in glucose-induced activation of mTOR, I used stable cell lines INS1 sh scrambled and sh PI3K-C2 $\alpha$ . Specifically, I determined whether downregulation of PI3K-C2 $\alpha$  affects mTOR activation upon glucose reintroduction.

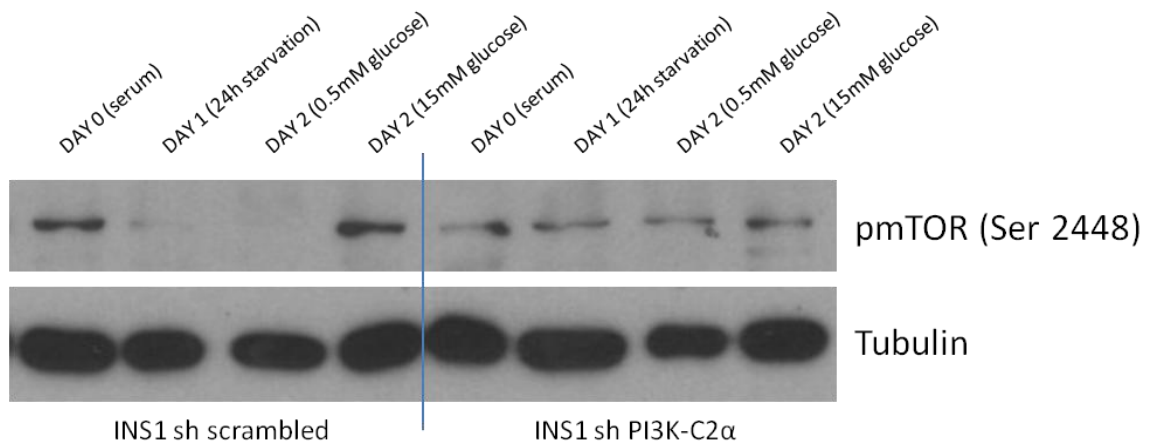


**Figure 5.10: Activation of mTOR upon nutrients deprivation and glucose reintroduction. Stable INS1 cell lines were deprived of nutrients for 24 hours and then incubated in serum free medium supplemented with 15 mM glucose or left in nutrients deprivation. Lysates were analysed by Western Blot and incubated with a specific antibody recognising phosphorylated Ser 2448 of mTOR. Tubulin was used as loading control. Representative blot of 2 independent experiments is shown.**

Ser 2448 of mTOR was phosphorylated in both INS1 sh scrambled and sh PI3K-C2 $\alpha$  cells when cells were grown in complete medium supplemented with serum. Upon nutrients deprivation, the residue Ser 2448 progressively decreased its phosphorylation in sh scrambled cells. Consistent with data obtained in parental cells (Figure 5.3), reintroduction of stimulatory concentrations of glucose induced the phosphorylation of mTOR Ser 2448 in sh scrambled cells. Interestingly, upon

nutrients deprivation or glucose reintroduction, the phosphorylation of Ser 2448 was not significantly modified in INS1 sh PI3K-C2 $\alpha$  cells. This data suggests that PI3K-C2 $\alpha$  is required for glucose-induced phosphorylation of mTOR at Ser 2448.

In order to further assess the effect of downregulation of PI3K-C2 $\alpha$  in glucose-induced activation of mTOR pathway, mTOR downstream signalling cascade was analysed by Western blot.

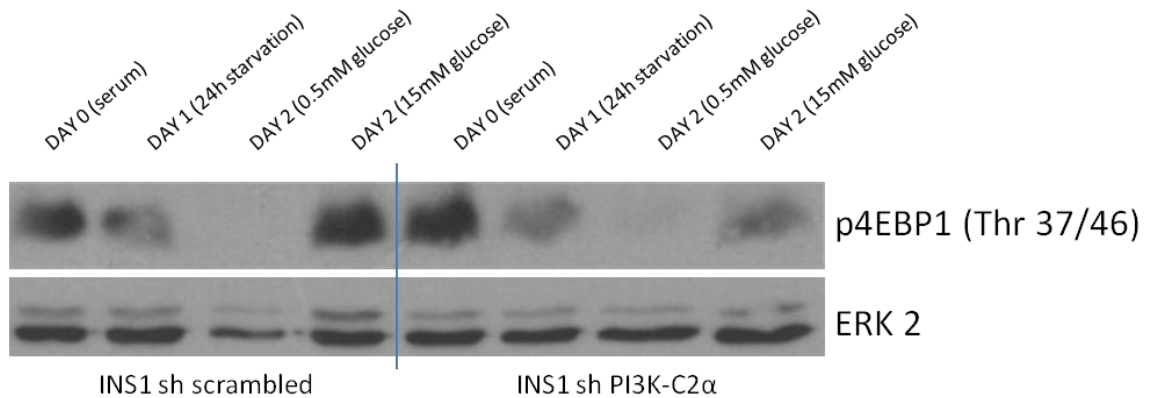


**Figure 5.11: Activation of 4EBP1 upon nutrients deprivation and glucose reintroduction. Stable INS1 cell lines were deprived from nutrients for 24 hours and then incubated in serum free medium supplemented with 15 mM glucose or left in nutrients deprivation. Lysates were analysed by Western Blot and incubated with a specific antibody recognising phosphorylated Thr 37/46 of 4EBP1. ERK2 was used as loading control. Representative blot of 2 independent experiments is shown.**

Consistent with data shown in Figure 5.4, Thr 37/46 of 4EBP1 was phosphorylated in serum, and the level of its phosphorylation progressively decreased upon 24 and 48 hours of nutrients deprivation in both cell lines (Figure 5.11). Upon reintroduction of stimulatory concentrations of glucose, strong phosphorylation of 4EBP1 on Thr

37/46 was detected in sh scrambled cells. Interestingly, in the same experimental conditions, sh PI3K-C2 $\alpha$  cells showed a decreased phosphorylation of 4EBP1 compared to control cells. This suggests that the activity of PI3K-C2 $\alpha$  is required for glucose-induced phosphorylation of 4EBP1 at residues Thr 37/46.

Densitometric analysis of Western Blots for p4EBP1 was then performed and results are shown in Figure 5.12. Western blot films from 2 different experiments were scanned and analysed with the software ImageJ.

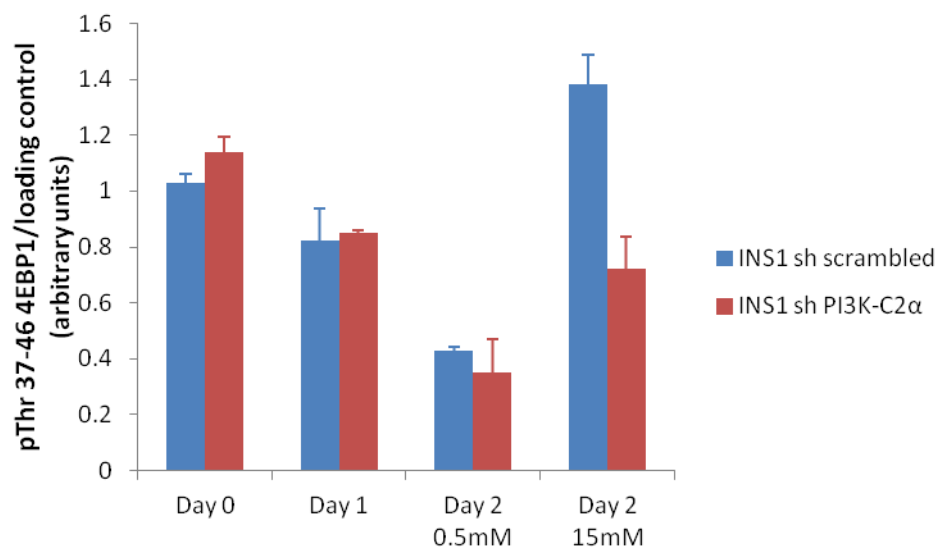


**Figure 5.12: Densitometric analysis of Western Blots for p4EBP1 (Thr 37/46) Data are means  $\pm$  s.e.m. from 2 independent experiments.**

Data showed that in both cell lines Thr 37/46 of 4EBP1 was phosphorylated in serum and the phosphorylation of Thr 37/46 was progressively decreased by nutrients deprivation for 24 and 48 hours. When glucose was reintroduced in the culture medium, the phosphorylation of Thr 37/46 of 4EBP1 was increased in INS1 sh

scrambled cells. Notably, INS1 sh PI3K-C2 $\alpha$  cells showed a strongly impaired phosphorylation of Thr 37/46 of 4EBP1 upon glucose reintroduction, compared to the scrambled control. Specifically, downregulation of PI3K-C2 $\alpha$  seemed to impair glucose-induced phosphorylation by ~50%.

In the same experimental conditions, the phosphorylation status of the protein S6K was also investigated (Figure 5.13).

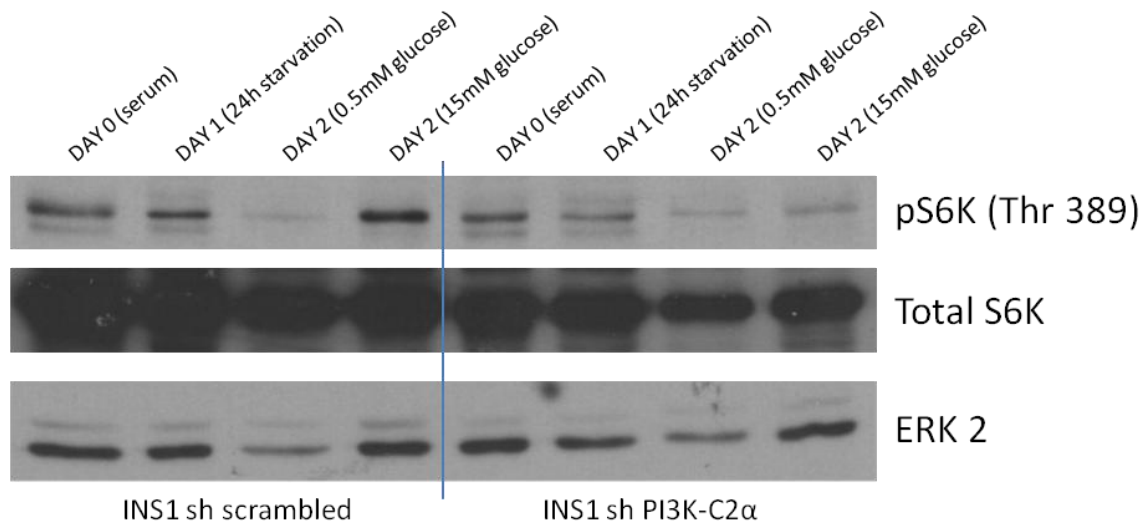


**Figure 5.13: Activation of S6K upon prolonged nutrients deprivation and 24 hours glucose reintroduction. Stable INS1 cell lines were deprived from nutrients for 24 hours and then incubated in serum free medium supplemented with 15 mM glucose or left in nutrients deprivation. Lysates were analysed by Western Blot and incubated with a specific antibody recognising phosphorylated Thr 389 of S6K, then stripped and incubated with an antibody recognising total S6K. ERK2 was also used as loading control. Representative blot of 3 independent experiments is shown.**

Results showed that Thr 389 S6K was phosphorylated in serum, and its phosphorylation level gradually decreased upon nutrients deprivation. In sh



scrambled cells, reintroduction of stimulatory concentrations of glucose induced the phosphorylation of Thr 389, consistent with data obtained using parental cells (Figure 5.5). On the other hand, glucose-induced S6K phosphorylation at Thr 389 was impaired in INS1 sh PI3K-C2 $\alpha$  cells, indicating that downregulation of PI3K-C2 $\alpha$  inhibits the activation of S6K in these experimental conditions.

In order to further clarify glucose-induced activation of S6K, additional experimental conditions were investigated. Stable INS1 cell lines were deprived from nutrients for 24 hours and then stimulatory concentrations of glucose were added to serum-free medium for further 24 or 48 hours. Results are shown in Figure 5.14.

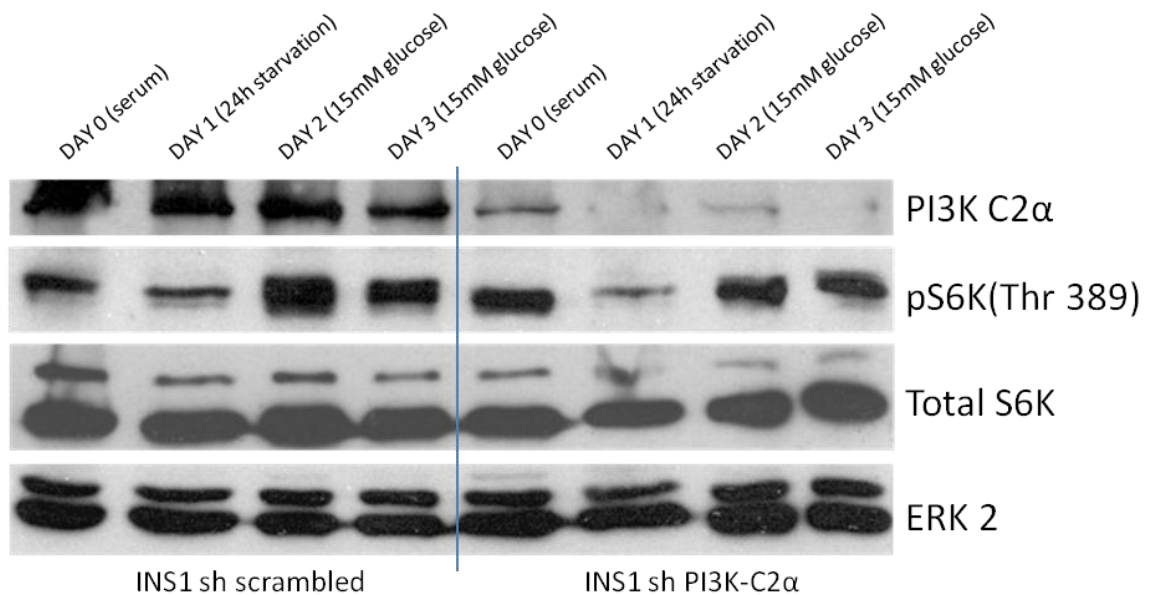


**Figure 5.14: Activation of S6K upon nutrients deprivation and 24 or 48 hours of glucose reintroduction. Stable INS1 cell lines were deprived from nutrients for 24 hours and then incubated in serum free medium supplemented with 15 mM glucose for 24 and 48 hours. Lysates were analysed by Western Blot and incubated with a specific antibody recognising phosphorylated Thr 389 of S6K, then stripped and incubated with an antibody recognising total S6K. ERK2 was also used as loading control. Representative blot of 3 independent experiments is shown.**

Consistent with data previously shown, Thr 389 S6K was phosphorylated in serum and the phosphorylation was decreased upon nutrients starvation in both cell lines. After reintroduction of stimulatory concentrations of glucose, phosphorylation of S6K increased in sh scrambled cells at both 24 and 48 hours post treatment. Downregulation of PI3K-C2 $\alpha$  inhibited glucose-induced phosphorylation of S6K, compared to control cells.

These data provide further evidence of the involvement of PI3K-C2 $\alpha$  in the activation of mTOR pathway upon glucose stimulation.

Densitometric analysis of Western Blots for pS6K was also performed, analysing scanned blots from 3 different experiments with the software ImageJ.

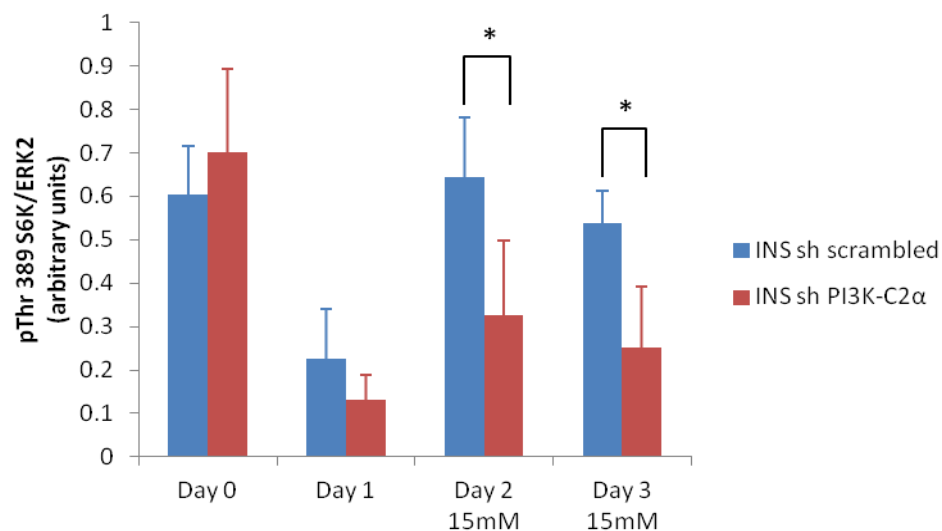


**Figure 5.15: Densitometric analysis of Western Blots for pS6K (Thr 389).** Stable INS1 cell lines were deprived from nutrients for 24 hours and then incubated in serum free medium supplemented with 15 mM glucose for further 24 or 48 hours. Scanned blots were analysed using the software ImageJ. Data are means  $\pm$  s.e.m. from 3 independent experiments. \* indicates INS1 sh scrambled vs INS1 sh PI3K-C2 $\alpha$ . p value < 0.05.

Upon nutrient starvation (day 1), phosphorylation of Thr 389 of S6K was reduced compared to cells in serum (day 0) in both cell lines. Following 24 or 48 hours reintroduction of stimulatory concentrations of glucose (days 2 and 3, respectively), phosphorylation of S6K was increased in sh scrambled cells, suggesting that glucose is able to activate S6K. Interestingly, glucose-induced phosphorylation of Thr 389 S6K was impaired in INS1 sh PI3K-C2 $\alpha$  cells, either upon 24 or 48 hours treatment. Specifically, INS1 sh PI3K-C2 $\alpha$  cells showed a ~50% decrease in the phosphorylation levels, compared to sh scrambled cells.

Taken together, these data indicate that PI3K-C2 $\alpha$  is required for the phosphorylation and activation of S6K upon reintroduction of stimulatory concentrations of glucose, at both 24 and 48 hours post treatment.

### **5.2.5 Effects of stimulatory glucose concentrations on the activation of other components of mTOR pathway**

In order to further investigate the role of PI3K-C2 $\alpha$  in glucose-induced activation of mTOR pathway, the activation of other members of the mTOR signalling cascade was investigated.

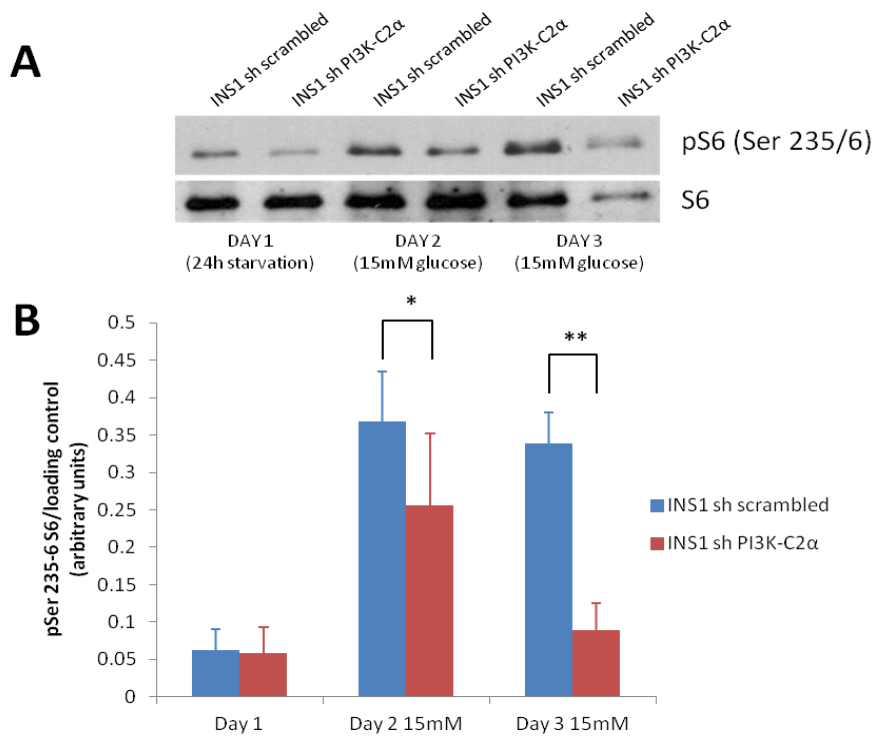


**Figure 5.16: Representative blot (A) and densitometric analysis (B) of Western Blots for pS6 (Ser 235/236).** Stable INS1 cell lines were deprived from nutrients for 24 hours and then incubated in serum free medium supplemented with 15 mM glucose for further 24 or 48 hours. Scanned blots were analysed using the software ImageJ. Data are means  $\pm$  s.e.m. from 3 independent experiments. \* $p < 0.05$  and \*\* $p < 0.01$ , indicating INS1 sh scrambled vs INS1 sh PI3K-C2 $\alpha$ .

Densitometric analysis of levels of S6 phosphorylation at its residue Ser 235/236 revealed that both cell lines showed a low phosphorylation upon 24 hours nutrients deprivation. Reintroduction of stimulatory concentrations of glucose increased the phosphorylation of S6 in sh scrambled cells, upon either 24 or 48 hours post treatment. Glucose-induced phosphorylation of Ser 235/236 was significantly reduced in INS1 sh PI3K-C2 $\alpha$ , at both 24 and 48 hours post treatment.

In addition, phosphorylation of residue 240/244 of S6 was analysed in the same experimental conditions (Figure 5.17).

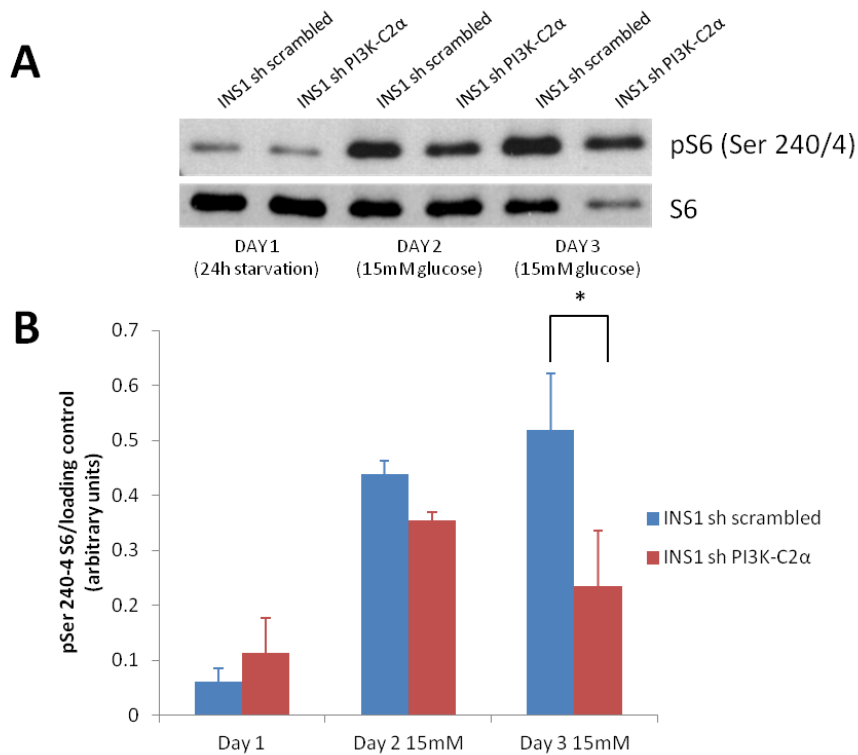


**Figure 5.17: Representative blot (A) and densitometric analysis (B) of Western Blots for pS6 (Ser 240/244).** Stable INS1 cell lines were deprived from nutrients for 24 hours and then incubated in serum free medium supplemented with 15 mM glucose for further 24 or 48 hours. Scanned blots were analysed using the software ImageJ. Data are means  $\pm$  s.e.m. from 3 independent experiments. \* indicates INS1 sh scrambled vs INS1 sh PI3K-C2 $\alpha$ . p value < 0.01.

Results indicated that both cell lines displayed low level of Ser 240/244 phosphorylation upon nutrients deprivation. Consistent with results showed in Figure 5.16, sh scrambled cells treated with stimulatory concentrations of glucose for 24 or 48 hours showed an increase in the phosphorylation levels of S6. The level of glucose-induced phosphorylation was slightly decreased in INS1 sh PI3K-C2 $\alpha$  cells after 24 hours of treatment and significantly decreased after 48 hours.

In summary, my results showed that glucose was able to activate the downstream effector of S6K, S6 ribosomal protein, as assessed by phosphorylation of the residues Ser 235/236 and Ser 240/244. The activation of S6, upon nutrients deprivation and glucose reintroduction, was impaired in INS1 sh PI3K-C2 $\alpha$  cells compared to the control.

Taken together, these data indicate for the first time that PI3K-C2 $\alpha$  is involved in glucose-induced activation of mTOR and its downstream targets.

### **5.2.6 Akt activation upon nutrients starvation and glucose stimulation**

In order to determine the upstream signalling involved in the PI3K-C2 $\alpha$ -dependent activation of mTOR pathway, additional Western blots experiments were performed.

Serum stimulation can activate the PI3K/Akt pathway, which can ultimately lead to the stimulation of mTOR catalytic activity (Sekulic et al. 2000). The serine threonine protein kinase B/Akt, is a key regulator of cell growth, differentiation, and survival and a key activator of mTOR (Vadlakonda et al. 2013). Some studies suggested that PI3K-C2 $\alpha$  can activate Akt in pancreatic  $\beta$  cells (Leibiger et al. 2010) and therefore, I decided to investigate whether Akt is involved in PI3K-C2 $\alpha$ -dependent mTOR activation. First, I investigated whether glucose stimulation could lead to the activation of Akt. Therefore, control cells lines were deprived from nutrients and

then treated with stimulatory concentrations of glucose, as previously described. Phosphorylation of residue Ser 473 of Akt was examined by Western blot.

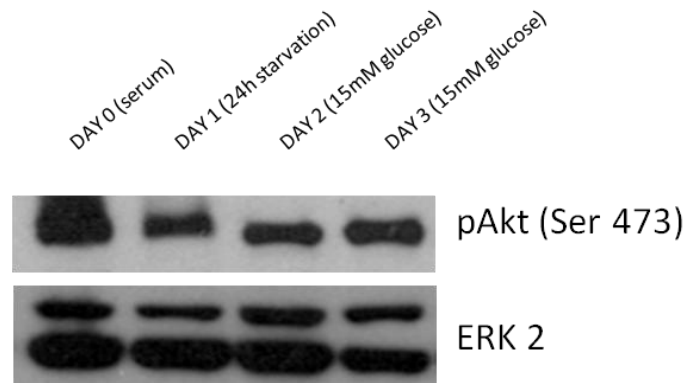


**Figure 5.18: Activation of Akt upon nutrients deprivation and glucose reintroduction.** INS1 cells were deprived of nutrients for 24 hours and then incubated with the indicated concentrations of glucose. Lysates were analysed by Western Blot analysis, incubated with a specific antibody recognising phosphorylated Ser 473 of Akt, stripped and incubated for total Akt. Representative blot of 3 independent experiments is shown.

Results showed that the phosphorylation of Ser 473 Akt was not clearly modified by nutrients deprivation and glucose reintroduction. This residue was phosphorylated in serum and, upon 24 hours of nutrients deprivation, a clear band corresponding to phosphorylated Ser 473 was still detectable and not modified by further treatment with glucose. These data suggested that phosphorylation of Ser 473 Akt is not involved in the glucose-induced proliferation object of my study.

### **5.2.7 PI3K-C2 $\alpha$ has a role in AMPK signalling**

In order to further investigate the intracellular signalling triggered by nutrients deprivation and reintroduction of stimulatory concentrations of glucose in INS1 cells, the phosphorylation status of the protein AMPK was studied, as this protein is an upstream regulator of mTOR.

AMPK plays a key role as a master regulator of cellular energy homeostasis. When cells are in a low energy state, scarce supplies of ATP, the intracellular source of energy, and large supplies of AMP are available. The binding of AMP to AMPK promotes AMPK phosphorylation and subsequent activation, inhibiting ATP-consuming pathways and restoring ATP supplies by promoting catabolic pathways (Canto and Auwerx 2010). Interestingly, AMPK can negatively regulate mTOR through the activation of the TSC pathway (Inoki et al. 2003) and therefore contribute to regulate cell proliferation.

Therefore, I sought to investigate whether glucose-induced stimulation of mTOR was mediated by inhibition of AMPK, and whether this pathway was regulated by PI3K-C2 $\alpha$ . To this end, INS1 sh scrambled and sh PI3K-C2 $\alpha$  cells were deprived from nutrients for 24 hours, 15 mM glucose was supplied to the culture medium, and the phosphorylation of AMPK was analysed.



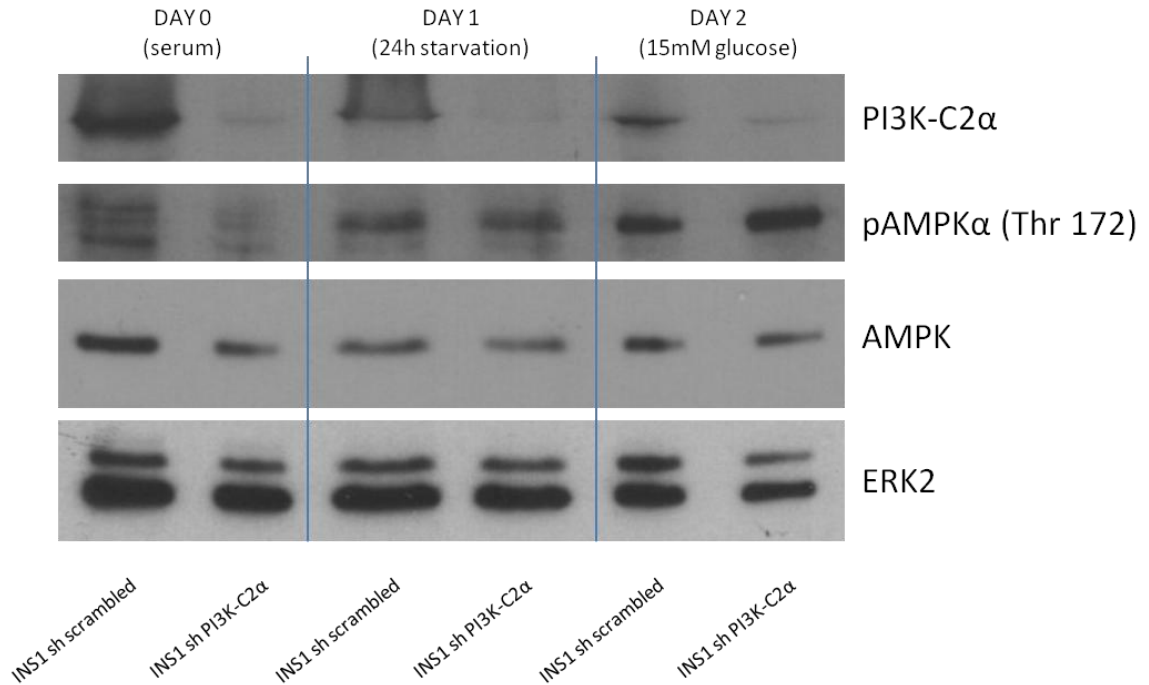


**Figure 5.19: Activation of AMPK upon nutrients deprivation and glucose reintroduction** Stable INS1 cell lines were deprived of nutrients for 24 hours and then incubated in serum free medium supplemented with 15 mM glucose. Lysates were analysed by Western Blot and incubated with an antibody recognising phosphorylated Thr 172 of AMPK, then stripped and reincubated with an antibody anti AMPK. Representative blot of 5 independent experiments is shown.

As shown in Figure 5.19, phosphorylation of AMPK was low when cells were grown in complete medium. Upon 24 hours of nutrients deprivation (Day 1), AMPK phosphorylation increased in both scrambled and PI3K-C2 $\alpha$  knock down cells, as a result of the low energy status. After incubation with stimulatory concentrations of glucose for 24 hours, phosphorylation of AMPK was still clear in both sh scrambled and sh PI3K-C2 $\alpha$  cells. However, sh PI3K-C2 $\alpha$  cells showed higher phosphorylation of AMPK compared to sh scrambled cells, in these experimental conditions.

Densitometric analysis of Western blot for pAMPK was performed and the results are shown in Figure 5.20.

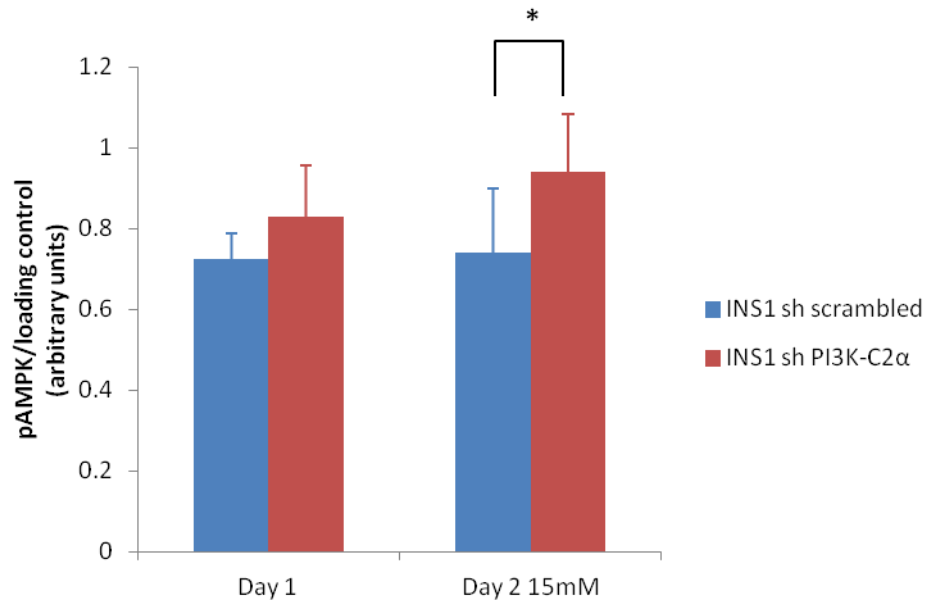


**Figure 5.20: Densitometric analysis of Western Blots for pAMPK. Data are means  $\pm$  s.e.m. from 5 independent experiments. \* indicates INS1 sh scrambled vs INS1 sh PI3K-C2 $\alpha$ . p value < 0.05.**

Following nutrients deprivation (Day 1), sh scrambled and PI3K-C2 $\alpha$  knock down cell lines showed comparable phosphorylation of AMPK. After glucose reintroduction, the phosphorylation level of AMPK did not change in control cells. Interestingly, sh PI3K-C2 $\alpha$  cells showed a further increase in the phosphorylation level of AMPK. Specifically, AMPK resulted ~25% more phosphorylated in INS1 sh PI3K-C2 $\alpha$  compared to sh scrambled cells upon glucose reintroduction. This indicates that downregulation of PI3K-C2 $\alpha$  leads to hyperactivation of AMPK, which might explain the inhibition of mTOR and its downstream effectors observed in Figures 5.10-5.17.

This observation provides a potential explanation on how PI3K-C2 $\alpha$  is involved in the activation of mTOR pathway upon glucose stimulation.

### **5.2.8 Short term signalling following 24 hours of nutrients deprivation.**

Long term starvation can activate survival mechanisms within the cells, activating intracellular pathways which do not necessarily depend on glucose reintroduction, and are rather due to prolonged nutrient deprivation. In order to further investigate the activation of mTOR pathway upon glucose stimulation and the potential role for PI3K-C2 $\alpha$  in modulating this signalling pathway, additional experimental conditions were investigated.

Specifically, I decided to perform time-course experiments to study whether glucose-stimulated intracellular signalling activates mTOR pathway components at earlier time points than those previously investigated. Therefore, INS1 sh scrambled and sh PI3K-C2 $\alpha$  cells were deprived from nutrients as described for the previous experiments, and then treated with stimulatory concentrations of glucose for 5, 10 and 30 minutes. Cells were lysed and samples were prepared for Western blot analysis.

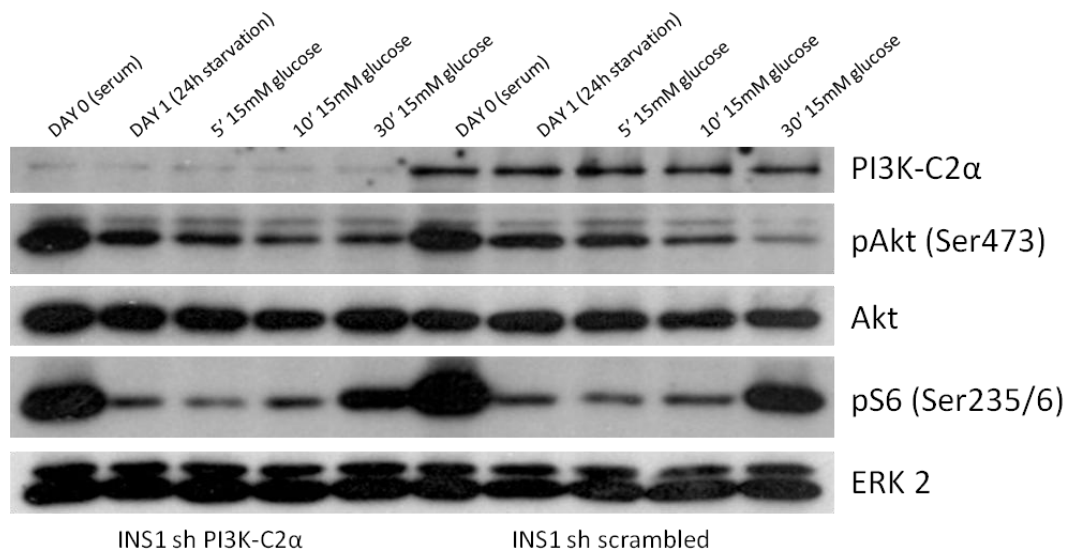


**Figure 5.21: Activation of Akt and S6 upon nutrients deprivation and short time points of glucose stimulation. Stable INS1 cell lines were deprived from nutrients for 24 hours and then incubated in serum free medium supplemented with 15 mM glucose for the indicated time points. Lysates were analysed by Western Blot and incubated with the indicated primary antibodies specific for ERK2, the phosphorylated forms of Akt and S6. Membranes were stripped and reincubated with the appropriate antibodies recognising total Akt or S6.**

As shown in Figure 5.21, Ser 473 of Akt was phosphorylated when the cells were grown in complete medium. This is consistent with data in literature reporting the activation of Akt in serum following activation of class I PI3Ks. Upon 24 hours of nutrients deprivation the phosphorylation of Ser 473 was strongly reduced but, interestingly, still clearly detectable. Following 5, 10 or 30 minutes of reintroduction of stimulatory glucose concentration, no changes in the levels of phosphorylated Ser 473 were observed. This observation is consistent with previous studies reporting that stimulation with 15 mM glucose has no effect on Akt activation (Dickson et al. 2001).

In serum conditions, Ser 235/6 of S6 was highly phosphorylated. This phosphorylation was significantly decreased after 24 hours of nutrients deprivation, consistent with data previously shown (Figure 5.16). Upon 5 or 10 minutes of glucose reintroduction, the phosphorylation levels of Ser 235/6 of S6 were not modified. Following 30 minutes of glucose reintroduction, the phosphorylation level of S6 increased. This suggests that glucose-induced activation of mTOR pathway begins already 30 minutes after treatment. Furthermore, the activation of S6 was achieved in experimental conditions that did not seem to induce Akt activation. This suggests that the intracellular signalling triggered by glucose reintroduction does not require the activation of the canonical class I PI3Ks/Akt axis.

Importantly, S6 phosphorylation was inhibited in INS1 sh PI3K-C2 $\alpha$  cells compared to scrambled control. This observation indicates that class II PI3K-C2 $\alpha$  is required for the activation of mTOR pathway induced by short time points of stimulation with glucose.

In addition, the phosphorylation levels of Thr 308 of Akt and Ser 240/4 of S6 were investigated.

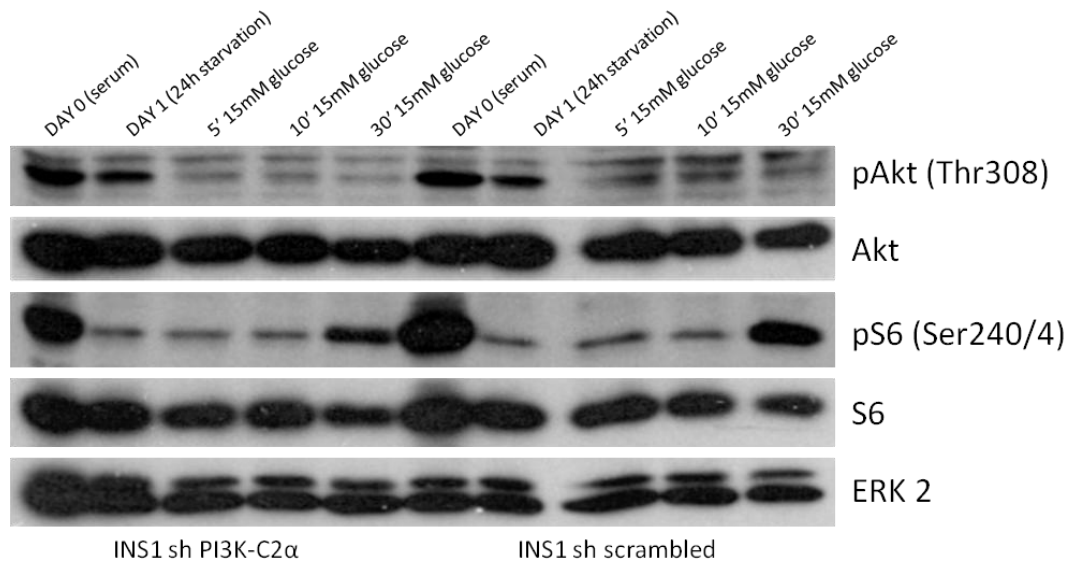


**Figure 5.22: Activation of Akt and S6 upon nutrients deprivation and short time points of glucose stimulation (II).** Stable INS1 cell lines were deprived from nutrients for 24 hours and then incubated in serum free medium supplemented with 15 mM glucose for the indicated time points. Lysates were analysed by Western Blot and incubated with the indicated primary antibodies specific for ERK2, the phosphorylated forms of Akt and S6. Membranes were stripped and reincubated with the appropriate antibodies recognising the total Akt or S6.

Results showed that the residues Thr 308 of Akt and Ser 240/4 of S6 were phosphorylated at Day 0. Upon 24 hours of nutrients deprivation, Thr 308 displayed a slight decrease in the phosphorylation level. After 5, 10 or 30 minutes of glucose reintroduction, activation of Akt was not observed. Following 24 hours of nutrients deprivation, Ser 240/4 of S6 showed a decreased phosphorylation compared to cells in serum. Consistent with the results shown in Figure 5.17, glucose reintroduction induced the phosphorylation and subsequent activation of S6 after 30 minutes of treatment (Figure 5.22). Interestingly, in INS1 sh PI3K-C2 $\alpha$  cells the phosphorylation of S6 at this specific residue resulted impaired compared to the scrambled control. These data suggest that in the experimental conditions examined, reintroduction of

stimulatory concentrations of glucose is able to activate S6 after 30 minutes treatment, independently of Akt activation and in a mechanism involving PI3K-C2 $\alpha$ .

In order to further investigate whether treatment with stimulatory concentrations of glucose is able to induce Akt activation, longer time points of stimulation were also examined. Therefore, Western Blot analysis was performed and the phosphorylation of Ser 473 of Akt was investigated after 45 and 60 minutes of glucose reintroduction.

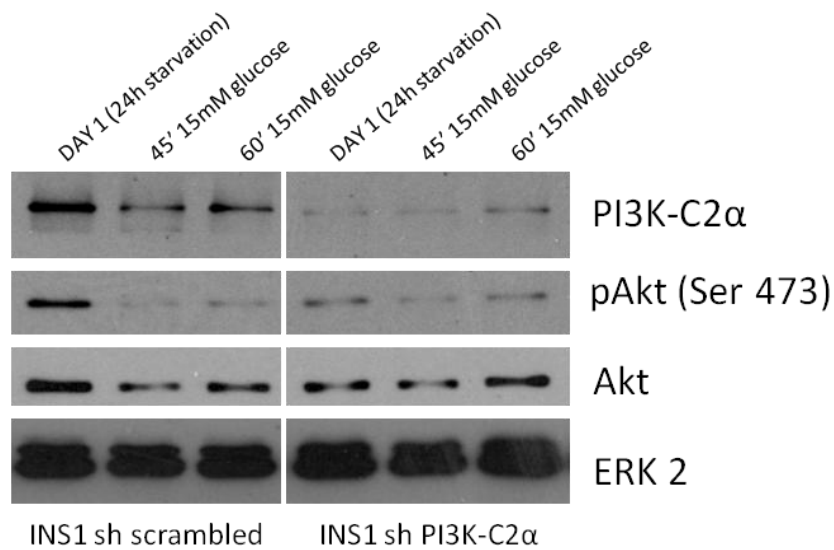


**Figure 5.23: Activation of Akt upon nutrients deprivation and glucose reintroduction** Stable INS1 cell lines were deprived from nutrients for 24 hours and then incubated in serum free medium supplemented with 15 mM glucose for the indicated time points. Lysates were analysed by Western Blot and incubated with the indicated primary antibodies specific for ERK2 and phosphorylated Ser 473 of Akt. Membrane incubated with pAkt was stripped and reincubated with an antibody recognising the total Akt. Representative blot is shown.

In these experimental conditions, Ser 473 of Akt was still phosphorylated upon 24 hours of nutrients deprivation, consistent with data on Akt activation previously

shown. Interestingly, the phosphorylation was not increased by treatment with stimulatory concentrations of glucose for either 45 or 60 minutes. These data further indicate that reintroduction of glucose does not result in Akt activation.

In the same experimental conditions, I also investigated the activation of the protein S6K. INS1 sh scrambled and sh PI3K-C2 $\alpha$  cells were deprived from nutrients and glucose was reintroduced in the culture medium, in the presence or absence of IGF1.

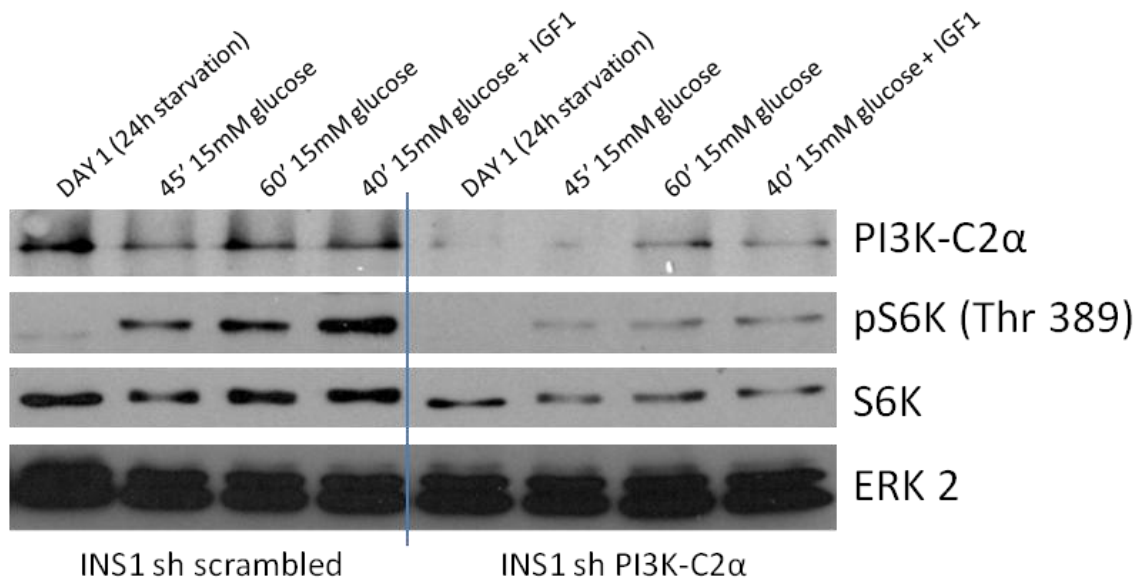


**Figure 5.24: Activation of S6K upon nutrients deprivation and glucose reintroduction** Stable INS1 cell lines were deprived from nutrients for 24 hours and then incubated in serum free medium supplemented with 15 mM glucose for the indicated time points, with or without IGF1. Lysates were analysed by Western Blot and incubated with the indicated primary antibodies specific for ERK2 and phosphorylated Thr 389 of S6K. Membrane incubated with pS6K was stripped and reincubated with an antibody recognising total S6K. Representative blot is shown.

As shown in Figure 5.24, the phosphorylation of S6K was not detectable following 24 hours of nutrients deprivation, consistent with data previously discussed in Chapter



5.2.4. The phosphorylation of Thr 389 S6K was increased by glucose reintroduction, as it was detectable after both 45 minutes and 60 minutes treatment. Also, the phosphorylation of Thr 389 was potentiated in the presence of IGF1, which suggests that two different intracellular pathways are activated by stimulatory concentrations of glucose and IGF1. Importantly, downregulation of PI3K-C2 $\alpha$  impaired both IGF1-induced and glucose-induced activation of S6K.

In the same conditions of nutrients deprivation, shorter time points of glucose stimulation were also used to investigate S6 phosphorylation. INS1 sh scrambled control and INS1 sh PI3K-C2 $\alpha$  cells were deprived from serum and glucose for 24 hours and then stimulated with 15 mM glucose from a minimum of 5 minutes to a maximum of 40 minutes. Results are shown in Figure 5.25.

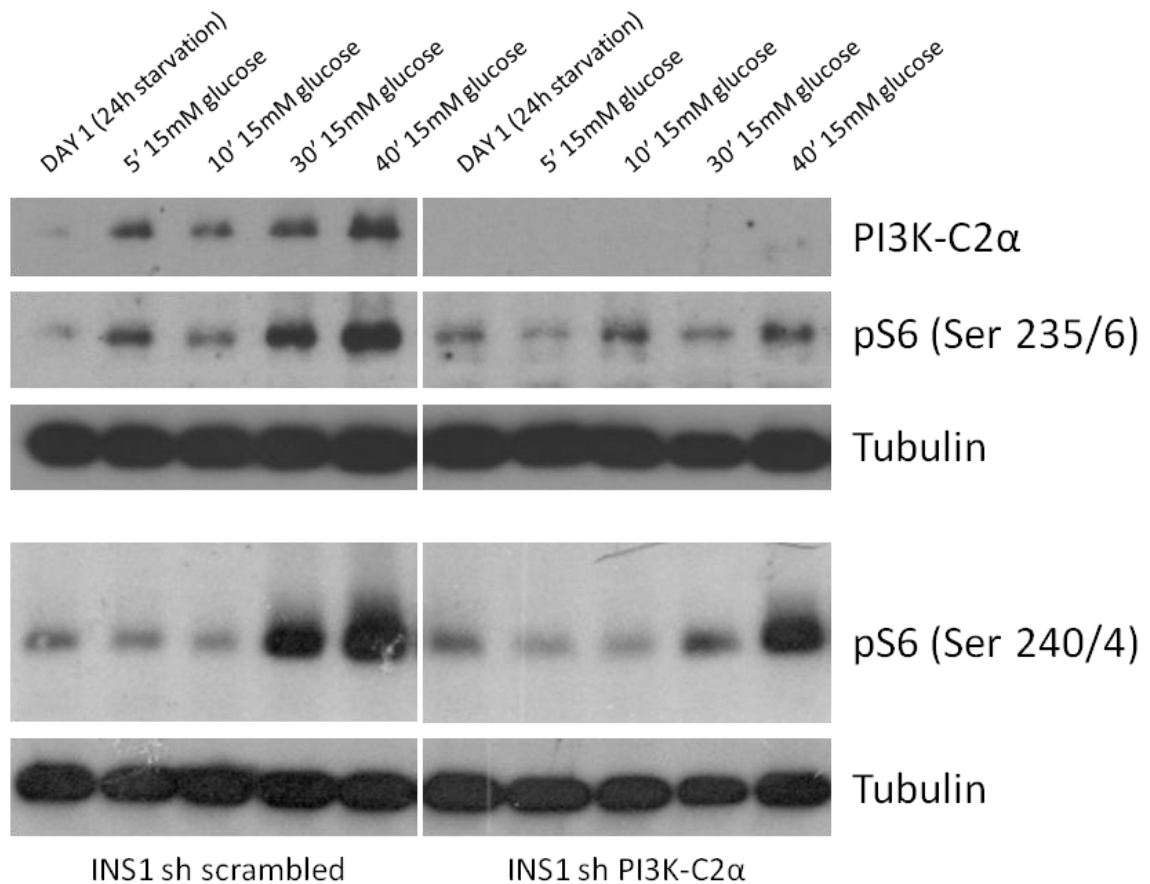


**Figure 5.25: Activation of S6 upon nutrients deprivation and short time points of glucose stimulation. Stable INS1 cell lines were deprived from nutrients for 24 hours and then incubated with 15 mM glucose for the indicated time points. Lysates were analysed by Western Blot and incubated with primary antibodies specific for the phosphorylated forms of S6. Tubulin was used as loading control. Representative blot is shown.**

The phosphorylation of both residues of S6 was very low upon 24 hours of starvation, consistent with data in Figures 5.16 and 5.17. Treatment with stimulatory concentrations of glucose induced the activation of S6 and the phosphorylation of both residues Ser 235/236 and 240/244 after 30 and 40 minutes of treatment. Interestingly, the activation of S6 resulted remarkably decreased in INS1 sh PI3K-C2α cells, compared to the scrambled control (Figure 5.25). This is consistent with data

previously discussed in Chapter 5.2.5 and indicates that the intracellular pathway activated by glucose requires PI3K-C2 $\alpha$ , also during short time stimulation.

Furthermore, the phosphorylation of Thr 37/46 of 4EBP1 was investigated upon short time points of glucose reintroduction.

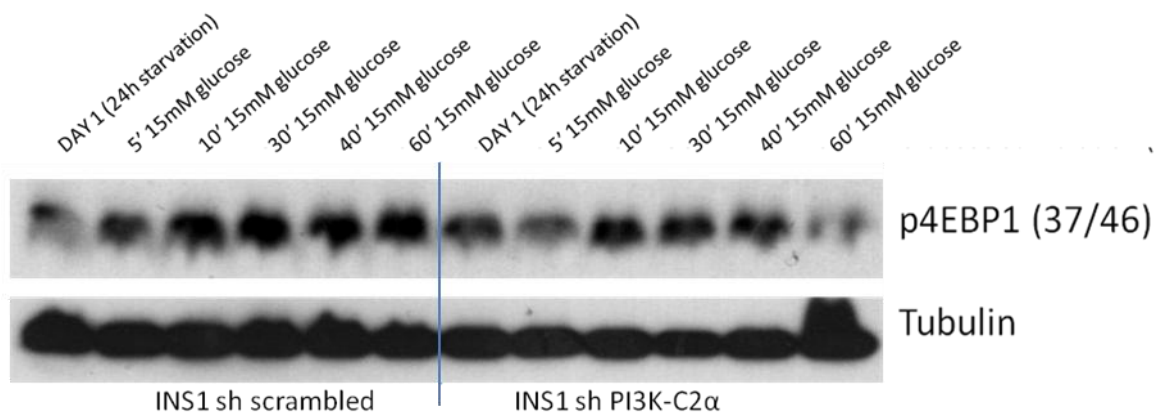


**Figure 5.26: Activation of 4EBP1 upon nutrients deprivation and short time points of glucose stimulation. Stable INS1 cell lines were deprived from nutrients for 24 hours and then incubated with 15 mM glucose for the indicated time points. Lysates were analysed by Western Blot. Representative blot of 2 independent experiments is shown.**

Upon nutrients deprivation, Thr 37/46 of 4EBP1 showed basal phosphorylation. Reintroduction of stimulatory concentrations of glucose induced the progressive activation of 4EBP1 in scrambled cells. The increase in 4EBP1 phosphorylation started after 10 minutes of glucose reintroduction and was clearly detectable after 60 minutes. The activation of 4EBP1 was impaired in INS1 sh PI3K-C2 $\alpha$  cells, as the intensity of the band corresponding to phosphorylated Thr 37/46 is less intense, particularly after 60 minutes of stimulation. These data further support the

conclusion that stimulation with 15 mM glucose is able to activate mTOR pathway, through an intracellular mechanism that involves the activation of PI3K-C2 $\alpha$ .

## 5.3 Discussion

In Chapter 4 I described the protective effect of stimulatory glucose concentrations upon nutrients deprivation in INS1 cells. In this Chapter I further investigated the molecular mechanisms by which glucose is able to prevent cell death, by analysing the activation of the key regulator of cell proliferation, mTOR and its downstream effectors by Western blot. The data presented in this chapter indicated that reintroduction of 15 mM glucose was able to induce the activation of mTOR pathway in pancreatic  $\beta$  cells (Figures 5.3, 5.4 and 5.5), consistent with data in literature (Cousin et al. 1999, Dickson et al. 2001, Kwon et al. 2004). Also consistent with my data (Figures 5.6 and 5.7), it was shown that glucose-induced activation of mTOR pathway is rapamycin sensitive in isolated  $\beta$  cell lines and rat islets (Dickson et al. 2001, Kwon et al. 2004). The fact that glucose-induced proliferation was affected by rapamycin suggested that the intracellular pathway triggered in INS1 cells involves mTORC1, in these experimental conditions. However, mTORC2 complex can also be inhibited by long term treatment (24 hours or more) with rapamycin in many cell types (Sarbasov et al. 2006) and therefore, it was not possible to completely rule out its involvement. Moreover, data in literature indicate that both complexes induce cell proliferation mechanisms (Xie and Herbert 2012). However, my data indicated that stimulatory concentrations of glucose were able to induce the phosphorylation of the direct downstream targets of mTORC1, 4EBP1 and S6K, and S6K downstream effector S6 (Figures 5.4, 5.5 and 5.7). Moreover, glucose did not

seem to induce phosphorylation of Ser 473 of Akt, which is modulated by mTORC2 in certain cell types (Sarbasov et al. 2006). These data confirm the hypothesis of a specific glucose-induced activation of mTORC1.

Once assessed that glucose was able to activate mTORC1 in INS1 cells, I then decided to investigate the potential role of PI3K-C2 $\alpha$  in this glucose-stimulated and mTORC1-dependent intracellular signalling pathway. The protective effect of stimulatory concentrations of glucose on cell viability was affected by both rapamycin (Figure 5.8) and downregulation of PI3K-C2 $\alpha$  (Figure 4.8). Importantly, my data indicated that rapamycin treatment had no effect on cell viability in INS1 sh PI3K-C2 $\alpha$  cells. This suggests that both rapamycin and downregulation of PI3K-C2 $\alpha$  affect the same intracellular pathway. Therefore, I further investigated the activation of mTORC1 and its pathway upon downregulation of PI3K-C2 $\alpha$ .

To this end, I analysed glucose-induced activation of mTORC1 pathway in INS1 sh scrambled sh PI3K-C2 $\alpha$  cells by Western blot and densitometric analysis. Results indicated that downregulation of PI3K-C2 $\alpha$  affected the phosphorylation of mTOR on Ser 2448, 4EBP1 Thr on 37/46, S6K on Thr 389 and S6 on both Ser 235/236 and 240/244. These data are consistent with a previous report indicating that downregulation of PI3K-C2 $\alpha$  affects mTORC1 activity in 3T3-L1 adipocytes upon insulin stimulation, with no effect on the phosphorylation of Akt (Bridges et al. 2012) Importantly, my data indicate that PI3K-C2 $\alpha$  mediates the intracellular signalling

triggered by glucose and stimulating mTORC1 and its downstream effectors. To the best of my knowledge, this has never been reported before.

Previous studies reported a role for class III PI3K hVps34 in amino acids and glucose-induced stimulation of mTORC1 pathway (Byfield et al. 2005). The specific contribution of hVps34 has not been investigated in my study. However, the downregulation of PI3K-C2 $\alpha$  was able to reduce, and not completely suppress, the activation of mTORC1 pathway in INS1 cells. Therefore, my study does not rule out the possibility that class III hVps34 is also involved in glucose-stimulated mTOR activation. However, my data indicated that glucose-induced cell survival was not affected by the inhibitors wortmannin and LY294002.

Moreover, my results indicated that nutrients deprivation induced the phosphorylation of AMPK, consistent with the activation of this protein following a low energy status (Canto and Auwerx 2010). Downregulation of PI3K-C2 $\alpha$  caused hyperactivation of AMPK, as assessed by phosphorylation of Thr 172 (Figure 5.19). Evidence in literature indicated that downregulation of PI3K-C2 $\alpha$  affects the expression of  $\beta$  glucokinase, the enzyme that phosphorylates glucose modulating the rate limiting step of ATP production using glucose as substrate (Leibiger et al. 2010). As a consequence, the reduced expression of  $\beta$  glucokinase affects ATP production, leading to AMPK hyperactivation. Therefore, it is possible that PI3K-C2 $\alpha$  regulates AMPK activation by modulating  $\beta$  glucokinase expression. Moreover, since active AMPK inhibits mTOR phosphorylation, this could explain the decreased

glucose-induced activation of mTOR pathway in INS1 sh PI3K-C2 $\alpha$  cells. However, AMPK phosphorylation was clearly detectable in sh scrambled cells upon glucose reintroduction, and this did not affect mTOR phosphorylation or the activation of its downstream effectors.

It has been reported that downregulation of PI3K-C2 $\alpha$  affected Akt1 activity and subsequently  $\beta$  glucokinase expression, and the resulting decreased ATP production upon glucose stimulation could account, at least in part, for the observed decrease in insulin secretion in MIN6 cells (Leibiger et al. 2010). In contrast with this, my data indicated that downregulation of PI3K-C2 $\alpha$  did not affect the phosphorylation levels of either Ser 473 or Thr 308 of Akt, in these experimental conditions (Figures 5.18, 5.21 and 5.22). In fact, no clear modification of the phosphorylation levels of Akt was detected in INS1 sh scrambled or sh PI3K-C2 $\alpha$  cells upon nutrients starvation and glucose reintroduction. This discrepancy might be explained by the different cellular system and experimental approach used to assess Akt activity. Furthermore, it has been reported that the duration of glucose deprivation can modulate site-specific activation of Akt in several cell types, protecting cells from death (Gao et al. 2013). In my experimental conditions, neither residue Thr 308 nor Ser 473 of Akt seemed to be affected by glucose stimulation. On the other hand, nutrients deprivation induced clear inhibition of mTORC1 and its downstream effectors, suggesting that glucose-induced activation of mTORC1 pathway is independent of Akt activity.



Importantly, short term glucose stimulation of mTOR downstream effectors suggested that the activation of this intracellular pathway is specific, glucose dependent and requires the activation of PI3K-C2 $\alpha$  in INS1 cells. Hence, my data indicate that PI3K-C2 $\alpha$  is required for glucose-induced mTOR activation and that this novel PI3K-C2 $\alpha$ /mTORC1 pathway is able to protect pancreatic  $\beta$  cell from death induced by nutrients deprivation. This finding is particularly relevant for understanding the progression of T2D and the mechanisms underlying the failure of pancreatic  $\beta$  cells in this context.

## Chapter 6

### Mechanisms of PI3K-C2 $\alpha$ activation

#### 6.1 Introduction

Insulin secretion is physiologically triggered in pancreatic  $\beta$  cell by stimulation with glucose, which is metabolised and increases ATP/ADP ratio, causing the depolarisation of the plasma membrane and the influx of calcium. Ultimately, it is the rise in intracellular calcium concentration that causes the fusion of insulin granules to the plasma membrane, allowing the release of their insulin content in the extracellular space. Treatment with high concentrations of KCl induces insulin secretion *in vitro* in pancreatic  $\beta$  cells, allowing studying insulin exocytosis without the metabolic component activated by glucose. Specifically, treatment with KCl causes depolarisation of the plasma membrane, which opens the voltage-gated Ca<sup>2+</sup> channels increasing the intracellular concentration of Ca<sup>2+</sup> and inducing insulin exocytosis through a mechanism not fully understood (Jewell et al. 2010).

In this context, previous work from my laboratory has shown that PI3K-C2 $\alpha$  is necessary for insulin secretion and, in particular, that downregulation of PI3K-C2 $\alpha$  in INS1 cells affects insulin granules exocytosis upon stimulation with KCl (Dominguez et al. 2011). Also, several studies reported that PI3K-C2 $\alpha$  is required for exocytosis in different contexts. Specifically, it has been found that PI3K-C2 $\alpha$  is involved in the

exocytosis of neurosecretory granules in neuroendocrine cells and that this process requires the intracellular second messenger PtdIns3P (Meunier et al. 2005). In L6 cells, it has been found that PI3K-C2 $\alpha$  is necessary for maximal GLUT4 translocation to the plasma membrane, in an exocytotic-like process that also involves the synthesis of PtdIns3P (Falasca et al. 2007). These lines of evidence suggest a role for PI3K-C2 $\alpha$  and, possibly, PtdIns3P in the fusion of intracellular granules to the plasma membrane.

Furthermore, evidence in literature reported that glucose-induced insulin secretion requires PI3K-C2 $\alpha$  in MIN6 cells, and that insulin-induced synthesis of the lipid second messenger PtdIns(3,4)P<sub>2</sub> is affected by downregulation of PI3K-C2 $\alpha$ , with no changes in PtdIns3P and PtdIns(3,4,5)P<sub>3</sub> levels (Leibiger et al. 2010).

Therefore, I sought to investigate the precise role of PI3K-C2 $\alpha$  in pancreatic  $\beta$  cells in the context of insulin granules exocytosis. In particular, I investigated which lipid product(s) were synthesised upon stimulation of insulin granules exocytosis induced by KCl and whether PI3K-C2 $\alpha$  was involved in this process.

To this end, I performed High Pressure Liquid Chromatography (HPLC) analysis of intracellular PIs upon stimulation of insulin secretion. HPLC is one of the few quantitative techniques that can be used to study lipids, which allows detecting modifications in the PIs profile within a cell. PIs are amphipathic phospholipids that are minor components of cellular membranes. They are made up of a soluble inositol head which is linked, through a phosphodiester bond in position 1, to two

fatty acid chains that constitute its insoluble tails. As mentioned before, the inositol head has five hydroxyl groups, three of which (positions 3, 4 and 5) can be phosphorylated in different combinations generating different PIs that play critical regulatory roles in several intracellular functions.

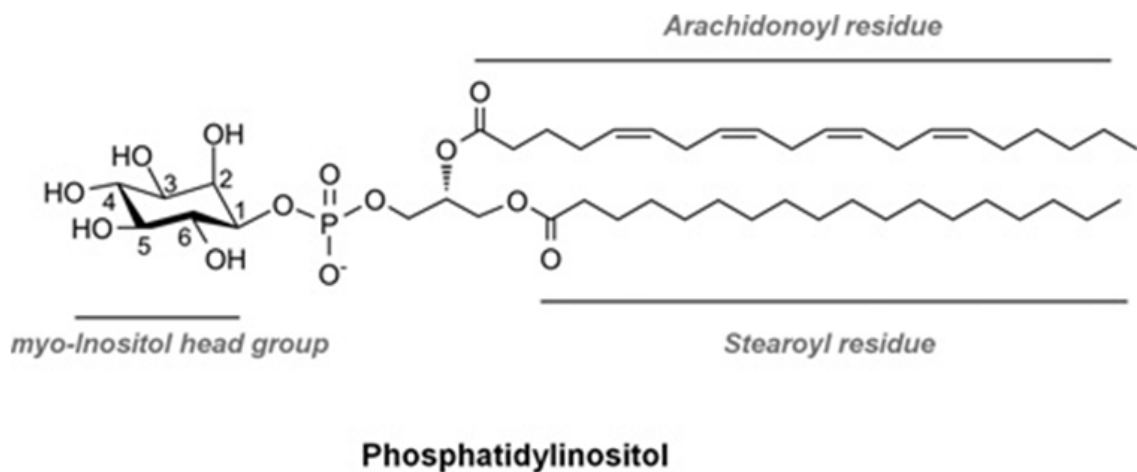


**Figure 6.1: Chemical structure of phosphatidylinositol (PtdIns), the building block of all PIs (Falasca and Maffucci 2012).**

Previous work optimised the conditions to extract and detect intracellular PIs using this technique, and Prof. Falasca and his group optimised the conditions to detect specifically PtdIns3P. In brief, cells are labelled with *myo*-[<sup>3</sup>H]inositol, which is incorporated in the neosynthesised PIs and inositol phosphates. This is achieved with incubation of cells in inositol-free medium supplemented with *myo*-[<sup>3</sup>H]inositol for the time necessary to reach isotopic equilibrium, which depends on the cell type and requires optimisation. Then, cells are lysed and lipids are extracted by phase

separation using a mix of hydrochloric acid, methanol and chloroform. During this step, water soluble inositol phosphates accumulate in the aqueous fraction and can therefore be separated by PIs that accumulate in the organic phase, due to their hydrophobic acyl chains. Once the organic phase containing phosphoinositides is retrieved, solvents are evaporated and PIs can be deacylated using a mix of monomethylamine, water, butanol and methanol. This step allows to chemically remove the water-soluble glycerophosphoinositol head groups from the acyl chains (Figure 6.2), that can affect the binding to the HPLC column.

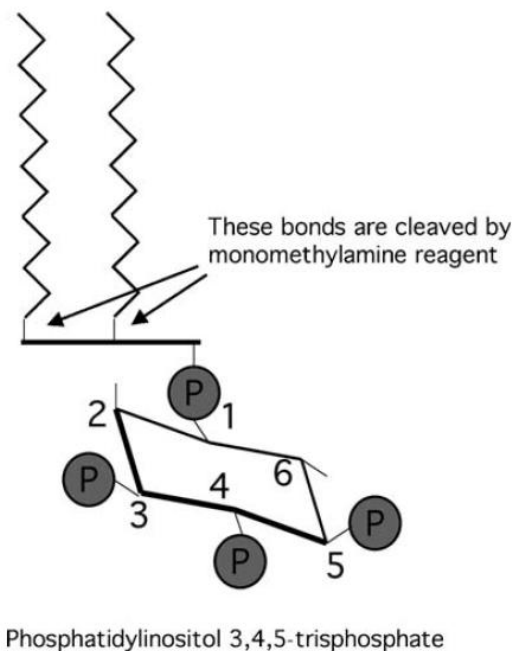


**Figure 6.2:** Schematic diagram of PtdIns(3,4,5)P<sub>3</sub>. The cleavage site of monomethylamine reagent is shown (Cooke 2009).

Aqueous phase containing glycerophosphoinositides is then separated by the organic phase containing fatty acyl chains using a mix of butanol, petroleum ether and ethyl acetate. Glycerophosphoinositides are then separated from the solvents and resuspended in water for HPLC analysis with a strong anion exchange column. The number and the position of the phosphate groups on the glycerophosphoinositides determine the strength of their bond to the column. Therefore, they can be gradually eluted by increasing the ionic force of the buffer used, with the non phosphorylated species being eluted first, then the mono, bis and the trisphosphorylated glycerophosphoinositides being progressively detached from the column at later stages of the run. In order to gradually increase the ionic force of the buffer, a mix of two solutions is used (referred to as buffer A and buffer B). The ratio between buffer A (1mM EDTA) and buffer B [1.3M  $(\text{NH}_4)_2\text{HPO}_4$  + 1mM EDTA] and how the percentage of buffer B increases with time has been optimised to better separate the phosphorylated PIs, and to specifically detect PtdIns3P. This is achieved through elution of the sample from the ion exchange column with a non linear composition gradient, which is schematically represented in Figure 6.3.

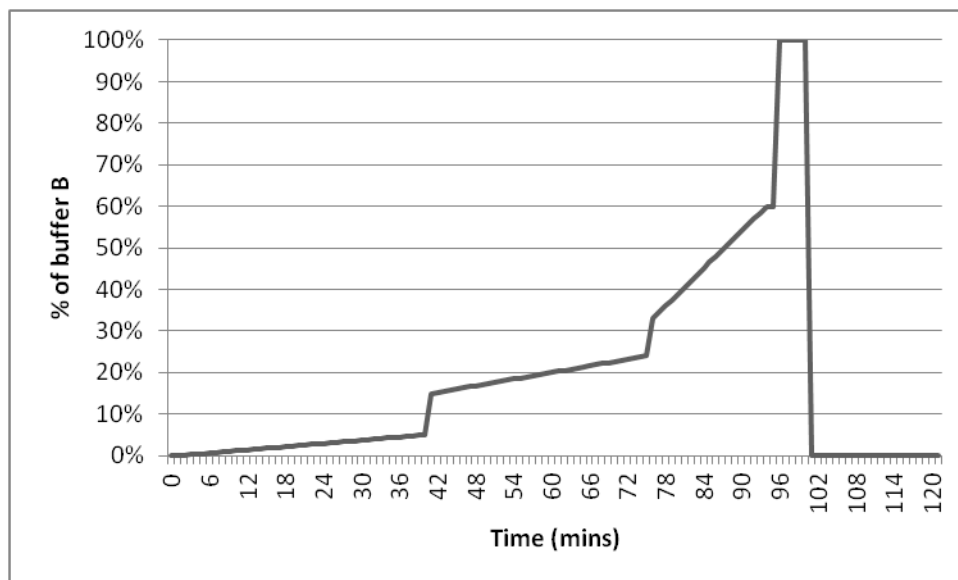


**Figure 6.3: Schematic diagram of the non linear gradient of buffer A (1mM EDTA) and buffer B [1.3M (NH<sub>4</sub>)<sub>2</sub>HPO<sub>4</sub> + 1mM EDTA].**

The percentage of buffer B in the elution buffer rapidly increases at minutes 40, 75 and 96. This creates three steps of elution. In the first step, from minute 1 to 39 the unphosphorylated phosphatidylinositol is eluted, followed by the monophosphorylated species. In the second, from minute 41 to 74, the bisphosphorylated PIs are detached from the column, followed in the third step (minute 76-95) by the trisphosphorylated species. At minute 96, the percentage of buffer B in the elution buffer increases rapidly from 60 to 100%, ensuring the removal of any remaining species from the chromatography column. Then, the HPLC column is washed with 100% buffer A and re-equilibrated to the initial high aqueous solvent composition, which allows subsequent use and loading of a new sample for analysis.

Eluted sample are collected in fractions, mixed with the appropriate amount of scintillation fluid and radioactivity is detected using a beta counter. PIs are characterised by high-phosphate content, especially in the later part of run, when the bis and trisphosphorylated species are eluted. Therefore, the scintillation fluid of choice has to be able to solubilise samples containing high levels of phosphate in order to reduce the error and improve counting efficiency (Cooke 2009).



## 6.2 Results

### 6.2.1 Optimisation – Labelling and starvation

In order to investigate what lipid species are synthesised in pancreatic  $\beta$  cells upon KCl-induced insulin exocytosis, HPLC was performed.

As mentioned before, the process of labelling cells with *myo*-[ $^3\text{H}$ ]inositol depends on the specific cell line used. The incubation time and conditions had to be optimised specifically for INS1 cells. To this purpose, INS1 cells were incubated with an inositol-free medium (M199) supplied with *myo*-[ $^3\text{H}$ ]inositol. The use of inositol free medium ensures that the only inositol present in the culture medium is the *myo*-[ $^3\text{H}$ ]inositol supplied. INS1 cells would internalise the tritiated compound, using it for the synthesis and the turnover of phospholipids. In this type of studies, the amount of FBS used tends to be minimised, since it is source of cold inositol which could compete with *myo*-[ $^3\text{H}$ ]inositol. Therefore, INS1 cells were incubated with 5  $\mu\text{Ci}$  *myo*-[ $^3\text{H}$ ]inositol/ml, in serum free or 1% FBS-supplemented M199 medium for 24 or 48 hours. Then, INS1 cells were washed, lysed and the radioactivity of the whole lysate was measured using a beta counter. In all cases, incubation medium was supplemented with 1% fresh glutamine. Results indicated that the presence of FBS decreased the amount of internalised compound, while the amount of tritiated inositol was slightly increased from 24 to 48 hours incubation. Therefore, I decided to set the experimental conditions to 5  $\mu\text{Ci}$  *myo*-[ $^3\text{H}$ ]inositol/ml in serum-free M199 for 24 hours, as a shorter incubation would less affect cell viability. This explorative

experiment indicated that INS1 cells were able to survive starvation in inositol free medium supplemented with tritiated inositol. Also, cells were able to internalise the radioactive compound under these experimental conditions.

In order to confirm that cells were healthy and still responsive after starvation, Western blot experiments were performed in parallel with the HPLC experiments. To this end, I assessed whether INS1 cells and stable cell lines were able to respond to insulin stimulation, as this stimulus is known to activate class I PI3Ks, leading to Akt activation and phosphorylation. Using the same conditions as the HPLC experiments, INS1 cells were starved for 24 hours in serum free M199 medium, followed by 30 minutes starvation in Krebs Ringer buffer and 30 minutes stimulation with 100nM insulin. Phosphorylation of Ser 473 of Akt was then analysed by Western blot. A representative experiment is shown in Figure 6.4.

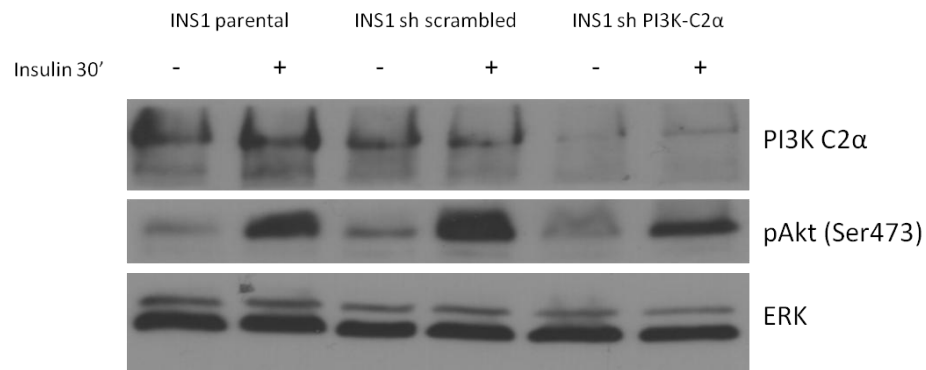


**Figure 6.4: Representative blot of the indicated INS1 cell lines untreated or stimulated with 100 nM insulin for 30 min. Downregulation of PI3K-C2 $\alpha$  was determined by using a specific antibody. Activation of Akt was assessed by monitoring its phosphorylation at residue Ser473.**

Western Blot analysis confirmed the efficient knock down of PI3K-C2 $\alpha$  in INS1 sh PI3K-C2 $\alpha$  cells. Upon serum starvation, phosphorylation of Ser 473 of Akt was reduced in INS1 parental, sh scrambled and sh PI3K-C2 $\alpha$  cells. The phosphorylation levels of Akt were increased upon 30 minutes treatment with insulin in all the cell lines. This indicated that INS1 parental, sh scrambled and sh PI3K-C2 $\alpha$  cells were all able to respond to cellular stimulation under the same starvation conditions used for HPLC experiments.

### **6.2.2 Optimisation – HPLC analysis**

HPLC analysis of intracellular PIs had been already optimised and performed in my laboratory (Iacovelli et al. 1993, Razzini et al. 2000, Falasca et al. 2007). Therefore, I decided to assess whether the same HPLC experimental conditions would allow to study the PIs profile in INS1 cells.

To this end, INS1 cells were labelled with *myo*-[<sup>3</sup>H]inositol as previously described. Cells were then washed, lysed and cellular extracts were prepared for HPLC analysis as described in Chapters 2.6.1 and 6.1. After the run, each sample was collected in 80 eluted fractions corresponding to 1 ml/min and radioactivity was measured using a beta counter. Figure 6.5 shows a representative chromatogram of intracellular glycerophosphoinositides from INS1 cells. Y axes shows the amount of radioactivity detected, expressed in counts per minute (cpm), x axes shows the retention time of each fraction of a single sample. The peaks highlighted by the arrows correspond to

the indicated species of PIs and measuring the height of each peak allows to estimate its abundance.

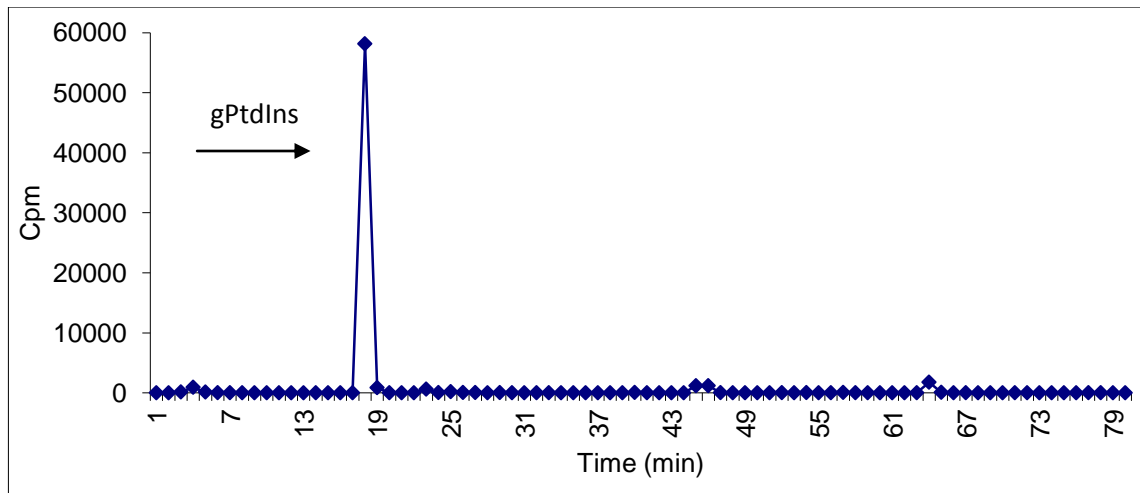


**Figure 6.5: Representative chromatogram of glycerophosphoinositides extracted from INS1 cells and analysed by HPLC.**

The peak visible at minute 18 corresponds to gPtdIns, the most abundant type of PIs, accounting for 90-96% of the total (Falasca and Maffucci 2012). The scale of y axes is adjusted to the maximum value of cpm detected. Using this scale, the rest of the run appears undistinguishable from the baseline.

In order to better visualise the different PIs species, which are present in different amounts within the cells, the scale of y axes has been gradually decreased for next figures.

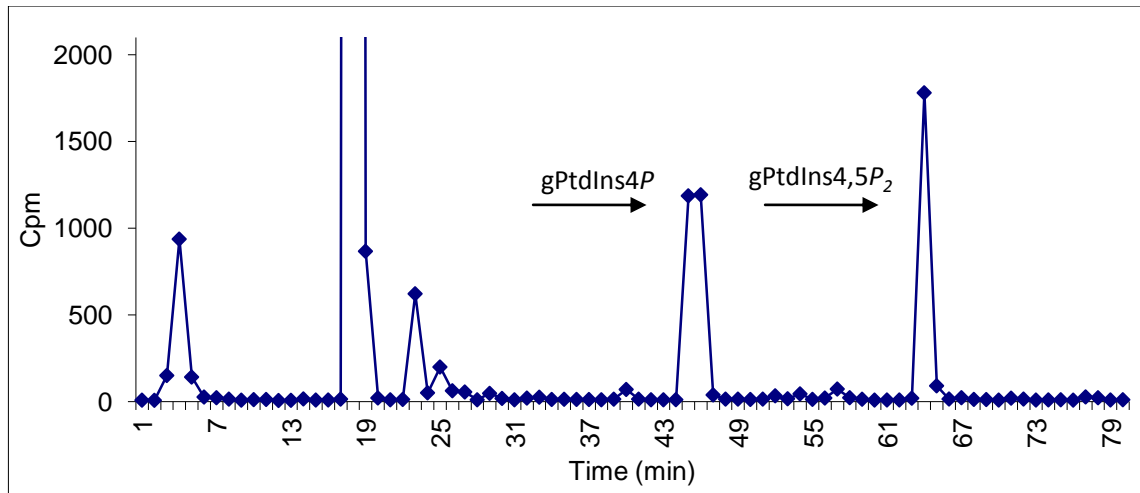


**Figure 6.6: Representative chromatogram of glycerophosphoinositides extracted from INS1 cells and analysed by HPLC.**

Figure 6.6 shows the HPLC run of the same sample as in Figure 6.5, adjusting the scale of y axes to a maximum of 2000 cpm. It is possible to detect a peak at 5 minutes, corresponding to the fraction of sample which did not bind the chromatography column (void volume) and therefore, was eluted quickly. Two other peaks are detected at minutes 45 and 64, and they correspond to the most abundant species of phosphorylated PIs, gPtdIns4P and gPtdIns(4,5)P<sub>2</sub> respectively. PtdIns4P is the most abundant of the monophosphorylated PIs. PtdIns4P and the bisphosphorylated PtdIns(4,5)P<sub>2</sub> represent each 0.05% of total membrane lipids (Maffucci 2012).

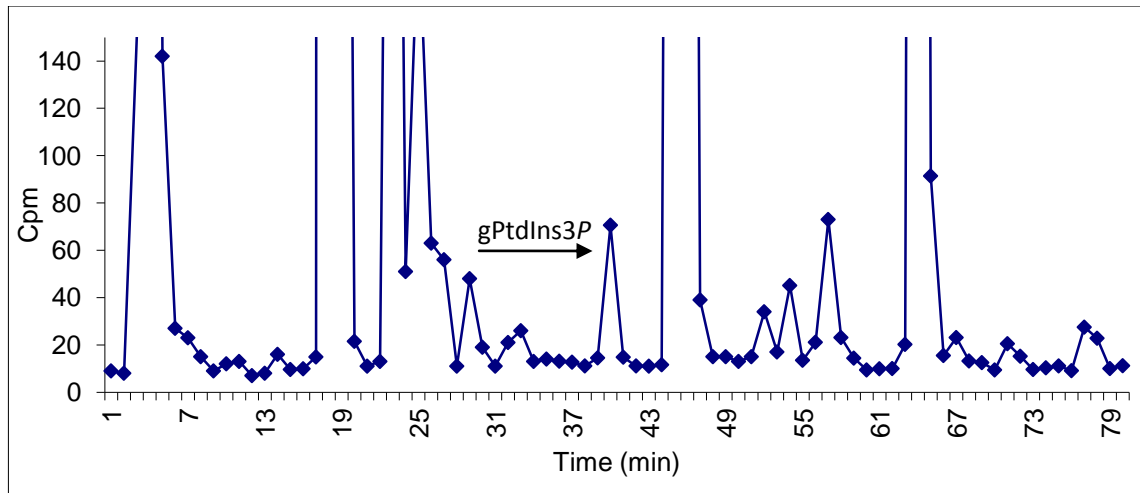


**Figure 6.7: Representative chromatogram of glycerophosphoinositides extracted from INS1 cells and analysed by HPLC.**

Further adjusting the scale of y axes, less abundant species of PIs can be visualised. At minute 39 on Figure 6.7, a small peak is visible and it corresponds to gPtdIns3P. PtdIns3P is the most abundant of the 3-phosphorylated PIs in unstimulated cells and it represents 0.1–0.5% of all PIs. PtdIns(3,4)P<sub>2</sub> and PtdIns(3,4,5)P<sub>3</sub> are barely detectable in unstimulated cells, and their level increase only upon cellular stimulation (Falasca and Maffucci 2009).

This optimisation step indicated that this HPLC protocol allowed to detect PIs species present in INS1 cells in unstimulated conditions.

Previous data from my laboratory have shown that treatment with 60 mM KCl induced insulin secretion in INS1 cells (Dominguez et al. 2011). Treatment with KCl, rather than a high glucose stimulus, allows to study exclusively the last step of

insulin secretion, namely the exocytosis of insulin granules. I then decided to investigate which lipid species are synthesised upon KCl stimulation in INS1 cells.

### **6.2.3 Stimulation of INS1 cells with KCl induces PtdIns3P de novo synthesis**

To the best of my knowledge, HPLC analysis of intracellular PIs of INS1 cells upon KCl stimulation has never been investigated before. Therefore, an additional optimisation step under these experimental conditions was necessary. INS1 cells were labelled with *myo*-[<sup>3</sup>H]inositol, starved in Krebs Ringer buffer for 30 minutes and stimulated with 60 mM KCl, to induce insulin secretion as previously described (Dominguez et al. 2011). Time-course experiments (0, 2.5, 5 and 10 minutes) were necessary to determine whether KCl stimulation was able to alter the PIs profile in INS1 cells.

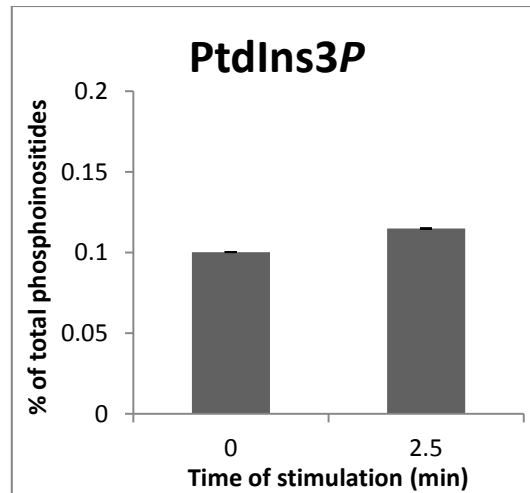


**Figure 6.8:** Analysis of the levels of PtdIns3P in INS1 cells upon stimulation with KCl. Cells were stimulated with 60mM KCl for 2.5 minutes and levels of PtdIns3P were analysed by HPLC. Data are expressed as percentage of total PIs.

Data showed that stimulation with KCl for 2.5 minutes only slightly increased the levels of PtdIns3P compared to the unstimulated sample (Figure 6.8).

Then, the levels of PtdIns3P, PtdIns4P and PtdIns(4,5)P<sub>2</sub> of INS1 cells in starved conditions, and upon 5 and 10 minutes of KCl stimulation were analysed. Data showed that treatment of INS1 cells with KCl induced *de novo* synthesis of the lipid second messenger PtdIns3P (Figure 6.9).



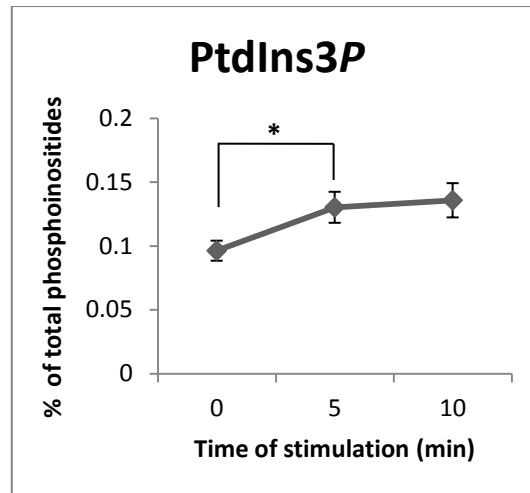


**Figure 6.9:** Analysis of the levels of PtdIns3P in INS1 cells upon stimulation with KCl. Cells were stimulated with 60mM KCl for the indicated time points and levels of PIs were analysed by HPLC. Data are expressed as percentage of total PIs and are means  $\pm$  S.E.M. of 2-6 independent experiments. \* p value < 0.01 vs unstimulated control.

This data was also confirmed by analysis of intracellular localisation of the pool of PtdIns3P upon KCl stimulation by confocal microscopy (see Chapter 7).

Analysis of other PIs species showed that the levels of PtdIns4P and PtdIns(4,5)P<sub>2</sub> were not significantly modified by treatment with KCl (Figure 6.10).

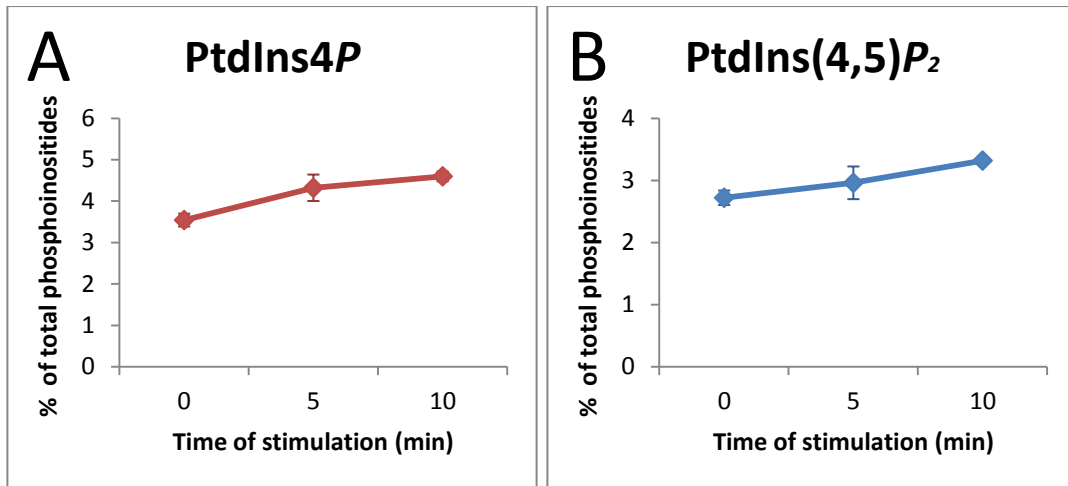


**Figure 6.10:** Analysis of the levels of PIs in INS1 cells upon stimulation with KCl. Cells were stimulated with 60mM KCl for the indicated time points and levels of PIs were analysed by HPLC. Data are expressed as percentage of total PIs and are means  $\pm$  S.E.M. of 2-6 independent experiments.

These data suggest that the observed increase in the levels of PtdIns3P is specifically induced by treatment with KCl.

Data in literature showed that the intracellular second messenger PtdIns3P is the product of PI3K-C2 $\alpha$  in L6 cells upon stimulation with insulin (Falasca et al. 2007). In contrast with these data, it was reported that PI3K-C2 $\alpha$  regulates the glucose-induced synthesis of PtdIns(3,4)P<sub>2</sub> in MIN6 cells (Leibiger et al. 2010). Also, data showed that downregulation of PI3K-C2 $\alpha$  decreased insulin secretion upon stimulation with KCl in INS1 cells. In order to investigate whether the KCl-dependent pool of PtdIns3P was synthesised upon activation of PI3K-C2 $\alpha$ , HPLC analysis of PIs profile was performed in INS1 sh scrambled and sh PI3K-C2 $\alpha$  upon KCl stimulation.

#### 6.2.4 Stimulation of INS1 sh-scrambled and sh-PI3K-C2 $\alpha$ cells with KCl induces *de novo* synthesis of PtdIns3P

INS1 sh scrambled and sh PI3K-C2 $\alpha$  cells were labelled with *myo*-[ $^3$ H]inositol and then incubated in Krebs-Ringer buffer as previously described. Then, cells were treated for 5 or 10 minutes with KCl and samples were prepared for HPLC analysis as previously described.

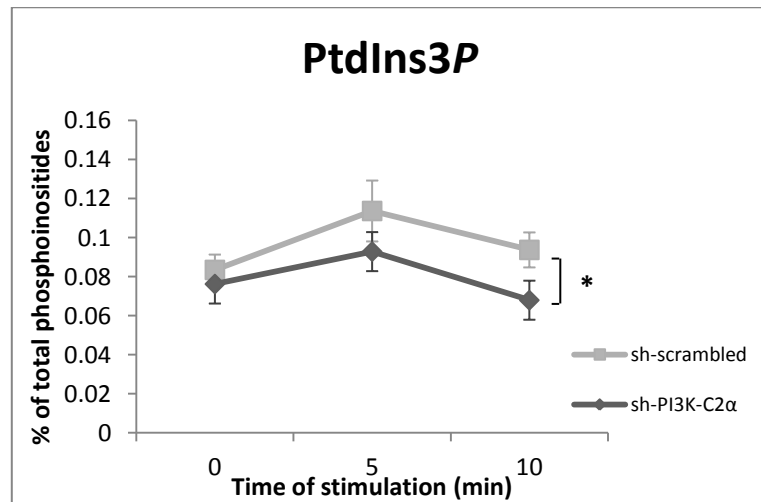
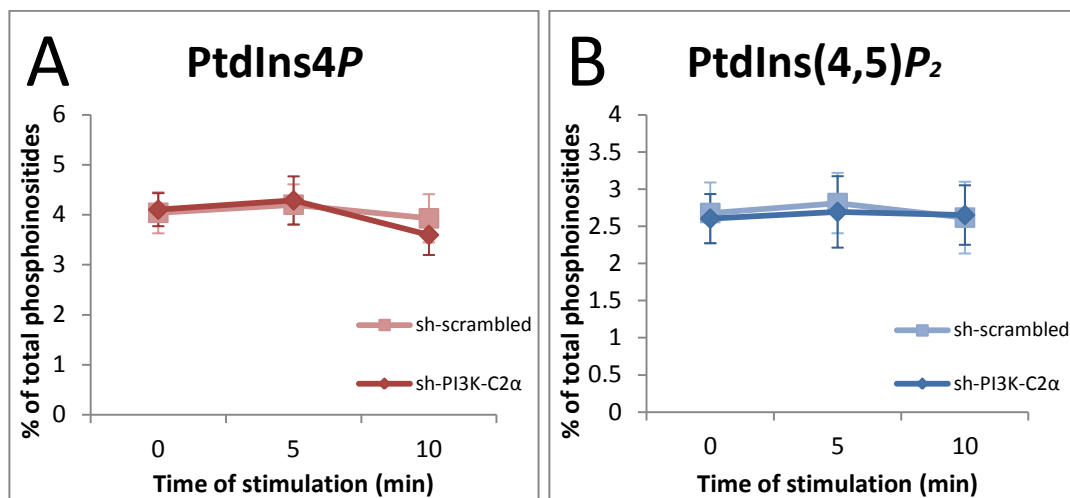


Figure 6.11: Analysis of the levels of PtdIns3P in INS1 sh scrambled and sh PI3K-C2 $\alpha$  cells upon stimulation with KCl. Cells were stimulated with 60mM KCl for the indicated time points and levels of PtdIns3P were analysed by HPLC. Data are expressed as percentage of total PIs and are means  $\pm$  S.E.M. of 3-4 independent experiments. 5 minutes stimulation with KCl induced a statistically significant increase of PtdIns3P compared to the unstimulated control in both cell lines (not shown). \*p value < 0.05 (sh scrambled cells vs sh PI3K-C2 $\alpha$  cells upon 10 minutes stimulation with KCl)

Results indicated that treatment with KCl for 5 minutes induced a significant increase in the levels of PtdIns3P in both cell lines (Figure 6.11). Interestingly, the amount of PtdIns3P detected in sh PI3K-C2 $\alpha$  cells upon treatment with KCl was

reduced compared to control cells. Also, the amount of PtdIns3P detected upon 10 minutes of stimulation with KCl was significantly higher in control cells compared to INS1 sh PI3K-C2 $\alpha$  cells.

Furthermore, levels of PtdIns4P and PtdIns(4,5)P<sub>2</sub> were investigated (Figure 6.12 A and B, respectively).



**Figure 6.12:** Analysis of the levels of PIs in INS1 sh-scrambled and sh-PI3K-C2 $\alpha$  cells upon stimulation with KCl. Cells were stimulated with 60mM KCl for the indicated time points and levels of PIs were analysed by HPLC. Data are expressed as percentage of total PIs and are means  $\pm$  S.E.M. of 3-4 independent experiments.

Results indicated that there was no change in the levels of PtdIns4P and PtdIns(4,5)P<sub>2</sub> upon treatment with KCl.

Taken together, these results further suggest that KCl specifically increases the levels of PtdIns3P, as the profile of the other PIs analysed did not change. Also, data indicated that KCl-induced increase of PtdIns3P is affected by downregulation of

PI3K-C2 $\alpha$ . This suggests that the KCl-dependent pool of PtdIns3P might be synthesised through PI3K-C2 $\alpha$  activation. These data were also investigated by fluorescent microscope analysis of the intracellular pool of PtdIns3P (see Chapter 7).

### **6.2.5 Glucose induces the synthesis of the lipid product PtdIns3P**

Data shown in Chapter 6.2.4 suggested that synthesis of PtdIns3P induced by cellular stimulation able to induce insulin secretion stimulus such as KCl stimulation is affected by downregulation of PI3K-C2 $\alpha$  in INS1 cells. Also, data shown in Chapter 5 defined a role for PI3K-C2 $\alpha$  in the intracellular signalling cascade activated by stimulatory concentrations of glucose. Insulin secretion is induced, *in vivo*, by a rise in glucose concentration in the blood. Therefore, I decided to investigate whether glucose was able to modulate the levels of PtdIns3P in a mechanism involving PI3K-C2 $\alpha$ .

These experiments required a further optimisation of the HPLC protocol, since the starvation conditions previously used for HPLC experiments did not deprive INS1 cells from glucose. Also, as glucose induces insulin secretion through a different intracellular mechanism than KCl, a wider time course was used to analyse the profile of intracellular PIs. Preliminary experiments were performed by incubating INS1 cells with serum-free M199 medium supplied with 5  $\mu$ Ci *myo*-[ $^3$ H]inositol/ml, as previously described. Then, cells were further incubated with Hank's Balanced Salt Solution (HBSS), with low glucose and in the absence of amino acids for 1 hour and

then stimulated with serum-free RPMI supplemented with 15mM glucose for 2.5, 5, 10 or 20 minutes or left in HBSS as a control. As an additional control, one sample was left in serum-free, inositol-free M199 medium. This additional condition allowed to assess whether incubation in amino acid-free, low glucose HBSS medium itself was able to affect the levels of PtdIns3P of unstimulated INS1. The results of these experiments are shown in Figure 6.13.

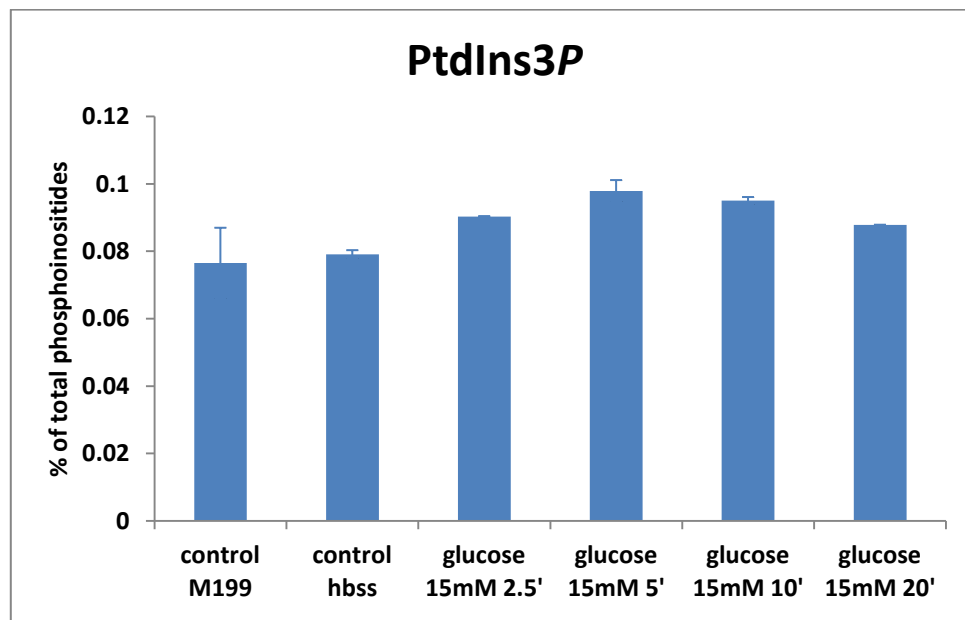


**Figure 6.13: Analysis of the levels of PtdIns3P in INS1 cells upon stimulation with 15mM glucose. Cells were stimulated for the indicated time points and levels of PIs were analysed by HPLC. Data are expressed as percentage of total PIs. n = 1 - 2**

Levels of PtdIns3P were analysed and they are expressed as a percentage of total intracellular PIs. Controls in M199 and in HBSS showed comparable basal levels of PtdIns3P. This indicated that 1 hour incubation in low glucose and amino acid-free

medium did not induce variations of PtdIns3P levels compared to samples in M199. Moreover, stimulation with RPMI supplemented with 15 mM glucose induced a time-dependent increase in the levels of PtdIns3P, which peaked at 5 minutes stimulation and slowly declined at longer time points. These experiments indicated that PtdIns3P levels are increased upon treatment with RPMI supplemented with stimulatory concentrations of glucose.

Since HBSS contains low concentrations of glucose and no amino acids, additional experimental conditions were also tested to further investigate the mechanisms of glucose-dependent increase of PtdIns3P levels. Therefore, in order to determine whether glucose or amino acids were responsible for the observed increase in PtdIns3P levels, I decided to incubate cells with RPMI supplemented with 0.5 mM glucose for 1 hour rather than HBSS.

Therefore, INS1 cells were labelled with tritiated inositol in serum-free M199 medium as previously described and then they were incubated with RPMI supplemented with 0.5 mM glucose for 1 hour. In contrast with previous experiments, in these experimental conditions INS1 cells were incubated in low glucose concentrations. As an additional control, one sample was left in inositol-free M199 medium for 1 hour, to assess whether the levels of PtdIns3P were altered by the starvation conditions. Results are shown in figure 6.14.

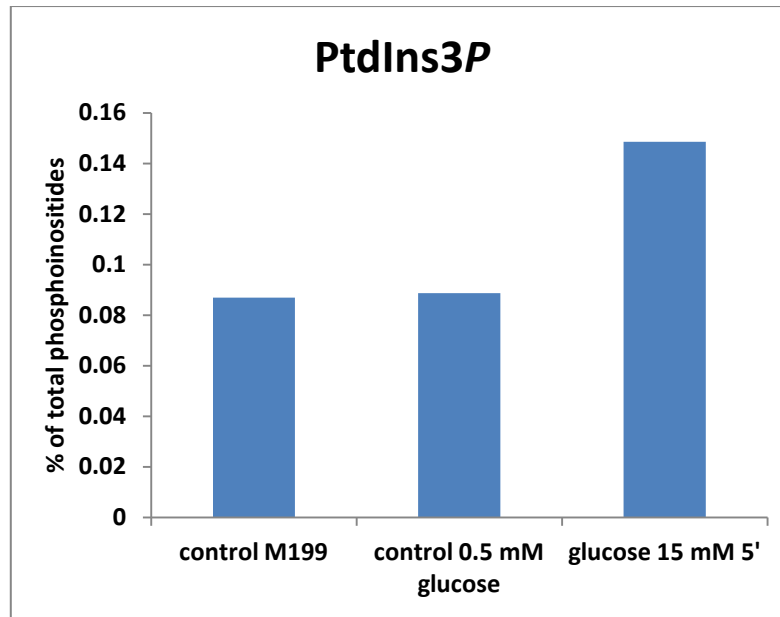


**Figure 6.14: Analysis of the levels of PtdIns3P in INS1 cells upon stimulation with 15mM glucose. Cells were stimulated for the indicated time points and the levels of PIs were analysed by HPLC. Data are expressed as percentage of total PIs.**

Data indicated that levels of PtdIns3P were not modified by treatment with RPMI supplemented with 0.5 mM glucose for 1 hour. Indeed, levels of PtdIns3P upon 24 incubation in serum free medium containing 0.5 mM glucose were comparable to those observed upon incubation in M199 or HBSS. This indicates that glucose deprivation has no effect on the levels of PtdIns3P, in these experimental conditions. Interestingly, reintroduction of stimulatory concentrations of glucose induced a remarkable increase in the levels of PtdIns3P. This suggests that reintroduction of glucose in INS1 cells is able to induce synthesis of the lipid second messenger PtdIns3P.



Taken together, these preliminary results suggest that glucose is able to induce synthesis of the 3-phosphorylated phosphoinositide PtdIns3P in INS1 cells. Further experiments are needed to confirm these data and to investigate whether or not PI3K-C2 $\alpha$  has a role in glucose-induced synthesis of PtdIns3P.

## 6.3 Discussion

PI3Ks have a well established role in regulating many intracellular processes and deregulation of their pathway is associated with the onset of several diseases, including diabetes and cancer. There is currently an increasing interest in understanding the specific role of distinct PI3Ks isoforms and to determine whether their function within the cell is redundant or complementary. Among the three classes of PI3Ks, class II is the least investigated. Nevertheless, accumulating evidence suggest a role for these enzymes in several cellular functions. For instance, it has been shown that PI3K-C2 $\alpha$  has a role in glucose-induced insulin secretion in MIN6 cells (Leibiger et al. 2010). Also, previous studies reported that downregulation of PI3K-C2 $\alpha$  impairs the fusion of insulin granules to the plasma membrane upon KCl stimulation in INS1 cells, with no effect on total insulin content, on the number of insulin granules proximal to the plasma membrane or on the expression of proteins involved in exocytosis (Dominguez et al. 2011). This, together with the fact that high mRNA levels of PI3K-C2 $\alpha$  were detected in human pancreatic  $\beta$  cells (Muller et al. 2006), suggests that PI3K-C2 $\alpha$  has a role in the complex mechanism of insulin secretion.

Interestingly, different studies highlighted a more general role for PI3K-C2 $\alpha$  in exocytosis in different cellular contexts, suggesting a common role of the enzyme in the fusion of different types of granules or vesicles to the plasma membrane (Mazza and Maffucci 2011, Falasca and Maffucci 2012). For instance, it has been shown that

PI3K-C2 $\alpha$  is implicated in the fusion of neurosecretory granules in adrenal chromaffin cells (Meunier et al. 2005) and it is required for maximal translocation of GLUT4 to the plasma membrane in L6 muscle cells (Falasca et al. 2007). Therefore, these data suggest that PI3K-C2 $\alpha$  may represent a key regulator of exocytosis, with a role in the very late steps of this process.

In order to analyse the final steps of insulin granules exocytosis, I stimulated INS1 cells with KCl. This treatment induces membrane depolarisation which opens the voltage-gated Ca<sup>2+</sup> channel, increasing the intracellular concentration of Ca<sup>2+</sup>, which triggers the fusion of insulin granules to the plasma membrane (Jewell et al. 2010). This approach allows studying exclusively the exocytotic steps of insulin secretion, without the metabolic component activated by glucose stimulation. As mentioned before, it was shown that PI3K-C2 $\alpha$  is involved in KCl-induced insulin secretion, but the precise role of the enzyme and the specific mechanisms by which PI3K-C2 $\alpha$  can regulate this step are still unclear. Therefore, I performed HPLC analysis of PIs of INS1 cells in order to determine whether these lipids are synthesised upon KCl-induced insulin exocytosis.

Data shown in figure 6.9 indicate that KCl treatment induced a significant increase of PtdIns3P levels. Also, the levels of the other PIs analysed were not modified under these experimental conditions, suggesting that KCl treatment specifically induced an increase in PtdIns3P levels. Consistent with these results, preliminary experiments performed using glucose to trigger insulin exocytosis also indicated an increase in

the levels of PtdIns3P. However, previous studies on insulin secreting HIT T15 cells reported a glucose-induced increase of PtdIns(3,4,5)P<sub>3</sub>, PtdIns(3,4)P<sub>2</sub> and PtdIns(3,5)P<sub>2</sub>, with no effect on PtdIns3P levels. (Yu et al. 2007). This difference can be explained by the different experimental conditions and cellular model used.

In order to study whether the observed increase in PtdIns3P levels was dependent on the action of PI3K-C2α, I compared the PIs profile in INS1 sh scrambled and sh PI3K-C2α cells.

Results indicated that there was no difference in the PIs profile between the two cell lines in unstimulated conditions (Figure 6.11). This suggests that the lack of PI3K-C2α does not affect the levels of the PIs detected when the cells are in resting conditions. Moreover, KCl treatment for 5 minutes increased PtdIns3P levels in both cell lines. Interestingly, data showed that the levels of PtdIns3P upon 10 minutes stimulation with KCl were significantly lower in INS1 sh PI3K-C2α cells compared to the scrambled control. Also, there was a trend for a reduced PtdIns3P increase in cells lacking PI3K-C2α after 5 minutes stimulation. These data indicate that KCl-dependent synthesis of PtdIns3P is affected by downregulation of PI3K-C2α. Therefore, these data suggest that PI3K-C2α is activated in INS1 cells under these experimental conditions. The fact that PtdIns3P synthesis was only partially inhibited in PI3K-C2α knock down cells is consistent with previous data showing that downregulation of PI3K-C2α in INS1 cells resulted in an impaired but not totally blunted insulin secretion (Dominguez et al. 2011). Furthermore, these data are

consistent with the observation that, in a different cell type and context, PI3K-C2 $\alpha$  is involved in PtdIns3P synthesis. Specifically, it has been reported that PI3K-C2 $\alpha$  is responsible for PtdIns3P synthesis at the plasma membrane in L6 cells upon insulin stimulation, contributing to the exocytotic-like process of GLUT4 translocation (Falasca et al. 2007). Also, depletion of PI3K-C2 $\alpha$  in HUVEC cells caused a decreased intracellular content of PtdIns3P, but not of PtdIns(3,4)P<sub>2</sub>, PtdIns(3,5)P<sub>2</sub> or PtdIns(3,4,5)P<sub>3</sub> and reduced motility, fusion and fission of vesicles containing PtdIns3P (Yoshioka et al. 2012).

In contrast with this, previous data reported that transient downregulation of PI3K-C2 $\alpha$  in pancreatic  $\beta$  cells MIN6 affects insulin-induced synthesis of PtdIns(3,4)P<sub>2</sub>, whereas no change in PtdIns3P or PtdIns(3,4,5)P<sub>3</sub> was detected in control or knockdown cells (Leibiger et al. 2010). A possible explanation to this could be the different cellular model and stimulation conditions, the presence of serum and the use of inhibitors. Also, the fact that KCl does not seem to induce synthesis of PtdIns(3,4)P<sub>2</sub> or PtdIns(3,4,5)P<sub>3</sub> could be attributed to the time points of stimulation used or to the experimental conditions that might not have allowed to detect less abundant species of PIs. In any case, it was reported that KCl-dependent insulin secretion in INS1 cells does not induce phosphorylation and activation of either Akt or the insulin receptor (Dominguez et al. 2011). This observation further suggests that class I PI3Ks are not involved in KCl-dependent insulin exocytosis in these experimental conditions, as the classical pathway class I PI3Ks/PtdIns(3,4,5)P<sub>3</sub>/Akt is not activated. Also, KCl stimulation does not seem to activate a feedback loop

(Dominguez et al. 2011) as previously reported in glucose-stimulated MIN6 (Leibiger et al. 2010). Taken together, these data indicate that both KCl and glucose-induced insulin exocytosis induce an intracellular increase of PtdIns3P levels. The fact that the increase in PtdIns3P levels is lower in PI3K-C2 $\alpha$  knock down cells suggest that this enzyme is involved, but it is not necessarily the sole responsible, of PtdIns3P synthesis upon KCl or glucose stimulation. Moreover, both KCl and glucose ultimately lead to an intracellular increase of Ca<sup>2+</sup> levels, which triggers insulin exocytosis. It was proposed that the increase in Ca<sup>2+</sup> levels is able to activate PI3K-C2 $\alpha$ , as shown by in vitro kinase assays performed on endogenous protein immunoprecipitated from de-endotheliased rabbit aortic vascular smooth muscle (Wang et al. 2006). This could represent a possible explanation of the mechanism of action of PI3K-C2 $\alpha$ .

## Chapter 7

### Mechanisms of PI3K-C2 $\alpha$ action

#### 7.1 Introduction

Insulin secretion is a complex mechanism that ultimately requires the fusion of insulin granules to the plasma membrane and the release of their insulin content in the extracellular space. The fusion of insulin granules to the plasma membrane of pancreatic  $\beta$  cells is an exocytotic process mediated by SNAREs. KCl and other nonnutrient stimuli induce the 'first phase insulin release', which occurs 5-10 minutes after  $\beta$  cell stimulation. Glucose and fuel type secretagogues also induce a 'second phase insulin release', which might last several hours if the insulin-secreting stimulus persists (Jewell et al. 2010). These two mechanisms involve distinct SNARE isoforms. KCl-induced insulin secretion requires two SNARE proteins associated to the plasma membrane, SNAP 25 and syntaxin 1 or syntaxin 4, which associate with VAMP2 on the secretory granule, forming a stable complex (Jewell et al. 2010, Torrejon-Escribano et al. 2011).

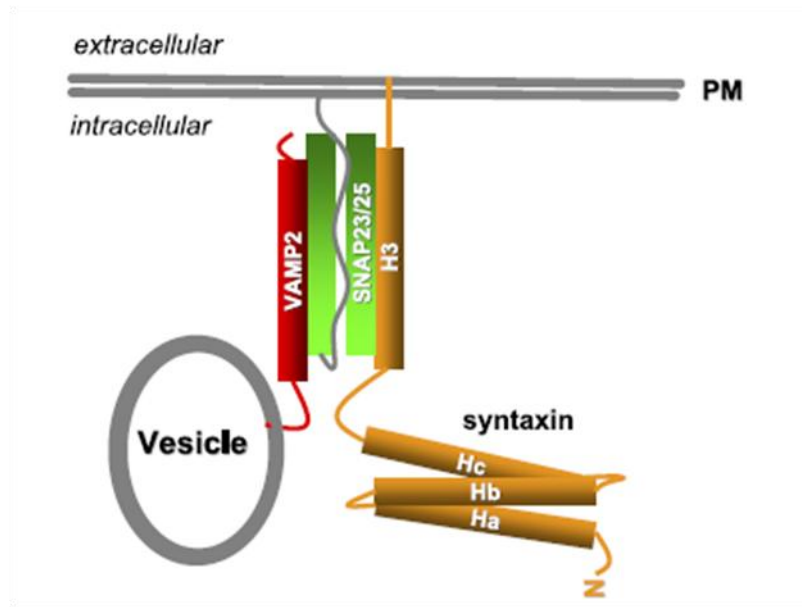


**Figure 7.1: SNAREs core complex.** Interactions between VAMP2 on the vesicle and SNAP 23/25 and syntaxin at the plasma membrane are necessary for exocytosis. Adapted from Jewell et al., 2010.

Glucose-induced insulin secretion is regulated by the same SNAREs isoforms that modulate glucose uptake in insulin target cells. This process requires syntaxin 4, SNAP 23, and VAMP2. The isoform syntaxin 1 is involved in the first, but not the second phase of insulin release (Jewell et al. 2010). The assembly of this core complex is also influenced by accessory proteins that interact with the SNARE core complex (Renström and Rorsman 2008).

Previous work demonstrated that PI3K-C2 $\alpha$  downregulation inhibited KCl-induced insulin secretion in INS1 cells, without affecting the expression levels of key proteins involved in the exocytotic machinery, such as SNAP 25, VAMP2, syntaxin 1 and syntaxin 4 (Dominguez et al. 2011). Nevertheless, a potential role for PI3K-C2 $\alpha$  in regulating the assembly or the activity of the complex cannot be excluded.



Interestingly, it was reported that downregulation of PI3K-C2 $\alpha$  in INS1 cells was associated with a reduced proteolysis of SNAP 25 upon KCl stimulation (Dominguez et al. 2011). Hence, this observation and the fact that SNAP 25 proteolysis is associated with insulin secretion (Marshall et al. 2005) suggested that PI3K-C2 $\alpha$  might be involved in the association or the functioning of the SNARE complex during the fusion step of insulin granules.

SNAP 25 proteolysis has been reported to depend on calpain 10 activity. Calpains are a family of proteases that are able to cleave cytoskeletal proteins and therefore, they might be involved in vesicle trafficking. Calpain 10 in particular has been reported to bind the SNAREs core complex and the inhibition of its activity reduced SNAP 25 cleavage (Marshall et al. 2005). Also, it has been reported that glucose stimulation increased calpain activity and protein expression of calpain 10 and genome scan studies identified the protein calpain 10 as a susceptibility gene for T2D (Turner et al. 2007). Therefore, it is possible that PI3K-C2 $\alpha$  has a role in modulating the assembly of the SNAREs complex necessary for insulin exocytosis, or its activity through calpains family members.

Data presented in the previous chapter indicated that stimulation of insulin secretion with KCl (and possibly also with glucose) induced the synthesis of the lipid second messenger PtdIns3P. PtdIns3P can derive from direct phosphorylation of PtdIns by class III PI3K hVps34 or members of class II PI3Ks (Maffucci 2012). It was proposed that PtdIns3P might have different functions, based on its intracellular

localisation and stimulation (Falasca and Maffucci 2009, Maffucci 2012). Results presented so far showed that synthesis of PtdIns3P was affected by downregulation of class II PI3K-C2 $\alpha$  in INS1 cells. In addition, it has been observed that PI3K-C2 $\alpha$  was localised in nuclear and perinuclear regions in L6 cells in resting conditions, and that a rapid and transient translocation of the enzyme to the plasma membrane occurred upon insulin stimulation (Falasca et al. 2007). Moreover, it has been shown that PI3K-C2 $\alpha$  associates with secretory granules in chromaffin cells (Meunier et al. 2005). It is still unknown whether PI3K-C2 $\alpha$  translocates to the plasma membrane or associates to insulin vesicles in pancreatic  $\beta$  cells following cellular stimulation. Nevertheless, based on these observations, it was proposed that PI3K-C2 $\alpha$  and/or its lipid product PtdIns3P might have a general role in exocytotic mechanisms, facilitating the fusion of insulin granules and other intracellular vesicles to the plasma membrane in different cell types (Mazza and Maffucci 2011). In an effort to determine how PI3K-C2 $\alpha$  regulates insulin secretion, in this chapter I sought to investigate the localisation of the PI3K-C2 $\alpha$ -dependent pool of PtdIns3P generated upon stimulation with KCl in INS1 cells and the potential role of PI3K-C2 $\alpha$ .

## **7.2 Results**

### **7.2.1 Analysis of calpain family members protein expression**

As mentioned before, the protein expression of the protease calpain 10 is positively regulated in response to glucose stimulation (Turner et al. 2007). It has also been proposed that calpain 10 is involved in the proteolysis of SNAP 25, an event associated with insulin granule fusion (Marshall et al. 2005). Furthermore, previous data showed an impaired proteolysis of SNAP 25 in INS1 upon downregulation of PI3K-C2 $\alpha$ , and a concomitant decrease in insulin secretion (Dominguez et al. 2011). Therefore, I decided to test whether downregulation of PI3K-C2 $\alpha$  would affect calpain 10 protein expression using Western Blot analysis. To this end, the expression of calpain 10 and of the two major ubiquitously expressed calpain family members, calpain 1 and 2, was investigated in INS1 parental, sh scrambled and sh PI3K-C2 $\alpha$  cells.

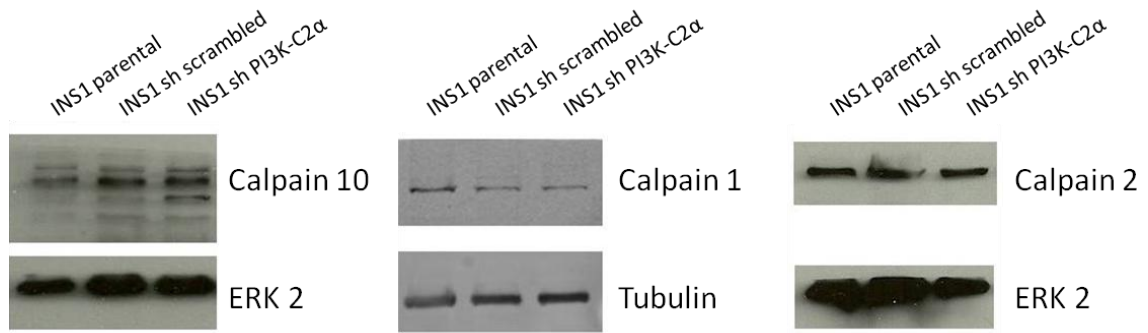


**Figure 7.2: Analysis of calpain family members protein expression. Lysates from stable INS1 cell lines were analysed by Western Blot and incubated with the indicated antibodies. Representative blots are shown.**

Results indicated that the protein expression of calpain 10, calpain 1 and calpain 2 was not affected by the downregulation of PI3K-C2 $\alpha$  in unstimulated conditions.

This suggests that PI3K-C2 $\alpha$  is not involved in modulating the expression levels of the examined calpains isoforms. However, a potential role for PI3K-C2 $\alpha$  in modulating calpain family members activity cannot be excluded.

### **7.2.2 Investigation of potential effects of PI3K-C2 $\alpha$ downregulation on SNAREs interaction**

The exocytosis of insulin granules requires the formation of a complex of proteins (SNAREs core complex and accessory proteins) which allows the fusion of the vesicle with the plasma membrane.

Specifically, insulin release requires the association of VAMP2, located on the insulin granule, with syntaxin and SNAP proteins on the plasma membrane, securing the

physical interaction of the two cellular compartments. Specifically, the first phase of insulin secretion requires syntaxin 1 isoform, while the second phase of insulin release involves either syntaxin 1 or syntaxin 4 (Jewell et al. 2010). It has been shown that downregulation of PI3K-C2 $\alpha$  did not affect the expression of key proteins involved in the insulin secreting machinery, including syntaxin 1 and VAMP2 (Dominguez et al. 2011). This finding, however, does not rule out a role for PI3K-C2 $\alpha$  in the formation of the complex and/or its activity.

In order to investigate whether downregulation of PI3K-C2 $\alpha$  affects the association of syntaxin 1 and VAMP2, I performed coimmunoprecipitation assays. Sh scrambled and sh PI3K-C2 $\alpha$  cells were starved for 30 minutes in Krebs Ringer buffer and then stimulated for 30 minutes with KCl to induce insulin secretion or left untreated as previously described (Dominguez et al. 2011). Then, an antibody anti VAMP2 was used to immunoprecipitate and isolate the complex from the whole lysate and the amount of VAMP2 and syntaxin 1 was investigated by Western blot (Figure 7.3).

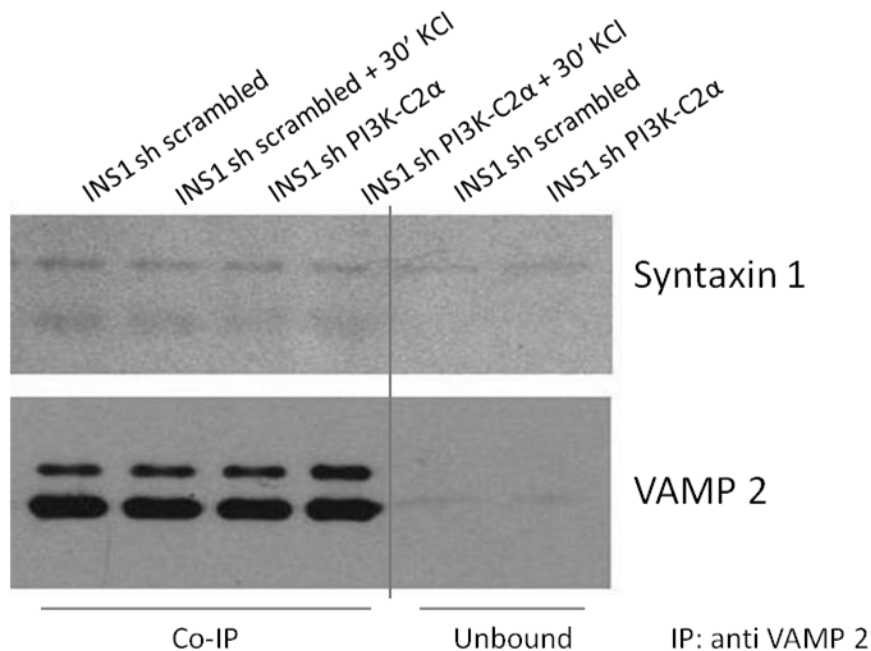


**Figure 7.3: Association between syntaxin 1 and VAMP 2 in the presence or absence of KCl.** Cell lysates were immunoprecipitated with an antibody anti VAMP2. Previous data from my laboratory showed that no VAMP2 or syntaxin 1 were immunoprecipitated by control IgG in these experimental conditions.

Results showed that a basal interaction between VAMP2 and Syntaxin 1 is detectable in both sh scrambled and sh PI3K-C2 $\alpha$  cells. This is consistent with previous reports indicating that a number of insulin granules is already pre-docked to the plasma membrane in unstimulated conditions (Rorsman and Renstrom 2003). Treatment with KCl for 30 minutes did not seem to increase the association of the SNAREs complex in these experimental conditions. This suggested that these experimental conditions did not allow to appreciate any changes in syntaxin 1/VAMP2 association. Nevertheless, they showed that there was no difference in

syntaxin 1/VAMP2 association between sh scrambled and sh PI3K-C2 $\alpha$  cells in unstimulated conditions or upon KCl treatment for 30 minutes.

Therefore, I decided to perform time-course experiments to test whether an increase in the association of the two proteins occurred at earlier time points. Preliminary experiments were performed in INS1 cells, varying the time of KCl stimulation from a minimum of 1 to a maximum of 30 minutes. A representative experiment is shown in Figure 7.4.

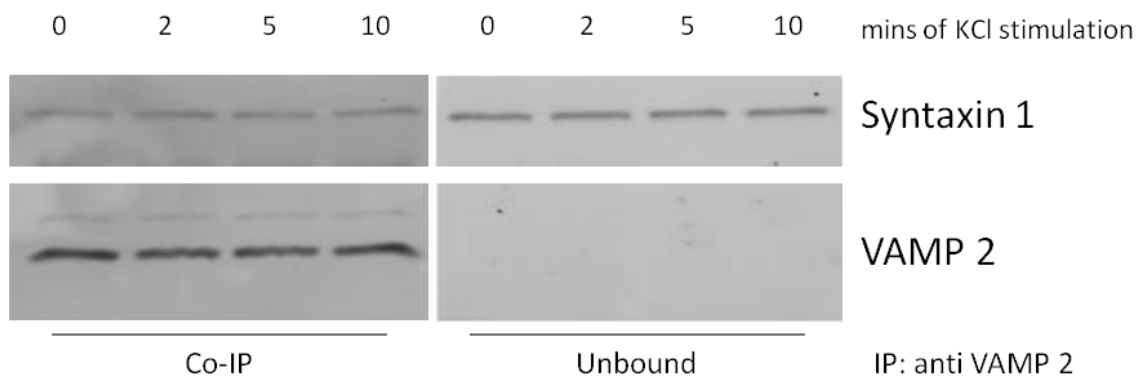


**Figure 7.4: Association between syntaxin 1 and VAMP 2 in the presence or absence of KCl.** Cell lysates were immunoprecipitated with an antibody anti VAMP2. Previous data from my laboratory showed that no VAMP2 or syntaxin 1 were immunoprecipitated by control IgG in these experimental conditions.

Results indicated that no clear increase in the amount of syntaxin 1 coimmunoprecipitated with VAMP2 was detected upon KCl stimulation even at shorter time points.

### 7.2.3 Optimisation of GFP-2XFYVE<sup>Hrs</sup> plasmid transfection

As mentioned before, PI3K-C2 $\alpha$  has a role in KCl-induced insulin secretion. Data presented in Chapter 6 indicated that KCl stimulation induced de novo synthesis of the lipid second messenger PtdIns3P in a mechanism involving PI3K-C2 $\alpha$ . In order to clarify the role of this PI3K-C2 $\alpha$ /PtdIns3P pathway in insulin secretion, I investigated the intracellular localisation of this PI3K-C2 $\alpha$  dependent PtdIns3P pool using a specific fluorescent probe. GFP-2XFYVE<sup>Hrs</sup> can be inserted into the cells by transfection of a plasmid containing its sequence using transfecting agents or electroporation. Once expressed by the cells, it selectively binds PtdIns3P and it can be detected by fluorescent or confocal microscopy because of its GFP tag, allowing the study of the intracellular localisation of PtdIns3P. The method of insertion of GFP-2XFYVE<sup>Hrs</sup> plasmid had to be optimised for INS1 cells. First, I decided to use electroporation to transfect INS1 cells.

INS1 cells were detached from the flask and counted as described in Materials and Methods, electroporated with Amaxa Nucleofector<sup>®</sup> according to the manufacturer's instructions and seeded. Plated cells were monitored for 72 hours by fluorescent microscope observation to assess the efficiency of transfection and GFP-2XFYVE<sup>Hrs</sup> plasmid expression. INS1 cells began to express GFP-2XFYVE<sup>Hrs</sup> plasmid ~30 hours post electroporation. The maximal intensity of GFP expressed was observed 48 hours post transfection. Although the protocol allowed a good efficiency of transfection (~60%), the overall intensity of fluorescence was low.



Therefore, I decided to try alternative methods to insert GFP-2XFYVE<sup>Hrs</sup> in INS1 cells, such as transfection using Lipofectamine®.

In order to optimise the transfection protocol, different factors were considered. Transfection efficiency may vary based on the confluence of cells, the ratio of plasmid DNA/transfecting agent, the amount of DNA and transfecting agent used.

INS1 cells were seeded on coverslips in 12 wells plates at a confluence of 0.6, 1.2 or 1.8 x10<sup>6</sup> cells/plate. Transfection was then performed, using GFP-2XFYVE<sup>Hrs</sup> and Lipofectamine® as a transfecting reagent. Different ratios of plasmid DNA/transfecting agent were used (1:2, 1:3, 1:4) and transfection efficiency was monitored by fluorescence microscopy. Results showed that 48 hours were necessary to obtain a maximal plasmid expression, as assessed by GFP fluorescence intensity, consistent with experiments performed using electroporation. Also, results indicated that the best combination was obtained by plating 1.2x10<sup>6</sup> cells/plate and using 0.5µg of plasmid and 2µl of Lipofectamine®/well (DNA/Lipofectamine® ratio 1:4) in a 12-well plate. Although the transfection efficiency was lower compared to the electroporated cells (~30%), the intensity of the fluorescence was higher.

In parallel experiments, transfection using Lipofectamine® 2000 was performed and the transfection efficiency was comparable to those obtained with Lipofetamine®. However, the viability of INS1 cells was more affected by Lipofectamine® 2000

compared to INS1 cells treated with Lipofectamine<sup>®</sup>. Therefore, Lipofectamine<sup>®</sup> was used as transfection reagent for the following experiments.

#### **7.2.4 GFP-2XFYVE<sup>Hrs</sup> translocates to the plasma membrane upon KCl treatment**

INS1 parental cells were plated on coverslips and transfected after 24 hours with GFP-2XFYVE<sup>Hrs</sup> plasmid. After 48 hours cells were starved in Krebs Ringer buffer for 30 minutes and stimulated with KCl for 30 minutes, following a protocol previously established in my laboratory to induce insulin secretion (Dominguez et al. 2011). Then, coverslips were fixed in paraformaldehyde and analysed by confocal microscopy.

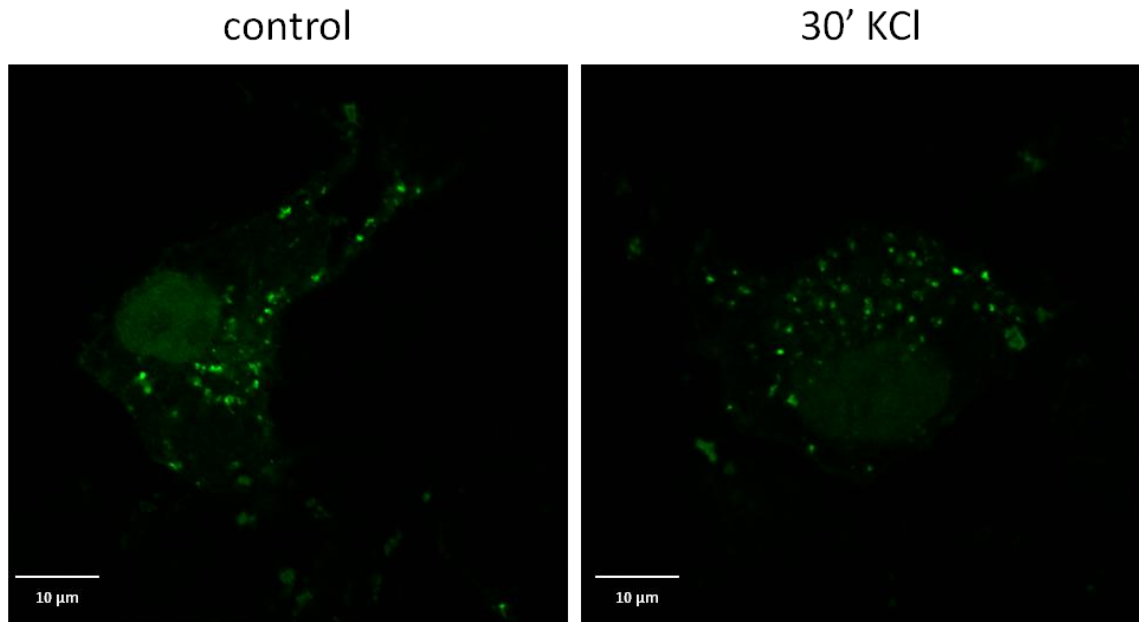


**Figure 7.5: Analysis of intracellular localisation of PtdIns3P.** INS1 cells were transfected with GFP-2XFYVE<sup>Hrs</sup>, starved in Krebs Ringer buffer for 30 minutes and then stimulated with 60 mM KCl for 30 minutes or left untreated. Cells were then analysed by confocal microscopy.

The results of this preliminary experiment indicated that GFP-2XFYVE<sup>Hrs</sup> plasmid was expressed in INS1 cells 48 hours post transfection. The expression of GFP-2XFYVE<sup>Hrs</sup> appeared as the typical punctuate staining (Figure 7.5), consistent with the localisation of PtdIns3P in intracellular endosomes (Maffucci 2012). The localisation of PtdIns3P was not modified by stimulation with KCl for 30 minutes. Therefore, I decided to perform a time-course analysis.

INS1 cells were plated on coverslips and transfected with GFP-2XFYVE<sup>Hrs</sup> as previously described. Then, cells were starved in Krebs Ringer buffer for 30 minutes and stimulated with KCl, for 2.5, 5, 7.5 and 10 minutes, respectively. Coverslips were fixed in paraformaldehyde and analysed by epifluorescent microscopy. Results

indicated that KCl treatment induced the translocation of the GFP tagged 2XFYVE probe to the plasma membrane upon 2.5 and 5 minutes treatment with KCl. The number of cells displaying a plasma membrane localisation of GFP-2XFYVE<sup>Hrs</sup> was maximal after 2.5 minutes stimulation and it was decreased upon 5 minutes treatment. The intracellular localisation of GFP-2XFYVE<sup>Hrs</sup> upon 7.5 and 10 minutes stimulation was comparable to control cells. This suggested that the synthesis of PtdIns3P induced by KCl is time-dependent, since the neosynthesised pool of PtdIns3P is undetectable 7.5 minutes after KCl stimulation.

In order to better visualise the plasma membrane localisation of GFP-2XFYVE<sup>Hrs</sup>, I decided to investigate the intracellular localisation of PtdIns3P using confocal microscopy analysis. INS1 cells on coverslips were transfected with GFP-2XFYVE<sup>Hrs</sup> and, 48 hours post transfection, they were starved in Krebs Ringer buffer and stimulated with KCl for 2.5 or 5 minutes, or they were left in starvation buffer.

Results obtained by confocal microscopy analysis are shown in Figure 7.6 and confirmed the result observed in the preliminary experiments.

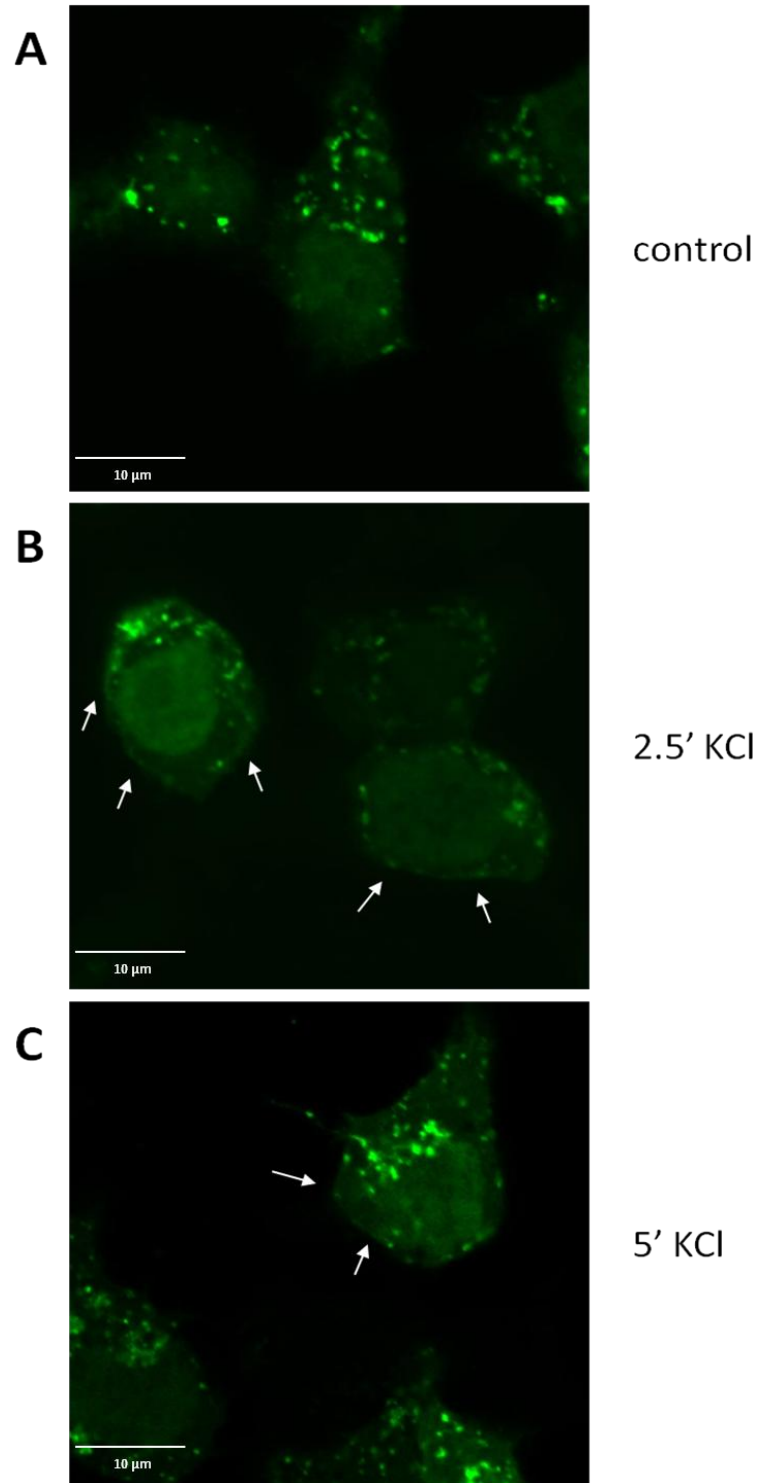


**Figure 7.6:** Analysis of intracellular localisation of PtdIns3P. INS1 cells were transfected with GFP-2XFYVE<sup>Hrs</sup>, starved in Krebs Ringer buffer for 30 minutes and then stimulated with 60 mM KCl for 2.5 and 5 minutes or left untreated. Cells were then analysed by confocal microscopy. GFP-2XFYVE<sup>Hrs</sup> translocation is indicated by arrows.

Results indicated that GFP-2XFYVE<sup>Hrs</sup> translocated to the plasma membrane upon 2.5 minutes of KCl stimulation. This suggested that a pool of PtdIns3P is specifically synthesised in this cellular compartment following stimulation with KCl. Consistent with the previous experiment, a reduced number of cells displaying plasma membrane staining with GFP-2XFYVE<sup>Hrs</sup> was observed upon 5 minutes of stimulation.

In order to further investigate the intracellular localisation of the KCl-dependent pool of PtdIns3P, co-staining with syntaxin 1 was performed. Syntaxin 1 is an intrinsic transmembrane protein localised at the plasma membrane, and its staining allowed to better visualise this intracellular compartment in INS1 cells. Therefore, it was possible to assess whether the newly synthesised PtdIns3P pool was on the plasma membrane or in its proximity. INS1 cells were transfected with GFP-2XFYVE<sup>Hrs</sup> plasmid, starved in Krebs Ringer buffer and stimulated for 2.5 minutes with KCl.

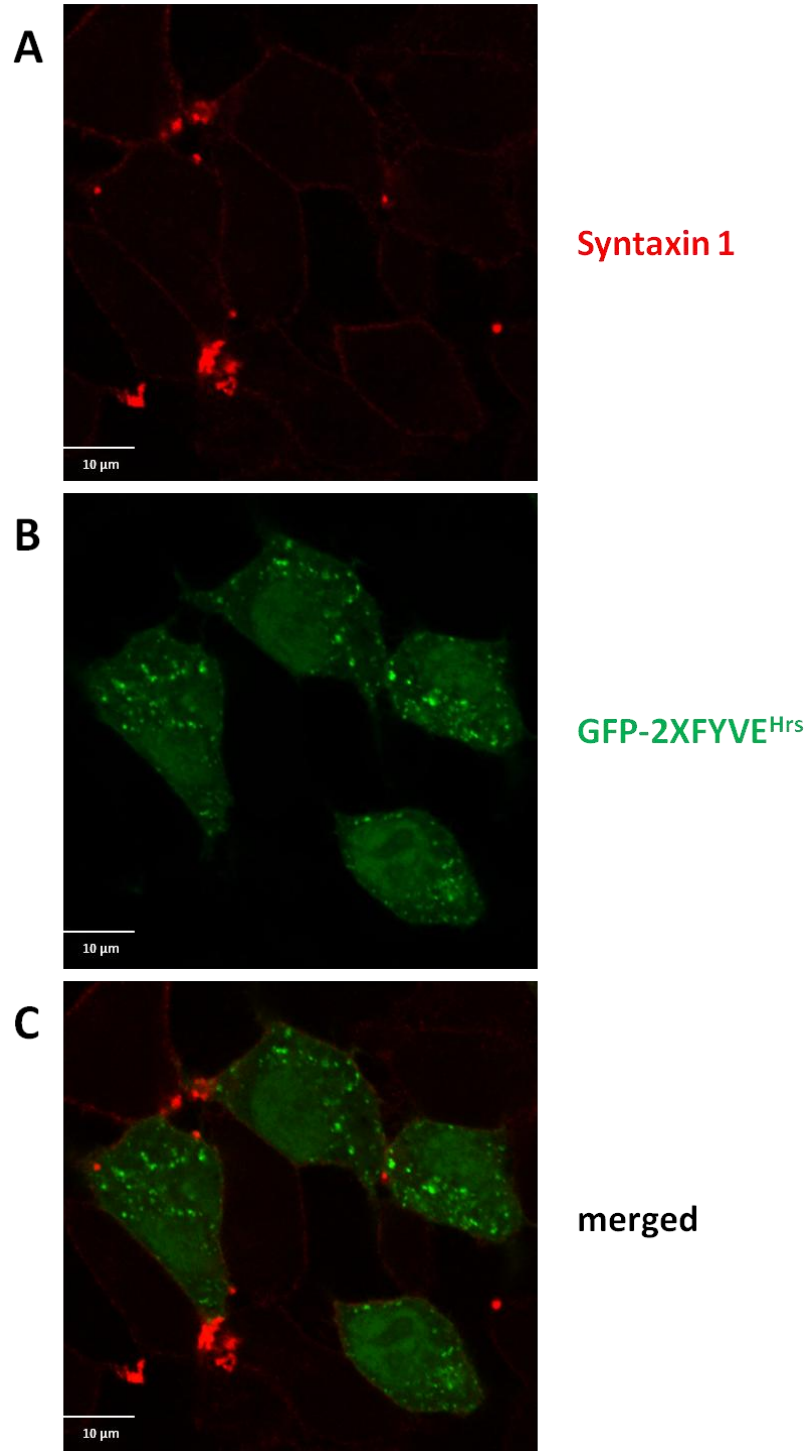


**Figure 7.7:** Analysis of intracellular localisation of PtdIns3P. INS1 cells were transfected with GFP-2XFYVE<sup>Hrs</sup>, starved in Krebs Ringer buffer for 30 minutes and then stimulated with 60 mM KCl for 2.5 minutes or left untreated. Cells were permeabilised, incubated with an antibody specific for syntaxin 1 and then with Alexa Fluor 555 Goat Anti-Mouse IgG. Cells were then fixed in paraformaldehyde and analysed by confocal microscopy using a 63X objective. Staining with syntaxin 1 (A), GFP-2XFYVE<sup>Hrs</sup> (B), and merged (C) images are shown.

These preliminary results indicated that staining with syntaxin 1 was specific and clearly outlined the plasma membrane of INS1 cells. GFP-2XFYVE<sup>Hrs</sup> fluorescent probe was located close to the plasma membrane upon 2.5 minutes of KCl stimulation. Merged images suggested the absence of colocalisation of the two fluorescent signals. Therefore, it appeared that KCl-dependent pool of PtdIns3P is synthesised in close proximity to the inner plasma membrane of INS1 cells.

In order to investigate whether the newly synthesised, KCl-dependent pool of PtdIns3P is produced through the action of PI3K-C2 $\alpha$ , similar experiments were performed using INS1 sh scrambled and sh PI3K-C2 $\alpha$  cells. Stable cell lines were transfected, starved and stimulated as previously described. Then, the number of cells displaying plasma membrane staining of GFP-2XFYVE<sup>Hrs</sup> was counted using epifluorescent microscopy.



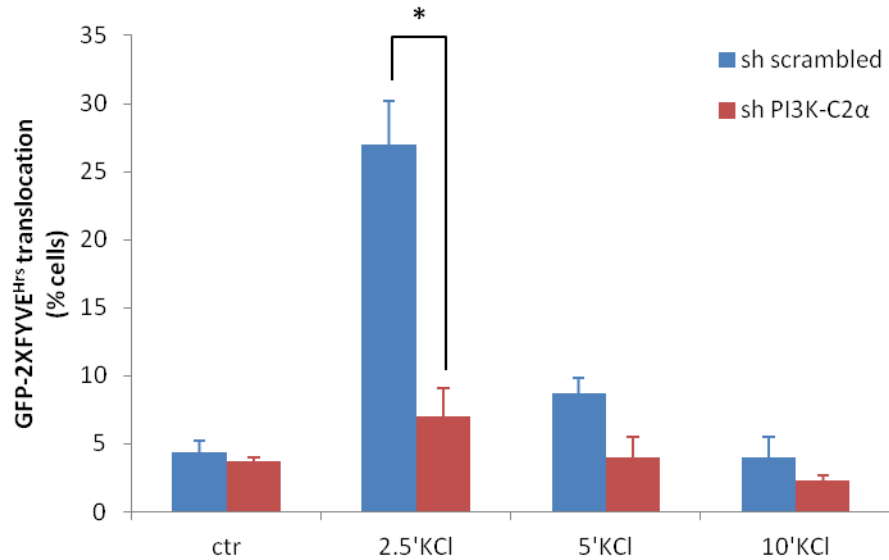


**Figure 7.8: Quantitative analysis of GFP-2XFYVE<sup>Hrs</sup> translocation.** INS1 cells plated on coverslips were transfected with GFP-2XFYVE<sup>Hrs</sup> and analysed by epifluorescent microscopy. Data are expressed as percentage of cells displaying plasma membrane localisation of GFP-2XFYVE<sup>Hrs</sup> and are means  $\pm$  s.e.m. from 3 independent experiments. \*p value < 0.05 sh scrambled vs sh PI3K-C2 $\alpha$  cells.

Results indicated that upon KCl stimulation, GFP-2XFYVE<sup>Hrs</sup> translocated to the plasma membrane in sh scrambled cells. The higher percentage of cells displaying plasma membrane staining with GFP-2XFYVE<sup>Hrs</sup> was detectable upon 2.5 minutes of KCl stimulation, and it progressively decreased at later time points, becoming comparable to unstimulated cells upon 10 minutes of KCl treatment. Quantitative analysis indicated that there was no difference between sh scrambled and sh PI3K-C2 $\alpha$  cells in the number of GFP-2XFYVE<sup>Hrs</sup> staining at the plasma membrane in unstimulated conditions. Also, downregulation of PI3K-C2 $\alpha$  did not affect the endosomal staining of GFP-2XFYVE<sup>Hrs</sup>, suggesting that PI3K-C2 $\alpha$  does not alter the endosomal pool of PtdIns3P. Results indicated that downregulation of PI3K-C2 $\alpha$

impaired translocation of GFP-2XFYVE<sup>Hrs</sup> to the plasma membrane upon KCl stimulation. Specifically, the percentage of cells displaying plasma membrane staining with GFP-2XFYVE<sup>Hrs</sup> upon KCl stimulation was not statistically significant at any time points.

These results indicated that PI3K-C2 $\alpha$  regulates the synthesis of a KCl-dependent pool of PtdIns3P at the plasma membrane.

### 7.3 Discussion

Evidence in literature reported that PI3K-C2 $\alpha$  is involved in the fusion of neurosecretory granules in adrenal chromaffin cells (Meunier et al. 2005), in insulin exocytosis in INS1 cells (Dominguez et al. 2011) and in the translocation of glucose transporter GLUT 4 to the plasma membrane in muscle cells (Falasca et al. 2007). Although these studies focus on different cell lines, contexts and cellular mechanisms, taken together they indicate that PI3K-C2 $\alpha$  might have a general role in exocytotic-like processes. However, the precise role for PI3K-C2 $\alpha$  and the specific mechanisms by which this enzyme might regulate exocytosis are still unclear. In order to investigate this aspect, I focused my research on the proteins involved in insulin granules exocytosis. The SNARE core complex necessary for insulin secretion requires the association of VAMP2 on the insulin granules and syntaxin 1 and SNAP 25 on the plasma membrane. During insulin exocytosis SNAP 25 undergoes a Ca<sup>2+</sup> dependent proteolytic cleavage, probably through the action of the protease calpain 10 (Marshall et al. 2005, Turner et al. 2007). It was also reported that the protein expression and the activity of calpain 10 are increased by glucose stimulation (Turner et al. 2007) and that the proteolytic cleavage of SNAP 25 was affected by PI3K-C2 $\alpha$  downregulation during KCl-induced insulin secretion (Dominguez et al. 2011). Nevertheless, data presented in this chapter indicated that downregulation of PI3K-C2 $\alpha$  did not affect the protein expression of either calpain 10 or the isoforms calpain 1 and 2 (Figure 7.2). However, the present study does not rule out the

possibility that PI3K-C2 $\alpha$  might regulate the activity of calpain 10 or other calpain family members, therefore affecting insulin secretion.

Another hypothesis might be that PI3K-C2 $\alpha$  has a role in regulating the assembly or the activity of the SNAREs core complex during the fusion of insulin granules to the plasma membrane. In order to investigate this aspect, coimmunoprecipitation studies were performed. Data showed that, PI3K-C2 $\alpha$  downregulation did not seem to modify the association between VAMP2 and syntaxin 1 in unstimulated conditions or after 30 minutes of stimulation with KCl. More specifically, no increase in the association of VAMP2 and syntaxin 1 was detected upon stimulation with KCl and therefore, it was not possible to determine the potential contribution of PI3K-C2 $\alpha$  in this context. Nevertheless, no difference in the basal association was detected between sh scrambled and sh PI3K-C2 $\alpha$  cells. This is consistent with the findings that insulin granules are docked to the plasma membrane of pancreatic  $\beta$  cells in resting conditions (Jewell et al. 2010) and that downregulation of PI3K-C2 $\alpha$  does not affect the number of granules proximal to the plasma membrane (Dominguez et al. 2011).

Results shown in Chapter 6 indicated that a pool of PtdIns3P is neosynthesised in INS1 cells upon stimulation of insulin secretion induced by KCl. In order to further investigate the role of PI3K-C2 $\alpha$  in the context of insulin granules exocytosis, I investigated the intracellular localisation of the KCl-dependent pool of PtdIns3P. PtdIns3P constitutes 0.1–0.5% of all intracellular PIs and it is the most abundant

among the 3-phosphorylated PIs species in mammalian cells in resting conditions. The majority of PtdIns3P is localised in intracellular endosomes and it is regulated by class III PI3K hVps34 (Maffucci 2012). The role of this constitutive pool of PtdIns3P is mainly to modulate receptor-independent trafficking events, such as endocytic membrane traffic and autophagy (Lindmo and Stenmark 2006). It was reported that an inducible pool of PtdIns3P was detected upon cellular stimulation at the plasma membrane in different cell types, together with an increase of PtdIns3P levels (Maffucci et al. 2005, Falasca et al. 2007). Evidence suggested that the function of this specific pool of PtdIns3P is distinct from the endosomal pool and its synthesis depends on the action of class II PI3Ks, rather than class III hVps34 (Maffucci 2012). In particular, it was shown that insulin stimulation induced PI3K-C2 $\alpha$ -dependent PtdIns3P synthesis at the plasma membrane in L6 cells, facilitating GLUT4 translocation (Falasca et al. 2007). It is possible then that PI3K-C2 $\alpha$  and PtdIns3P might facilitate the fusion of insulin granules in pancreatic  $\beta$  cells using a similar mechanism. Data obtained with HPLC analysis revealed that the KCl-dependent pool of PtdIns3P involves PI3K-C2 $\alpha$  activation. In order to further investigate this aspect, I investigated the localisation of PtdIns3P in INS1 cells following KCl stimulation using the specific PtdIns3P probe GFP-2XFYVE<sup>Hrs</sup>.

Results indicated that the inducible pool of PtdIns3P was synthesised in close proximity to the plasma membrane of INS1 cells (Figure 7.7). In addition, downregulation of PI3K-C2 $\alpha$  impaired GFP-2XFYVE<sup>Hrs</sup> translocation to the plasma membrane, further suggesting that PI3K-C2 $\alpha$  is involved in the synthesis of the

inducible pool of PtdIns3P in this cellular compartment. Consistent with this, preliminary data indicated that PtdIns3P is synthesised in INS1 cells following treatment with glucose, the physiological stimulus for insulin secretion.

These data, together with the observation that PI3K-C2 $\alpha$  downregulation affects insulin exocytosis following stimulation with KCl or with secretagogue mixture, with no effect on total insulin content or on the expression of proteins involved in exocytotic machinery (Dominguez et al. 2011), suggest that PI3K-C2 $\alpha$  and PtdIns3P have a role specifically in the fusion step of insulin secretion in INS1 cells.

# Chapter 8

## Final conclusions and future work

### 8.1 Conclusions

PI3Ks have a well established role in many intracellular functions, and impairment of their signalling pathway has been associated with defects in metabolic regulation. Most of our knowledge about PI3Ks signalling comes from the study of class I PI3Ks, and it is now generally accepted that these enzymes have a central role in both insulin target tissues and insulin producing tissues. These observations highlighted that deregulation of PI3Ks or their intracellular pathway is crucial for the pathogenesis and progression of metabolic diseases, such as T2D. Amongst all PI3Ks, class II remains, to date, the least investigated. However, in the last few years interest in the function of class II PI3K, and particularly PI3K-C2 $\alpha$ , has increased.

This study focussed on the investigation of the intracellular functions and signalling pathways regulated by PI3K-C2 $\alpha$  and its mechanisms of activation. Evidence indicated PI3K-C2 $\alpha$  has an important role in insulin signalling, regulating glucose uptake in muscle cells through the synthesis of its lipid product PtdIns3P. In addition, it was demonstrated that PI3K-C2 $\alpha$  mRNA is highly expressed in human pancreatic  $\beta$  cells, while it is reduced in islets from T2D subjects compared to non-diabetic controls. Also, PI3K-C2 $\alpha$  contributes to glucose and KCl-induced insulin

granules exocytosis. The dual role of PI3K-C2 $\alpha$  in insulin release and action suggests that this enzyme may represent a novel therapeutic target for T2D.

Results from this study indicated that the protein levels of class I p110 $\alpha$  and class II PI3K-C2 $\alpha$  were selectively downregulated by addition of free fatty acids in the culture medium of INS1 cells. As PI3K-C2 $\alpha$  is important for pancreatic  $\beta$  cell function, this might add important information to understand the role of lipotoxicity in the context of pancreatic  $\beta$  cell failure and diabetes progression. The reduced levels of PI3K-C2 $\alpha$  do not seem to be responsible for reduced  $\beta$  cell viability in lipotoxic conditions, since INS1 cells lacking PI3K-C2 $\alpha$  were as prone as control cells to death induced by lipotoxicity.

On the other hand, these results indicated for the first time that PI3K-C2 $\alpha$  is involved in intracellular signalling activated by stimulatory concentrations of glucose following nutrients deprivation. Specifically, glucose was able to prevent cell death induced by nutrients deprivation in control cells. Downregulation of PI3K-C2 $\alpha$  significantly inhibited the glucose-dependent survival effect. Nutrients deprivation was able to trigger both apoptotic and autophagic processes in INS1 cells. Notably, reintroduction of stimulatory concentrations of glucose was not able to revert autophagy, while it was able to inhibit apoptosis, in a mechanism involving PI3K-C2 $\alpha$ . This suggests that PI3K-C2 $\alpha$  is involved in the anti-apoptotic role of stimulatory glucose concentrations in INS1 cells.



Further analysis on the intracellular pathway revealed that glucose activated mTORC1 and its downstream effectors, and this is required for the anti-apoptosis effect. This conclusion was confirmed by the use of mTOR inhibitor rapamycin, which impaired cell viability in the presence of glucose. The reduced cell viability caused by treatment with rapamycin was similar to the one observed in cells lacking PI3K-C2 $\alpha$ , suggesting that PI3K-C2 $\alpha$  and mTORC1 are part of the same signalling pathway. Indeed, Western Blot analysis indicated that glucose-induced activation of mTORC1 pathway was impaired by downregulation of PI3K-C2 $\alpha$ . Specifically, downregulation of PI3K-C2 $\alpha$  inhibited phosphorylation of mTORC1 and the downstream effectors S6K, 4EBP1 and S6. Notably, glucose-induced effect on cell viability was not inhibited by classical PI3K inhibitors, suggesting that glucose was not able to activate mTOR pathway through the class I PI3K/Akt/mTOR pathway. Investigation of Akt activation at both long and short time points of stimulation with glucose confirmed this hypothesis, as mTOR and downstream targets resulted activated in absence of detectable Akt phosphorylation. Taken together, these data indicated for the first time that stimulatory concentrations of glucose are able to activate mTOR and its downstream effectors, through an intracellular pathway that involves the activation of PI3K-C2 $\alpha$ .

The second part of this project focussed on the investigation of the mechanisms of activation of PI3K-C2 $\alpha$  and the identification of the lipid product specifically synthesised by this enzyme in pancreatic  $\beta$  cells. Previous work had demonstrated that downregulation of PI3K-C2 $\alpha$  impaired insulin granules exocytosis in INS1 cells

(Dominguez et al., 2011). Preliminary data suggested that PtdIns3P is synthesised in pancreatic  $\beta$  cells upon stimulation with glucose, the physiological stimulus for insulin secretion. Also, results indicated that KCl stimulation induced the synthesis of the lipid second messenger PtdIns3P in  $\beta$  cells. Importantly, the levels of PtdIns3P were significantly reduced by downregulation of PI3K-C2 $\alpha$  upon KCl stimulation. This suggests that PI3K-C2 $\alpha$  is activated in INS1 cells upon depolarisation of the plasma membrane, and that it specifically catalyses the synthesis of PtdIns3P, which can then facilitate insulin granules exocytosis. Indeed, fluorescence microscopy analysis revealed that the KCl-induced pool of PtdIns3P was localised in close proximity to the plasma membrane. Importantly, this specific pool of PtdIns3P was reduced by downregulation of PI3K-C2 $\alpha$ . Furthermore, PtdIns3P synthesis was not completely inhibited in PI3K-C2 $\alpha$  knock down cells, consistent with the previous observation that ~80% downregulation of PI3K-C2 $\alpha$  levels in INS1 cells resulted in an impaired but not totally blunted insulin secretion (Dominguez et al. 2011). These data are also consistent with previous reports showing that PtdIns3P and PI3K-C2 $\alpha$  were involved in the exocytotic-like process of GLUT4 translocation in muscle cells (Falasca et al. 2007). Interestingly, insulin secretion and GLUT4 translocation require the assembly of an exocytotic machinery that involves similar proteins. Analysis of the SNAREs syntaxin 1 and VAMP2 in the presence or absence of KCl stimulation showed that PI3K-C2 $\alpha$  did not seem to be involved in this process. Similar mechanisms were also observed in different cell types, and a role for PI3K-C2 $\alpha$  was reported in the exocytosis of neurosecretory granules (Meunier et al. 2005). Given these similarities,

it is likely that PI3K-C2 $\alpha$  has a general role in exocytosis in distinct cellular contexts. Therefore, further experiments are needed to elucidate the precise role of PI3K-C2 $\alpha$  in this context.

## **8.2 Future work**

Several questions arisen from the experiments showed in this thesis remain pending. Observation of the phenotype of a conditional knock-out mouse model with deletion of the kinase specifically in pancreatic  $\beta$  cells would be the best option to study the function of PI3K-C2 $\alpha$  in this specific cell type.

Other short-term future work will focus on:

### **Function of PI3K-C2 $\alpha$**

Since PI3K-C2 $\alpha$  does not seem to affect the exocytotic machinery, its precise role in the context of insulin secretion is still unclear. Further work will clarify how PI3K-C2 $\alpha$  and PtdIns3P are involved in fusion of granules to the plasma membrane.

### **Lipid product of PI3K-C2 $\alpha$ in pancreatic $\beta$ cells**

Further experiments are required to identify the lipid product of PI3K-C2 $\alpha$  upon glucose stimulation in pancreatic  $\beta$  cells.

### **mTORC1 activation**

Data showed that downregulation of PI3K-C2 $\alpha$  impaired mTORC1 and its downstream targets upon glucose stimulation. Additional experiments are required to understand the involvement of signalling pathway(s) involved upstream of mTORC1. Also, further work is necessary to elucidate whether the glucose reintroduction and PI3K-C2 $\alpha$  activation are needed for cell proliferation, rescue from apoptosis or a combination of these processes. Cell cycle analysis and investigation of specific markers for proliferation and apoptosis are necessary.

## Bibliography

16, U. K. p. d. s. (1995). "U.K. prospective diabetes study 16. Overview of 6 years' therapy of type II diabetes: a progressive disease. U.K. Prospective Diabetes Study Group." *Diabetes* 44(11): 1249-1258.

Alessi, D. R., M. Andjelkovic, B. Caudwell, P. Cron, N. Morrice, P. Cohen and B. A. Hemmings (1996). "Mechanism of activation of protein kinase B by insulin and IGF-1." *EMBO J* 15(23): 6541-6551.

Backer, J. M. (2008). "The regulation and function of Class III PI3Ks: novel roles for Vps34." *Biochem J* 410(1): 1-17.

Barker, C. J., I. B. Leibiger and P. O. Berggren (2013). "The pancreatic islet as a signaling hub." *Adv Biol Regul* 53(1): 156-163.

Barlow, J. and C. Affourtit (2013). "Novel insights in pancreatic beta cell glucolipototoxicity from real-time functional analysis of mitochondrial energy metabolism in INS-1E insulinoma cells." *Biochem J*.

Bartolome, A. and C. Guillen (2014). "Role of the mammalian target of rapamycin (mTOR) complexes in pancreatic beta-cell mass regulation." *Vitam Horm* 95: 425-469.

Bernal-Mizrachi, E., R. N. Kulkarni, D. K. Scott, F. Mauvais-Jarvis, A. F. Stewart and A. Garcia-Ocaña (2014). "Human  $\beta$ -Cell Proliferation and Intracellular Signaling Part 2: Still Driving in the Dark Without a Road Map." *Diabetes* 63(3): 819-831.

Bi, L., I. Okabe, D. J. Bernard and R. L. Nussbaum (2002). "Early embryonic lethality in mice deficient in the p110beta catalytic subunit of PI 3-kinase." *Mamm Genome* 13(3): 169-172.

Bi, L., I. Okabe, D. J. Bernard, A. Wynshaw-Boris and R. L. Nussbaum (1999). "Proliferative defect and embryonic lethality in mice homozygous for a deletion in the p110alpha subunit of phosphoinositide 3-kinase." *J Biol Chem* 274(16): 10963-10968.

Blandino-Rosano, M., A. Y. Chen, J. O. Scheys, E. U. Alejandro, A. P. Gould, T. Taranukha, L. Elghazi, C. Cras-Meneur and E. Bernal-Mizrachi (2012). "mTORC1 signaling and regulation of pancreatic beta-cell mass." *Cell Cycle* 11(10): 1892-1902.

Blommaart, E. F., U. Krause, J. P. Schellens, H. Vreeling-Sindelarova and A. J. Meijer (1997). "The phosphatidylinositol 3-kinase inhibitors wortmannin and LY294002 inhibit autophagy in isolated rat hepatocytes." *Eur J Biochem* 243(1-2): 240-246.

Bogan, J. S. (2012). "Regulation of glucose transporter translocation in health and diabetes." *Annu Rev Biochem* 81: 507-532.

Bonner-Weir, S. (2000). "Life and death of the pancreatic beta cells." *Trends Endocrinol Metab* 11(9): 375-378.

Bonner-Weir, S., D. Deery, J. L. Leahy and G. C. Weir (1989). "Compensatory growth of pancreatic beta-cells in adult rats after short-term glucose infusion." *Diabetes* 38(1): 49-53.

Bouzakri, K., P. Ribaux, A. Tomas, G. Parnaud, K. Rickenbach and P. A. Halban (2008). "Rab GTPase-activating protein AS160 is a major downstream effector of protein kinase B/Akt signaling in pancreatic beta-cells." *Diabetes* 57(5): 1195-1204.

Brachmann, S. M., K. Ueki, J. A. Engelman, R. C. Kahn and L. C. Cantley (2005). "Phosphoinositide 3-kinase catalytic subunit deletion and regulatory subunit deletion have opposite effects on insulin sensitivity in mice." *Mol Cell Biol* 25(5): 1596-1607.

Briaud, I., M. K. Lingohr, L. M. Dickson, C. E. Wrede and C. J. Rhodes (2003). "Differential activation mechanisms of Erk-1/2 and p70(S6K) by glucose in pancreatic beta-cells." *Diabetes* 52(4): 974-983.

Bridges, D., J. T. Ma, S. Park, K. Inoki, L. S. Weisman and A. R. Saltiel (2012). "Phosphatidylinositol 3,5-bisphosphate plays a role in the activation and subcellular localization of mechanistic target of rapamycin 1." *Mol Biol Cell* 23(15): 2955-2962.

Brown, R. A., J. Domin, A. Arcaro, M. D. Waterfield and P. R. Shepherd (1999). "Insulin activates the alpha isoform of class II phosphoinositide 3-kinase." *J Biol Chem* 274(21): 14529-14532.

Butler, A. E., J. Janson, S. Bonner-Weir, R. Ritzel, R. A. Rizza and P. C. Butler (2003). "Beta-cell deficit and increased beta-cell apoptosis in humans with type 2 diabetes." *Diabetes* 52(1): 102-110.

Byfield, M. P., J. T. Murray and J. M. Backer (2005). "hVps34 is a nutrient-regulated lipid kinase required for activation of p70 S6 kinase." *J Biol Chem* 280(38): 33076-33082.

Canto, C. and J. Auwerx (2010). "AMP-activated protein kinase and its downstream transcriptional pathways." *Cell Mol Life Sci* 67(20): 3407-3423.

Cheng, J. Q., B. Ruggeri, W. M. Klein, G. Sonoda, D. A. Altomare, D. K. Watson and J. R. Testa (1996). "Amplification of AKT2 in human pancreatic cells and inhibition of AKT2 expression and tumorigenicity by antisense RNA." *Proc Natl Acad Sci U S A* 93(8): 3636-3641.

Chiang, G. G. and R. T. Abraham (2005). "Phosphorylation of mammalian target of rapamycin (mTOR) at Ser-2448 is mediated by p70S6 kinase." *J Biol Chem* 280(27): 25485-25490.

Chiang, S. H., C. A. Baumann, M. Kanzaki, D. C. Thurmond, R. T. Watson, C. L. Neudauer, I. G. Macara, J. E. Pessin and A. R. Saltiel (2001). "Insulin-stimulated GLUT4 translocation requires the CAP-dependent activation of TC10." *Nature* 410(6831): 944-948.

Cho, H., J. Mu, J. K. Kim, J. L. Thorvaldsen, Q. Chu, E. B. Crenshaw, 3rd, K. H. Kaestner, M. S. Bartolomei, G. I. Shulman and M. J. Birnbaum (2001). "Insulin resistance and a diabetes mellitus-like syndrome in mice lacking the protein kinase Akt2 (PKB beta)." *Science* 292(5522): 1728-1731.

Cho, H. J., J. Park, H. W. Lee, Y. S. Lee and J. B. Kim (2004). "Regulation of adipocyte differentiation and insulin action with rapamycin." *Biochem Biophys Res Commun* 321(4): 942-948.

Ciraolo, E., M. Iezzi, R. Marone, S. Marengo, C. Curcio, C. Costa, O. Azzolino, C. Gonella, C. Rubinetto, H. Wu, W. Dastru, E. L. Martin, L. Silengo, F. Altruda, E. Turco, L. Lanzetti, P. Musiani, T. Ruckle, C. Rommel, J. M. Backer, G. Forni, M. P. Wymann and E. Hirsch (2008). "Phosphoinositide 3-kinase p110beta activity: key role in metabolism and mammary gland cancer but not development." *Sci Signal* 1(36): ra3.

Cooke, F. T. (2009). "Measurement of polyphosphoinositides in cultured mammalian cells." *Methods Mol Biol* 462: 43-58.

Cousin, S. P., S. R. Hugl, M. G. Myers, Jr., M. F. White, A. Reifel-Miller and C. J. Rhodes (1999). "Stimulation of pancreatic beta-cell proliferation by growth hormone is glucose-dependent: signal transduction via janus kinase 2 (JAK2)/signal transducer and activator of transcription 5 (STAT5) with no crosstalk to insulin receptor substrate-mediated mitogenic signalling." *Biochem J* 344 Pt 3: 649-658.

Cousin, S. P., S. R. Hügl, C. E. Wrede, H. Kajio, M. G. Myers and C. J. Rhodes (2001). "Free Fatty Acid-Induced Inhibition of Glucose and Insulin-Like Growth Factor I-Induced Deoxyribonucleic Acid Synthesis in the Pancreatic  $\beta$ -Cell Line INS-1." *Endocrinology* 142(1): 229-240.

Cross, D. A., D. R. Alessi, P. Cohen, M. Andjelkovich and B. A. Hemmings (1995). "Inhibition of glycogen synthase kinase-3 by insulin mediated by protein kinase B." *Nature* 378(6559): 785-789.

Czech, M. P. and S. Corvera (1999). "Signaling mechanisms that regulate glucose transport." *J Biol Chem* 274(4): 1865-1868.

Dann, S. G., A. Selvaraj and G. Thomas (2007). "mTOR Complex1-S6K1 signaling: at the crossroads of obesity, diabetes and cancer." *Trends Mol Med* 13(6): 252-259.

Devereaux, K., C. Dall'armi, A. Alcazar-Roman, Y. Ogasawara, X. Zhou, F. Wang, A. Yamamoto, P. De Camilli and G. Di Paolo (2013). "Regulation of Mammalian Autophagy by Class II and III PI 3-Kinases through PI3P Synthesis." *PLoS One* 8(10): e76405.



Dickson, L. M., M. K. Lingohr, J. McCuaig, S. R. Hugl, L. Snow, B. B. Kahn, M. G. Myers, Jr. and C. J. Rhodes (2001). "Differential activation of protein kinase B and p70(S6)K by glucose and insulin-like growth factor 1 in pancreatic beta-cells (INS-1)." *J Biol Chem* 276(24): 21110-21120.

Domin, J., I. Gaidarov, M. E. Smith, J. H. Keen and M. D. Waterfield (2000). "The class II phosphoinositide 3-kinase PI3K-C2alpha is concentrated in the trans-Golgi network and present in clathrin-coated vesicles." *J Biol Chem* 275(16): 11943-11950.

Domin, J., L. Harper, D. Aubyn, M. Wheeler, O. Florey, D. Haskard, M. Yuan and D. Zicha (2005). "The class II phosphoinositide 3-kinase PI3K-C2beta regulates cell migration by a PtdIns3P dependent mechanism." *J Cell Physiol* 205(3): 452-462.

Domin, J., F. Pages, S. Volinia, S. E. Rittenhouse, M. J. Zvelebil, R. C. Stein and M. D. Waterfield (1997). "Cloning of a human phosphoinositide 3-kinase with a C2 domain that displays reduced sensitivity to the inhibitor wortmannin." *Biochem J* 326 ( Pt 1): 139-147.

Domin, J. and M. D. Waterfield (1997). "Using structure to define the function of phosphoinositide 3-kinase family members." *FEBS Lett* 410(1): 91-95.

Dominguez, V., C. Raimondi, S. Somanath, M. Bugliani, M. K. Loder, C. E. Edling, N. Divecha, G. da Silva-Xavier, L. Marselli, S. J. Persaud, M. D. Turner, G. A. Rutter, P. Marchetti, M. Falasca and T. Maffucci (2011). "Class II phosphoinositide 3-kinase regulates exocytosis of insulin granules in pancreatic beta cells." *J Biol Chem* 286(6): 4216-4225.

Dowling, R. J., I. Topisirovic, T. Alain, M. Bidinosti, B. D. Fonseca, E. Petroulakis, X. Wang, O. Larsson, A. Selvaraj, Y. Liu, S. C. Kozma, G. Thomas and N. Sonenberg (2010). "mTORC1-mediated cell proliferation, but not cell growth, controlled by the 4E-BPs." *Science* 328(5982): 1172-1176.

Dufner, A. and G. Thomas (1999). "Ribosomal S6 Kinase Signaling and the Control of Translation." *Experimental Cell Research* 253(1): 100-109.

Ebato, C., T. Uchida, M. Arakawa, M. Komatsu, T. Ueno, K. Komiyama, K. Azuma, T. Hirose, K. Tanaka, E. Kominami, R. Kawamori, Y. Fujitani and H. Watada (2008). "Autophagy is

important in islet homeostasis and compensatory increase of beta cell mass in response to high-fat diet." *Cell Metab* 8(4): 325-332.

Edling, C. E., F. Selvaggi, R. Buus, T. Maffucci, P. Di Sebastiano, H. Friess, P. Innocenti, H. M. Kocher and M. Falasca (2010). "Key role of phosphoinositide 3-kinase class IB in pancreatic cancer." *Clin Cancer Res* 16(20): 4928-4937.

El-Assaad, W., J. Buteau, M. L. Peyot, C. Nolan, R. Roduit, S. Hardy, E. Joly, G. Dbaibo, L. Rosenberg and M. Prentki (2003). "Saturated fatty acids synergize with elevated glucose to cause pancreatic beta-cell death." *Endocrinology* 144(9): 4154-4163.

Elghazi, L., L. Rachdi, A. J. Weiss, C. Cras-Meneur and E. Bernal-Mizrachi (2007). "Regulation of beta-cell mass and function by the Akt/protein kinase B signalling pathway." *Diabetes Obes Metab* 9 Suppl 2: 147-157.

Elis, W., E. Triantafellow, N. M. Wolters, K. R. Sian, G. Caponigro, J. Borawski, L. A. Gaither, L. O. Murphy, P. M. Finan and J. P. Mackeigan (2008). "Down-regulation of class II phosphoinositide 3-kinase alpha expression below a critical threshold induces apoptotic cell death." *Mol Cancer Res* 6(4): 614-623.

Engelman, J. A., J. Luo and L. C. Cantley (2006). "The evolution of phosphatidylinositol 3-kinases as regulators of growth and metabolism." *Nat Rev Genet* 7(8): 606-619.

Falasca, M., W. E. Hughes, V. Dominguez, G. Sala, F. Fostira, M. Q. Fang, R. Cazzolli, P. R. Shepherd, D. E. James and T. Maffucci (2007). "The role of phosphoinositide 3-kinase C2alpha in insulin signaling." *J Biol Chem* 282(38): 28226-28236.

Falasca, M. and T. Maffucci (2006). "Emerging roles of phosphatidylinositol 3-monophosphate as a dynamic lipid second messenger." *Arch Physiol Biochem* 112(4-5): 274-284.

Falasca, M. and T. Maffucci (2007). "Role of class II phosphoinositide 3-kinase in cell signalling." *Biochem Soc Trans* 35(Pt 2): 211-214.

Falasca, M. and T. Maffucci (2009). "Rethinking phosphatidylinositol 3-monophosphate." *Biochim Biophys Acta* 1793(12): 1795-1803.

Falasca, M. and T. Maffucci (2012). "Regulation and cellular functions of class II phosphoinositide 3-kinases." *Biochem J* 443(3): 587-601.

Foster, F. M., C. J. Traer, S. M. Abraham and M. J. Fry (2003). "The phosphoinositide (PI) 3-kinase family." *J Cell Sci* 116(Pt 15): 3037-3040.

Foukas, L. C., M. Claret, W. Pearce, K. Okkenhaug, S. Meek, E. Peskett, S. Sancho, A. J. Smith, D. J. Withers and B. Vanhaesebroeck (2006). "Critical role for the p110alpha phosphoinositide-3-OH kinase in growth and metabolic regulation." *Nature* 441(7091): 366-370.

Foukas, L. C. and D. J. Withers (2010). "Phosphoinositide signalling pathways in metabolic regulation." *Curr Top Microbiol Immunol* 346: 115-141.

Franco, I., F. Gulluni, C. C. Campa, C. Costa, J. P. Margaria, E. Ciruolo, M. Martini, D. Monteyne, E. De Luca, G. Germena, Y. Posor, T. Maffucci, S. Marengo, V. Haucke, M. Falasca, D. Perez-Morga, A. Boletta, G. R. Merlo and E. Hirsch (2014). "PI3K Class II alpha Controls Spatially Restricted Endosomal PtdIns3P and Rab11 Activation to Promote Primary Cilium Function." *Dev Cell* 28(6): 647-658.

Franke, T. F., D. R. Kaplan and L. C. Cantley (1997). "PI3K: downstream AKTion blocks apoptosis." *Cell* 88(4): 435-437.

Fresno Vara, J. A., E. Casado, J. de Castro, P. Cejas, C. Belda-Iniesta and M. Gonzalez-Baron (2004). "PI3K/Akt signalling pathway and cancer." *Cancer Treat Rev* 30(2): 193-204.

Fujitani, Y., T. Ueno and H. Watada (2010). "Autophagy in health and disease. 4. The role of pancreatic beta-cell autophagy in health and diabetes." *Am J Physiol Cell Physiol* 299(1): C1-6.

Gaidarov, I., M. E. Smith, J. Domin and J. H. Keen (2001). "The class II phosphoinositide 3-kinase C2alpha is activated by clathrin and regulates clathrin-mediated membrane trafficking." *Mol Cell* 7(2): 443-449.

Ganley, I. G., H. Lam du, J. Wang, X. Ding, S. Chen and X. Jiang (2009). "ULK1.ATG13.FIP200 complex mediates mTOR signaling and is essential for autophagy." *J Biol Chem* 284(18): 12297-12305.

Gao, M., J. Liang, Y. Lu, H. Guo, P. German, S. Bai, E. Jonasch, X. Yang, G. B. Mills and Z. Ding (2013). "Site-specific activation of AKT protects cells from death induced by glucose deprivation." *Oncogene*.

Gao, W., J. Z. Li, J. Y. Chan, W. K. Ho and T. S. Wong (2012). "mTOR Pathway and mTOR Inhibitors in Head and Neck Cancer." *ISRN Otolaryngol* 2012: 953089.

Geissler, E. K. and H. J. Schlitt (2010). "The potential benefits of rapamycin on renal function, tolerance, fibrosis, and malignancy following transplantation." *Kidney Int* 78(11): 1075-1079.

Guariguata, L., D. R. Whiting, I. Hambleton, J. Beagley, U. Linnenkamp and J. E. Shaw (2014). "Global estimates of diabetes prevalence for 2013 and projections for 2035." *Diabetes Research and Clinical Practice* 103(2): 137-149.

Guillen, C., A. Bartolome, C. Nevado and M. Benito (2008). "Biphasic effect of insulin on beta cell apoptosis depending on glucose deprivation." *FEBS Lett* 582(28): 3855-3860.

Hardie, D. G., I. P. Salt, S. A. Hawley and S. P. Davies (1999). "AMP-activated protein kinase: an ultrasensitive system for monitoring cellular energy charge." *Biochem J* 338 ( Pt 3): 717-722.

Harris, D. P., P. Vogel, M. Wims, K. Moberg, J. Humphries, K. G. Jhaver, C. M. DaCosta, M. K. Shadoan, N. Xu, G. M. Hansen, S. Balakrishnan, J. Domin, D. R. Powell and T. Oravec (2011). "Requirement for class II phosphoinositide 3-kinase C2alpha in maintenance of glomerular structure and function." *Mol Cell Biol* 31(1): 63-80.

Herman, S. E. and A. J. Johnson (2012). "Molecular pathways: targeting phosphoinositide 3-kinase p110-delta in chronic lymphocytic leukemia." *Clin Cancer Res* 18(15): 4013-4018.

Hinchliffe, K. A. (2001). "Cellular signalling: stressing the importance of PIP3." *Curr Biol* 11(9): R371-372.

Hosokawa, N., T. Hara, T. Kaizuka, C. Kishi, A. Takamura, Y. Miura, S. Iemura, T. Natsume, K. Takehana, N. Yamada, J. L. Guan, N. Oshiro and N. Mizushima (2009). "Nutrient-dependent mTORC1 association with the ULK1-Atg13-FIP200 complex required for autophagy." *Mol Biol Cell* 20(7): 1981-1991.

Huang, J. and B. D. Manning (2008). "The TSC1-TSC2 complex: a molecular switchboard controlling cell growth." *Biochem J* 412(2): 179-190.

Hugl, S. R., M. F. White and C. J. Rhodes (1998). "Insulin-like growth factor I (IGF-I)-stimulated pancreatic beta-cell growth is glucose-dependent. Synergistic activation of insulin receptor substrate-mediated signal transduction pathways by glucose and IGF-I in INS-1 cells." *J Biol Chem* 273(28): 17771-17779.

Iacovelli, L., M. Falasca, S. Valitutti, D. D'Arcangelo and D. Corda (1993). "Glycerophosphoinositol 4-phosphate, a putative endogenous inhibitor of adenylcyclase." *J Biol Chem* 268(27): 20402-20407.

Inoki, K., T. Zhu and K. L. Guan (2003). "TSC2 mediates cellular energy response to control cell growth and survival." *Cell* 115(5): 577-590.

Jewell, J. L., E. Oh, L. Ramalingam, M. A. Kalwat, V. S. Tagliabracchi, L. Tackett, J. S. Elmendorf and D. C. Thurmond (2011). "Munc18c phosphorylation by the insulin receptor links cell signaling directly to SNARE exocytosis." *J Cell Biol* 193(1): 185-199.

Jewell, J. L., E. Oh and D. C. Thurmond (2010). "Exocytosis mechanisms underlying insulin release and glucose uptake: conserved roles for Munc18c and syntaxin 4." *Am J Physiol Regul Integr Comp Physiol* 298(3): R517-531.

Jung, H. S., K. W. Chung, J. Won Kim, J. Kim, M. Komatsu, K. Tanaka, Y. H. Nguyen, T. M. Kang, K. H. Yoon, J. W. Kim, Y. T. Jeong, M. S. Han, M. K. Lee, K. W. Kim, J. Shin and M. S. Lee (2008). "Loss of autophagy diminishes pancreatic beta cell mass and function with resultant hyperglycemia." *Cell Metab* 8(4): 318-324.

Kaneko, K., K. Ueki, N. Takahashi, S. Hashimoto, M. Okamoto, M. Awazawa, Y. Okazaki, M. Ohsugi, K. Inabe, T. Umehara, M. Yoshida, M. Kakei, T. Kitamura, J. Luo, R. N. Kulkarni, C. R. Kahn, H. Kasai, L. C. Cantley and T. Kadowaki (2010). "Class IA phosphatidylinositol 3-kinase in pancreatic beta cells controls insulin secretion by multiple mechanisms." *Cell Metab* 12(6): 619-632.

Kang, S., J. Song, J. Kang, H. Kang, D. Lee, Y. Lee and D. Park (2005). "Suppression of the alpha-isoform of class II phosphoinositide 3-kinase gene expression leads to apoptotic cell death." *Biochem Biophys Res Commun* 329(1): 6-10.

Knight, Z. A., B. Gonzalez, M. E. Feldman, E. R. Zunder, D. D. Goldenberg, O. Williams, R. Loewith, D. Stokoe, A. Balla, B. Toth, T. Balla, W. A. Weiss, R. L. Williams and K. M. Shokat (2006). "A pharmacological map of the PI3-K family defines a role for p110alpha in insulin signaling." *Cell* 125(4): 733-747.

Kok, K., B. Geering and B. Vanhaesebroeck (2009). "Regulation of phosphoinositide 3-kinase expression in health and disease." *Trends Biochem Sci* 34(3): 115-127.

Koshkin, V., F. F. Dai, C. A. Robson-Doucette, C. B. Chan and M. B. Wheeler (2008). "Limited mitochondrial permeabilization is an early manifestation of palmitate-induced lipotoxicity in pancreatic beta-cells." *J Biol Chem* 283(12): 7936-7948.

Krag, C., E. K. Malmberg and A. E. Salcini (2010). "PI3KC2alpha, a class II PI3K, is required for dynamin-independent internalization pathways." *J Cell Sci* 123(Pt 24): 4240-4250.

Kubota, N., K. Tobe, Y. Terauchi, K. Eto, T. Yamauchi, R. Suzuki, Y. Tsubamoto, K. Komeda, R. Nakano, H. Miki, S. Satoh, H. Sekihara, S. Sciacchitano, M. Lesniak, S. Aizawa, R. Nagai, S. Kimura, Y. Akanuma, S. I. Taylor and T. Kadowaki (2000). "Disruption of insulin receptor

substrate 2 causes type 2 diabetes because of liver insulin resistance and lack of compensatory beta-cell hyperplasia." *Diabetes* 49(11): 1880-1889.

Kulkarni, R. N. (2005). "New insights into the roles of insulin/IGF-I in the development and maintenance of beta-cell mass." *Rev Endocr Metab Disord* 6(3): 199-210.

Kwon, G., C. A. Marshall, K. L. Pappan, M. S. Remedi and M. L. McDaniel (2004). "Signaling Elements Involved in the Metabolic Regulation of mTOR by Nutrients, Incretins, and Growth Factors in Islets." *Diabetes* 53(suppl 3): S225-S232.

Lamming, D. W. and D. M. Sabatini (2013). "A Central role for mTOR in lipid homeostasis." *Cell Metab* 18(4): 465-469.

Laplane, M. and D. M. Sabatini (2012). "mTOR signaling in growth control and disease." *Cell* 149(2): 274-293.

Lee, Y., H. Hirose, M. Ohneda, J. H. Johnson, J. D. McGarry and R. H. Unger (1994). "Beta-cell lipotoxicity in the pathogenesis of non-insulin-dependent diabetes mellitus of obese rats: impairment in adipocyte-beta-cell relationships." *Proc Natl Acad Sci U S A* 91(23): 10878-10882.

Leibiger, B., I. B. Leibiger, T. Moede, S. Kemper, R. N. Kulkarni, C. R. Kahn, L. M. de Vargas and P. O. Berggren (2001). "Selective insulin signaling through A and B insulin receptors regulates transcription of insulin and glucokinase genes in pancreatic beta cells." *Mol Cell* 7(3): 559-570.

Leibiger, B., T. Moede, S. Uhles, C. J. Barker, M. Creveaux, J. Domin, P. O. Berggren and I. B. Leibiger (2010). "Insulin-feedback via PI3K-C2alpha activated PKBalpha/Akt1 is required for glucose-stimulated insulin secretion." *FASEB J* 24(6): 1824-1837.

Leslie, N. R. and C. P. Downes (2002). "PTEN: The down side of PI 3-kinase signalling." *Cell Signal* 14(4): 285-295.

Lindmo, K. and H. Stenmark (2006). "Regulation of membrane traffic by phosphoinositide 3-kinases." *J Cell Sci* 119(Pt 4): 605-614.

Loveland, B. E., T. G. Johns, I. R. Mackay, F. Vaillant, Z. X. Wang and P. J. Hertzog (1992). "Validation of the MTT dye assay for enumeration of cells in proliferative and antiproliferative assays." *Biochem Int* 27(3): 501-510.

MacDonald, P. E., J. W. Joseph, D. Yau, J. Diao, Z. Asghar, F. Dai, G. Y. Oudit, M. M. Patel, P. H. Backx and M. B. Wheeler (2004). "Impaired glucose-stimulated insulin secretion, enhanced intraperitoneal insulin tolerance, and increased beta-cell mass in mice lacking the p110gamma isoform of phosphoinositide 3-kinase." *Endocrinology* 145(9): 4078-4083.

Maffucci, T. (2012). "An introduction to phosphoinositides." *Curr Top Microbiol Immunol* 362: 1-42.

Maffucci, T., A. Brancaccio, E. Piccolo, R. C. Stein and M. Falasca (2003). "Insulin induces phosphatidylinositol-3-phosphate formation through TC10 activation." *EMBO J* 22(16): 4178-4189.

Maffucci, T., F. T. Cooke, F. M. Foster, C. J. Traer, M. J. Fry and M. Falasca (2005). "Class II phosphoinositide 3-kinase defines a novel signaling pathway in cell migration." *J Cell Biol* 169(5): 789-799.

Mannaa, M., S. Kramer, M. Boschmann and M. Gollasch (2013). "mTOR and regulation of energy homeostasis in humans." *J Mol Med (Berl)* 91(10): 1167-1175.

Manning, B. D. and L. C. Cantley (2007). "AKT/PKB signaling: navigating downstream." *Cell* 129(7): 1261-1274.

Marchetti, P., F. Dotta, D. Lauro and F. Purrello (2008). "An overview of pancreatic beta-cell defects in human type 2 diabetes: implications for treatment." *Regul Pept* 146(1-3): 4-11.

Marchetti, P., R. Lupi, M. Federici, L. Marselli, M. Masini, U. Boggi, S. Del Guerra, G. Patane, S. Piro, M. Anello, E. Bergamini, F. Purrello, R. Lauro, F. Mosca, G. Sesti and S. Del Prato (2002). "Insulin secretory function is impaired in isolated human islets carrying the Gly(972)->Arg IRS-1 polymorphism." *Diabetes* 51(5): 1419-1424.



Marshall, C., G. A. Hitman, C. J. Partridge, A. Clark, H. Ma, T. R. Shearer and M. D. Turner (2005). "Evidence that an isoform of calpain-10 is a regulator of exocytosis in pancreatic beta-cells." *Mol Endocrinol* 19(1): 213-224.

Masini, M., R. Lupi, M. Bugliani, U. Boggi, F. Filipponi, P. Masiello and P. Marchetti (2009). "A role for autophagy in beta-cell life and death." *Islets* 1(2): 157-159.

Mavrommati, I. and T. Maffucci (2011). "mTOR inhibitors: facing new challenges ahead." *Curr Med Chem* 18(18): 2743-2762.

Mazza, S. and T. Maffucci (2011). "Class II phosphoinositide 3-kinase C2alpha: what we learned so far." *Int J Biochem Mol Biol* 2(2): 168-182.

Mazza, S. and T. Maffucci (2014). "Autophagy and pancreatic beta-cells." *Vitam Horm* 95: 145-164.

McCulloch, L. J., M. van de Bunt, M. Braun, K. N. Frayn, A. Clark and A. L. Gloyn (2011). "GLUT2 (SLC2A2) is not the principal glucose transporter in human pancreatic beta cells: implications for understanding genetic association signals at this locus." *Mol Genet Metab* 104(4): 648-653.

McGarry, J. D. (2002). "Banting lecture 2001: dysregulation of fatty acid metabolism in the etiology of type 2 diabetes." *Diabetes* 51(1): 7-18.

Meunier, F. A., S. L. Osborne, G. R. Hammond, F. T. Cooke, P. J. Parker, J. Domin and G. Schiavo (2005). "Phosphatidylinositol 3-kinase C2alpha is essential for ATP-dependent priming of neurosecretory granule exocytosis." *Mol Biol Cell* 16(10): 4841-4851.

Modrak-Wojcik, A., M. Gorka, K. Niedzwiecka, K. Zdanowski, J. Zuberek, A. Niedzwiecka and R. Stolarski (2013). "Eukaryotic translation initiation is controlled by cooperativity effects within ternary complexes of 4E-BP1, eIF4E, and the mRNA 5' cap." *FEBS Lett* 587(24): 3928-3934.

Morgan, N. G. and S. Dhayal (2010). "Unsaturated fatty acids as cytoprotective agents in the pancreatic beta-cell." *Prostaglandins Leukot Essent Fatty Acids* 82(4-6): 231-236.

Muller, D., G. C. Huang, S. Amiel, P. M. Jones and S. J. Persaud (2006). "Identification of insulin signaling elements in human beta-cells: autocrine regulation of insulin gene expression." *Diabetes* 55(10): 2835-2842.

Muoio, D. M. and C. B. Newgard (2008). "Mechanisms of disease: molecular and metabolic mechanisms of insulin resistance and beta-cell failure in type 2 diabetes." *Nat Rev Mol Cell Biol* 9(3): 193-205.

Ng, S. K. L., S.-Y. Neo, Y.-W. Yap, R. K. M. Karuturi, E. S. L. Loh, K.-H. Liao and E.-C. Ren (2009). "Ablation of phosphoinositide-3-kinase class II alpha suppresses hepatoma cell proliferation." *Biochemical and Biophysical Research Communications* 387(2): 310-315.

Ono, F., T. Nakagawa, S. Saito, Y. Owada, H. Sakagami, K. Goto, M. Suzuki, S. Matsuno and H. Kondo (1998). "A novel class II phosphoinositide 3-kinase predominantly expressed in the liver and its enhanced expression during liver regeneration." *J Biol Chem* 273(13): 7731-7736.

Pende, M., S. C. Kozma, M. Jaquet, V. Oorschot, R. Burcelin, Y. Le Marchand-Brustel, J. Klumperman, B. Thorens and G. Thomas (2000). "Hypoinsulinaemia, glucose intolerance and diminished beta-cell size in S6K1-deficient mice." *Nature* 408(6815): 994-997.

Pende, M., S. H. Um, V. Mieulet, M. Sticker, V. L. Goss, J. Mestan, M. Mueller, S. Fumagalli, S. C. Kozma and G. Thomas (2004). "S6K1(-)/S6K2(-) mice exhibit perinatal lethality and rapamycin-sensitive 5'-terminal oligopyrimidine mRNA translation and reveal a mitogen-activated protein kinase-dependent S6 kinase pathway." *Mol Cell Biol* 24(8): 3112-3124.

Peng, G., L. Li, Y. Liu, J. Pu, S. Zhang, J. Yu, J. Zhao and P. Liu (2011). "Oleate Blocks Palmitate-Induced Abnormal Lipid Distribution, Endoplasmic Reticulum Expansion and Stress, and Insulin Resistance in Skeletal Muscle." *Endocrinology* 152(6): 2206-2218.

Pigeau, G. M., J. Kolic, B. J. Ball, M. B. Hoppa, Y. W. Wang, T. Ruckle, M. Woo, J. E. Manning Fox and P. E. MacDonald (2009). "Insulin granule recruitment and exocytosis is dependent on p110gamma in insulinoma and human beta-cells." *Diabetes* 58(9): 2084-2092.

Posor, Y., M. Eichhorn-Gruenig, D. Puchkov, J. Schoneberg, A. Ullrich, A. Lampe, R. Muller, S. Zerbakhsh, F. Gulluni, E. Hirsch, M. Krauss, C. Schultz, J. Schmoranz, F. Noe and V. Haucke (2013). "Spatiotemporal control of endocytosis by phosphatidylinositol-3,4-bisphosphate." *Nature* 499(7457): 233-237.

Prentki, M., F. M. Matschinsky and S. R. Madiraju (2013). "Metabolic signaling in fuel-induced insulin secretion." *Cell Metab* 18(2): 162-185.

Prentki, M. and C. J. Nolan (2006). "Islet beta cell failure in type 2 diabetes." *J Clin Invest* 116(7): 1802-1812.

Razzini, G., A. Brancaccio, M. A. Lemmon, S. Guarnieri and M. Falasca (2000). "The role of the pleckstrin homology domain in membrane targeting and activation of phospholipase Cbeta(1)." *J Biol Chem* 275(20): 14873-14881.

Renström, E. and P. Rorsman (2008). Regulation of Insulin Granule Exocytosis. *Pancreatic Beta Cell in Health and Disease*. S. Seino and G. Bell, Springer Japan: 147-176.

Rorsman, P. and M. Braun (2013). "Regulation of insulin secretion in human pancreatic islets." *Annu Rev Physiol* 75: 155-179.

Rorsman, P. and E. Renstrom (2003). "Insulin granule dynamics in pancreatic beta cells." *Diabetologia* 46(8): 1029-1045.

Saltiel, A. R. and C. R. Kahn (2001). "Insulin signalling and the regulation of glucose and lipid metabolism." *Nature* 414(6865): 799-806.

Samuels, Y., Z. Wang, A. Bardelli, N. Silliman, J. Ptak, S. Szabo, H. Yan, A. Gazdar, S. M. Powell, G. J. Riggins, J. K. Willson, S. Markowitz, K. W. Kinzler, B. Vogelstein and V. E. Velculescu (2004). "High frequency of mutations of the PIK3CA gene in human cancers." *Science* 304(5670): 554.

Sano, H., S. Kane, E. Sano, C. P. Miinea, J. M. Asara, W. S. Lane, C. W. Garner and G. E. Lienhard (2003). "Insulin-stimulated phosphorylation of a Rab GTPase-activating protein regulates GLUT4 translocation." *J Biol Chem* 278(17): 14599-14602.

Sarbassov, D. D., S. M. Ali, S. Sengupta, J. H. Sheen, P. P. Hsu, A. F. Bagley, A. L. Markhard and D. M. Sabatini (2006). "Prolonged rapamycin treatment inhibits mTORC2 assembly and Akt/PKB." *Mol Cell* 22(2): 159-168.

Schepeler, T., A. Holm, P. Halvey, I. Nordentoft, P. Lamy, E. M. Riising, L. L. Christensen, K. Thorsen, D. C. Liebler, K. Helin, T. F. Orntoft and C. L. Andersen (2012). "Attenuation of the beta-catenin/TCF4 complex in colorectal cancer cells induces several growth-suppressive microRNAs that target cancer promoting genes." *Oncogene* 31(22): 2750-2760.

Schultze, S. M., J. Jensen, B. A. Hemmings, O. Tschopp and M. Niessen (2011). "Promiscuous affairs of PKB/AKT isoforms in metabolism." *Arch Physiol Biochem* 117(2): 70-77.

Sekulic, A., C. C. Hudson, J. L. Homme, P. Yin, D. M. Otterness, L. M. Karnitz and R. T. Abraham (2000). "A direct linkage between the phosphoinositide 3-kinase-AKT signaling pathway and the mammalian target of rapamycin in mitogen-stimulated and transformed cells." *Cancer Res* 60(13): 3504-3513.

Skelin, M., M. Rupnik and A. Cencic (2010). "Pancreatic beta cell lines and their applications in diabetes mellitus research." *ALTEX* 27(2): 105-113.

Soos, M. A., J. Jensen, R. A. Brown, S. O'Rahilly, P. R. Shepherd and J. P. Whitehead (2001). "Class II phosphoinositide 3-kinase is activated by insulin but not by contraction in skeletal muscle." *Arch Biochem Biophys* 396(2): 244-248.

Sotsios, Y. and S. G. Ward (2000). "Phosphoinositide 3-kinase: a key biochemical signal for cell migration in response to chemokines." *Immunol Rev* 177: 217-235.

Srivastava, S., L. Di, O. Zhdanova, Z. Li, S. Vardhana, Q. Wan, Y. Yan, R. Varma, J. Backer, H. Wulff, M. L. Dustin and E. Y. Skolnik (2009). "The class II phosphatidylinositol 3 kinase C2beta is required for the activation of the K<sup>+</sup> channel KCa3.1 and CD4 T-cells." *Mol Biol Cell* 20(17): 3783-3791.

Subbiah, V., R. E. Brown, Y. Jiang, J. Buryanek, A. Hayes-Jordan, R. Kurzrock and P. M. Anderson (2013). "Morphoproteomic profiling of the mammalian target of rapamycin

(mTOR) signaling pathway in desmoplastic small round cell tumor (EWS/WT1), Ewing's sarcoma (EWS/FLI1) and Wilms' tumor(WT1)." PLoS One 8(7): e68985.

Sujobert, P., V. Bardet, P. Cornillet-Lefebvre, J. S. Hayflick, N. Prie, F. Verdier, B. Vanhaesebroeck, O. Muller, F. Pesce, N. Ifrah, M. Hunault-Berger, C. Berthou, B. Villemagne, E. Jourdan, B. Audhuy, E. Solary, B. Witz, J. L. Harousseau, C. Himmerlin, T. Lamy, B. Lioure, J. Y. Cahn, F. Dreyfus, P. Mayeux, C. Lacombe and D. Bouscary (2005). "Essential role for the p110delta isoform in phosphoinositide 3-kinase activation and cell proliferation in acute myeloid leukemia." Blood 106(3): 1063-1066.

Suzuki, A., J. L. de la Pompa, V. Stambolic, A. J. Elia, T. Sasaki, I. del Barco Barrantes, A. Ho, A. Wakeham, A. Itie, W. Khoo, M. Fukumoto and T. W. Mak (1998). "High cancer susceptibility and embryonic lethality associated with mutation of the PTEN tumor suppressor gene in mice." Curr Biol 8(21): 1169-1178.

Taniguchi, C. M., B. Emanuelli and C. R. Kahn (2006). "Critical nodes in signalling pathways: insights into insulin action." Nat Rev Mol Cell Biol 7(2): 85-96.

Taylor, R. (2012). "Insulin resistance and type 2 diabetes." Diabetes 61(4): 778-779.

Taylor, R. C., S. P. Cullen and S. J. Martin (2008). "Apoptosis: controlled demolition at the cellular level." Nat Rev Mol Cell Biol 9(3): 231-241.

Tibolla, G., R. Pineiro, D. Chiozzotto, I. Mavrommati, A. P. Wheeler, G. D. Norata, A. L. Catapano, T. Maffucci and M. Falasca (2013). "Class II phosphoinositide 3-kinases contribute to endothelial cells morphogenesis." PLoS One 8(1): e53808.

Tomiyama, K., H. Nakata, H. Sasa, S. Arimura, E. Nishio and Y. Watanabe (1995). "Wortmannin, a specific phosphatidylinositol 3-kinase inhibitor, inhibits adipocytic differentiation of 3T3-L1 cells." Biochem Biophys Res Commun 212(1): 263-269.

Torrejon-Escribano, B., J. Escoriza, E. Montanya and J. Blasi (2011). "Glucose-dependent changes in SNARE protein levels in pancreatic beta-cells." Endocrinology 152(4): 1290-1299.

Turner, M. D., F. K. Fulcher, C. V. Jones, B. T. Smith, E. Aganna, C. J. Partridge, G. A. Hitman, A. Clark and Y. M. Patel (2007). "Calpain facilitates actin reorganization during glucose-stimulated insulin secretion." *Biochem Biophys Res Commun* 352(3): 650-655.

Ueki, K., D. A. Fruman, S. M. Brachmann, Y. H. Tseng, L. C. Cantley and C. R. Kahn (2002). "Molecular balance between the regulatory and catalytic subunits of phosphoinositide 3-kinase regulates cell signaling and survival." *Mol Cell Biol* 22(3): 965-977.

Vadlakonda, L., A. Dash, M. Pasupuleti, K. Anil Kumar and P. Reddanna (2013). "The Paradox of Akt-mTOR Interactions." *Front Oncol* 3: 165.

Vanhaesebroeck, B., J. Guillermet-Guibert, M. Graupera and B. Bilanges (2010). "The emerging mechanisms of isoform-specific PI3K signalling." *Nat Rev Mol Cell Biol* 11(5): 329-341.

Vanhaesebroeck, B., S. J. Leever, K. Ahmadi, J. Timms, R. Katso, P. C. Driscoll, R. Woscholski, P. J. Parker and M. D. Waterfield (2001). "Synthesis and function of 3-phosphorylated inositol lipids." *Annu Rev Biochem* 70: 535-602.

Vanhaesebroeck, B. and M. D. Waterfield (1999). "Signaling by distinct classes of phosphoinositide 3-kinases." *Exp Cell Res* 253(1): 239-254.

Visnjic, D., J. Curic, V. Crljen, D. Batinic, S. Volinia and H. Banfic (2003). "Nuclear phosphoinositide 3-kinase C2beta activation during G2/M phase of the cell cycle in HL-60 cells." *Biochim Biophys Acta* 1631(1): 61-71.

Wang, X. and C. G. Proud (2009). "Nutrient control of TORC1, a cell-cycle regulator." *Trends Cell Biol* 19(6): 260-267.

Wang, Y., K. Yoshioka, M. A. Azam, N. Takuwa, S. Sakurada, Y. Kayaba, N. Sugimoto, I. Inoki, T. Kimura, T. Kuwaki and Y. Takuwa (2006). "Class II phosphoinositide 3-kinase alpha-isoform regulates Rho, myosin phosphatase and contraction in vascular smooth muscle." *Biochem J* 394(Pt 3): 581-592.

Wen, P. J., S. L. Osborne, I. C. Morrow, R. G. Parton, J. Domin and F. A. Meunier (2008). "Ca<sup>2+</sup>-regulated pool of phosphatidylinositol-3-phosphate produced by phosphatidylinositol 3-kinase C2alpha on neurosecretory vesicles." *Mol Biol Cell* 19(12): 5593-5603.

Withers, D. J., J. S. Gutierrez, H. Towery, D. J. Burks, J. M. Ren, S. Previs, Y. Zhang, D. Bernal, S. Pons, G. I. Shulman, S. Bonner-Weir and M. F. White (1998). "Disruption of IRS-2 causes type 2 diabetes in mice." *Nature* 391(6670): 900-904.

Wu, J. J., C. Quijano, E. Chen, H. Liu, L. Cao, M. M. Fergusson, Rovira, II, S. Gutkind, M. P. Daniels, M. Komatsu and T. Finkel (2009). "Mitochondrial dysfunction and oxidative stress mediate the physiological impairment induced by the disruption of autophagy." *Aging (Albany NY)* 1(4): 425-437.

Xie, J. and T. P. Herbert (2012). "The role of mammalian target of rapamycin (mTOR) in the regulation of pancreatic beta-cell mass: implications in the development of type-2 diabetes." *Cell Mol Life Sci* 69(8): 1289-1304.

Yamaguchi, S., H. Ishihara, T. Yamada, A. Tamura, M. Usui, R. Tominaga, Y. Munakata, C. Satake, H. Katagiri, F. Tashiro, H. Aburatani, K. Tsukiyama-Kohara, J. Miyazaki, N. Sonenberg and Y. Oka (2008). "ATF4-mediated induction of 4E-BP1 contributes to pancreatic beta cell survival under endoplasmic reticulum stress." *Cell Metab* 7(3): 269-276.

Yoshioka, K., K. Yoshida, H. Cui, T. Wakayama, N. Takuwa, Y. Okamoto, W. Du, X. Qi, K. Asanuma, K. Sugihara, S. Aki, H. Miyazawa, K. Biswas, C. Nagakura, M. Ueno, S. Iseki, R. J. Schwartz, H. Okamoto, T. Sasaki, O. Matsui, M. Asano, R. H. Adams, N. Takakura and Y. Takuwa (2012). "Endothelial PI3K-C2alpha, a class II PI3K, has an essential role in angiogenesis and vascular barrier function." *Nat Med* 18(10): 1560-1569.

Yu, J., P. O. Berggren and C. J. Barker (2007). "An autocrine insulin feedback loop maintains pancreatic beta-cell 3-phosphorylated inositol lipids." *Mol Endocrinol* 21(11): 2775-2784.

Zhao, F. and Q. Wang (2012). "The protective effect of peroxiredoxin II on oxidative stress induced apoptosis in pancreatic beta-cells." *Cell Biosci* 2(1): 22.

This work was supported by Diabetes UK



# Copyright permission

## AMERICAN DIABETES ASSOCIATION LICENSE TERMS AND CONDITIONS

May 08, 2014

---

This is a License Agreement between Simona Mazza ("You") and American Diabetes Association ("American Diabetes Association") provided by Copyright Clearance Center ("CCC"). The license consists of your order details, the terms and conditions provided by American Diabetes Association, and the payment terms and conditions.

**All payments must be made in full to CCC. For payment instructions, please see information listed at the bottom of this form.**

License Number	3381430222433
License date	May 03, 2014
Licensed content publisher	American Diabetes Association
Licensed content publication	Diabetes
Licensed content title	Signaling Elements Involved in the Metabolic Regulation of mTOR by Nutrients, Incretins, and Growth Factors in Islets
Licensed copyright line	Copyright © 2004, American Diabetes Association
Licensed content author	Guim Kwon, Connie A. Marshall, Kirk L. Pappan et al.
Licensed content date	Dec 1, 2004
Volume number	53
Issue number	suppl 3
Type of Use	Thesis/Dissertation
Requestor type	Student
Format	Print, Electronic
Portion	chart/graph/table/figure
Number of charts/graphs/tables/figures	1
Rights for	Main product
Duration of use	Life of current edition
Creation of copies for the disabled	no
With minor editing privileges	no
For distribution to	U.K. and Commonwealth (excluding Canada)
In the following language(s)	Original language of publication
With incidental promotional use	no
The lifetime unit quantity of new product	0 to 499
Specified additional information	FIG. 1. Proposed model of metabolic and autocrine regulation of the mTOR pathway by beta cells. Figure will be used only in my PhD dissertation

The requesting person/organization is:	Simona Mazza - Queen Mary University of London
Order reference number	None
Title of your thesis / dissertation	role of PI3K-C2alpha in pancreatic beta cells
Expected completion date	May 2014
Expected size (number of pages)	230
Total	0.00 USD

**SPRINGER LICENSE  
TERMS AND CONDITIONS**

May 08, 2014

---

This is a License Agreement between Simona Mazza ("You") and Springer ("Springer") provided by Copyright Clearance Center ("CCC"). The license consists of your order details, the terms and conditions provided by Springer, and the payment terms and conditions.

**All payments must be made in full to CCC. For payment instructions, please see information listed at the bottom of this form.**

License Number	3381280017843
License date	May 03, 2014
Licensed content publisher	Springer
Licensed content publication	Springer eBook
Licensed content title	An Introduction to Phosphoinositides
Licensed content author	Tania Maffucci
Licensed content date	Jan 1, 2012
Type of Use	Thesis/Dissertation
Portion	Figures
Author of this Springer article	No
Order reference number	None
Original figure numbers	Figures 2, 3, 5
Title of your thesis / dissertation	role of PI3K-C2alpha in pancreatic beta cells
Expected completion date	May 2014
Estimated size(pages)	230
Total	0.00 GBP

**SPRINGER LICENSE  
TERMS AND CONDITIONS**

May 08, 2014

---

---

This is a License Agreement between Simona Mazza ("You") and Springer ("Springer") provided by Copyright Clearance Center ("CCC"). The license consists of your order details, the terms and conditions provided by Springer, and the payment terms and conditions.

**All payments must be made in full to CCC. For payment instructions, please see information listed at the bottom of this form.**

License Number	3380841466570
License date	May 02, 2014
Licensed content publisher	Springer
Licensed content publication	Springer eBook
Licensed content title	Measurement of Polyphosphoinositides in Cultured Mammalian Cells
Licensed content author	Frank T. Cooke
Licensed content date	Jan 1, 2009
Type of Use	Thesis/Dissertation
Portion	Figures
Author of this Springer article	No
Order reference number	None
Original figure numbers	Fig. 3.2 of the protocol. Schematic diagram of PtdIns(3,4,5) P2 .
Title of your thesis / dissertation	role of PI3K-C2alpha in pancreatic beta cells
Expected completion date	May 2014
Estimated size(pages)	230
Total	0.0 USD

**NATURE PUBLISHING GROUP LICENSE  
TERMS AND CONDITIONS**

May 08, 2014

---

---

This is a License Agreement between Simona Mazza ("You") and Nature Publishing Group ("Nature Publishing Group") provided by Copyright Clearance Center ("CCC"). The license consists of your order details, the terms and

conditions provided by Nature Publishing Group, and the payment terms and conditions.

**All payments must be made in full to CCC. For payment instructions, please see information listed at the bottom of this form.**

License Number	3380840444939
License date	May 02, 2014
Licensed content publisher	Nature Publishing Group
Licensed content publication	Kidney International
Licensed content title	The potential benefits of rapamycin on renal function, tolerance, fibrosis, and malignancy following transplantation
Licensed content author	Edward K Geissler and Hans J Schlitt
Licensed content date	Sep 22, 2010
Volume number	78
Issue number	11
Type of Use	reuse in a dissertation / thesis
Requestor type	academic/educational
Format	print and electronic
Portion	figures/tables/illustrations
Number of figures/tables/illustrations	1
High-res required	no
Figures	Figure 1 mTORC1 pathway basics.
Author of this NPG article	no
Your reference number	None
Title of your thesis / dissertation	role of PI3K-C2alpha in pancreatic beta cells
Expected completion date	May 2014
Estimated size (number of pages)	230
Total	0.00 USD

**JOHN WILEY AND SONS LICENSE  
TERMS AND CONDITIONS**

May 08, 2014

---

---

This is a License Agreement between Simona Mazza ("You") and John Wiley and Sons ("John Wiley and Sons") provided by Copyright Clearance Center ("CCC"). The license consists of your order details, the terms and conditions provided by John Wiley and Sons, and the payment terms and conditions.

**All payments must be made in full to CCC. For payment instructions, please see information listed at the bottom of this form.**

License Number	3380840155274
License date	May 02, 2014
Licensed content publisher	John Wiley and Sons
Licensed content publication	Diabetes, Obesity and Metabolism
Licensed content title	Regulation of $\beta$ -cell mass and function by the Akt/protein kinase B signalling pathway
Licensed copyright line	2007 Blackwell Publishing Ltd
Licensed content author	L. Elghazi, L. Rachdi, A. J. Weiss, C. Cras-Méneur, E. Bernal-Mizrachi
Licensed content date	Oct 4, 2007
Start page	147
End page	157
Type of use	Dissertation/Thesis
Requestor type	University/Academic
Format	Print and electronic
Portion	Figure/table
Number of figures/tables	1
Original Wiley figure/table number(s)	Figure 2 Schematic representation of Akt/protein kinase B (PKB) signalling
Will you be translating?	No
Title of your thesis / dissertation	role of PI3K-C2alpha in pancreatic beta cells
Expected completion date	May 2014
Expected size (number of pages)	230
Total	0.00 GBP

**ELSEVIER LICENSE  
TERMS AND CONDITIONS**

May 08, 2014

This is a License Agreement between Simona Mazza ("You") and Elsevier ("Elsevier") provided by Copyright Clearance Center ("CCC"). The license consists of your order details, the terms and conditions provided by Elsevier, and the payment terms and conditions.

**All payments must be made in full to CCC. For payment instructions, please see information listed at the bottom of this form.**

Supplier	Elsevier Limited The Boulevard, Langford Lane Kidlington, Oxford, OX5 1GB, UK
Registered Company Number	1982084
Customer name	Simona Mazza
Customer address	Blizard Institute London, greater london E1 2RD
License number	3380831158293
License date	May 02, 2014
Licensed content publisher	Elsevier
Licensed content publication	Trends in Molecular Medicine
Licensed content title	mTOR Complex1-S6K1 signaling: at the crossroads of obesity, diabetes and cancer
Licensed content author	Stephen G. Dann, Anand Selvaraj, George Thomas
Licensed content date	June 2007
Licensed content volume number	13
Licensed content issue number	6
Number of pages	8
Start Page	252
End Page	259
Type of Use	reuse in a thesis/dissertation
Intended publisher of new work	other
Portion	figures/tables/illustrations
Number of figures/tables/illustrations	1
Format	both print and electronic
Are you the author of this Elsevier article?	No
Will you be translating?	No
Title of your thesis/dissertation	role of PI3K-C2alpha in pancreatic beta cells
Expected completion date	May 2014
Estimated size (number of pages)	230
Elsevier VAT number	GB 494 6272 12

Permissions price	0.00 USD
VAT/Local Sales Tax	0.00 USD / 0.00 GBP
Total	0.00 USD

**NATURE PUBLISHING GROUP LICENSE  
TERMS AND CONDITIONS**

May 08, 2014

This is a License Agreement between Simona Mazza ("You") and Nature Publishing Group ("Nature Publishing Group") provided by Copyright Clearance Center ("CCC"). The license consists of your order details, the terms and conditions provided by Nature Publishing Group, and the payment terms and conditions.

**All payments must be made in full to CCC. For payment instructions, please see information listed at the bottom of this form.**

License Number	3380830909048
License date	May 02, 2014
Licensed content publisher	Nature Publishing Group
Licensed content publication	Nature Reviews Molecular Cell Biology
Licensed content title	The renaissance of GSK3
Licensed content author	Philip CohenandSheelagh Frame
Licensed content date	Oct 1, 2001
Volume number	2
Issue number	10
Type of Use	reuse in a dissertation / thesis
Requestor type	academic/educational
Format	print and electronic
Portion	figures/tables/illustrations
Number of figures/tables/illustrations	1
Figures	Figure 1   The signalling pathway by which insulin inhibits GSK3 and contributes to the stimulation of glycogen and protein synthesis.
Author of this NPG article	no
Your reference number	None
Title of your thesis / dissertation	role of PI3K-C2alpha in pancreatic beta cells
Expected completion date	May 2014
Estimated size (number of pages)	230
Total	0.00 USD

**NATURE PUBLISHING GROUP LICENSE  
TERMS AND CONDITIONS**

May 08, 2014

This is a License Agreement between Simona Mazza ("You") and Nature Publishing Group ("Nature Publishing Group") provided by Copyright Clearance Center ("CCC"). The license consists of your order details, the terms and conditions provided by Nature Publishing Group, and the payment terms and conditions.

**All payments must be made in full to CCC. For payment instructions, please see information listed at the bottom of this form.**

License Number	3380830554538
License date	May 02, 2014
Licensed content publisher	Nature Publishing Group
Licensed content publication	Nature Reviews Molecular Cell Biology
Licensed content title	The emerging mechanisms of isoform-specific PI3K signalling
Licensed content author	Bart Vanhaesebroeck, Julie Guillermet-Guibert, Mariona Graupera and Benoit Bilanges
Licensed content date	May 1, 2010
Volume number	11
Issue number	5
Type of Use	reuse in a dissertation / thesis
Requestor type	academic/educational
Format	print and electronic
Portion	figures/tables/illustrations
Number of figures/tables/illustrations	1
High-res required	no
Figures	Figure 2 Title: The emerging mechanisms of isoform-specific PI3K signalling Author: Bart Vanhaesebroeck, Julie Guillermet-Guibert, Mariona Graupera and Benoit Bilanges
Author of this NPG article	no
Your reference number	None
Title of your thesis / dissertation	role of PI3K-C2alpha in pancreatic beta cells
Expected completion date	May 2014
Estimated size (number of pages)	230
Total	0.0 GBP